



**HAL**  
open science

## RESEARCH AT GANIL A COMPILATION 1996-1997

E. Balanzat, M. Bex, J. Galin, S. Geswend

► **To cite this version:**

E. Balanzat, M. Bex, J. Galin, S. Geswend. RESEARCH AT GANIL A COMPILATION 1996-1997. 1998, pp.1-189. in2p3-00384381

**HAL Id: in2p3-00384381**

**<https://hal.in2p3.fr/in2p3-00384381>**

Submitted on 15 May 2009

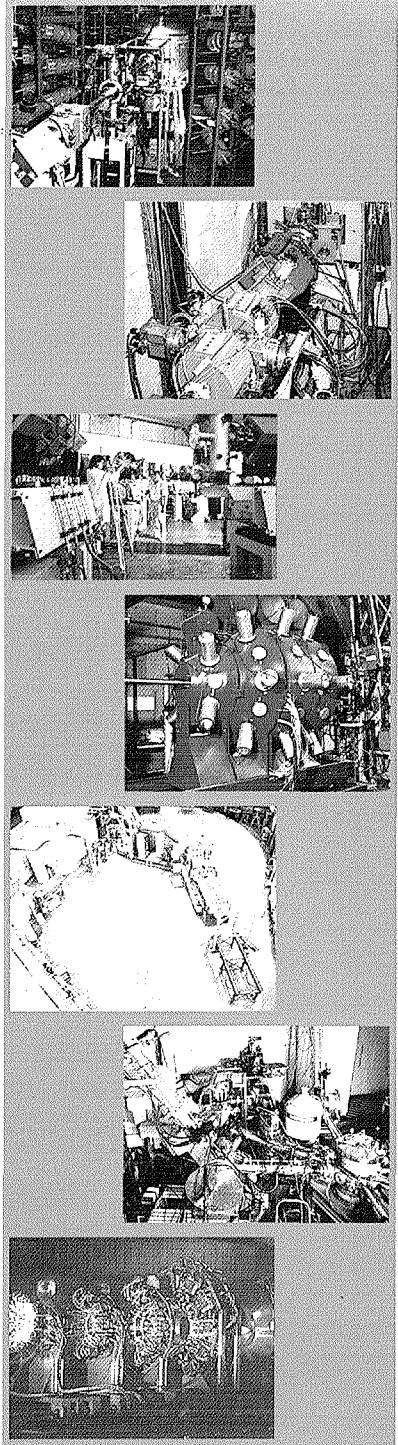
**HAL** is a multi-disciplinary open access archive for the deposit and dissemination of scientific research documents, whether they are published or not. The documents may come from teaching and research institutions in France or abroad, or from public or private research centers.

L'archive ouverte pluridisciplinaire **HAL**, est destinée au dépôt et à la diffusion de documents scientifiques de niveau recherche, publiés ou non, émanant des établissements d'enseignement et de recherche français ou étrangers, des laboratoires publics ou privés.

IMS-FR--044



FR9901033



**RESEARCH**  
at  
**GANIL**  
**1996-1997**

**A COMPILATION**

30 - 38

Grand Accélérateur National d'Ions Lourds

**GANIL**

Laboratoire commun CEA / DSM - CNRS / IN<sup>2</sup>P<sup>3</sup>

Section IUS  
Doc. no. : 15/2/98  
N° TMI : .....  
Destination : I, I-D, D

# RESEARCH AT GANIL

A COMPILATION

1996 - 1997

Editors : E. BALANZAT, M. BEX, J. GALIN  
Typing and layout of the manuscript : S. GESWEND

December 1998

## FOREWORD

The present compilation gives an overview of experimental results obtained with the GANIL facility during the period 1996-1997. For the first time, it includes nuclear physics activities as well as interdisciplinary research. The latter was previously published independently by the CIRIL laboratory which is acting as a host laboratory for this community.

The GANIL and the CIRIL laboratories agreed to present one single report in order to emphasize the broad scientific activity favored by the large variety of beams, energies and experimental equipments offered by the GANIL facility. Therefore the scientific domain ~~which is~~ presented here extends well beyond the traditional nuclear physics and includes atomic physics, condensed matter physics, nuclear astrophysics, radiation chemistry, radiobiology as well as applied physics.

In the nuclear physics field, many new results have been obtained during that period concerning nuclear structure as well as the dynamics of nuclear collisions, and

Further experiments have been performed with the INDRA device which should largely contribute to get a well detailed knowledge of the nuclear disassembly of complex systems. Results which are presented so far deal in particular with the problem of energy equilibration, timescales and the origin of multifragmentation.

Nuclear structure studies using both stable and radioactive beams have led to quite exciting results on the behaviour of exotic systems at the limits of stability. They deal with halo systems, study of shell closures far from stability, the existence of nuclear molecules as well as measurements of fundamental data as half lives, nuclear masses, nuclear radii, quadrupole and magnetic moments. In this domain, LISE and SPEG spectrometers have been heavily used.

Investigations of nuclear structure by means of nuclear reactions have also been performed, especially using SPEG and ORION devices.

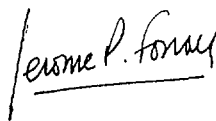
Besides nuclear physics, activities have evolved towards an increased diversification. In addition to traditional fields of atomic and solid state physics, which remain very active, covering an even broader energetic domain through the use of ECR sources, new thematics such as radiation chemistry and radiobiology are progressively being tackled. Such promising is their development that the old denomination of " swift heavy ion physics " given to this field of activity happened to be more and more inappropriate and had to be replaced by the new one of " interdisciplinary research ".

With the forthcoming SPIRAL radioactive beam facility and the undergoing developments of new experimental lines (irradiation lines after the C0 injector) and devices (VAMOS spectrometer and EXOGAM detector), there is no doubt that a rich research programme is expected to be pursued in the future.

We are much indebted to the authors for the quality of their contributions.



D. GUERREAU  
Director  
GANIL



J.P. FOUAN  
Deputy Director  
GANIL



J.P. GRANDIN  
Director  
CIRIL

# CONTENTS

*FOREWORD*

SUMMARY

## A-C) NUCLEAR PHYSICS

A - NUCLEAR STRUCTURE

- A1 - NUCLEAR SPECTROSCOPY
- A2 - EXOTIC NUCLEI AND DECAY MODES

B - NUCLEAR REACTIONS

- B1 - PERIPHERAL COLLISIONS
- B2 - DISSIPATIVE COLLISIONS
- B3 - MULTIFRAGMENT EMISSION
- B4- LIFETIMES OF EXCITED NUCLEI

C - MISCELLANEOUS

PUBLICATION LIST

## D - INTERDISCIPLINARY RESEARCH

- 1 - BASIC COLLISION PROCESSES
- 2 - SWIFT HEAVY ION INDUCED MODIFICATION IN MATERIALS
- 3 - RADIATION CHEMISTRY AND RADIOBIOLOGY
- 4 - PHYSICS AND CHEMISTRY WITH TRACKS

AUTHOR INDEX

# **I. COMPILATION**

## A - NUCLEAR PHYSICS

### A1 - NUCLEAR SPECTROSCOPY

#### TWO-NEUTRON CORRELATIONS AT SMALL RELATIVE MOMENTA IN $^{86}\text{Kr} + ^{165}\text{Ho}$ AND $^{40}\text{Ar} + ^{197}\text{Au}$ REACTIONS AT 60 MeV/u

PLUTA J., LESZCZYNSKI P., PAWLAK T., PRZEWLOCKI M., *Warsaw Univ. of Tech. - Warsaw*

BIZARD G., DURAND D., LECOLLEY F.R., TAMAIN B., *LPC - Caen*

DESEQUELLES P., *ISN - Grenoble*

DORVAUX O., STUTTGE L., *IReS Univ. Louis Pasteur - Strasbourg*

ERAZMUS B., LEBRUN C., *SUBATECH - Nantes*

HANAPPE F., *ULB - Bruxelles*

JAKOBSSON B., NOREN B., *Lund Univ. - Lund*

LEDNICKY R., *Czech Ac. of Sc. - Prague*

MIKHAILOV K., STAVINSKY A., *ITEP - Moscow*

SKEPPSTEDT O., *Chalmers Univ. of Tech. - Göteborg*

9

#### ELASTIC AND INELASTIC PROTON SCATTERING ON THE UNSTABLE $^{20}\text{O}$ NUCLEUS MEASURED WITH THE "MUST" DETECTOR ARRAY

KHAN E., BLUMENFELD Y., SUOMIJARVI T., FRASCARIA N., GODWIN M., LHENRY I., MARECHAL

F., ROYNETTE J.C., SANTONOCITO D., SCARPACI J.A., *IPN - Orsay*

ALAMANOS N., AUGER F., GILLIBERT A., LAPOUX V., MUSUMARA A., OTTINI S., POLLACCO E.C., *CEA Saclay - Gif sur Yvette*

GLASCHAMER T., MORISSEY D.J., *NSCL MSU - East Lansing*

ORR N., *LPC - Caen*

PIATTELLI P., *INFN LNS - Catania*

ROUSSEL-CHOMAZ P., *GANIL - Caen*

SAUVESTRE J.E., *CEA Bruyères - Bruyères-le-Château*

11

#### ANOMALOUS E1 AND E2 STRENGTHS IN $^{40}\text{Ca}$ AND $^{48}\text{Ca}$ AT LOW EXCITATION ENERGY : A COMPARATIVE STUDY

OTTINI-HUSTACHE S., ALAMANOS N., AUGER F., CHISTE V., GILLIBERT A., LAPOUX V., MARIE F., *CEA Saclay - Gif sur Yvette*

CASTEL B., *Queen's Univ. - Kingston*

BLUMENFELD Y., FRASCARIA N., JOUANNE C., ROYNETTE J.C., SCARPACI J.A., *IPN - Orsay*

MITTIG W., *GANIL - Caen*

14

#### SPECTROSCOPY OF THE UNBOUND $^{11}\text{N}$ NUCLEUS BY THE $^{12}\text{C}(^{14}\text{N}, ^{15}\text{C})^{11}\text{N}$ TRANSFER REACTION

LEPINE-SZILY A., LICHTENTHALER R., *IFUSP - Sao Paulo Univ. - Sao Paulo*

OLIVEIRA J.M., *Sorocaba Univ. - Sorocaba*

OSTROWSKI A.N., *Edinburgh Univ. - Edinburgh*

BOHLEN H.G., BLASEVIC A., von OERTZEN W., STOLLA Th., *HMI - Berlin*

BORCEA C., *IAP - Bucharest*

GUIMARAES V., *UNIP - Sao Paulo*

KALPAKCHIEVA R., *LNR JINR - Dubna*

LAPOUX V., *CEA Saclay - Gif sur Yvette*

MACCORMICK M., OLIVEIRA F., ROUSSEL-CHOMAZ P., *GANIL - Caen*

ORR N.A., WINFIELD J.S., *LPC ISMRA - Caen*

19

#### NUCLEAR RADII OF PROTON-RICH RADIOACTIVE NUCLEI AT A = 60-80

LIMA G.F., LEPINE-SZILY A., VILLARI A.C.C., LICHTENTHALER R., *IFUSP Sao Paulo Univ. - Sao Paulo*

MITTIG W., CASANDJIAN J.M., CHARTIER M., LEWITOWICZ M., MACCORMICK M., OSTROWSKI

A.N., *GANIL - Caen*

HIRATA D., *SPring-8 - Hyogo*

ANGELIQUE J.C., ORR N.A., *LPC ISMRA - Caen*  
AUDI G., *CSNSM - Orsay*  
CUNSOLO A., FOTI A., *INFN - Catania*  
DONZEAUD C., STEPHAN C., SUOMIJARVI T., TASSAN-GOT L., *IPN - Orsay*  
GILLIBERT A., *CEN Saclay - Gif sur Yvette*  
LUKYANOV S., *LNR JINR - Dubna*  
MORRISSEY D.J., SHERRILL B.M., *NSCL MSU - East Lansing*  
VIEIRA D.J., WOUTERS J.M., *LANL - Los Alamos* 20

**STUDY OF SUBSHELL CLOSURE AT N=40 BY COULOMB EXCITATION**

LEENHARDT S., AZAIEZ F., SORLIN O., BELLEGUIC M., BOURGEOIS C., DONZAUD C., DUPRAT J., GREVY S., GUILLEMAUD-MUELLER D., MUELLER A.C., POUGHEON F., *IPN - Orsay*  
DELONCLE I., KIENER J., PORQUET M.G., *CSNSM - Orsay*  
DAUGAS J.M., LEWITOWICZ M., de OLIVEIRA F., SAINT-LAURENT M.G., WINFIELD J., *GANIL - Caen*  
ANGELIQUE J.C., MARIE F., ORR N., *LPC - Caen*  
GILLIBERT A., *CEA Saclay - Gif sur Yvette*  
BORCEA C., *IAP - Bucharest*  
PENIONZHKEVICH Yu.E., SOBOLEV Yu., *FLNR JINR - Dubna* 21

**INTERPLAY BETWEEN THE NEUTRON HALO STRUCTURE AND REACTION MECHANISMS IN COLLISIONS OF 35 MeV/NUCLEON  $^6\text{He}$  WITH Au**

PERIER Y., LOTT B., GALIN J., LIENARD E., MORJEAN M., PEGHAIRE A., QUEDNAU B.M., VILLARI A.C.C., *GANIL - Caen*  
ORR N.A., *LPC - Caen* 23

**EXOTIC MOLECULAR AND HALO STATES IN  $^{12,14}\text{Be}$**

FREER M., CLARKE N.M., FULTON B.R., MURGATROYD J.T., SINGER S., *Birmingham Univ. - Birmingham*  
ORR N.A., LABICHE M., MARQUES F.M., ANGELIQUE J.C., BENOIT B., GREVY S., LE BRUN C., *LPC ISMRA - Caen*  
AXELSSON L., JONSON B., MARKENROTH K., NILSSON T., NYMAN G., *Chalmers Tekniska Högskola - Göteborg*  
BENOIT B., D'ARRIGO A., de GOES BRENNARD E., HANAPPE F., *ULB - Bruxelles*  
BERGMANN U., RIISAGER K., *Aarhus univ. - Aarhus*  
CATFORD W.N., CURTIS N., *Surrey Univ. - Guildford*  
CHAPPELL S.P.G., *Oxford Univ. - Oxford*  
COSTA G., DORVAUX O., HEUSCH B., STUTTGE L., *IReS - Strasbourg*  
GARDINA G., MOTTA M., *Messina Univ. - Messina*  
GREGORI C., PIQUERAS I., *IEM - Madrid*  
GUILLEMAUD-MUELLER D., LEENHARDT S., MUELLER A.C., SORLIN O., *IPN - Orsay*  
KELLY G., *Staffordshire Univ. - Stoke-on-Trent*  
de OLIVEIRA F., LEWITOWICZ M., SAINT-LAURENT M.G., SARAZIN F., *GANIL - Caen*  
NINANE A., *UCL - Louvain-la-Neuve*  
WATSON D.L., *York Univ. - York* 25

**QUADRUPOLE AND MAGNETIC MOMENT OF SPIN-ORIENTED  $^{18}\text{N}$  FRAGMENTS MEASURED WITH THE COMBINED  $\beta$ -LMR-NMR METHOD**

NEYENS G., COULIER N., TEUGHELS S., GEORGIEV G., TERNIER S., VYVEY K., COUSSEMENT R., BALABANSKI D.L., *Leuven Univ. - Leuven*  
de OLIVEIRA F., LEWITOWICZ M., MITTIG W., ROUSSEL-CHOMAZ P., *GANIL - Caen*  
ROGERS W.F., *Westmont College - Santa Barbara*  
LEPINE-SZILY A., *Sao Paulo Univ. - Sao Paulo*  
CORTINA GIL M.D., *GSI - Darmstadt* 30

**CHARGE-EXCHANGE REACTION INDUCED BY  $^6\text{He}$**

CORTINA-GIL M.D., ROUSSEL-CHOMAZ P., CASANDJIAN J.M., CHARTIER M., MITTIG W., *GANIL - Caen*  
PAKOU A., ALAMANOS N., AUGER F., FEKOU-YOUMBI V., FERNANDEZ B., GILLIBERT A., LAURENT H., SIDA J.L., *CEA Saclay - Gif sur Yvette*  
BARRETTE J., *Mc Gill Univ. - Montreal*  
BLUMENFELD Y., FRASCARIA N., PASCALON V., SCARPACI J.A., SUOMIJARVI T., *IPN - Orsay*  
LEPINE A., *IFUSP - Sao Paulo*  
ORR N., *LPC ISMRA - Caen* 32



## A2 - EXOTIC NUCLEI AND DECAY MODES

### DECAY SPECTROSCOPY OF NEUTRON RICH NUCLEI

REED A.T., PAGE R.D., ALLATT R.G., NOLAN P.J., *Liverpool Univ. - Liverpool*  
TARASOV O., PENIONZHKEVICH Yu., LUKYANOV S., SOKOL E., *FLNR JINR - Dubna*  
DONZAUD C., GUILLEMAUD-MUELLER D., MUELLER A.C., GREVY S., POUGHEON F., SORLIN O.,  
*IPN - Orsay*  
ANGELIQUE J.C., MARQUES F.M., ORR N.A., *LPC - Caen*  
ANNE R., LEWITOWICZ M., MARTINEZ G., SAINT-LAURENT M.G., TRINDER W., *GANIL - Caen*  
BORCEA C., *IAP - Bucharest*  
BURJAN V., DLOUHY Z., *NPI - Rez*  
CATFORD W.N., REGAN P.H., VINCENT S., *Surrey Univ. - Guildford*  
NOVAK J., SIISKONEN T., SUHONEN J., *Jyvaskylä Univ. - Jyvaskylä* 39

### STUDY OF NEUTRON-RICH NUCLEI NEAR THE N=20 NEUTRON CLOSED SHELL

LUKYANOV S., PENIONZHKEVICH Yu.E., SOKOL E., TARASOV O., *FLNR JINR - Dubna*  
ALLATT R., PAGE R.D., REED A., *Liverpool Univ. - Liverpool*  
ANGELIQUE J.C., ORR N.A., *LPC - Caen*  
ANNE R., LEWITOWICZ M., NOWACKI F., SAINT-LAURENT M.G., TRINDER W., WINFIELD J.S.,  
*GANIL - Caen*  
BORCEA C., *IAP - Bucharest-Magurele*  
DLOUHY Z., *NPI - Rez*  
DONZAUD C., GREVY S., GUILLEMAUD-MUELLER D., MUELLER A.C., POUGHEON F., SCHWAB  
W., *IPN - Orsay* 40

### BETA DECAY HALF-LIVES OF NEUTRON RICH Ti-Co ISOTOPES AROUND N=40

DONZAUD C., SORLIN O., AXELSSON L., BELLEGUIC M., GUILLEMAUD-MUELLER D., LEENHARD  
S., POUGHEON F., *IPN - Orsay*  
DAUGAS J.M., LEWITOWICZ M., LOPEZ M.J., de OLIVEIRA F., SAINT-LAURENT M.G., BORCEA C.,  
*GANIL - Caen*  
BERAUD R., CHABANNAT E., CANCEL G., EMSALLEM A., *IPN - Lyon*  
LONGOUR C., *IReS - Strasbourg*  
SAUVESTRE J.E., *CEA DAM - Bruyères-Le-Château* 42

### BETA-DECAY STUDIES OF THE NEUTRON-RICH ISOTOPES $^{53-55}\text{Sc}$ , $^{54-57}\text{Ti}$ , $^{56-59}\text{V}$ .

SORLIN O., BORREL V., GREVY S., GUILLEMAUD-MUELLER D., MUELLER A.C., POUGHEON F.,  
*IPN - Orsay*  
BÖHMER W., KRATZ K.L., MEHREN T., MÖLLER P., PFEIFFER B., RAUSCHER T., *Mainz Univ. - Mainz*  
SAINT-LAURENT M.G., ANNE R., LEWITOWICZ M., OSTROWSKI A., *GANIL - Caen*  
DÖRFLER T., SCHMIDT-OTT W.D., *Göttingen Univ. - Göttingen* 44

### A MASS MEASUREMENT EXPERIMENT TO INVESTIGATE THE SHELL CLOSURES FAR FROM STABILITY

SARAZIN F., SAVAJOLS H., MITTIG W., ROUSSEL-CHOMAZ P., AUGER G., LALLEMAN A.S.,  
LEWITOWICZ M., de OLIVEIRA F., REN Z., RIDIKAS D., de VISMES A., *GANIL - Caen*  
BAIBORODIN D., DLOUHY Z., *Nucl.Phys.Inst. - Rez*  
BELOZYOROV A.V., LUKYANOV S.M., PENIONZHKEVICH Y.E., *LNR JINR - Dubna*  
BORCEA C., *IAP - Bucharest*  
GILLIBERT A., *CEA Saclay - Gif sur Yvette*  
ORR N., *LPC - Caen*  
SAKURAI H., *RIKEN - Saitama* 46

### OBSERVATION OF THE Z = N+1 NUCLEI $^{77}_{39}\text{Y}$ , $^{79}_{40}\text{Zr}$ , and $^{83}_{42}\text{Mo}$

JANAS Z., BLANK B., CZAJKOWSKI S., FLEURY A., MARCHAND C., PRAVIKOFF M.S., *CENBG -*  
*Gradignan*  
GRZYWACZ R., *Inst. Exp. Phys. Warsaw Univ. - Warsaw*  
CHANDLER C., REGAN P.H., CATFORD W.N., CURTIS N., GELLETLY W., PEARSON C.J., SHEIKH  
J.A., VINCENT S.M., *Dept. Phys. Surrey Univ. - Guildford*  
BRUCE A.M., *Dept. Mechan. Eng. Univ. of Brighton - Brighton*  
DESSAGNE Ph., GIOVINAZZO J., LONGOUR C., MIEHE Ch., *IReS - Strasbourg*  
LEWITOWICZ M., SAINT-LAURENT M.G., WINFIELD J.S., *GANIL - Caen*

ORR N.A., *LPC ISMRA - Caen*  
PAGE R.D., REED A.T., *Oliver Lodge Lab. Univ. of Liverpool - Liverpool*  
WADSWORTH R., *Dept. Phys. Univ. of York - York*  
WARNER D.D., *CCLRC Daresbury Lab. - Warrington*

47

**HALF-LIVES OF HEAVY ODD-ODD N=Z NUCLEI SELECTED WITH THE LISE3 SPECTROMETER**

LONGOUR C., MIEHE Ch., DESSAGNE Ph., *IReS et Univ. Louis Pasteur - Strasbourg*  
GARCES NARRO J., REGAN P.H., CATFORD W.N., CHANDLER C., GELLETLY W., JONES K.L.,  
PEARSON C.J., *Dept. Phys. Univ. of Surrey - Guildford*  
BLANK B., CZAJKOWSKI S., FLEURY A., GIOVINAZZO J., *CENBG - Gradignan*  
LEWITOWICZ M., DAUGAS J.M., *GANIL - Caen*  
APPLEBE D., CULLEN D.M., PAGE R.D., REED A.T., *Oliver Lodge Lab. Univ. of Liverpool - Liverpool*  
AXELSSON L., *Chamers Univ. of Tech. - Göteborg*  
BRUCE A.M., FRANKLAND L., HARDER M., *Dept. Mech. Eng. Univ. of Brighton - Brighton*  
CLARK R.M., *Nucl. Sci. Div. LBNL - Berkeley*  
GREENHALGH B., KELSALL N., WADSWORTH R., *Dept. Phys. Univ. of York - York*  
GRZYWACZ R., KSZCZOT T., *Inst. Exp. Phys. Warsaw Univ. - Warsaw*  
SORLIN O., *IPN - Orsay*

49

**MASS MEASUREMENTS NEAR N=Z AND  $^{100}\text{Sn}$**

CHARTIER M., AUGER G., MITTIG W., CASANDJIAN J.M., CHABERT M., FERME J., LEPINE-SZILY  
A., LEWITOWICZ M., MAC CORMICK M., MOSCATELLO M.H., OSTROWSKI A., SPITAELS C.,  
VILLARI A.C.C., *GANIL - Caen*  
ANGELIQUE J.C., ORR N.A., *LPC ISMRA - Caen*  
AUDI G., *CSNSM - Orsay*  
CUNSOLO A., FOTI A., *INFN - Catania*  
DONZAUD C., STEPHAN C., SUOMIJARVI T., TASSAN-GOT L., *IPN - Orsay*  
LUKYANOV S., *LNR JINR - Dubna*  
MORRISSEY D.J., SHERRILL B.M., *NSCL MSU - Esat Lansing*  
VIEIRA D.J., WOUTERS J.M., *LANL - Los Alamos*  
FIFIELD L.K., *Dept. Nucl. Phys. Austr. Nat. Univ. - Australia*  
GILLIBERT A., *CEN Saclay - Gif sur Yvette*  
POLITI G., *Universita di Catania - Catani*  
ODLAND O.H., *Universitet i Bergen - Bergen*

51

## B - NUCLEAR REACTIONS

### B1 - PERIPHERAL COLLISIONS

#### SOME REGULARITIES IN THE PRODUCTION OF ISOTOPES IN $^{32,34,36}\text{S}$ - INDUCED REACTIONS IN THE ENERGY RANGE 6-75 A MeV

TARASOV O.B., PENIONZHKEVICH Yu.E., BAIBORODIN D.S., BELOZYOROV A.V.,  
KALPAKCHIEVA R., LUKYANOV S.M., MAIDIKOV V.Z., OGANESSIAN Yu.Ts., SKOBELEV N.K.,  
*FLNR JINR - Dubna*

ANNE R., LEWITOWICZ M., SAINT-LAURENT M.G., TRINDER W., *GANIL - Caen*

BORCEA C., *Bucharest-Magurele*

DLOUHY Z., *NPI - Rez*

GUILLEMAUD-MUELLER D., MUELLER A.C., SORLIN O., *IPN - Orsay*

TONEEV V.D., *Bogoliubov Lab. Theor. Phys. JINR - Dubna*

## B2 - DISSIPATIVE COLLISIONS

### THERMAL AND CHEMICAL EQUILIBRIUM FOR VAPORIZING SOURCES

BORDERIE B., RIVET M.F., TASSAN-GOT L., *IPN - Orsay*

GULMINELLI F., *LPC ISMRA et Université - Caen*

61

### ENERGY SHARING IN BINARY COLLISIONS

NALPAS L., BUCHET Ph., CHARVET J.L., DAYRAS R., DORE D., *CEN Saclay - Gif sur Yvette* 63

### CHEMICAL AND KINEMATICAL PROPERTIES OF MID-RAPIDITY EMISSIONS IN Ar+Ni COLLISIONS FROM 52 TO 95 A.MeV.

LEFORT T., DORE D., CUSSOL D., PETER J., *LPC - Caen*

65

### COMPARISON BETWEEN DATA MEASURED BY INDRA AND THE PREDICTION OF THE BNV TRANSPORT MODEL FOR $^{36}\text{Ar} + ^{58}\text{Ni}$ REACTION AT 95 A.MeV

GULMINELLI F., *LPC - Caen*

GALICHET E., GUINET D.C.R., *IPN - Lyon*

67

### NON EQUILIBRIUM EMISSION EFFECTS ON QUASI-PROJECTILE PROPERTIES

DORE D., CHARVET J.L., DAYRAS R., NALPAS L., *CEA Saclay - Gif sur Yvette*

BORDERIE B., RIVET M.F., *IPN - Orsay*

BUCHET Ph., *DAPNIA CEN Saclay - Gif sur Yvette*

70

### EVIDENCE FOR DYNAMICAL PROTON EMISSION IN Xe+Sn COLLISIONS AT 50 MeV/u

GERMAIN M., GOURIO D., EUDES Ph., LAVILLE J.L., ARDOUIN D., ASSENARD M., LAUTRIDOU P.,

LEBRUN C., METIVIER V., RAHMANI A., REPOSEUR T., *SUBATECH - Nantes*

72

### **B3 - MULTIFRAGMENT EMISSION**

- EXPANSION COLLECTIVE ENERGIES AND FREEZE-OUT VOLUME IN THE MULTIFRAGMENTING Xe + Sn SYSTEMS FROM 32 TO 50 A.MeV INCIDENT ENERGIES**  
CHBIHI A., SALOU S., WIELECZKO J.P., *GANIL - Caen*  
FRIEDMAN W.A., *Wisconsin Univ. - Madison* 77
- DYNAMICAL EFFECTS IN PERIPHERAL AND SEMI-CENTRAL COLLISIONS AT INTERMEDIATE ENERGY**  
TIREL O., *GANIL - Caen*  
AICHELIN J., NEBAUER R., *SUBATECH - Nantes* 78
- INDEPENDENCE OF FRAGMENT CHARGE DISTRIBUTIONS OF THE SIZE OF HEAVY MULTIFRAGMENTING SOURCES**  
RIVET M.F., BACRI Ch.O., BORDERIE B., FRANKLAND J.D., SQUALLI M., *IPN - Orsay*  
GUARNERA A., COLONNA M., CHOMAZ P., *GANIL - Caen* 82
- SPACE TIME CHARACTERIZATION OF NUCLEAR MATTER IN FRAGMENTATION PROCESSES**  
NGUYEN A.D., *LPC - Caen* 84
- FRAGMENT EXCITATION ENERGIES IN MULTIFRAGMENTATION**  
CHBIHI A., MARIE N., WIELECZKO J.P., *GANIL - Caen*  
NATOWITZ J.B., *Texas A&M Univ. - College Station* 86
- COLLECTIVE MOTION AND ANGULAR MOMENTUM IN 50 A.MeV Xe+Sn CENTRAL COLLISIONS**  
LE FEVRE A., SCHAPIRO O., WIELECZKO J.P., CHBIHI A., *GANIL - Caen* 87
- MULTIFRAGMENTATION, SCALING LAW AND BINARY DISSIPATIVE COLLISIONS**  
CHARVET J.L., *DAPNIA CEN Saclay - Gif sur Yvette* 89

## **B4 - LIFETIMES OF EXCITED NUCLEI**

### **A STRAIGHTFORWARD MEASUREMENT OF FISSION LIFETIMES BY THE CRYSTAL BLOCKING TECHNIQUE**

CHEVALLIER M., DAUVERGNE D., KIRSCH R., POIZAT J.C., REMILLIEUX J., *IPNL - Villeurbanne*

COHEN C., PREVOT G., SCHMAUS D., *GPS - Paris*

DURAL J., TOULEMONDE M., *CIRIL - Caen*

GALIN J., GOLDENBAUM F., LIENARD E., LOTT B., MORJEAN M., PEGHAIRE A., PERIER Y., *GANIL - Caen*

JACQUET D., *IPN - Orsay*

93

### **COMPOUND NUCLEAR LIFETIMES AT HIGH EXCITATION ENERGIES VIA A NEW STATISTICAL FLUCTUATION METHOD**

CASANDJIAN J.M., MITTIG W., AUGER G., CHARTIER M., CORTINA-GIL D., LEPINE A.,

MACCORMICK M., OSTROWSKI A., ROUSSEL-CHOMAZ P., *GANIL - Caen*

PAKOU A., ALAMANOS N., AUGER F., FEKOU-YOUMBI V., FERNANDEZ B., GILLIBERT A., SIDA

J.L., *CEA Saclay - Gif sur Yvette*

95

## C - MISCELLANEOUS

### **TOURNESOL : A NEW HIGH EFFICIENCY, POSITION SENSITIVE, TIME-OF-FLIGHT SPECTROMETER FOR NEUTRONS**

PEGHAIRE A., GALIN J., LOTT B., PATOIS Y., *GANIL - Caen*  
LIENARD E., *LPC - Caen*

99

### **NEUTRON PRODUCTION IN THICK Pb TARGETS FOLLOWING SPALLATION REACTIONS**

LOTT B., CNIGNIET F., GALIN J., GOLDENBAUM F., LIENARD A., PEGHAIRE A., PERIER Y., QIAN X., *GANIL - Caen*

HILSCHER D., *HMI - Berlin*

101

### **COSMIC RAY INSTRUMENT CALIBRATION (E-285)**

DEL PERAL L., BRONCHALO E., MEDINA J., *Departamento de Fisica Alcala Univ. - Madrid*

SANCHEZ S., CARBAJO M., MEZIAT D., *Departamento de Automatica Alcala Univ. - Madrid*

103

### **ANGULAR DISTRIBUTION OF PROTONS EMITTED FROM ORIENTED NUCLEI : TOWARDS IMAGING SINGLE-PARTICLE WAVE FUNCTIONS**

CARJAN N., TALOU P., *CENBG - Gradignan*

STROTTMAN D., *LANSCE and LANL - Los Alamos*

105

# INTERDISCIPLINARY RESEARCH

## 1 - BASIC COLLISION PROCESSES

### SEARCH FOR RESONANT TRIELECTRONIC RECOMBINATION IN CHANNELING CONDITIONS

CHEVALLIER M., DAUVERGNE D., KIRSCH R., POIZAT J.C., REMILLIEUX J., SANUY F., *IPNL - Villeurbanne*

CHOMAZ P., GANGNAN P., LIBIN J.F., *GANIL - Caen*

COHEN C., L'HOIR A., ROZET J.P., SCHMAUS D., VERNHET D., *GPS Univ. Paris VI et VII - Paris*

CUE N., *The Hong Kong Univ. of Sci. and Tech. - Hong Kong*

DURAL J., LELIEVRE D., RAMILLON J.M., TOULEMONDE M., *CIRIL - Caen*

MOKLER P., PRINZ H.T., WARCZAK A., *GSI - Darmstadt*

STEPHAN C., *IPN - Orsay*

111

### SINGLE AND MULTIPLE EXCITATION PROCESSES IN HEAVY ION-ATOM COLLISIONS AT INTERMEDIATE VELOCITY

ADOUI L., RAMILLON J.M., CASSIMI A., GRANDIN J.P., *CIRIL - Caen*

VERNHET D., ROZET J.P., FOURMENT C., *GPS - Paris*

STEPHAN C., TASSAN-GOT L., *IPN - Orsay*

112

### PRODUCTION AND TRANSPORT OF PROJECTILE EXCITED STATES IN SOLIDS

VERNHET D., ROZET J.P., FOURMENT C., *GPS - Paris*

GERVAIS B., CASSIMI A., RAMILLON J.M., LELIEVRE D., ROTHARD H., LAMOUR E., ADOUI L., GRANDIN J.P., *CIRIL - Caen*

STEPHAN C., TASSAN-GOT L., *IPN - Orsay*

114

### TWO- AND THREE-BODY EFFECTS IN SINGLE IONIZATION OF Li BY 95 MeV/u Ar<sup>18+</sup> PROJECTILES : ANALOGIES WITH PHOTOIONIZATION

STOLTERFOHT N., CHESNEL J.Y., GREYER M., *HMI - Berlin*

SKOGVALL B., *Technische Univ. Berlin - Berlin*

FREMONT F., LECLER D., HENNECART D., HUSSON X., *LSA ISMRA - Caen*

GRANDIN P., *CIRIL - Caen*

SULIK B., GULYAS L., *INR - Debrecen*

TANIS J.A., *Western Michigan Univ. - Michigan*

116

### ELECTRON ANGULAR DISTRIBUTIONS AS A FUNCTION OF MOMENTUM TRANSFER IN DOUBLE IONIZATION OF HELIUM BY 100 MeV/u C<sup>6+</sup> IMPACT

BAPAT B., MOSHAMMER R., KOLLMUS H., ULLRICH J., *Freiburg Univ. - Freiburg*

SCHMITT W., MANN R., *GSI - Darmstadt*

DORNER R., WEBER Th., KHAYYAT K., *Frankfurt Univ. - Frankfurt*

CASSIMI A., ADOUI L., GRANDIN J.P., *CIRIL - Caen*

117

### FAST ELECTRON SPECTRA FROM SWIFT HEAVY ION IMPACT ON SOLIDS

LANZANO G., De FILIPPO E., AIELLO S., GERACI M., PAGANO A., POLITI G., *INFN - Catania*

CAVALLARO S., LOPIANO F., MAHBOUB D., *INFN LNS - Catania*

POLLACCO E.C., VOLANT C., VUILLIER S., *DAPNIA CEN Saclay - Gif sur Yvette*

BECK C., NOUCER R., *IReS and Univ. Louis Pasteur - Strasbourg*

JAKUBASSA-AMUNDSEN D.H., *Munich Univ. - Garching*

ROTHARD H., *CIRIL - Caen*

119

### SOLID STATE EFFECTS IN BINARY ENCOUNTER ELECTRON EMISSION

ROTHARD H., *CIRIL - Caen*

JAKUBASSA-AMUNDSEN D.H., *Munich Univ. - Garching*

BILLEBAUD A., *ISN Univ. Joseph Fourier - Grenoble*

120

### ELECTRON YIELDS AS PROBE OF SWIFT HEAVY ION-SOLID INTERACTION

ROTHARD H., CARON M., GRANDIN J.P., GERSVAIS B., JUNG M., *CIRIL - Caen*



BILLEBAUD A., <i>ISN Univ. Joseph Fourier - Grenoble</i> CLOUVAS A., <i>Aristotelian Univ. - Thessaloniki</i> WÜNSCH R., <i>J.W. Goethe Univ. - Frankfurt</i>	121
<b>ENHANCEMENT OF DIELECTRONIC PROCESSES IN <math>\text{Ne}^{10+} + \text{He}</math> COLLISIONS AT ENERGIES AS LOW AS 1 keV</b>	
CHESNEL J.Y., BEDOUEY C., FREMONT F., HUSSON X., <i>LSA ISMRA - Caen</i> MERABET H., <i>Nevada Univ. - Reno</i> SULIK B., <i>INR of the Hungarian Acad. of Sci. - Debrecen</i> GREYER M., SPIELER A., STOLTERFOHT N., <i>HMI - Berlin</i>	123
<b>SCALING LAWS FOR SINGLE AND DOUBLE ELECTRON CAPTURE IN <math>\text{A}^{q+} + \text{He}</math> COLLISIONS (<math>q \geq Z_A - 2</math>) AT LOW IMPACT VELOCITIES</b>	
FREMONT F., BEDOUEY C., CHESNEL J.Y., HUSSON X., <i>LSA ISMRA - Caen</i>	124
<b>INVESTIGATION OF CHARGE EXCHANGE REACTIONS AT LOW ENERGY BY RECOIL ION MOMENTUM SPECTROSCOPY</b>	
FLECHARD X., LEPOUTRE A., HENNECART D., <i>LSA ISMRA - Caen</i> DUPONCHEL S., ADOUI L., CASSIMI A., <i>CIRIL - Caen</i> RONCIN P., <i>LCAM Univ. Paris Sud - Orsay</i> OLSON R.E., <i>Missouri-Rolla Univ. - Missouri</i>	125
<b><math>(n, l, m_l)</math> SELECTIVITY OF THE SINGLE ELECTRON CAPTURE FOR LOW ENERGY <math>\text{X}^{8+} (\text{X} \equiv \text{Ar}, \text{Kr}, \text{O}) - \text{Li}(2s)</math> COLLISIONS</b>	
BODUCH P., CHANTEPIE M., CREMER G., JACQUET E., LAULHE C., LECLER D., <i>LSA ISMRA - Caen</i> PASCALE J., <i>CEN Saclay - Gif sur Yvette</i> DRUETTA M., <i>Lab. du traitement du signal - Saint Etienne</i> WILSON M., <i>Royal Holloway Univ. of London - Surrey</i>	126
<b>FAST ION-INDUCED MOLECULE FRAGMENTATION</b>	
CARABY C., CASSIMI A., ADOUI L., GRANDIN J.P., LELIEVRE D., <i>CIRIL - Caen</i> DUBOIS A., <i>Pierre et Marie Curie Univ. - Paris</i>	127

## 2 - SWIFT HEAVY ION INDUCED MODIFICATION IN MATERIALS

### TEMPERATURE DEPENDANCE OF DAMAGE CREATION IN BISMUTH BY SWIFT HEAVY IONS

DUFOUR Ch., PAUMIER E., *LERMAT-ISMRA - Caen*

BENEU F., *LSI Ecole Polytechnique - Palaiseau*

TOULEMONDE M., *CIRIL - Caen*

131

### ELECTRONIC STOPPING POWER THRESHOLD OF SPUTTERING IN YTTRIUM IRON GARNET : COMPARISON TO THE LATENT TRACK APPEARANCE

MEFTAH A., *ENSET - Skikda*

DJEBARA M., *USTHB - Alger*

STOQUERT J.P., *Lab. PHASE - Strasbourg*

STUDER F., *CRISMAT ISMRA - Caen*

TOULEMONDE M., *CIRIL - Caen*

133

### ANGULAR DISTRIBUTION OF NEUTRAL ATOMS SPUTTERED BY HEAVY ION BOMBARDMENT

SCHLUTIG S., BOUFFARD S., *CIRIL - Caen*

DURAUD J.P., MOSBAH M., *LPS CEA Saclay - Gif sur Yvette*

134

### EFFECT OF THE ENERGY DENSITY NEAR THE ION PATH ON THE TRACK FORMATION IN MICA

BOUFFARD S., LEROY C., *CIRIL - Caen*

COSTANTINI J.M., *CEA Bruyères Le Châtel - Bruyères Le Châtel*

135

### MODIFICATIONS INDUCED BY SWIFT HEAVY ION IRRADIATIONS IN METALLIC OXIDE POWDERS ( $Y_2O_3$ AND Sn O<sub>2</sub>)

HEMON S., LEVESQUE F., *CIRIL - Caen*

BERTHELOT A., DUFOUR C., GOURBILLEAU F., PAUMIER E., *LERMAT ISMRA - Caen*

DOORYHEE E., *ESRF - Grenoble*

136

### SWELLING OF INSULATORS UNDER ION IRRADIATION

TOULEMONDE M., *CIRIL - Caen*

COSTANTINI J.M., *CEA Bruyères le Châtel - Bruyères Le Châtel*

MEFTAH A., *ENSET - Skikda*

STOQUERT J.P., *Lab. PHASE - Strasbourg*

SCHWARTZ K., TRAUTMANN C., *GSI - Darmstadt*

137

### DAMAGE MORPHOLOGY OF ION IRRADIATED LITHIUM FLUORIDE

TRAUTMANN C., SCHWARTZ K., STECKENREITER T., *GSI - Darmstadt*

TOULEMONDE M., *CIRIL - Caen*

139

### STRUCTURAL AND MAGNETIC MODIFICATION INDUCED BY HEAVY IONS IRRADIATION IN Fe-R-B AMORPHOUS ALLOYS

RAVACH G., FNIDIKI A., TEILLET J., *Rouen Univ. - Mont Saint-Aignan*

TOULEMONDE M., *CIRIL - Caen*

140

### ION IRRADIATION EFFECTS ON bcc-Fe/Tb MULTILAYERS

JURASZEK J., FNIDIKI A., TEILLET J., *Rouen Univ. - Mont-Saint-Aignan*

RICHOMME F., TOULEMONDE M., *CIRIL - Caen*

141

### SWIFT HEAVY ION EFFECTS IN POLYMERS

BETZ N., LE BOUEDEC A., ESNOUF S., AYMES-CHODUR C., DAPOZ S., PETERSOHN E., SCHLOSSER

D., LE MOEL A., *CEA Saclay - Gif sur Yvette*

142

### CROSS-LINKING INDUCED BY HIGH DENSITY OF IONISATION OF POLYSTYRENE

BOUFFARD S., LEROY C., BALANZAT E., *CIRIL - Caen*

BUSNEL J.P., *Lab. de Physico-Chimie Macromoléculaire - Le Mans*

144

### ION INDUCED ALKYNE FORMATION IN POLYMERS

STECKENREITER T., FUJESS H., *TU-Darmstadt - Darmstadt*

BALANZAT E., *CIRIL - Caen*

**"POLYMER-LIKE" AMORPHOUS DEUTERATED CARBON FILMS IRRADIATED BY SWIFT  
HEAVY IONS : DAMAGE AND HYDROGEN PUMPING**

PAWLAK F., TOULEMONDE M., *CIRIL - Caen*

DUFOUR Ch., PAUMIER E., *LERMAT ISMRA - Caen*

LAURENT A., PERRIERE J., *GPS Univ. Paris VII et VI - Paris*

STOQUERT J.P., *Lab. PHASE - Strasbourg*

### 3 - RADIATION CHEMISTRY AND RADIOBIOLOGY

#### **DIRECT TIME-RESOLVED MEASUREMENT OF RADICAL SPECIES FORMED IN WATER BY HEAVY IONS IRRADIATION**

BALDACCHINO G., HICKEL B., *CEA Saclay - Gif sur Yvette*

BOUFFARD S., BALANZAT E., *CIRIL - Caen*

GARDES-ALBERT M., ABEDINZADEH Z., JORE D., *Lab. de Chimie-Physique - Paris*

DEYCARD S., *Faculté de Pharmacie - Caen*

151

#### **RADIATION YIELDS OF THE FREE RADICALS FORMED BY HEAVY IONS WATER RADIOLYSIS**

GARDES-ALBERT M., JORE D., ABEDINZADEH Z., ROUSCILLES A., *Lab. de Chimie-Physique - Paris*

DEYCARD S., *Faculté de Pharmacie - Caen*

BOUFFARD S., BALANZAT E., *CIRIL - Caen*

152

#### **DNA DAMAGE INDUCED IN PLASMID DNA BY HEAVY IONS AND MUTAGENIC CONSEQUENCES**

SAGE E., GIUSTRANTI C., PEREZ C., ROUSSET S., *Institut Curie - Paris*

BALANZAT E., *CIRIL - Caen*

153

#### 4 - PHYSICS AND CHEMISTRY WITH TRACKS

##### **SWIFT HEAVY ION RADIATION GRAFTING OF POLYMERS / OBTENTION OF HAEMOCOMPATIBLE SURFACES**

AYMES-CHODUR C., DAPOZ S., BETZ N., LE MOËL A., *CEA Saclay - Gif sur Yvette*  
PORTE-DURRIEU M.C., BAQUEY C., *INSERM Univ. Victor Segalen-Bordeaux - Bordeaux* 157

##### **SIMULATION DES DOMMAGES DE FISSION DANS LES MATERIAUX ENVISAGES POUR LA TRANSMUTATION DES ACTINIDES MINEURS**

MATZKE H., WISS T., *Joint Research Centre - Karlsruhe*  
BEAUVY M., *CEA Cadarache - Saint Paul-lez-Durance* 159

##### **A COMPARATIVE STUDY OF THE IRRADIATION EFFECTS IN HIGH RESISTIVITY SILICON USED IN THE SEMICONDUCTOR DETECTORS MANUFACTURING**

MANGIAGALLI P., LEVALOIS M., MARIE P., *LERMAT ISMRA - Caen* 161

##### **VORTEX PINNING BY COLUMNAR DEFECTS IN HIGH- $T_c$ SUPERCONDUCTORS**

HARDY V., HEBERT S., WARMONT F., SIMON Ch., PROVOST J., HERVIEU M., VILLARD G., *CRISMAT ISMRA - Caen*  
LEJAY P., *CRTBT - Grenoble* 162

**A-C) - NUCLEAR PHYSICS**

# **A - NUCLEAR STRUCTURE**

## **A1 - NUCLEAR SPECTROSCOPY**



## TWO-NEUTRON CORRELATIONS AT SMALL RELATIVE MOMENTA IN $^{86}\text{Kr} + ^{165}\text{Ho}$ AND $^{40}\text{Ar} + ^{197}\text{Au}$ REACTIONS AT 60 MeV/u

J.Pluta<sup>1</sup>, G.Bizard<sup>2</sup>, P.Desesquelles<sup>3</sup>, O.Dorvaux<sup>4</sup>, D.Durand<sup>2</sup>, B.Erasmus<sup>5</sup>, F.Hanappe<sup>6</sup>,  
B.Jakobsson<sup>7</sup>, C.Lebrun<sup>5</sup>, F.R.Lecolley<sup>2</sup>, R.Lednicky<sup>8</sup>, P.Leszczynski<sup>1</sup>, K.Mikhailov<sup>9</sup>,  
B.Noren<sup>7</sup>, T.Pawlak<sup>1</sup>, M.Przewlocki<sup>1</sup>, Ö.Skeppstedt<sup>10</sup>, A.Stavinsky<sup>9</sup>, L.Stuttgé<sup>4</sup>, B.Tamain<sup>2</sup>

<sup>1</sup>Warsaw Univ. of Technology, Poland; <sup>2</sup>LPC, Caen, France; <sup>3</sup>ISN, Univ. J.Fourier, Grenoble, France; <sup>4</sup>IReS, Univ. L.Pasteur, Strasbourg, France; <sup>5</sup>SUBATECH, Nantes, France; <sup>6</sup>ULB, Bruxelles, Belgium; <sup>7</sup>Univ. of Lund, Sweden; <sup>8</sup>Czech Ac. of Sc., Prague, Czech Rep.; <sup>9</sup>ITEP, Moscow, Russia; <sup>10</sup>Chalmers Univ. of Techn., Göteborg, Sweden

Correlations between particles emitted with small relative velocities are widely used to study the space-time properties of the emission process in lepton, hadron and heavy-ion collisions[1]. Charged particle correlations are affected by the long range Coulomb forces from the emitting source or from other fragments of nuclear disintegration rendering ambiguous the interpretation of the results. Two-neutron correlations are free of it. Despite this favorable property the data on neutron-neutron correlations are very scarce. The cross-talk effects in the detection of neutrons in coincidence usually preclude the measurement of two-neutron correlation in the region of small relative momenta.

In the frame of the GANIL E236[2] and E240[3] experiments performed with the neutron detector DEMON, the two-neutron correlations were measured by looking at a cluster of 12 detectors installed at three different distances from the target. The cross-talk effects in the two-neutron correlations were eliminated using the combination of geometrical and kinematical relations[4]. The cluster for correlation measurements was placed at the mean angle about 50 degrees with respect to the beam axis.

The dependences of the experimental two-neutron correlation functions on  $k^*$ , half of momentum difference in the rest system of two-neutron pair, are presented in the Fig.1. The data are for two different reactions:  $^{86}\text{Kr} + ^{165}\text{Ho}$  (E236 experiment) and  $^{40}\text{Ar} + ^{197}\text{Au}$  (E240 experiment). The incident energy per nucleon, 60 MeV/u, was the same in both experiments and geometrical configurations of detectors were identical. The results are presented together for comparison.

The left hand part of the figure shows the correlation functions for neutrons with laboratory kinetic energies greater than 3MeV; the right hand part is for neutron energies greater than 10 MeV. In the first case the forms of correlation functions are the same for both reactions; in the second case, a clear difference appears. Note that higher correlation effect corresponds, in general, to smaller space-time intervals between the emission of particles.

The detected neutrons come from different sources and their origin can be related to the neutron energies. Low energies correspond predominately to the target fragmentation, mid-rapidity region is mostly populated by the promptly emitted particles from the compact system formed at the early stage of the collision, the highest energies can be attributed to the projectile disintegration.

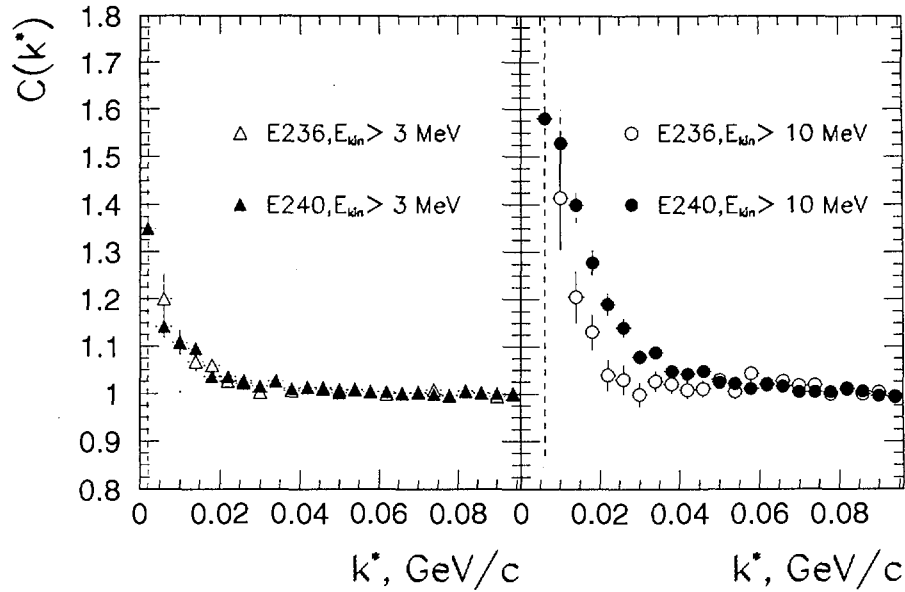


Fig.1 Neutron-neutron correlation functions for different reactions and different minimal neutron energies; see text for details.

The tendencies seen in the figures are in qualitative agreement with this expectation. Low energy neutrons seem to be emitted from the sources of similar space-time properties in both reactions. The prompt stage of the collision process shows different behavior in the space and time for the two reactions studied.

It should be noted here[1] that the form of correlation function is also very sensitive to the details of the reaction dynamics and thus, the two-particle correlations in the region of small relative velocities can be used as a tool to verify the validity of dynamical models. The works on comparison of the experimental data presented here with several dynamical descriptions are in progress.

## References

- [1] B.Erazmus et al., Nuclear Interferometry from Low Energy to Ultra-Relativistic Nucleus-Nucleus Collisions, Proc. of the Winter Meeting on Nuclear Physics, Bormio, Italy (1996)
- [2] O.Dorvaux et al., 8-th Int. Conf. on Nuclear Reaction Mechanisms, Varenna, Italy, June 9-12, (1997)
- [3] F.R.Lecolley et al., Nucl.Phys. A620, 327 (1997),
- [4] J.Pluta et al., Rapport.Int. SUBATECH 97-28, (Nucl.Instr. Meth.A, in print).

# ELASTIC AND INELASTIC PROTON SCATTERING ON THE UNSTABLE $^{20}\text{O}$ NUCLEUS MEASURED WITH THE "MUST" DETECTOR ARRAY

E. Khan<sup>a)</sup>, Y. Blumenfeld<sup>a)</sup>, T. Suomijärvi<sup>a)</sup>, N. Alamanos<sup>b)</sup>, F. Auger<sup>b)</sup>, N. Frascaria<sup>a)</sup>, A. Gillibert<sup>b)</sup>, T. Glasmacher<sup>c)</sup>, M. Godwin<sup>a)</sup>, V. Lapoux<sup>b)</sup>, I. Lhenry<sup>a)</sup>, F. Maréchal<sup>a)</sup>, D.J. Morissey<sup>c)</sup>, A. Musumara<sup>b)</sup>, N. Orr<sup>d)</sup>, S. Ottini<sup>b)</sup>, P. Piattelli<sup>e)</sup>, E.C. Pollacco<sup>b)</sup>, P. Roussel-Chomaz<sup>f)</sup>, J.C. Roynette<sup>a)</sup>, D. Santonocito<sup>a)</sup>, J.E. Sauvestre<sup>g)</sup>, and J.A. Scarpaci<sup>a)</sup>

- a) Institut de Physique Nucléaire, IN<sub>2</sub>P<sub>3</sub>-CNRS, 91406 Orsay, France*  
*b) SPhN, DAPNIA, CEA Saclay, 91191 Gif sur Yvette Cedex, France*  
*c) NSCL, Michigan State University, East Lansing, Mi 48824, USA*  
*d) LPC, IN<sub>2</sub>P<sub>3</sub>-CNRS, Bd. Maréchal Juin, 14050 Caen Cedex, France*  
*e) INFN-Laboratorio Nazionale del Sud, Via S. Sofia 44, Catania, Italy*  
*f) GANIL, BP 5027, 14021 Caen Cedex, France*  
*g) DPTA/SPN-CEA Bruyères, 91680 Bruyères-le-Châtel Cedex 12, France*

## Abstract.

A 43 MeV/nucleon  $^{20}\text{O}$  secondary beam obtained by using the SISSI solenoid at GANIL was scattered on a  $\text{CH}_2$  target. The angle and energy of the recoiling protons were measured with the MUST Silicon-strip array yielding an excitation energy spectrum and angular distributions for elastic and inelastic proton scattering. For comparison, data was also measured for the  $^{18}\text{O}$  stable isotope.

## INTRODUCTION

The availability of radioactive nuclear beams with reasonable intensity and optical quality furnishes the tantalizing opportunity to study direct nuclear reactions, such as elastic and inelastic scattering and transfer reactions, induced by unstable nuclei on light particles. Such reactions are performed in inverse kinematics, where the radioactive nucleus of interest bombards a target containing the light particles. An efficient method to gain access to the excitation energy and scattering angle characterizing the reaction is to measure the energy and angle of the recoiling particle. Experiments of this type, concerning elastic and inelastic proton scattering, have already been performed at RIKEN [1] and the NSCL/MSU [2]. To perform such studies at GANIL, a silicon-strip array named MUST was recently constructed by the collaboration between IPN-Orsay, CEA Bruyères-le-Châtel and CEA Saclay. In the following we will report on the preliminary results obtained for the  $^{20}\text{O}(p,p')$  experiment performed at GANIL by using the MUST array.

## EXPERIMENTAL SETUP AND PRELIMINARY RESULTS

A subject of current interest is the evolution of density and transition density distributions for nuclei far from stability. The measurement of the angular distributions of elastic and inelastic proton scattering allows us to test theoretical predictions of these quantities through microscopic folding model analyses. As a first experiment with the MUST detector, we have measured at GANIL  $^{20}\text{O}(p,p')$  angular distributions of elastic scattering and inelastic scattering towards the first collective  $2^+$  and  $3^-$  states.  $^{18}\text{O}$  scattering was also measured for comparison. The secondary beams, produced by fragmentation of a 77 MeV/u  $^{40}\text{Ar}$  beam and re-focused with the SISSI solenoid, impinged on a  $2\text{mg}/\text{cm}^2$   $\text{CH}_2$  target. The  $^{20}\text{O}$  beam had an intensity of approximately  $5 \times 10^3$  pps and was 98% pure. The energy of the secondary beam was 43 MeV/nucleon. The  $^{18}\text{O}$  beam, also produced by fragmentation, had the same energy as  $^{20}\text{O}$  and an intensity of  $3 \times 10^4$  pps.

The angle and energy of recoiling protons were measured by the MUST array [3-5]. The array is composed of 8 telescopes consisting of 300  $\mu\text{m}$  silicon strip detector with 60 vertical and 60 horizontal strips of 1 mm wide, backed by a 3 mm Si(Li) detector and a 15 mm CsI detector, read out by a photodiode allowing us to measure protons up to 70 MeV. In this first experiment only 4 telescopes were available. The telescopes were placed at 20 cm from the target and covered laboratory angles from  $54^\circ$  to  $82^\circ$ . This setup yielded a recoil angle measurement with an accuracy of  $0.3^\circ$ . Low energy particles which stopped in the strip detector were identified by an energy and a time of flight measurement and higher energy particles by the  $\Delta E$ -E method. The time resolution of the strip detector was better than 1 ns.

Two low pressure multi-wire proportional chambers [5] were used for beam tracking and one of them furnished the start signal for the time of flight measurement. The scattered projectiles were detected in the SPEG spectrometer in coincidence with recoiling light particles.

Fig.1 displays elastic angular distributions measured for  $^{18}\text{O}$  and  $^{20}\text{O}$ . The solid lines correspond to coupled channel predictions using the ECIS code [6]. The optical potential was obtained from the Becchetti-Greenlees parameterization [7] developed for proton scattering on medium heavy nuclei. A remarkably good agreement is observed between the calculation and the data for both nuclei. It is noted that no arbitrary normalization is involved here.

## CONCLUSIONS

The use of Silicon-strip arrays is a powerful method to obtain high resolution light particle scattering data for unstable nuclei. Proton scattering on  $^{20}\text{O}$  and  $^{18}\text{O}$  was recently studied at GANIL by using the MUST array. Preliminary results show that elastic scattering angular distributions are in good agreement with coupled channels

calculations using macroscopic optical potentials. A microscopic analysis, which will be undertaken in the near future, should give information on the differences of the density profiles between  $^{20}\text{O}$  and  $^{18}\text{O}$ . Moreover, the inelastic scattering data will yield transition strengths for the first  $2^+$  and  $3^-$  states and comparison of these values with microscopic calculations should give information on the structure of the  $^{20}\text{O}$  nucleus.

Apart from the  $^{20}\text{O}(p,p')$  experiment described above, measurements of proton scattering on  $^6\text{He}$ ,  $^{30}\text{S}$  and  $^{34}\text{Ar}$  have recently been performed at GANIL. The versatility of the MUST array will allow studies of transfer reactions and 2-proton decay when the SPIRAL facility comes on-line in the near future.

## REFERENCES

1. Korshennikov, A.A., et al. *Phys. Rev. Lett.* 78 (1997) 2317.
2. J.H. Kelley et al., *Phys. Rev.* 56 (1997) R1206.
3. Y. Blumenfeld et al., *Nucl. Instr. and Meth. in Phys. Research A*, to be published.
4. F. Maréchal, *PhD Thesis, Orsay* (1998).
5. Ottini, S. *PhD thesis, CEA Saclay, internal report Dapnia/SPhN 98-01-T* (1998).
6. J. Raynal, *Phys. Rev. C* 23 (1981) 2571.
7. F.D. Becchetti and G.W. Greenlees, *Phys. Rev.* 182 (1969) 1190.

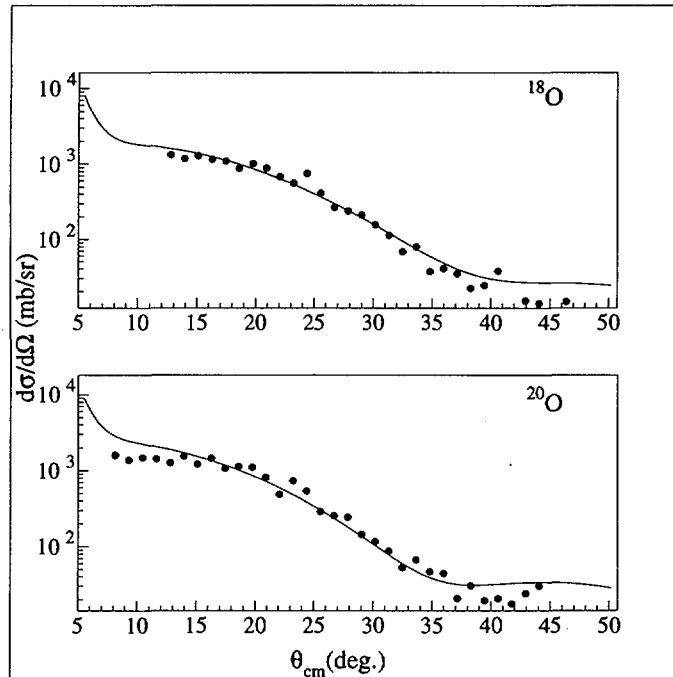


FIGURE 1. Angular distributions for the  $^{18}\text{O}(p,p)$  and  $^{20}\text{O}$  reactions at 43 MeV/nucleon. Solid lines correspond to calculated angular distributions using the ECIS code.

## Anomalous E1 and E2 Strengths in $^{40}\text{Ca}$ and $^{48}\text{Ca}$ at low excitation energy : A Comparative Study

S. Ottini-Hustache<sup>(1,\*)</sup>, N. Alamanos<sup>(1)</sup>, F. Auger<sup>(1)</sup>, B. Castel<sup>(2)</sup>, Y. Blumenfeld<sup>(3)</sup>, V. Chiste<sup>(1)</sup>, N. Frascaria<sup>(3)</sup>,  
A. Gillibert<sup>(1)</sup>, C. Jouanne<sup>(3)</sup>, V. Lapoux<sup>(1)</sup>, F. Marie<sup>(1)</sup>, W. Mittig<sup>(4)</sup>, J.C. Roynette<sup>(3)</sup>, J.A. Scarpaci<sup>(3)</sup>

(1) : CEA DSM/DAPNIA/SPhN, CE Saclay, 91191 Gif sur Yvette Cedex, France

(2) : Dept. of Physics, Queen's University, Kingston, Canada.

(3) : IPN Orsay, IN2P3 - CNRS, 91406 Orsay Cedex, France

(4) : GANIL, B.P. 5027, 14076 Caen Cedex 5, France

Can the addition of neutrons modify the structure of nuclear isotopes to the point of affecting their Giant Resonances ? This is a particularly important question in light of the current general interest generated by neutron halo nuclei in which low energy resonances are expected. We present here the results of an experimental comparative study of the  $^{40,48}\text{Ca}$  resonance spectra between 6 and 12 MeV. The power of the heavy ion reaction  $^{40,48}\text{Ca}(^{86}\text{Kr}, ^{86}\text{Kr}')^{40,48}\text{Ca}^*$  at 60 MeV per nucleon was exploited to enhance greatly the low energy part of inclusive spectra in order to look for the possible presence of a low energy dipole mode in  $^{48}\text{Ca}$  due to a neutron skin. We did not observe any difference in the  $l = 1$  channel and therefore found no evidence of this mode. In the  $l = 2$  channel, an important excess of strength was observed in  $^{40}\text{Ca}$  compared to  $^{48}\text{Ca}$ . These results challenge traditional RPA descriptions of dipole and quadrupole resonances and suggest that a refinement of our theoretical understanding of giant resonances is necessary to explain the data.

To what extent does the addition of eight neutrons modify the structure of  $^{48}\text{Ca}$  compared to the doubly magic  $^{40}\text{Ca}$  ? Are these modifications, if any, likely to affect also the collective observables like giant resonances ? These are important questions in nuclear structure especially in light of the current interest generated by neutron halo low energy vibration modes expected to occur in unstable neutron-rich nuclei. In  $^{48}\text{Ca}$ , the precursor of such phenomena could be seen as an out-of-phase oscillation of the  $f_{7/2}$  neutrons against the  $N=Z=20$  core. This would manifest itself as a decoupling of the E1 strength from the GDR and appear as a small low energy  $l = 1$  resonance. Several years ago, Harvey and Khanna studied the occurrence of enhanced low energy resonances in  $^{208}\text{Pb}$  and showed that their strength and position would be sensitive markers of the parameters of the nuclear force [1]. More recently, Chambers et al. [2] used the RPA in the density functional method to predict the occurrence in neutron rich calcium isotopes of a "soft" E1 resonance. The calculated transition density shows the onset of such a "soft" E1 mode whose strength would increase linearly with neutron number, its largest signal standing at around 8 MeV in  $^{48}\text{Ca}$  and exhausting about 5% of the E1 EWSR. Since all RPA calculations predicted the onset of the GDR to be seen well above 15 MeV in both isotopes, the position and strength of the weaker E1 resonance in  $^{48}\text{Ca}$  should be visible in a comparison of  $l = 1$  spectra of  $^{40}\text{Ca}$  and  $^{48}\text{Ca}$  since it should not appear in the  $^{40}\text{Ca}$  spectrum.

A similar comparison in the  $l = 2$  channel is also very interesting. Indeed, experimental results for  $^{40}\text{Ca}$  are scattered : measured strengths of the GQR mainly stand around 50% of the EWSR but can vary up to 80% ([3-7]). This is anyway low compared to conventional RPA calculations which predict that this resonance exhausts almost 100% of the EWSR, with the same structure in both  $^{40}\text{Ca}$  and  $^{48}\text{Ca}$  with a centroid at  $E=16$  MeV and half-width of about 5 MeV (there is thus no theoretical basis to expect the occurrence of such a large spreading width in calcium). Recently, Kamerdzhiiev et al. [8] have suggested that effects beyond RPA, like ground state correlations induced by particle-hole -phonon coupling would redistribute some of the E2 strength to lower energy and produce a splitting of the familiar GQR. In  $^{48}\text{Ca}$  one would expect ground state correlations to be of a different nature than in  $^{40}\text{Ca}$ , leading there to a different distribution of quadrupole strength.

Thus, in both  $l = 1$  and  $l = 2$  channels, a comparative study of the  $^{40}\text{Ca}$  -  $^{48}\text{Ca}$  spectra is likely to yield interesting insight in the structure of giant resonances and their low energy manifestations. It is the purpose of this Letter to present results of such an investigation.

Heavy ion inelastic scattering is a very efficient tool to investigate low excitation energy states. Indeed, the strong Coulomb excitation provided by a high energy and high Z projectile *results in an enhancement of the very low energy part of the excitation cross section* [9,10]. For instance, for E1 transitions the differential cross section can be written as :

$$\frac{d^2\sigma}{d\Omega dE} = \left( \frac{d^2\sigma}{d\Omega dB(E1)} \right)_E b_{E1}(E) \uparrow$$

where  $(d^2\sigma/d\Omega dB(E1))_E$  is the DWBA cross section evaluated at excitation energy E for unit excitation strength,

$B(E1) \uparrow = 1e^2 fm^2$ . This cross section represents the pure Coulomb excitation generated by the colliding nuclei for uniform transition strength. The nuclear response to this solicitation is introduced via  $b_{E1}(E) \uparrow = dB(E1) \uparrow / dE$ , the distribution of E1 reduced matrix element per unit energy, which can be related to the photonuclear cross section  $\sigma_\gamma(E)$  by :

$$b_{E1}(E) \uparrow = \frac{9\hbar c}{16\pi^3} \frac{\sigma_\gamma(E)}{E}$$

The Coulomb excitation probability is a decreasing exponential function of excitation energy. As an example, the effect of the combination of the photoabsorption spectrum and the Coulomb excitation probability is shown in figure 1 in the case of  $^{84}\text{Kr} + ^{48}\text{Ca}$  inelastic scattering. The left part shows the results of Chambers et al. [2] for the photonuclear cross section in  $^{48}\text{Ca}$ . The broad resonance around 8 MeV is the "soft" E1 resonance mentioned above, exhausting about 5% of the EWSR. The right part is a calculation using these results combined with the formalism described above, for the  $^{84}\text{Kr}(^{48}\text{Ca}, ^{48}\text{Ca}^*)^{84}\text{Kr}$  reaction at 60 MeV/nucleon at an angle of 2.2 degrees in the center of mass frame. The results are striking in that one observes that the photoabsorption spectrum is greatly distorted by the diffusion with krypton, the low energy part of the spectrum being "amplified" with respect to the high energy side. The cross section of the "soft" resonance becomes even more important than the usual GDR's one, centered around 19 MeV. This demonstrates the power of the inelastic scattering of heavy ions for the study of low excitation energy transitions, such as the soft E1 resonance.

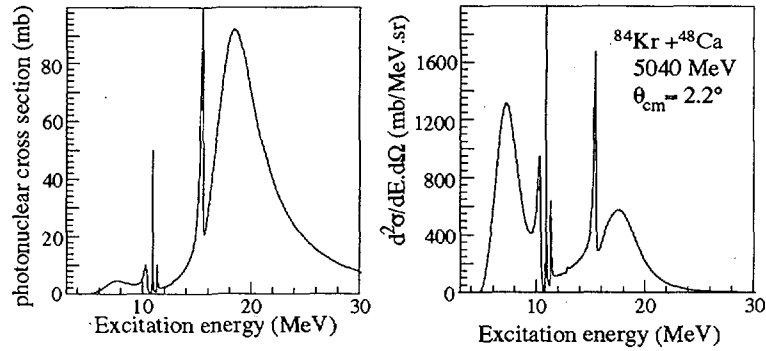


FIG. 1. Comparison between a photoabsorption spectrum calculated by Chambers et al. [2] (left side) and a calculation using these results combined with the Coulomb excitation for the reaction  $^{84}\text{Kr}(^{48}\text{Ca}, ^{48}\text{Ca}^*)^{84}\text{Kr}$  at 60 MeV per nucleon (right side) at an angle of 2.2 degrees in the center of mass frame.

Therefore, we have performed an experiment at GANIL, with a  $^{86}\text{Kr}$  beam at 60 MeV/nucleon impinging on two thin (about  $0.5 \text{ mg/cm}^2$ ) targets of  $^{40}\text{Ca}$  and  $^{48}\text{Ca}$ . The targets were fabricated, transported and installed in the scattering chamber under vacuum, to avoid any oxydization. There was no detectable impurity. The scattered  $^{86}\text{Kr}$ , in the charge state  $35^+$ , were detected and identified in the high resolution spectrometer SPEG, in which their scattering angle and energy were measured with an accuracy of 0.2 degree and 1.4 MeV ( $\Delta E/E = 2.7 \cdot 10^{-4}$ ) respectively. The spectrometer was centered at 2.2 degrees in the laboratory frame, covering an angular range from 0.3 to 4.2 degrees. The elastic and low energy inelastic scattering were partly suppressed by insertion of movable absorbers before the focal plane. The excitation energy was measured from about 5 MeV as can be seen on figure 2, and up to several hundreds of MeV. Due to the energy resolution, the low excitation energy transitions are superimposed on a strong tail of the elastic scattering which is highly probable. The spectra shown here are not normalized since the targets' thicknesses were not known precisely and the charge state distribution of the outgoing  $^{86}\text{Kr}$  was not measured. Therefore, the absolute normalization of the data was obtained using GDR and GQR results of ref. [5] for the excitation energy between 13 and 25 MeV. We have subtracted a constant background (following the results obtained in [7]) whose angular distribution was assumed to be similar to the angular distribution of the energy region located immediately above the giant resonances region. The consistency of this normalization method was verified with elastic scattering for the  $^{40}\text{Ca}$  target, indicating that the strengths measured in [5] are correct within experimental errors. The uncertainty on the absolute normalization is more important for  $^{48}\text{Ca}$ , for which data in ref. [5] are less precise ( $89 \pm 27\%$  for  $^{48}\text{Ca}$  compared to  $86 \pm 11\%$  for  $^{40}\text{Ca}$  for the giant quadrupole resonance).

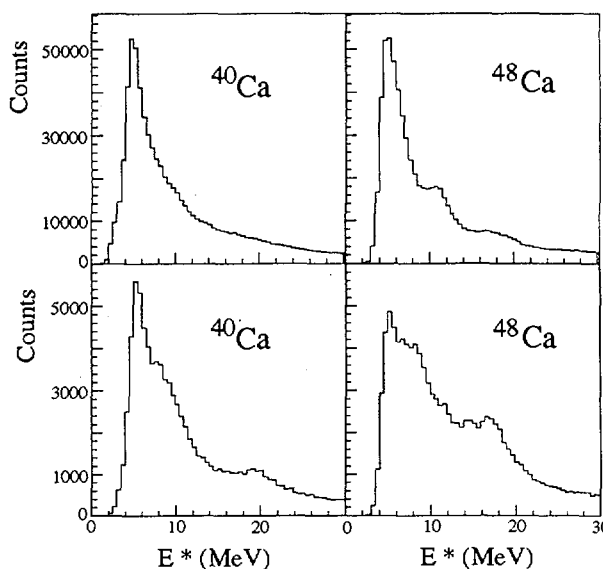


FIG. 2. Excitation energy spectra obtained with  $^{40}\text{Ca}$  (left side) and  $^{48}\text{Ca}$  (right side) targets, for  $0.85 \text{ deg} < \theta_{cm} \leq 1.15 \text{ deg}$  (upper part) and  $2.05 \text{ deg} < \theta_{cm} \leq 2.35 \text{ deg}$  (lower part) where dipole transitions dominate. The spectra binning is 500 keV.

Using these data, we have extracted the E1 and E2 transition strengths for both targets and for different bins in excitation energy. Since we cannot distinguish between target and projectile excitations, the strengths determined here concern the whole system. But  $^{86}\text{Kr}$  excitations show up in the same way with both targets, allowing us to make a comparative study of the calcium isotopes. A typical example is shown in figures 3 and 4. The cross section is plotted as a function of scattering angle in the center of mass system for an excitation energy between 6 and 8 MeV for both targets. Since we consider all kind of transitions, collective and single particle ones, and we make a comparative study of both targets, no background was subtracted. The grey area around the data corresponds to the uncertainty on the absolute global normalization factor applied to each point of the angular distribution. The data are fitted with calculations performed with ECIS, in the framework of coupled channels equations [11], using E1 and higher multipolarity electric transitions. These higher multipolarity transitions nevertheless should be dominated by  $l=2$  ones and therefore we performed the calculations with quadrupolar transition strength only. It should be noted that any small contribution of higher multipolarity would strongly decrease the strength attributed here to quadrupolar transitions. One can see that the behaviors of the two contributions with scattering angle are very different, allowing to determine the only combination of  $l=1$  and  $l=2$  cross sections reproducing the data. The relative contribution of each kind of transitions is therefore well determined. The uncertainty on the normalization factor, by far dominating other sources of error (particularly the multipolarity decomposition error), defines the precision on the absolute strength extracted for  $l=1$  and  $l=2$ .

The calculations are indeed very close to the experimental values for angles larger than 2.2 degrees. The discrepancy at lower angles comes from the elastic and inelastic to low lying states scattering tail which are not taken into account in the calculations. The contribution of these processes is very difficult to evaluate on account of the many low energy excited states of both targets and projectile. From 2.2 degrees, the contribution of elastic scattering is not dominating anymore, as can be seen on figure 2.

The E1 and E2 strengths extracted are summarized in table I. Note that calculations have been done assuming  $l=1$  and  $l=2$  excitations of the calcium targets only. For  $^{40}\text{Ca}$  target and for  $8 \text{ MeV} < E^* < 10 \text{ MeV}$  and  $10 \text{ MeV} < E^* < 12 \text{ MeV}$ , we have introduced 5% of EWSR for monopole transitions, following the results of [6]. For  $^{48}\text{Ca}$ , according to Kamedzhiev [12], the monopolar strength in this excitation energy region can be neglected and this difference between the two isotopes is caused by the difference in shell structure of the two nuclei. Above 10 MeV, the strength cannot be attributed to krypton excitations due to neutron emission.

The analysis of our  $l=2$  data indicates that there is a significant difference between the two targets for E2 strength below 12 MeV, with about 15% more E2 strength detected in the scattering on the lighter isotope. As mentioned earlier, this departure from RPA predictions can be explained by invoking the presence in that nucleus of strong ground state correlation effects [8]. There is no indication however why these mechanisms should be so much weaker in  $^{48}\text{Ca}$  as to reduce their contribution by the factor observed here.



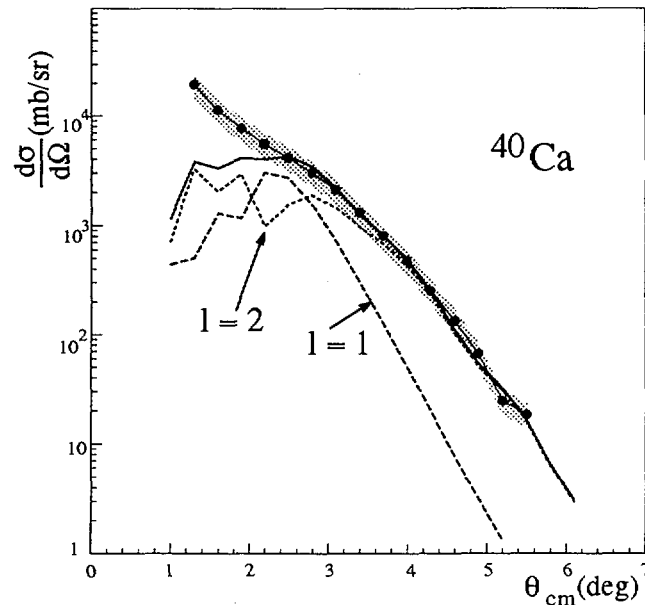


FIG. 3. Angular distribution obtained with the  $^{40}\text{Ca}$  target, for  $6\text{MeV} < E^* < 8\text{MeV}$ . The grey area represents the uncertainty on absolute normalization. The fit obtained with a coupled channel calculation is indicated by the solid line. The dashed lines respectively represent E1 and E2 transitions only.

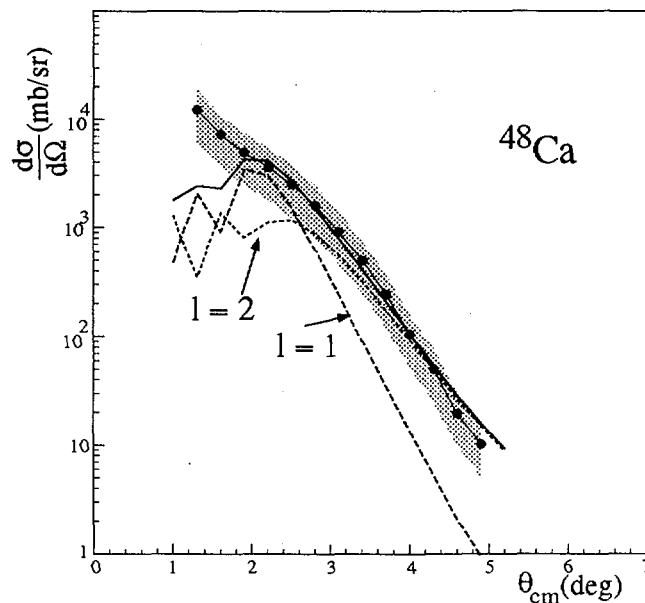


FIG. 4. Angular distribution obtained with the  $^{48}\text{Ca}$  target, for  $6\text{MeV} < E^* < 8\text{MeV}$ . The grey area represents the uncertainty on absolute normalization. The fit obtained with a coupled channel calculation is indicated by the solid line. The dashed lines respectively represent E1 and E2 transitions only.

In the  $l = 1$  case, two general observations come to mind :

- 1) One observes non negligible E1 strength with both targets in the low excitation energy region studied here. There is no theoretical basis for such a strength, since all RPA calculations (*with* or *without* ground state correlations) predict no E1 strength below 14 MeV in either isotope except in [2] for  $^{48}\text{Ca}$ .
- 2) We do not observe any E1 strength difference between  $^{48}\text{Ca}$  and  $^{40}\text{Ca}$ . Therefore, there is no evidence of the excitation of a soft dipole mode in  $^{48}\text{Ca}$ . Nevertheless, the E1 strength observed between 8 and 10 MeV is indeed consistent with the predictions of Chambers et al. [2]. A better study of the low excitation energy spectrum of  $^{40}, ^{48}\text{Ca}$  could be achieved in the forthcoming years with the improved energy resolution of the new focal plane detection of

SPEG. The expected energy resolution of 150 keV would allow to study whether the strength observed in  $^{48}\text{Ca}$  possesses the collective features i. e. resonance shape and transition density, expected for the soft E1 mode [2].

In conclusion, the results of our experiment using a particularly powerful and efficient probe for detecting low-lying excitations suggest that, in the E1 and E2 cases, our theoretical understanding of collective excitations should be critically reassessed. This is becoming especially important as higher resolution facilities are coming on line which will further test our understanding of the microscopic structure of collective excitations, as well as their coupling to more complex degrees of freedom.

E(MeV)	$^{40}\text{Ca}$		$^{48}\text{Ca}$		Difference	
	$l = 1$	$l = 2$	$l = 1$	$l = 2$	$l = 1$	$l = 2$
[6,8]	$2.6 \pm 0.6$	$8.3 \pm 2.0$	$3.1 \pm 1.5$	$4.2 \pm 2.1$	-0.5	+4.1
[8,10]	$4.9 \pm 1.2$	$15.6 \pm 3.9$	$3.6 \pm 1.8$	$8.8 \pm 4.4$	+1.3	+6.8
[10,12]	$6.6 \pm 1.6$	$15.8 \pm 3.9$	$7.0 \pm 3.5$	$10.0 \pm 5.0$	-0.4	+5.7

TABLE I. Percentage of the EWSR extracted from the data for  $l = 1$  and  $l = 2$  transitions for three energy regions. The errors are determined by the uncertainty on absolute normalization. The error due to multipolarity decomposition is negligible compared to this error. The percentage difference between  $^{40}\text{Ca}$  and  $^{48}\text{Ca}$  is given in the last column. The total strength between 6-12 MeV cannot be read as the cumulative sum because of the common boundaries. For  $^{40}\text{Ca}$  target and for  $8\text{MeV} \leq E^* \leq 10\text{MeV}$  and  $10\text{MeV} \leq E^* \leq 12\text{MeV}$ , we have introduced 5% of EWSR for monopole transitions, following the results of [6].

#### Acknowledgements :

The authors would like to thank J. Barrette for many fruitful discussions and for his very careful reading of this letter. They are also grateful to D.H. Youngblood for discussions and communication of his data.

- [1] M. Harvey and F. C. Khanna, *Nucl. Phys.* **A221**, 77 (1974).
- [2] J. Chambers et al., *Phys. Rev.* **C50**, 2671 (1994).
- [3] A. Van der Woude, *Prog. Part. Nucl. Phys.* **18**, 217 (1987)
- [4] J. Lisantti et al, *Phys. Rev.* **C40**, 211 (1989).
- [5] F.T. Baker et al., *Phys. Rev.* **C44**, 93 (1991).
- [6] D.H. Youngblood et al., *Phys. Rev.* **C55**, 2811 (1997).
- [7] J. A. Scarpaci et al., *Phys. Rev.* **C56**, 3187 (1997).
- [8] S. Kamerdzhiev, J. Speth and G. Tertychuy, *Phys. Rev. Letters* **74**, 3943 (1995).
- [9] J. Barrette et al., *Phys. Lett.* **B209**, 182 (1988).
- [10] J.R. Beene et al., *Phys. Rev.* **C41**, 920 (1990).
- [11] J. Raynal, *Phys. Rev.* **C23**, 2571 (1980).
- [12] S. Kamerdzhiev et al., *Nucl. Phys.* **A577**, 641 (1994).

\* Present address : GANIL, B.P. 5027, 14076 Caen Cedex 5, France

# SPECTROSCOPY OF THE UNBOUND $^{11}\text{N}$ NUCLEUS BY THE $^{12}\text{C}(^{14}\text{N},^{15}\text{C})^{11}\text{N}$ TRANSFER REACTION

A. Lépine-Szilý<sup>1</sup>, J. M. Oliveira Jr<sup>2</sup>, A. N. Ostrowski<sup>3</sup>, H. G. Bohlen<sup>4</sup>, R. Lichtenthaler<sup>1</sup>, A. Blasevic<sup>4</sup>, C. Borcea<sup>5</sup>, V. Guimarães<sup>6</sup>, R. Kalpakchieva<sup>7</sup>, V. Lapoux<sup>8</sup>, M. MacCormick<sup>9</sup>, F. Oliveira<sup>9</sup>, W. von Oertzen<sup>4</sup>, N. A. Orr<sup>10</sup>, P. Roussel-Chomaz<sup>9</sup>, Th. Stolla<sup>4</sup>, J. S. Winfield<sup>10</sup>

<sup>1</sup> IFUSP-Universidade de São Paulo, C.P.66318, 05315-970 São Paulo, Brasil <sup>2</sup> Universidade de Sorocaba, Sorocaba, Brasil <sup>3</sup> Universidade de Edinburgh, Edinburgh, EH9 3JZ United Kingdom <sup>4</sup> Hahn Meitner Institute, Berlin, Germany <sup>5</sup> Institute of Atomic Physics, Bucarest, Romania <sup>6</sup> UNIP-Objetivo, São Paulo, Brasil <sup>7</sup> LNR,JINR, Dubna, P.O.Box 79,101000 Moscow, Russia <sup>8</sup> CEA/DSM/DAPNIA/SPhN, CEN Saclay,91191 Gif-sur-Yvette, France. <sup>9</sup> GANIL, Bld Henri Becquerel, Bp 5027, 14021 Caen, Cedex, France <sup>10</sup> LPC-ISMRA,Bld du Marechal Juin, 14050 Caen, Cedex, France

Many interesting phenomena occur in the isobaric chain of nuclei with mass 11. The two-neutron halo of the  $^{11}\text{Li}$ , the  $s_{1/2}$  intruder halo ground state of the  $\text{Be}^{11}$  are some examples. The stability island is crossed from one shore to other with the five  $A=11$  nuclei. The unbound  $^{11}\text{N}$  is the mirror nucleus of  $^{11}\text{Be}$  at the other end of the  $T=3/2$  isospin quartet. It has been the object of many recent studies, mainly to establish if the spin inversion persists and the ground state is the continuum equivalent of a proton halo. However the observation of an unbound  $s_{1/2}$  resonance is a difficult task due to the lack of centrifugal barrier, which makes the width of the resonance fairly large. Previous experiments [1,2] claim the observation of the s-wave ground state resonance.

The spectroscopic study of the  $^{11}\text{N}$  was performed by using the  $^{12}\text{C}(^{14}\text{N},^{15}\text{C})^{11}\text{N}$  transfer reaction [3]. The experience was realized at GANIL with a  $^{14}\text{N}$  beam of 30A MeV incident energy using the SPEG spectrometer for the ejectil analysis. The selectivity, momentum calibration and resolution are also well demonstrated for other product nuclei as  $^{12}\text{N}$  and  $^{13}\text{N}$ .

The quality of the spectrum of the  $^{12}\text{C}(^{14}\text{N},^{15}\text{C})^{11}\text{N}$  reaction seems to be better than of previous measurements [1,2,4]. It presents several well defined resonances in the  $^{11}\text{N}$  with the  $^{15}\text{C}$  ejectile in its  $5/2^+$  excited state. The  $1/2^+$  ground state of the  $^{15}\text{C}$  is much less favoured in this transfer reaction. The  $^{11}\text{N}$  resonances observed in the spectrum have the decay energies (with respect to the  $^{10}\text{C}+p$  threshold) of  $E_{\text{decay}}=2.18(5)$ ,  $3.63(5)$ ,  $4.39(5)$ ,  $5.12(8)$  and  $5.87(15)$  MeV. The first two resonances correspond respectively to the fairly pure single-particle  $p_{1/2}$  and  $d_{5/2}$  levels, previously observed. For the higher resonances the spin-parity assignments are difficult, their structure can involve also core excitations and the estimated values of  $3/2^-$ ,  $5/2^-$  and  $7/2^-$  are only preliminary. Our observed widths are lower than those previously observed, possibly due to our energy resolution.

There is no clear evidence of the population of the  $s_{1/2}$  ground state of  $^{11}\text{N}$  in this experiment; however, our spectra of  $^{12}\text{N}$  and  $^{13}\text{N}$ , which have much better statistics, clearly corroborate the strong hindrance of any  $2s_{1/2}$  resonance. This does not exclude the existence of the  $s_{1/2}$  resonance in  $^{11}\text{N}$ , but reopens the debate about the missing s state.

## References

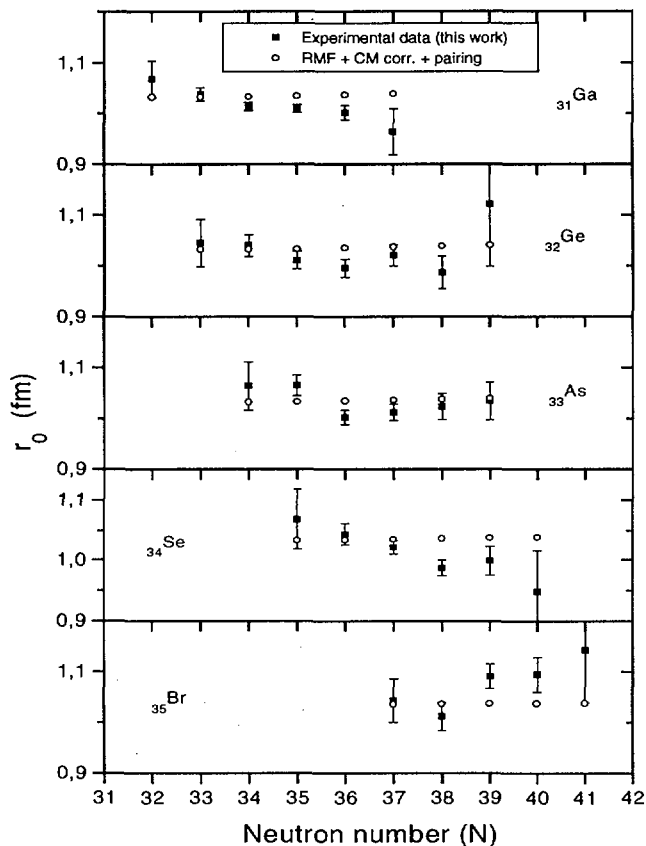
1. L. Axelsson et al Phys. Rev C54(1996) R1511.
2. A. Azhari et al Phys. Rev C57(1998)628.
3. A. Lépine-Szilý et al Phys. Rev. Lett 80(1998)1601.
4. W. Benenson et al Phys. Rev C9(1974)2130.

## NUCLEAR RADII OF PROTON-RICH RADIOACTIVE NUCLEI AT A=60-80

G. F. Lima<sup>1</sup>, A. Lépine-Szily<sup>1</sup>, A. C. C. Villari<sup>1,2</sup>, R. Lichtenthaler<sup>1</sup>, W. Mittig<sup>2</sup>, D. Hirata<sup>3</sup>, J. C. Angelique<sup>4</sup>, G. Audi<sup>5</sup>, J. M. Casandjian<sup>2</sup>, M. Chartier<sup>2</sup>, A. Cunsolo<sup>6</sup>, C. Donzeaud<sup>7</sup>, A. Foti<sup>6</sup>, A. Gillibert<sup>8</sup>, M. Lewitowicz<sup>2</sup>, S. Lukyanov<sup>9</sup>, M. MacCormick<sup>2</sup>, D. J. Morrissey<sup>10</sup>, N. A. Orr<sup>4</sup>, A. N. Ostrowski<sup>2</sup>, B. M. Sherrill<sup>10</sup>, C. Stephan<sup>7</sup>, T. Suomijarvi<sup>7</sup>, L. Tassan-Got<sup>7</sup>, D. J. Vieira<sup>11</sup>, J. M. Wouters<sup>11</sup>

<sup>1</sup> IFUSP-Universidade de São Paulo, C.P.66318, 05315-970 São Paulo, Brasil <sup>2</sup> GANIL, Bld Henri Becquerel, Bp 5027, 14021 Caen, Cedex, France <sup>3</sup> Spring-8, Kamigori cho, Ako gun, Hyogo, 678-12, Japan <sup>4</sup> LPC-ISMRA, Bld du Marechal Juin, 14050 Caen, Cedex, France <sup>5</sup> CSNSM, Batiment 108, 91406 Orsay Cedex, France <sup>6</sup> INFN, Corso Itàlia 57, 95129 Catania, Italy <sup>7</sup> IPN Orsay, BP1, 91406 Orsay Cedex, France <sup>8</sup> CEA/DSM/DAPNIA/SPhN, CEN Saclay, 91191 Gif-sur-Yvette, France. <sup>9</sup> LNR, JINR, Dubna, P.O.Box 79, 101000 Moscow, Russia <sup>10</sup> NSCL, MSU, East Lansing MI, 48824-1321, USA <sup>11</sup> LANL, Los Alamos NM, 87545, USA

The region of neutron-deficient nuclei with  $A \sim 60-80$  near the  $N=Z$  line presents interesting properties as shape-coexistence and reinforcing or switching of shell-gaps [1]. Very near to the spherical magic



number 40 strong ground-state deformations ( $\beta_2 \sim 0.44$ ) were found in the <sup>76</sup>Sr ( $Z=N=38$ ) and <sup>74,76</sup>Kr ( $Z=36, N=38,40$ ) nuclei, while neighbouring nuclides with lower  $Z$  values, as <sup>70,72</sup>Ge ( $Z=32, N=38,40$ ) and <sup>72,74</sup>Se ( $Z=34, N=38,40$ ) present spherical behaviour around  $N=38$  [1]. One first simple information concerning the deformations of nuclei in this region can be obtained from their radii, which can be deduced from the experimental data of reaction cross sections. Therefore we measured at GANIL (Grand Accélérateur National d'Ions Lourds), Caen, France the radii of proton-rich radioactive nuclei with masses between  $A=60-80$  near the  $N=Z$  line. They were produced via the fragmentation of a 73 MeV/nucleon <sup>78</sup>Kr primary beam on a <sup>nat</sup>Ni target. The secondary beams were analysed in the high precision magnetic spectrometer SPEG with complete identification of mass and atomic number of the incident particles. The nuclear reaction cross section of secondary nuclei on Silicon were measured using the Direct Method [2], where the detector plays also the role of the target. The reduced nuclear radii  $r_0$ , defined by Kox [3] from a large systematics using stable nuclear radii, can be obtained from the direct reaction cross-section [4]. The results of  $r_0$  for <sup>63,64,65,66,67</sup>Ga, <sup>65,66,67,68,69,70,71</sup>Ge, <sup>67,68,69,70,71,72</sup>As,

<sup>69,70,71,72,73,74</sup>Se and <sup>72,73,74,75,76</sup>Br are presented in the figure, compared with theoretical predictions. The nuclear densities were obtained in a spherical relativistic mean field (RMF) with center of mass correction including pairing correlation [5]. Finally Glauber calculations were performed to obtain the reaction cross sections and the values of the reduced radius  $r_0$ . The experimental radii are not constant as a function of  $N$ , presenting a minimum around  $N=36-38$ , possibly corresponding to the spherical configuration. For lower, as well as for higher  $N$  values the  $r_0$  values increase. The spherical RMF calculation gives a reasonable agreement, without reproducing the systematic trend of a minimum around  $N=38$ .

### References

1. J.H. Hamilton, Treatise on Heavy-Ion Science vol.8. Plenum Press. Ed. D. A. Bromley, 1988.
2. A. C. C. Villari et al., *Phys. Lett.* **B268**(1991)345.
3. S. Kox et al., *Phys. Rev.* **C35**(1987)1678.
4. W. Mittig et al., *Phys. Rev. Lett.* **59**(1987)1889.
5. I. Tanihata et al., *Phys. Lett.* **B289**(1992) and D. Hirata et al, *Phys. Lett.* **B314**(1993)168.

# Study of subshell closure at $N=40$ by Coulomb excitation

S. Leenhardt<sup>1)</sup>, F. Azaiez<sup>1)</sup>, O. Sorlin<sup>1)</sup>, M. Belleguic<sup>1)</sup>, J.C. Angelique<sup>4)</sup>,  
C. Borcea<sup>6)</sup>, C. Bourgeois<sup>1)</sup>, J.M. Daugas<sup>3)</sup>, I. Deloncle<sup>2)</sup>, C. Donzaud<sup>1)</sup>,  
J. Duprat<sup>1)</sup>, A. Gillibert<sup>5)</sup>, S. Grevy<sup>1)</sup>, D. Guillemaud-Mueller<sup>1)</sup>, J. Kiener<sup>2)</sup>,  
M. Lewitowicz<sup>3)</sup>, F. Marie<sup>4)</sup>, A.C. Mueller<sup>1)</sup>, F. de Oliveira<sup>3)</sup>, N. Orr<sup>4)</sup>,  
Yu-E. Penionzhkevich<sup>7)</sup>, M.G. Porquet<sup>2)</sup>, F. Pougheon<sup>1)</sup>, M.G. Saint-Laurent<sup>3)</sup>,  
Yu. Sobolev<sup>7)</sup>, J. Winfield<sup>3)</sup>.

<sup>1)</sup>Institut de Physique Nucléaire, IN2P3-CNRS, F-91406 Orsay Cedex, France.

<sup>2)</sup>Centre de Spectrométrie Nucléaire et de Spectrométrie de Masse, IN2P3-CNRS,  
F-91405 Orsay Campus, France.

<sup>3)</sup>Grand Accélérateur National d'Ions Lourds, BP 5027, F-14076 Caen Cedex, France.

<sup>4)</sup>Laboratoire de Physique Corpusculaire, F-14050 Caen Cedex, France.

<sup>5)</sup>C.E. Saclay, DAPNIA/SphN, Orme des Merisiers, F-91191 Gif-sur-Yvette, France.

<sup>6)</sup>Institute of Atomic Physics, P.O. Box M66, Bucharest, Romania.

<sup>7)</sup>Flerov Laboratory of Nuclear Reactions, JINR, PO Box 79, Dubna, Russia.

Coulomb excitation experiment has been achieved in order to study the subshell closure at  $N = 40$  for neutron-rich nuclei. This subshell effect is thought to be enhanced when large  $N/Z$  ratios are encountered. Therefore, the  $Z = 28$   $^{68}\text{Ni}$  is of particular interest in order to test this behaviour. In addition this nucleus would be a good starting point for describing other nickel isotopes up to the doubly magic  $^{78}\text{Ni}$ . Some experimental informations are already known for  $^{68}\text{Ni}$  at low excitation energy : a  $0_2^+$  isomer at  $1.770\text{MeV}$  <sup>1)</sup>, a  $2^+$  state at  $2.033\text{MeV}$  <sup>2)</sup> and a long-lived  $5^-$  state at  $2.847\text{MeV}$  <sup>2)</sup>. The high energy of the  $2^+$  state suggests the shell closure though its reduced transition probability  $B(E2)$  has never been measured.

The experiment, performed at GANIL with the LISE3 spectrometer, has been investigated by the method of Coulomb excitation of secondary beams into a thick target placed in the center of a large gamma-array detector. The nuclei were produced at an energy of about 50 A.MeV by the fragmentation of a  $^{86}\text{Kr}$  beam at 65 A.MeV on a  $\text{Ni}$  target.

Secondary beams were identified event-by-event by two large-area ( $25\text{ cm}^2$ ) silicon detectors mounted at a distance of 50 cm from the secondary lead target ( $220\text{ mg/cm}^2$ ). Two clover Ge-detectors were placed around the implantation detector in order to determine photons originating from the decay of isomers transmitted by the spectrometer. Deflection angle of the fragments (up to an angle of  $3^\circ$  in the laboratory frame) can be determined by position sensitive gas detectors located before and after lead target. At these small deflection angles, Coulomb inelastic contribution dominates the total cross-section. The lead target was surrounded by the 70  $\text{BaF}_2$  detectors of "Château de Cristal" mounted at a distance of 35

cm, in the  $4\pi$  geometry of the first generation TAPS-detector. The production rate of fragments was about 100 particles/second for  $^{76}\text{Ge}$  and  $^{72}\text{Zn}$ , and about 20 particles/second for  $^{68}\text{Ni}$  and  $^{70}\text{Zn}$ .  $\gamma$ -rays originating from Coulomb excitation are emitted in flight with a velocity of  $v/c=0.3$ .

Time-resolution between an incoming projectile and  $\gamma$ -ray in the total array is better than 3 ns. Achieved energy spectra are shown on Fig. 1.

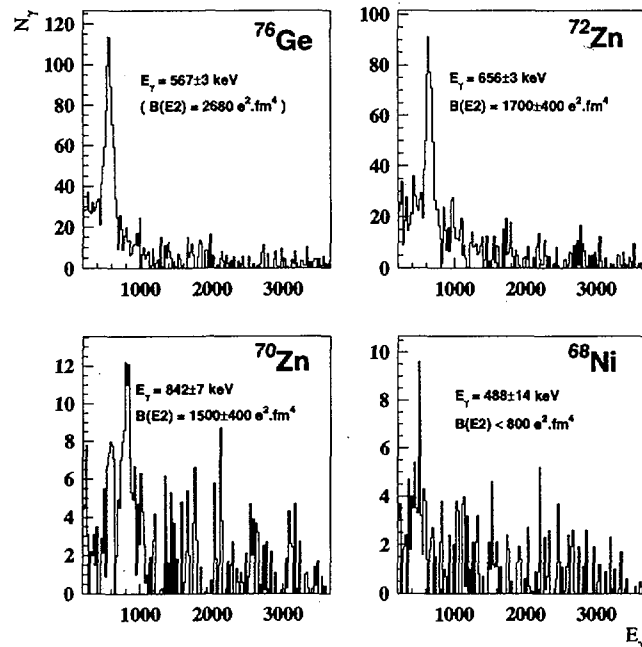


Figure 1: Doppler corrected energy-spectra and excitation probability obtained from Coulomb excitation of  $^{76}\text{Ge}$ ,  $^{72}\text{Zn}$ ,  $^{70}\text{Zn}$  and  $^{68}\text{Ni}$ . The x-axis is in keV.

$^{76}\text{Ge}$  is a well-known case of deformed nucleus with a low  $2^+$  state (562.9 keV) and a strong excitation probability ( $B(E2)_{\uparrow} = 2680 e^2.fm^4$ ). It has been used as a reference in order to determine  $B(E2)$  for other nuclei ( $^{72}\text{Zn}$ ,  $^{70}\text{Zn}$  and  $^{68}\text{Ni}$ ). Even if the spectrometer wasn't optimized for  $^{70}\text{Zn}$ , an excitation probability value has been determined for the  $2^+$  state at  $830 \pm 75$  MeV :  $B(E2) = 1500 \pm 400 e^2.fm^4$ . With regard to  $^{68}\text{Ni}$ , very few counts are found around the expected energy (2.03 MeV). Hence only an upper limit has been derived :  $B(E2) \leq 800 e^2.fm^4$ . This limit doesn't establish sphericity of this nucleus. Nevertheless a structure is yet visible around 490 keV, whose structure isn't still clear. Two assumptions can be made : on one hand, it could be a signature of the decay in flight of the  $0_2^+$  isomer, on the other hand, it could be due to the Coulomb excitation of one of the both isomers, present in the  $^{68}\text{Ni}$  beam as a contaminant.

Future investigations with majors improvements at GANIL are planned. First the use of a neutron-rich primary beam  $^{70}\text{Zn}$ , closer to  $^{68}\text{Ni}$  will enhance the production rate with a factor of at least 100, and secondly a higher resolution  $\gamma$ -array composed with segmented clover Ge detectors will increase the sensitivity of the set-up.

#### References:

- (1) M. Bernas et al., Phys. Lett. B **113**, (1982) p. 279.
- (2) R. Broda et al., Phys. Rev. Lett. **74**, (1995) p. 868.

Interplay between the neutron halo structure and reaction mechanisms in collisions of 35 MeV/nucleon  ${}^6\text{He}$  with Au.

Y.Périer<sup>1</sup>, B.Lott<sup>1</sup>, J.Galin<sup>1</sup>, E.Liénard<sup>1</sup>, M.Morjean<sup>1</sup>, N.A.Orr<sup>2</sup>, A. Péghaire<sup>1</sup>, B.M.Quednau<sup>1</sup>, A.C.C.Villari<sup>1</sup>

<sup>1</sup> GANIL (IN2P3-CNRS, DSM-CEA), BP 5027, F-14076 Caen Cedex 5, France  
<sup>2</sup> LPC (IN2P3-CNRS-University of Caen), F-14050 Caen Cedex, France

The halo structure of some nuclei has been mainly probed so far by considering the linear momentum distributions of either the core or the neutrons or both, emerging from breakup reactions. However, in most experiments, rather little attention has been paid to the influence of the reaction mechanism or to the considered reaction channels on these observables. At best, the choice of the target nucleus, either very heavy or very light, was made with the aim of either enhancing or inhibiting Coulomb breakup. Moreover, in many cases a rather simple experimental device was used not permitting both an energy and angular exploration of the detected cores, making most of these first generation experiments integral experiments. Furthermore, no attempt has so far been made to experimentally quantify the excitation energy deposited into the target-nucleus, which appears to be as an extremely valuable piece of information for characterizing the reaction channels.

Utilizing the experimental device sketched in Fig.1, the following reaction products were measured eventwise:

- the  ${}^4\text{He}$  projectile core (or its component(s) when breaking up) through its parallel and transverse linear momenta.
- the halo neutron(s) via its (their) momentum modulus.
- the target excitation energy through the multiplicity of evaporated neutrons.

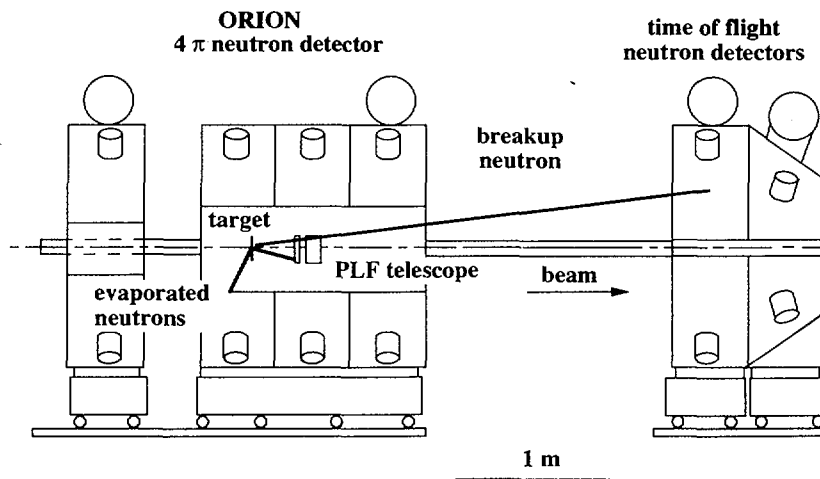


Fig.1: Schematic view of the experimental setup.

For the first time, when using all these measured parameters it was possible to follow the linear momentum distribution widths, for both the core and the halo neutrons, over a very broad domain of impact parameters and distinct reaction channels. The general trend observed in Fig.2 is an increase of the momentum widths for reactions presumably associated with smaller impact parameters. The probing of different parts of the wavefunction for different impact parameters on one hand and different final-state interactions, both in nature and magnitude, on the other hand are likely to be responsible for this behavior<sup>1)</sup>. Most of the published data so far were obtained in rather inclusive experiments and may thus depend considerably on the experimental conditions (position and opening angle of the detectors). This stresses the need of exclusive data for other halo nuclei might they be single- or double-neutron halos.

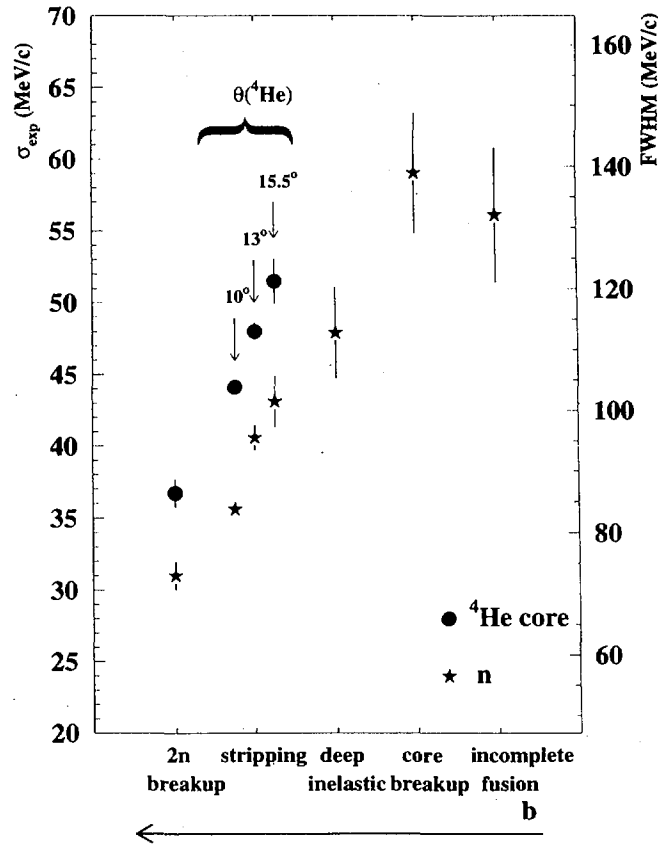


Fig.2: Comparison between the widths of the parallel momentum distributions of the core nucleus (dots) and the halo neutrons (stars) for the different reaction channels isolated in the experiment.

The present experiment has also shed new light on the nuclear structure of the  $^6\text{He}$  nucleus. According to theoretical predictions the ground state should appear with two configurations equally probable: one with the two neutrons as a di-neutron, the other with the two neutrons opposite with respect to the core, thus giving the nucleus a cigar-like shape. This could be checked experimentally, based on the following arguments. In stripping reactions there is a large probability to remove the two neutrons in the first configuration whereas this probability should be low in the second configuration. By measuring the probability for the one-neutron stripping and the two-neutron stripping one tends to confirm the predicted structure. However more data are needed as a function of impact parameters in order to be more quantitative.

In summary, a new approach has been followed in the investigation of neutron halo nuclei. Very exclusive data have shown the importance of reaction mechanisms in connection with the nuclear structure. A good understanding of the reaction mechanism appears to be a prerequisite to the investigation of the nuclear structure.

#### References:

- 1) Y.Périer, PhD thesis, Caen University, GANIL-T 9705, unpublished and Y. Périer et al., letter in preparation.
- 2) B.Lott et al. , Proceedings of the XXXVI International Winter Meeting on Nuclear Physics, Bormio 1998 and B.Lott et al., letter in preparation.



# Exotic Molecular and Halo States in $^{12,14}\text{Be}$

M. Freer<sup>a,b</sup>, N.A. Orr<sup>b</sup>, M. Labiche<sup>b</sup>, F.M. Marqués<sup>b</sup>, J.C. Angélique<sup>b</sup>, L. Axelsson<sup>c</sup>, B. Benoit<sup>d</sup>, U. Bergmann<sup>e</sup>, M.J.G. Borge<sup>j</sup>, W.N. Catford<sup>f</sup>, S.P.G. Chappell<sup>g</sup>, N.M. Clarke<sup>a</sup>, G. Costa<sup>h</sup>, N. Curtis<sup>f</sup>, A. D'Arrigo<sup>d</sup>, F. D'Oliviera<sup>m</sup>, E. de Goes Brennard<sup>d</sup>, O. Dorvaux<sup>h</sup>, B.R. Fulton<sup>a</sup>, G. Gardina<sup>i</sup>, C. Gregori<sup>j</sup>, S. Grévy<sup>b,k</sup>, D. Guillemaud-Mueller<sup>k</sup>, F. Hanappe<sup>d</sup>, B. Heusch<sup>h</sup>, B. Jonson<sup>c</sup>, G. Kelly<sup>l</sup>, C. Le Brun<sup>b</sup>, S. Leenhardt<sup>k</sup>, M. Lewitowicz<sup>m</sup>, K. Markenroth<sup>c</sup>, M. Motta<sup>i</sup>, A.C. Mueller<sup>k</sup>, J.T. Murgatroyd<sup>a</sup>, T. Nilsson<sup>c</sup>, A. Ninane<sup>n,b</sup>, G. Nyman<sup>c</sup>, I. Piqueras<sup>j</sup>, K. Riisager<sup>e</sup>, M.G. Saint Laurent<sup>m</sup>, F. Sarazin<sup>m,b</sup>, S. Singer<sup>a</sup>, O. Sorlin<sup>k</sup>, L. Stuttgé<sup>h</sup>, D.L. Watson<sup>o</sup>

<sup>a</sup> School of Physics and Astronomy, University of Birmingham, Birmingham B15 2TT, U. K.

<sup>b</sup> LPC-ISMRA, Bd Maréchal Juin, 14050 Caen Cedex, France.

<sup>c</sup> Fysiska Institutionen, Chalmers Tekniska Högskola, S-412 96 Göteborg, Sweden.

<sup>d</sup> Université Libre de Bruxelles, CP 226, B-1050 Bruxelles, Belgium.

<sup>e</sup> Det Fysiske Institut, Aarhus Universitet, DK 8000 Aarhus C, Denmark.

<sup>f</sup> Department of Physics, University of Surrey, Guildford, Surrey, GU2 5XH, U. K.

<sup>g</sup> Department of Nuclear Physics, University of Oxford, Keble Road, Oxford OX1 3RH, U. K.

<sup>h</sup> IReS, B.P.28, F-67037 Strasbourg Cedex, France.

<sup>i</sup> Dipartimento di Fisica, Università di Messina, Salita Sperone 31, I-98166 Messina, Italy.

<sup>j</sup> Instituto Estructura de la Materia, CSIC, E-28006 Madrid, Spain.

<sup>k</sup> Institut de Physique Nucléaire 91406 Orsay Cedex, France.

<sup>l</sup> School of Sciences, Staffordshire University, College Road, Stoke-on-Trent, ST4 2DE, U. K.

<sup>m</sup> GANIL, BP 5027, 14076 Caen Cedex, France.

<sup>n</sup> Institut de Physique, Université Catholique de Louvain, B-1328 Louvain-la-Neuve, Belgium.

<sup>o</sup> Department of Physics, University of York, York, YO1 5DD, U. K.

**Abstract.** The two nuclei  $^{12}\text{Be}$  and  $^{14}\text{Be}$  have been studied using breakup reactions on p,  $^{12}\text{C}$  and  $^{208}\text{Pb}$  targets. The decay of  $^{12}\text{Be}$  into two helium clusters ( $^6\text{He}+^6\text{He}$  and  $^4\text{He}+^8\text{He}$ ) was observed from a series of excited states between 10 and 25 MeV, with spins in the range  $4^+$  to  $8^+$ . The single neutron angular distributions for  $^{14}\text{Be}$  exhibit the narrow forward peak characteristic of a halo. The widths of these distributions in coincidence with  $^{12}\text{Be}$  fragments are  $\Gamma_L=78\pm 6$  and  $80\pm 1$  MeV/c for breakup on carbon and lead.

## I INTRODUCTION

The stability of the  $\alpha$ -cluster has a strong influence on the structure of light nuclei and has spawned an industry devoted to the understanding of the role of clustering in s-d shell nuclei dating from the early 1960's when heavy-ion beams were first exploited. The advent of radioactive beams has also revealed clustering in light, neutron-rich nuclei, in the guise of the halo, where the nucleus is composed of a core and valence halo neutrons, and the molecular type cluster states composed of  $\alpha$ -particles bound by the valence neutrons.

In the 1960's, Ikeda [1] developed a classification of clustering in light  $A=4n$ ,  $\alpha$ -conjugate nuclei, in which cluster structures appeared at, or close to, the decay threshold for the particular cluster partition. This scheme, which is on the whole verified by experimental observations, is based on the premise that to create the internal cluster structures an energy equivalent to the binding energy of the constituents is required. Thus systems that include weakly bound neutrons, e.g.  $^{11}\text{Be}$  ( $S_n=0.5$  MeV) and  $^{11}\text{Li}$  ( $S_{2n}\simeq 0.3$  MeV), should show strong clustering characteristics. Clustering is amplified in these systems by reduced centrifugal barriers for the weakly bound valence neutrons allowing a greater decoupling of the core and halo neutrons. The heaviest particle stable Be isotope,  $^{14}\text{Be}$  ( $S_{2n} = 1.34 \pm 0.11$  MeV), is Borromean and is known to exhibit a two-neutron halo. In contrast to other halo systems, the configuration of the valence neutrons is expected to contain a significant d-wave admixture. Additionally,  $^{14}\text{Be}$  is the heaviest two-neutron halo nucleus currently known. The investigation of  $^{14}\text{Be}$ , presented here, thus provides an opportunity to study the evolution of halo systems with binding energy, angular momentum and mass.

Another extreme manifestation of clustering is the formation of chain and ring structures composed of individual cluster units, such as  $\alpha$ -particles. Indeed there is some evidence for such structures in light nuclei. Similar arrangements have also been observed in atomic systems, for example carbon clusters [2] which are believed to be related to particular spectral lines in astronomical observations of stellar dust clouds. Another nuclear analogue of such phenomena are  $\alpha$ -ring and chain structures covalently bonded by valence neutrons, predicted by Wilkinson [3], much as the binding of atomic molecules through the exchange of electrons. Von Oertzen [4] has characterized the structure of the sequence of Be isotopes  $^9\text{Be}$  to  $^{11}\text{Be}$  in terms of dinuclear  $2\alpha$ -Xn structures, and certain carbon isotopes as trinuclear molecules. The present contribution reports a measurement of the  $2\alpha$ -4n cluster system  $^{12}\text{Be}$ .

## II EXPERIMENTAL MEASUREMENTS

The secondary beams of  $^{12,14}\text{Be}$  ( $\overline{E}_{12\text{Be}} = 31.5$  MeV/nucleon,  $i \approx 2.10^4$  pps,  $\overline{E}_{14\text{Be}} = 41.3$  MeV/nucleon,  $i \approx 10^2$  pps) were prepared from the fragmentation of an  $^{18}\text{O}$  beam (63 MeV/nucleon) on a thick Be target using the LISE3 spectrometer. In

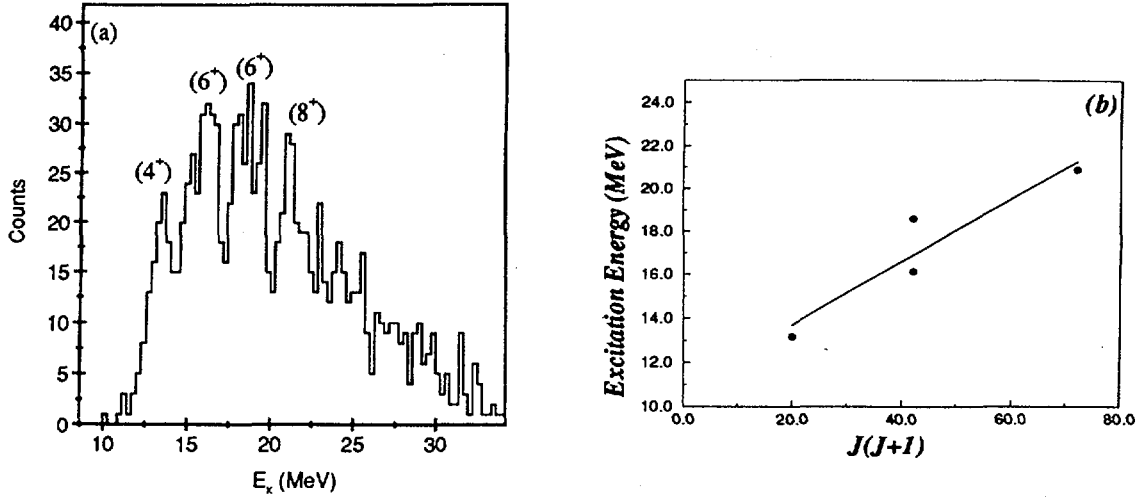


FIGURE 1. (a)  $^{12}\text{Be}$  excitation energy spectrum for  $^6\text{He}+^6\text{He}$  coincidences, (b) the energy-spin systematics of the breakup states.

the case of the  $^{14}\text{Be}$  studies, measurements were carried out on secondary reaction targets of carbon and lead ( $\bar{E}_{^{14}\text{Be}} = 35$  MeV/nucleon at target mid-point) in an attempt to disentangle the effects of nuclear and Coulomb induced breakup. For the  $^{12}\text{Be}$  measurements,  $^{12}\text{C}$  and  $(\text{CH}_2)_n$  target foils were used, with beam tracking and time-of-flight measurement provided by two parallel plate avalanche counters. The breakup of the  $^{12}\text{Be}$  nucleus into two helium fragments was detected in an array of ten Si-CsI telescopes placed around the beam axis. The silicon elements were two dimensional position sensitive detectors (2DPSDs), proving a measurement of the angle of the incident particles with a resolution of better than  $0.5^\circ$ . The telescopes provided a clean identification of the  $^4\text{He}$ ,  $^6\text{He}$  and  $^8\text{He}$  nuclei of interest, and a measurement of the energy with a resolution of 1.5%. For the  $^{14}\text{Be}$  experiment the charged reaction products were again detected using the 10 element position sensitive Si-CsI array with one of the elements placed at zero degrees. Neutrons were detected using the 99 modules of the DEMON array. A staggered arrangement

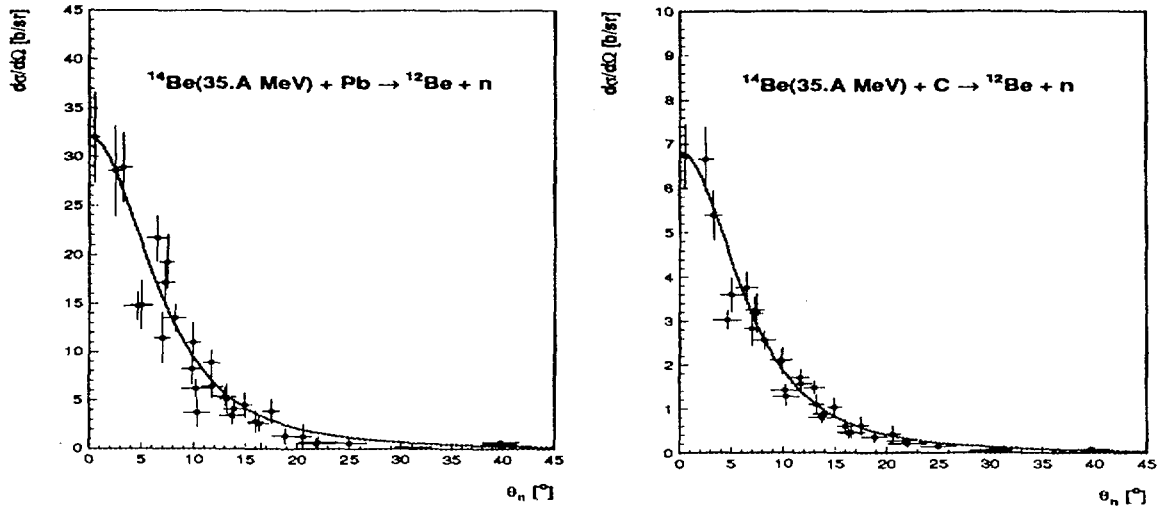
Reaction	Target	$\sigma$ (mb)
$p(^{12}\text{Be}, ^6\text{He}^6\text{He})p$	$(\text{CH}_2)_n$	0.76 (0.05)
$^{12}\text{C}(^{12}\text{Be}, ^6\text{He}^6\text{He})^{12}\text{C}$	$(\text{CH}_2)_n$	0.26 (0.06)
$^{12}\text{C}(^{12}\text{Be}, ^6\text{He}^6\text{He})^{12}\text{C}$	$^{12}\text{C}$	0.28 (0.04)
$p(^{12}\text{Be}, ^4\text{He}^8\text{He})p$	$(\text{CH}_2)_n$	2.91 (0.06)
$^{12}\text{C}(^{12}\text{Be}, ^4\text{He}^8\text{He})^{12}\text{C}$	$(\text{CH}_2)_n$	1.62 (0.11)
$^{12}\text{C}(^{12}\text{Be}, ^4\text{He}^8\text{He})^{12}\text{C}$	$^{12}\text{C}$	0.79 (0.07)

TABLE 1.  $^{12}\text{Be}$  breakup reaction cross sections.

Channel	$\sigma_{telescope}$ [mb]		$\Gamma_n$ [MeV/c]	
	C	Pb	C	Pb
$^{12}\text{Be}$	$460\pm 40$	$2300\pm 400$	—	—
$^{12}\text{Be}+n$	—	—	$78\pm 6$	$80\pm 1$
$^{11}\text{Be}$	$85\pm 15$	—	—	—
$^{10}\text{Be}$	$145\pm 20$	—	—	—
$^{10}\text{Be}+n$	—	—	$119\pm 44$	—

**TABLE 2.** Preliminary results for the breakup of  $^{14}\text{Be}$  on C and Pb targets. The single neutron angular distributions have been characterized in terms of a Lorentzian distribution.

for the neutron detectors was chosen so as to maximize the coverage at forward angles whilst minimizing the effects of cross talk (both geometrically and in the off-line analysis).



**FIGURE 2.** Single neutron angular distributions for the breakup of  $^{14}\text{Be}$  ( $E_n=10$  to  $100$  MeV).

## A $^{12}\text{Be}$ breakup

The  $Q$ -values for the reactions  $^{12}\text{C}(^{12}\text{Be},^x\text{He}^y\text{He})^{12}\text{C}$  and  $p(^{12}\text{Be},^x\text{He}^y\text{He})p$  were calculated from the energies of the two detected helium nuclei and the energy of the undetected recoil-like particle inferred from the measured momenta of the beam and detected reaction products. In the case of the  $(\text{CH}_2)_n$  target this technique was able to resolve the reactions taking place on the carbon and hydrogen. The cross

sections for the various reactions are given in Table 1. Selecting events identified with peaks in the Q-value spectra for the above reactions, it is possible to calculate the excitation energy, or invariant mass, of the  $^{12}\text{Be}$  nucleus prior to decay using the relationship

$$E_x = \frac{1}{2}\mu v_{rel}^2 + Q_{bu} \quad (1)$$

where  $v_{rel}$  is the relative velocity of the two breakup fragments,  $\mu$  the reduced mass and  $Q_{bu}$  the breakup Q-value, which for the  $^6\text{He}+^6\text{He}$  and  $^8\text{He}+^4\text{He}$  channels is 10.11 and 8.95 MeV respectively. Figure 1a shows the  $^{12}\text{Be}$  excitation energy spectrum for decays into two  $^6\text{He}$  nuclei. These states, which span the excitation energy region 10 to 25 MeV, are the first definitive evidence for the  $2\alpha$ -4n, molecular cluster structure in this nucleus [5]. Angular correlation measurements of the breakup products indicate that the states may be associated with spins from  $4^+$  to  $8^+$ , and the inferred excitation energy-spin sequence appears to be consistent with a rotational band with a large moment of inertia (Figure 1b).

## B $^{14}\text{Be}$ breakup

The  $^{14}\text{Be}$  reaction cross sections derived from the telescope data confirm that the two-neutron removal reaction channel is dominant, as seen in an earlier experiment [6]. The single neutron angular distributions (shown in Figure 2) exhibit the narrow, forward peaked form characteristic of a halo. Interestingly the characteristic widths of the distributions for the two targets are very similar and thus may suggest, as in the case of  $^{11}\text{Li}$  [7], the existence of a very low lying state in  $^{13}\text{Be}$ . The analysis of the  $^{12}\text{Be}+n$  invariant mass spectrum, presently underway, should shed further light on this conjecture. The  $^{12}\text{Be}+n+n$  invariant mass spectrum is being investigated in parallel with the objective of extracting the low-lying dipole strength function,  $dB(E1)/dE_x$ . The two-neutron correlations — relative momenta and correlation function,  $C(q)$  — are also under analysis, with the present effort concentrating on inclusion of the effects of neutron-neutron final state interactions. The results of these analyses when compared with realistic three-body models are expected to provide important insights into the halo structure of  $^{14}\text{Be}$ .

- [1] K. Ikeda, Suppl. Prog. Physics (Japan) Extra Numbers, 464 (1968).
- [2] S. Yang, *et al.*, Chem. Phys. Letts. 144, 431 (1988).
- [3] D.H. Wilkinson, Nucl. Phys. A 452, 296 (1986).
- [4] W. von Oertzen, Z. Phys. A 354, 249 (1996), Z. Phys. A 357, 355 (1997).
- [5] A.A. Korshinnikov, *et al.*, Phys. Letts. B 343, 53 (1995).
- [6] K. Riisager *et al.*, Nucl. Phys. A540, 365 (1992).
- [7] F. Barranco *et al.*, Phys. Lett. B319, 387 (1993).

## Quadrupole and magnetic moment of spin-oriented $^{18}\text{N}$ fragments measured with the combined $\beta$ -LMR-NMR method.

G. Neyens<sup>a</sup>, N. Coulier<sup>a</sup>, S. Teughels<sup>a</sup>, G. Georgiev<sup>a</sup>, S. Ternier<sup>a</sup>, K. Vyvey<sup>a</sup>, R. Coussement<sup>a</sup>, D.L. Balabanski<sup>a</sup>, F. de Oliveira Santos<sup>b</sup>, M. Lewitowicz<sup>b</sup>, W. Mittig<sup>b</sup>, P. Roussel Chomaz<sup>b</sup>, W.F. Rogers<sup>c</sup>, A. L epine Szily<sup>d</sup>, M.D. Cortina Gil<sup>e</sup>.

<sup>a</sup> Instituut voor Kern- en Stralingsfysica, University of Leuven, Celestijnenlaan 200 D, B-3001 Leuven, Belgium

<sup>b</sup> Grand Acc el erateur National d'Ions Lourds, BP 5027, F-14021 Caen Cedex, France

<sup>c</sup> Westmont College, 955 La Plaz Road, Santa Barbara, CA 93108 California USA

<sup>d</sup> Institute of Physics, University of Sao Paulo, C.P. 66318, 05389-970, Sao Paulo, Brasil

<sup>e</sup> Gesellschaft f ur Schwerionenforschung (GSI), D-64291 Darmstadt, Germany

We have produced spin-oriented projectile fragments by selecting a secondary beam in the forward direction after the reaction of a  $^{22}\text{Ne}$  (60.3 MeV/u) beam with a  $^{12}\text{C}$  (350 mg/cm<sup>2</sup>) target. The target was mounted on a rotating target frame in the LISE target chamber. A nearly pure secondary beam of  $^{18}\text{N}$ -fragment (5.5 % of  $^{20}\text{O}$  contamination) was selected using the LISE spectrometer and the Wien-filter. After reducing the beam energy by Al-degraders, the fragments were stopped in a Mg single crystal, which was mounted on the cold finger of a continuous flow cryostat into a vacuum chamber. The crystal was cooled to 40K, in order to reduce the influence of spin-lattice relaxation on the spin-orientation. A static magnetic field up to 2000 Gauss was induced by two coils mounted around the vacuum chamber. Around the Mg-crystal, a small RF-coil was build to induce a RF-field with constant frequency of 20 kHz. Due to the presence of 3 interactions, a static magnetic dipole interaction ( $v_B = g\mu_N B/h$ ), a static electric quadrupole interaction ( $v_Q = eQV_{zz}/h$ ) and a RF-interaction ( $v_{RF} = 20 \pm 3$  kHz), the spin-orientation of the fragment nuclei is modified resonantly at well-defined values for the static magnetic field strength B. The induced spin-polarization is measured by monitoring the  $\beta$ -decay asymmetry as a function of the magnetic field strength. From the position of the resonance fields, we can deduce unambiguously the magnetic moment and the quadrupole moment of the selected projectile fragment [1,2,3]. The measured high-precision LMR is in very good agreement with a first less-precise measurement [3,4,5]. From the NMR-resonances, measured as a function of B (fig. 1), we derive a very small magnetic moment  $\mu = 0.157(7)$  n.m.. Using this value together with the ratio  $\mu/Q$  derived from the LMR-resonance field, we deduce a rather large quadrupole moment  $Q = 32(3)$  emb for the  $^{18}\text{N}$ ,  $I^\pi = 1^-$  ground state [6,7]. Comparison to shell model calculations using the USD interaction of Brown and Wildenthal [8] shows that the magnetic moment is smaller than expected. However, modifying slightly the interaction parameters, such that the magnetic moment of the  $3/2^-$  first excited state in  $^{19}\text{O}$  is reproduced better, gives perfect agreement between experiment and theory [9]. No shell-model calculations for the quadrupole moment have been performed so far. Comparison to mean-field calculations [10], shows an experimental Q-moment which is about 60% larger than the theoretical value for the proton Q-moment, using the rotational model relation with  $K=0$  to relate the intrinsic theoretical and measured spectroscopic quadrupole moment ( $Q_0 = -(2I+3)/I Q_s$ ).

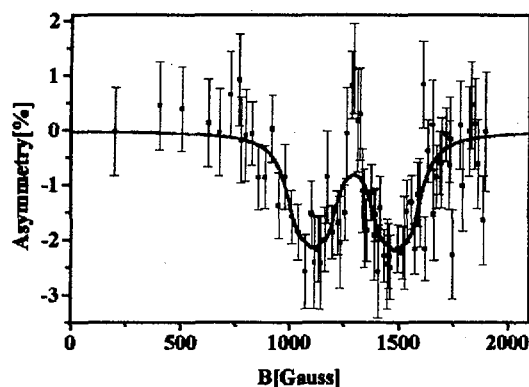


Figure 1 : NMR-resonances : At well-defined magnetic field values, polarization is induced resonantly by applying an RF-field with constant frequency, perpendicular to the static magnetic field. The  $^{18}\text{N}$ -fragments are stopped in a Mg single crystal oriented such that it's c-axis nearly coincides ( $1^\circ < \beta < 2^\circ$ ) with B.

- [1] G. Neyens, N. Coulier, S. Teughels, S. Ternier, K. Vyvey, R. Coussement, D.L. Balabanski, J.M. Casandjian, M. Chartier, M.D. Cortina-Gil, M. Lewitowicz, W. Mittig, A.N. Ostrowski, Heavy Ion Physics 7 (1998) 101-106
- [2] W.F. Rogers, G. Neyens, N. Coulier, S. Teughels, K. Vyvey, S. Ternier, G. Georgiev, R. Coussement, A. Lépine-Szily, Bulletin of the American Physical Society, 42 (1997) 1642
- [3] G.Neyens, N.Coulier, S.Ternier, K.Vyvey, R.Coussement, D. Balabanski, J.M. Casandjian, M. Chartier, D. Cortina-Gil, M.Lewitowicz, W.Mittig, A.N. Ostrowski, P. Roussel-Chomaz, N.Alamanos, A. Lépine-Szily, Physics Letters B393, 1-2 (1997) 36-41
- [4] G. Neyens, N. Coulier, S. Ternier, K. Vyvey, R. Coussement, D. Balabanski, J.M. Casandjian, M. Chartier, M.D. Cortina-Gil, M. Lewitowicz, W. Mittig, A.N. Ostrowski, P. Roussel-Chomaz, N. Alamanos, A. Lépine-Szily, Proc. of the First Int. Workshop on Physics of Unstable Nuclear Beams, Sao Paulo, Brazil, August 28-31, 1996, Eds. C.A. Bertulani, L.F. Canto, M.S. Hussein, World Scientific, Singapore, New Jersey, London, Hong Kong, p. 346-353
- [5] N. Coulier, G. Neyens, S. Ternier, K. Vyvey, R. Coussement, D. Balabanski, J.M. Casandjian, M. Chartier, M.D. Cortina-Gil, M. Lewitowicz, W. Mittig, A.N. Ostrowski, P. Roussel-Chomaz, N. Alamanos, A. Lépine-Szily, Acta Physica Polonica B28 (1997) 407-411
- [6] N. Coulier, G. Neyens, S. Teughels, G. Georgiev, S. Ternier, K. Vyvey, R. Coussement, D.L. Balabanski, M.D. Cortina-Gil, M. Lewitowicz, W. Mittig, F. De Oliveira Santos, P. Roussel-Chomaz, W.F. Rogers, A. Lépine-Szily, Nuovo Cimento, Proceedings of the XVI Nuclear Physics Divisional Conference - SNEC98 (March 31 - April 4, 1998, Padova, Italy)
- [7] G. Neyens et al., in preparation
- [8] B. A. Brown and B. H. Wildenthal, Ann. Rev. of Nucl. Part. Sci. 38, 29 (1988),
- [9] B.A. Brown, private communication
- [10] P.H. Heenen, private communication and S.K. Patra, Nucl. Phys. A559 (1992) 73

## Charge-exchange reaction induced by ${}^6\text{He}$

M.D. Cortina-Gil<sup>a,1</sup>, A. Pakou<sup>b,h</sup>, P. Roussel-Chomaz<sup>a</sup>, N. Alamanos<sup>b</sup>, F. Auger<sup>b</sup>,  
J. Barrette<sup>c</sup>, Y. Blumenfeld<sup>e</sup>, J. M. Casandjian<sup>a,2</sup>, M. Chartier<sup>a,3</sup>, V. Fekou-Youmbi<sup>b</sup>, B.  
Fernandez<sup>b</sup>, N. Frascaria<sup>e</sup>, A. Gillibert<sup>b</sup>, H. Laurent<sup>b</sup>, A. Lepine<sup>f</sup>, W. Mittig<sup>a</sup>,  
N. Orr<sup>g</sup>, V. Pascalon<sup>e</sup>, J. A. Scarpaci<sup>e</sup>, J. L. Sida<sup>b</sup>, T. Suomijarvi<sup>e</sup>

<sup>a</sup>GANIL(DSM/CEA, IN2P3/CNRS), BP 5027,14021 Caen Cedex, France

<sup>b</sup>CEA/DSM/DAPNIA/SPhN Saclay, 91191 Gif-sur-Yvette Cedex, France

<sup>c</sup>Foster Radiation Lab. Mc Gill University, Montreal, Canada H3A 2B1

<sup>d</sup>Lawrence Livermore National Laboratory, Livermore, California 94550

<sup>e</sup>IPN, IN2P3/CNRS 91406 Orsay Cedex, France

<sup>f</sup>IFUSP, DFN, C. P 66318, 05315-970, Sao Paulo, S. P Brasil

<sup>g</sup>LPC- ISMRA, Blud du Maréchal Juin, 1405 Caen, France

<sup>h</sup>Department of Physics , The University of Ioannina, Greece

Abstract: The charge exchange reaction  $p({}^6\text{He}, {}^6\text{Li})$  was studied in reverse kinematics with a secondary  ${}^6\text{He}$  beam at 41.6 MeV /nucleon. Angular distributions for the reactions connecting the ground states and the one leading from the ground state of  ${}^6\text{He}$  to its isobaric analogue state in  ${}^6\text{Li}$  have been obtained between  $0^\circ$  and  $20^\circ$  in the center of mass. The results were analyzed into the context of a microscopic calculation.

Nucleon-nucleus elastic scattering and charge exchange reactions have been widely studied in the past with stable targets and provided valuable information on nuclear properties such as the nucleon-nucleon interaction, energy levels or transition matrix elements [1-2]. It was shown by Lane that the inclusion of the isospin term in the optical potential has the effect of coupling all the channels with the same total isospin [3]. In this way the charge-exchange reaction  $(p,n)$  connecting two isobaric analogue states is coupled to the elastic scattering reaction because the structure of the target and the residual nucleus are essentially the same, differing only in the isospin. In this context, a consistent description of the  $(p,p)$  and  $(p,n)$  angular distributions could provide information on the isoscalar and isovector part of the nucleon-nucleon interaction and could also ideally probe differences between the proton and neutron density distributions [4].

Nowadays, the advent of intense secondary beam facilities allows to extend these studies to unstable nuclei by using secondary radioactive beams and inverse kinematics and test our understanding of the nuclear properties far from the valley of stability.

We have studied the  $p({}^6\text{He}, {}^6\text{Li})n$  reaction, which populates two states : the ground state of  ${}^6\text{Li}$  via a Gamow-Teller transition (GT) and the 3.56 MeV excited state of the same nucleus, which is the isobaric analogue state (IAS) of the  ${}^6\text{He}$  ground state. The 3.56 MeV state of  ${}^6\text{Li}$  is predicted theoretically to be a halo state [5]. Therefore this reaction provides the opportunity to



study simultaneously transitions connecting a halo state and either a standard or another halo state.

To analyze the data we have used an optical model potential, obtained by folding the standard JLM interaction [6] for stable nuclei ( $\lambda_v=1, \lambda_w=0.8$ ) with neutron and proton densities obtained by Hartree-Fock calculations [7] and assuming that the isoscalar and isovector strengths of the JLM interaction are known from direct reaction studies with stable nuclei. However, these calculations had failed to reproduce the experimental data, Figure 1. In this point, it has to be reminded that a fit to our previous elastic scattering data  $p(^6\text{He}, ^6\text{He})p$ , had also failed to reproduce the experimental differential cross sections with standard normalization parameters. It was suggested [8] that a good fit could be obtained by adjusting either the real part or the imaginary part of the optical potential. The effect of the normalization of the real and imaginary part of the entrance channel optical potential for the present (p, n) data is shown in Figures 1a and 1b respectively. Fig. 1a shows that it is not possible to reproduce the (p, n) angular distribution by a readjustment of the real potential. However this is possible through the imaginary potential (Fig. 1b). The best fit ( $\lambda_v=1, \lambda_w=1.8$ ), which was obtained for the elastic angular distribution, gives also a satisfactory agreement with the charge exchange reaction. This analysis shows that a consistent description of the elastic scattering  $p(^6\text{He}, ^6\text{He})p$  and  $p(^6\text{He}, ^6\text{Li}_{\text{IAS}})n$  charge exchange reaction can be obtained only by assuming a strong renormalization of the imaginary part of the optical potential.

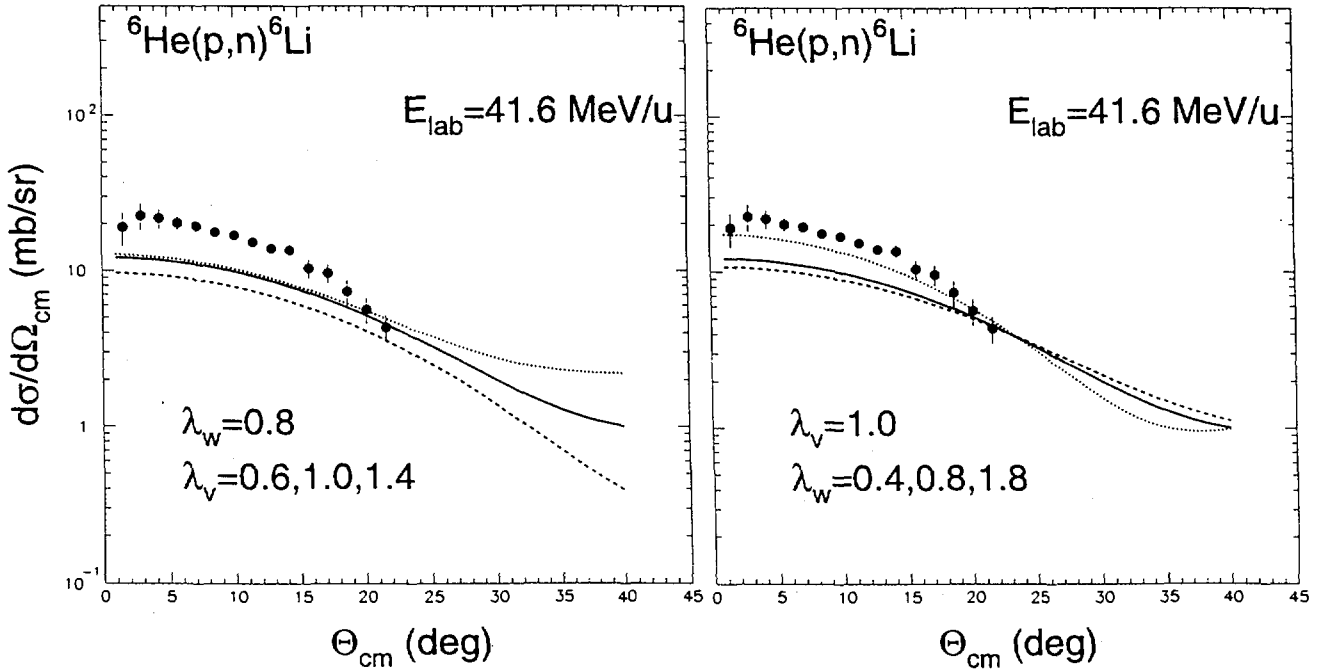


Figure 1: a) Comparison of the present results with JLM calculations adopting different normalization factors for the real part of the potential. b) same for the imaginary part.

Subsequently we have explored the sensitivity of our results against various density distributions. In Fig. 2, the data are compared with JLM predictions obtained with constant real and imaginary normalizing parameters of 1.0 and 1.8 respectively and the following density distributions: a) Hartree-Fock density distributions by Sagawa et al. [7] which give root mean square radii,  $R_p=1.90$  fm and  $R_n=2.36$  fm for protons and neutrons correspondingly-dashed line b) Similar distributions for both protons and neutron ( $\rho_n = (N/Z) \rho_p$ ) -dot-dashed line (where  $\rho_p$  is Sagawa's Hartree-Fock density distribution) c) Distributions calculated, assuming a two Gaussian shape and root mean square radii  $R_p=1.88$  and  $R_n=2.48$ , that is the values obtained from a Glauber analysis of recent  $p(^6\text{He}, ^6\text{He})p$  elastic scattering data obtained at high energy ( $R_p=1.88\pm 0.12$  fm,  $R_n=2.48\pm 0.11$  [9]) -solid line and d) Distributions calculated assuming a two Gaussian shape and root mean square radii  $R_p=1.9$ ,  $R_n=2.36$  that is the Sagawa root mean square radii -dotted line.

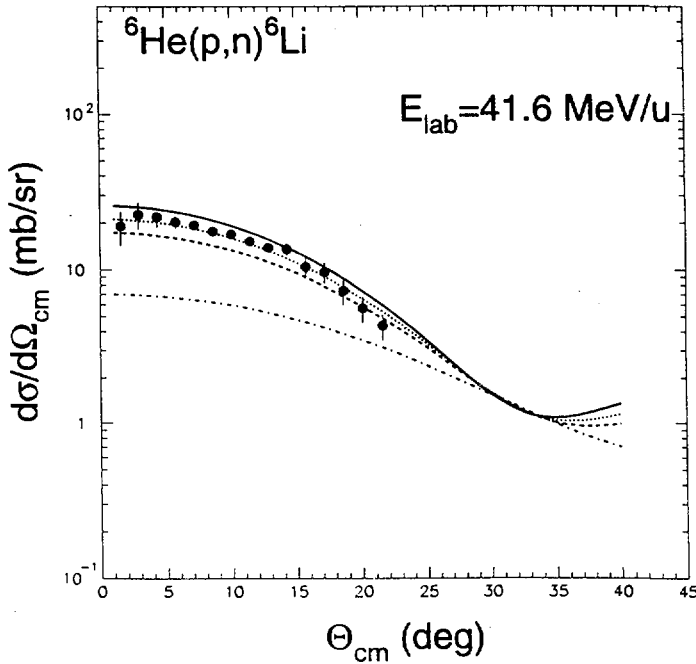


Figure 2: Comparison of the present (p,n) results and JLM calculations ( $\lambda v=1$ ,  $\lambda w=1.8$ ) assuming different density distributions. See text for more details.

It is obvious that the non-halo distributions give predictions way out of our results. The other distributions give results close to the experimental values, with the best fit obtained by the two Gaussian distributions with the values obtained by Sagawa for the root mean square radii. It is interesting to note the sensitivity of the (p,n) cross sections not only to different radii but also to different shapes of the distribution. For instance the angular distributions calculated assuming a two Gaussian shape density distribution and a Hartree-Fock density distribution with the same root mean square radii differ by 20%.

In summary, angular distributions for the reaction connecting the ground state of  $^6\text{He}$  and the ground and excited states of  $^6\text{Li}$  have been obtained. The angular distribution leading

from the  ${}^6\text{He}$  ground state to its isobaric analogue state in  ${}^6\text{Li}$  was analyzed together with the  $p({}^6\text{He}, {}^6\text{He})p$  elastic scattering data. A consistent description of both angular distributions was obtained by using experimental or theoretical density distributions. Precise elastic and  $(p,n)$  charge exchange reaction measurements, extending to larger angles, may be used to investigate the shape of the density distribution or when the density distribution is known from precise high energy measurements to investigate the isoscalar and isovector part of the nucleon-nucleon interaction far from the valley of stability.

## References

- [1] G. R. Satchler and W. G. Love, *Phys. Rep.* 55(1979) 183.
- [2] N. Alamanos and P. Roussel-Chomaz, *Ann. Phys. Fr.* 21 (1996) 601 and refer. therein
- [3] A.M. Lane, *Nucl. Phys.* 35 (1962) 676
- [4] C.J. Batty et al, *Advances in Nuclear Physics* 19 (1989), 1  
M. D. Cortina-Gil et al., *Nucl. Phys.* A641 (1998) 263
- [5] K. Arai et al, *Phys. Rev.* C51 (1995) 2488.
- [6] J. -P. Jeukenne, A. Lejeune and C. Mahaux, *Phys. ReV. C* 10(1974)1391 ; *Phys. Rev.* 15 (1977) 10 ; *Phys. Rev. C*16 (1977) 80.
- [7] H. Sagawa, *Phys. Lett* B286 (1992) 315.
- [8] M. D Cortina-Gil et al, *Phys. Lett.* B401 (1997) 9
- [9] G. D. Alkharov et al. *Phys. Rev. Lett.* 78 (1997) 2313.

**NEXT PAGE(S)  
left BLANK**

## **A2 - EXOTIC NUCLEI AND DECAY MODES**

# Decay Spectroscopy of Neutron Rich Nuclei

GANIL E267

A.T. Reed<sup>1</sup>, O. Tarasov<sup>2</sup>, C. Donzaud<sup>3</sup>, R.D. Page<sup>1</sup>, D. Guillemaud-Mueller<sup>3</sup>,  
Yu. Penionzhkevich<sup>2</sup>, R.G. Allatt<sup>1</sup>, J.C. Angélique<sup>4</sup>, R. Anne<sup>5</sup>, C. Borcea<sup>6</sup>, V. Burjan<sup>7</sup>,  
W.N. Catford<sup>8</sup>, Z. Dlouhý<sup>7</sup>, S. Grévy<sup>3</sup>, M. Lewitowicz<sup>5</sup>, S. Lukyanov<sup>2</sup>, F.M. Marques<sup>4</sup>,  
G. Martinez<sup>5</sup>, A.C. Mueller<sup>3</sup>, P.J. Nolan<sup>1</sup>, J. Novák<sup>9</sup>, N.A. Orr<sup>4</sup>, F. Pougheon<sup>3</sup>,  
P.H. Regan<sup>8</sup>, M.G. Saint-Laurent<sup>5</sup>, T. Siiskonen<sup>9</sup>, E. Sokol<sup>2</sup>, O. Sorlin<sup>3</sup>, J. Suhonen<sup>9</sup>,  
W. Trinder<sup>5</sup>, S. Vincent<sup>8</sup>

<sup>1</sup>University of Liverpool, <sup>2</sup>FLNR JINR Dubna, <sup>3</sup>IPN Orsay, <sup>4</sup>LPC Caen, <sup>5</sup>GANIL,  
<sup>6</sup>IAP Bucharest, <sup>7</sup>NPI Rez, <sup>8</sup>University of Surrey, <sup>9</sup>University of Jyväskylä

Nuclei possessing neutron/proton ratios radically larger than those of stable isotopes exhibit unexpected phenomena which have revolutionised our understanding of nuclear physics. Although the neutron drip line has probably been delimited for elements below neon [1] and atomic masses of many nuclei have been measured [2], comparatively little is known about their radioactive decay characteristics or spectroscopy. Such measurements can probe important details of the underlying microscopic structures which give rise to the novel phenomena.

The neutron rich nuclei of interest were produced by the fragmentation of a 0.5  $\mu$ A 77.7A MeV beam of the rare isotope  $^{36}\text{S}^{16+}$  in a range of tantalum targets mounted on carbon backings and separated using the LISE3 spectrometer [3]. The selected nuclei were implanted into a stack of six silicon detectors located at the focal plane of LISE3, which were used to provide an unambiguous identification of the ions on an event-by-event basis and to detect  $\beta$ -particles emitted in the radioactive decay of the implanted nuclei.

The energies of  $\gamma$ -rays emitted following  $\beta$ -decay were measured using 4 germanium detectors, each of 70 % relative efficiency, mounted in close proximity to the implantation point around 0° to the secondary beam direction. The silicon detector stack was surrounded on three sides by 42 cylindrical  $^3\text{He}$  proportional counters, which were used to determine  $\beta$ -delayed neutron emission probabilities.

In these measurements it was possible for the first time to identify  $\gamma$ -rays emitted in the  $\beta$ -decays of  $^{24}\text{O}$ ,  $^{25-27}\text{F}$  and  $^{28-30}\text{Ne}$  and to obtain candidate  $\gamma$ -ray lines in another 2 cases, which will provide the basis for further investigations. The half-lives of the selected nuclei were determined from the time intervals between their arrival and subsequent  $\beta$ -decay, with 4 half-lives being measured for the first time. The energy level schemes deduced from these spectra, the absolute  $\beta$ -decay strengths feeding these levels and the half-lives are being compared with shell model calculations in order to learn more about the structure of nuclei in this region.

[1] O. Tarasov *et al.*, Physics Letters **B409**, 64 (1997).

[2] N.A. Orr *et al.*, Physics Letters **B258**, 29 (1991).

[3] R. Anne *et al.*, Nuclear Instruments and Methods **A257**, 215 (1987).

## Study of neutron-rich nuclei near the N=20 neutron closed shell

R.Allatt<sup>b</sup>, J.C.Angelique<sup>c</sup>, R.Anne<sup>d</sup>, C.Borcea<sup>e</sup>, Z.Dlouhy<sup>f</sup>, C.Donzaud<sup>g</sup>, S.Grevy<sup>g</sup>,  
D.Guillemaud-Mueller<sup>g</sup>, M.Lewitowicz<sup>d</sup>, S.Lukyanov<sup>a</sup>, A.C.Mueller<sup>g</sup>, F.Nowacki<sup>d</sup>,  
N.A.Orr<sup>c</sup>, Yu.E.Penionzhkevich<sup>a</sup>, R.D.Page<sup>b</sup>, F.Pougheon<sup>g</sup>, A.Reed<sup>b</sup>, M.G.Saint-  
Laurent<sup>d</sup>, W.Schwab<sup>g</sup>, E.Sokol<sup>a</sup>, O.Tarasov<sup>a</sup>, W.Trinder<sup>d</sup>, J.S.Winfield<sup>d</sup>

<sup>a</sup> *Flerov Laboratory of Nuclear Reactions, Joint Institute for Nuclear Research, 141980  
Dubna, Moscow region, Russia*

<sup>b</sup> *Dept. of Physics, University of Liverpool, Liverpool, L69 7ZE, UK*

<sup>c</sup> *Laboratoire de Physique Gorpusculaire, CNRS-IN2P3, ISMRA et Universite de Caen,  
Boulevard du Marechal Juin, 14050 Caen Cedex, France*

<sup>d</sup> *Grand Accelérateur National d'Ions Lourds, BP 5027, 14076 Caen Cedex 5, France*

<sup>e</sup> *Institute of Atomic Physics, Bucharest-Magurele P.O. Box MG6, Rumania*

<sup>f</sup> *Nuclear Physics Institute, 250 68 Rez, Czech Republic*

<sup>g</sup> *Institut de Physique Nucleaire, CNRS-IN2P3, 91406 Orsay Cedex, France*

An interesting aspect of the region of N=20 nuclei is the transition from spherical to deformed shapes in the so-called “island of inversion”. The deformations in this region can also result in the appearance of the isomeric states of extremely neutron-rich isotopes. Such effects may influence the decay properties of these nuclei, such as half-life, neutron emission probability. The lack of experimental information on the very neutron-rich isotopes in the C-Al region is mainly due to the very low production cross section. Therefore a very exotic primary beam of <sup>36</sup>S (78 AMeV) ions, which give an opportunity to study the  $\beta$ -delayed neutron emission from neutron-rich nuclei with the magic neutron number N=20, such as <sup>29</sup>F, <sup>30</sup>Ne and <sup>31</sup>Na, was used in the experiment. The experiment was carried out at GANIL using the Si(Li) detectors telescope at the focal point. The implantation detectors were surrounded by 3He filled neutron detectors. This detector system was served as both the fragment identification and  $\beta$ -delayed neutron decay measurement. For the first time the  $\beta$ -decay half-lives and neutron emission probability were measured for <sup>30</sup>Ne, <sup>26,27,29</sup>F. Additionally, the cases of <sup>22</sup>N, <sup>24</sup>O, <sup>24-29</sup>Ne, <sup>25</sup>F, <sup>30,32</sup>Na were re-examined (see Table) [1].

The measured half-lives for <sup>28</sup>Ne and <sup>30,31</sup>Na agree within the error bars with the previous experiments. The only important discrepancy is observed for <sup>29</sup>Ne. The experimental half-lives obtained here are in good agreement (within a factor of two) with the sd shell-model calculations of Wildenthal et al. [2] including the values for <sup>27,29</sup>F and <sup>29,30</sup>Ne. The last suggest that the deformation phenomena, predicted and observed in the Mg - Na region, disappears below Z=11. Thus the standard shell-model space seems to be sufficient to predict half-lives of fluorine and neon isotopes in vicinity of N=20.

The attempt to synthesize  $^{28}\text{O}$  was carried out at GANIL using the LISE spectrometer, which collects projectile-like fragments. The fragmentation of a  $^{36}\text{S}^{16+}$  (78.1 AMeV) beam with a mean intensity 800 enA was expected to increase the production rate of the neutron-rich isotopes near  $N=20$ . Measurements of the momentum distributions of all fragments with  $N=20$  and an optimization of the target material (Be, C, Ni, Ta) and thickness were undertaken to determine the best setting of the LISE spectrometer for  $^{28}\text{O}$ . It was found that the Ta target produced the highest rates of the neutron-rich nuclei.

During 53-hours measurement with this average beam intensity no events corresponding to  $^{26}\text{O}$  and  $^{28}\text{O}$  have been obtained. In the addition to  $A/q$  and  $Z$  identification, a horizontal coordinate in the intermediate dispersive plane of the LISE spectrometer was in agreement with the computer simulation of horizontal images in the focal point. According to the estimation given by the modified formula of Summerer et al.c [2] one could expect about 11 events corresponding to  $^{28}\text{O}$ .

The results of the present experiment point to the particle instability of the  $^{28}\text{O}$  isotope as well as for  $^{26}\text{O}$ . An upper limit for the cross section of the formation of the oxygen isotopes extracted from the data is estimated to be 0.7 pb and 0.2 pb for  $^{26}\text{O}$  and  $^{28}\text{O}$ , respectively.

**Table.** Experimental values of the  $\beta$ -decay half-lives and neutron emission probability of neutron-rich nuclei close to  $N=20$

Isotope	Experimental results			
	This work		Table of Isotopes 1996	
	$T_{1/2}$ ms	$P_n$ %	$T_{1/2}$ ms	$P_n$ %
$^{22}\text{N}$	31 (5)	37 (14)	24 (7)	35 (5)
$^{24}\text{O}$	67 (10)	12 (8)	61 (26)	58 (12)
$^{25}\text{F}$	70 (10)	14 (5)	59 (4)	15 (10)
$^{27}\text{F}$	9.6 (0.8)	11 (4)		
$^{29}\text{F}$	2.4 (0.8)	100 (80)		
$^{27}\text{Ne}$	22 (6)	0 (3)	32 (2)	2 (0.5)
$^{28}\text{Ne}$	20 (3)	11 (3)	17 (4)	22 (3)
$^{29}\text{Ne}$	15 (3)	27(9)	200 (10)	
$^{30}\text{Ne}$	7 (2)	9 (17)		
$^{30}\text{Na}$	50 (4)			
$^{31}\text{Na}$	18 (2)		48 (2)	30 (4)

### References

1. O.Tarasov et al., Phys. Lett. B409 (1997) p.64.
2. B.H.Windenthal et al. Phys. Rev. C28 (1983), p.1343.
3. K.Summerer et al. Phys. Rev. C42 (1990) p.2546.

## Beta decay half-lives of neutron rich Ti-Co isotopes around N=40

C. Donzaud<sup>1</sup>, O. Sorlin<sup>1</sup>, L. Axelsson<sup>1,6</sup>, M. Belleguic<sup>1</sup>, D. Guillemaud-Mueller<sup>1</sup>,  
S. Leenhard<sup>1</sup>, F. Pougheon<sup>1</sup>, J.M. Daugas<sup>2</sup>, M. Lewitowicz<sup>2</sup>, M.J. Lopez<sup>2</sup>, F. De Oliveira<sup>2</sup>,  
M.G. Saint-Laurent<sup>2</sup>, R. Béraud<sup>3</sup>, E. Chabannat<sup>3</sup>, G. Cachel<sup>3</sup>, A. Emsallem<sup>3</sup>,  
C. Longour<sup>4</sup>, J.E. Sauvestre<sup>5</sup>, C. Borcea<sup>2,7</sup>  
<sup>1</sup>IPN Orsay, <sup>2</sup>Ganil, <sup>3</sup>IPN Lyon, <sup>4</sup>IREs Strasbourg, CEA-DAM Bruyeres-Le-Chatel<sup>5</sup>,  
<sup>6</sup>Chalmers University of technology, Sweden, <sup>7</sup>IAP Bucarest, Roumanie

The present work is a continuation of that presented in in ref. [1]. The isotopes <sup>57-59</sup>Ti, <sup>59-62</sup>V, <sup>61-64</sup>Cr, <sup>62-66</sup>Mn, <sup>65-68</sup>Fe, <sup>67-70</sup>Co were produced from the fragmentation of a <sup>86</sup>Kr 60,4 MeV/u beam impinging onto a Ni(140 μm)+C(9,5 mg/cm<sup>2</sup>) target. The primary beam intensity was on average 1.2 μA. A wedge-shape Be foil of 219 μm-thickness was placed in the intermediate focal plane of the LISE3 spectrometer in order to reduce the rate of contaminant nuclei. Two different magnetic settings were used to transmit nuclei with increasing neutron richness. Bρ-values of 2.6730 Tm and 2.7268 Tm were chosen in the first part of the spectrometer. Selected nuclei were identified in redundant way by means of 4 consecutive 300, 300, 500, 500 μm silicon detectors placed close to the final focal plane. Fragments were implanted in the last detector divided in twelve 2mm-wide vertical strips. Energy and time of each fragment and each β-particle were registered in the strips of interest. Each time a nucleus was implanted, the primary beam was switched off during 1.5 seconds, a duration long enough for the decay of the mother and daughter nuclei. All β-particles detected during this time are taken into account for half-life determination. A β-particle is accepted as an event coming from the β-decay of the implanted isotope if it is above the background of a given strip and detected in the same strip or in neighbouring strips as the precursor. Other β-events are counted as β-background. This background presents a period of 4.7±0.5 s and 5.3±0.1 s for the two explored tunings of the spectrometer coming from decays of long-lived nuclei. Background frequency values of less than 0.05 β-particles per second were obtained for each strip. The β-efficiency was found around 15 %. Preliminary results are given in Table 1.

The deduced Fe and Co half-lives are compatible with the values obtained at GSI [2] except for <sup>70</sup>Co and <sup>65</sup>Fe. The decay curve of <sup>65</sup>Fe, almost flat, can be reproduced only if the <sup>65</sup>Fe half-life is close to the half-life of the <sup>65</sup>Co daughter nucleus. This excludes to deduce a value as short as the one measured at GSI [2, 5]. To determine the <sup>65</sup>Mn half-life, our value of <sup>65</sup>Fe half-life (1317(279) ms) was used to fix the daughter nucleus half-life parameter. A value of 100(8) ms was found, between the values of ref. [2] and [7]. With a daughter half-life parameter of 800 ms, a value of 88(8) ms would be deduced. In <sup>64,66</sup>Mn isotopes, our values are shorter than those published in ref. [2] but are in very good agreement with those measured at CERN/Isolde [7].

The measured Cr half-lives are close to those of ref. [2]. For <sup>61-62</sup>Cr the decay curves were fitted using the known half-lives of the <sup>61-62</sup>Mn daughter nuclei. For <sup>63</sup>Cr, our <sup>63</sup>Mn half-life value was taken into account. The <sup>62</sup>Cr decay curve cannot be fitted using the known <sup>62</sup>Mn half-life of 880(150) ms ; the fit requires a much shorter value of 80(15) ms. The beta-decay may occur to a <sup>62</sup>Mn isomeric state which decays to the <sup>62</sup>Fe with an half-life of 80(15) ms. The <sup>64</sup>Cr half-life is found much smaller than the one of <sup>63</sup>Cr in contradiction with the prediction



of Möller (96.6 et 153.9 ms for  $^{63}\text{Cr}$  and  $^{64}\text{Cr}$  respectively with deformation parameter of 0.3 et 0.017 [8]).

In addition to the implantation set-up, 4 germanium detectors were placed in cross geometry around the last Si detector in order to detect the main  $\gamma$  transitions. In the decay of  $^{60}\text{V}$  a strong transition was observed for the first time at 646.3(1.5) KeV which probably corresponds to the  $2^+ \rightarrow 0^+$  transition in  $^{60}\text{Cr}$ . This energy is smaller than the  $2^+$ -energy of the isotone  $^{62}_{36}\text{Fe}$  measured at 878.6(1.5) KeV in decay of the  $^{62}\text{Mn}$ . We found that the decay of  $^{64}\text{Mn}$  feeds the  $2^+$ -level of the  $^{64}_{38}\text{Fe}$  at 745.5(1.5) KeV. This shows the decrease of the  $2^+$ -energy in the Fe towards N=40 and the weakening of this shell strength.

Isotope	N	$T_{1/2}$ (ms)	$T_{1/2}$ (ms) (previous measurements)
$^{57}\text{Ti}$	125	67(25)	180(30)[2], 56(20)[1]
$^{58}\text{Ti}$	286	47(10)	
$^{59}\text{Ti}$	86	58(17)	
$^{59}\text{V}$	2306	75(7)	130(20)[2], 70(40)[1] 200(40)[2]
$^{60}\text{V}$	1042	122(18)	
$^{61}\text{V}$	776	43(7)	
$^{62}\text{V}$	51	65(31)	
$^{61}\text{Cr}$	4455	251(22)	270(20)[2]
$^{62}\text{Cr}$	2771	187(15)	190(30)[2]
$^{63}\text{Cr}$	835	115(16)	110(70)[2]
$^{64}\text{Cr}$	215	44(12)	
$^{63}\text{Mn}$	7966	322(23)	240(30)[3], 250(40)[6], 275(4)[7]
$^{64}\text{Mn}$	7348	85(5)	140(30)[2], 89(4)[7]
$^{65}\text{Mn}$	3226	100(8)	110(20)[2], 88(4)[7]
$^{66}\text{Mn}$	400	62(14)	90(20)[2], 66(4)[7]
$^{65}\text{Fe}$	3541	1317(279)	600(100)[3], 450(150)[5]
$^{66}\text{Fe}$	3541	440(60)	440(60)[2]
$^{67}\text{Fe}$	2820	500(98)	470(50)[2]
$^{67}\text{Co}$	805	436(77)	370(100)[3], 420(70)[6]
$^{68}\text{Co}$	597	170(30)	230(20)[3], 180(100)[4]
$^{69}\text{Co}$	1961	187(38)	270(50)[4]
$^{70}\text{Co}$	259	92(25)	150(20)[2]

Table 1: Half-life values compared to previous measurements. N is the number of implanted isotopes.

## References

- [1] O. Sorlin et al, Nucl. Phys. A362 (1998) 205
- [2] F. Ameil et al, Eur. Phys. Jour. A1 (1998) 275
- [3] F. Ameil, thèse IPN Orsay 1997
- [4] M. Bernas et al, Phys. Rev. Lett. 67 (1991) 3661
- [5] S. Czajkowski et al, Z. Phys. A348 (1994) 267
- [6] U. Bosch et al, Phys. Lett. 164B (1985) 22
- [7] A. Wöhr, ENAM conference juin 1998
- [8] P. Möller et al, At. Data and Nucl. Data Tables 66 (1997) 131

## Beta-decay studies of the neutron-rich isotopes $^{53-55}\text{Sc}$ , $^{54-57}\text{Ti}$ , $^{56-59}\text{V}$ .

O. Sorlin, V. Borrel, S. Grévy, D. Guillemaud-Mueller, A.C. Mueller, F. Pougheon  
*Institut de Physique Nucléaire IN2P3-CNRS, F-91406 ORSAY, France*

W. Böhmer, K-L. Kratz, T. Mehren, P. Möller<sup>∇</sup>, B. Pfeiffer, T. Rauscher<sup>#</sup>  
*Institut für Kernchemie, Universität Mainz, D-55099 MAINZ, Germany*

M.G. Saint-Laurent, R. Anne, M. Lewitowicz, A. Ostrowski  
*Grand Accélérateur National d'Ions Lourds (GANIL), BP-5027, F-14021 CAEN, France*

T. Dörfler, W-D. Schmidt-Ott  
*II Physikalisches Institut, Universität Göttingen, D-37073 GÖTTINGEN, Germany*

The very short half-life of  $T_{1/2}=90\pm 15\text{ms}$  compared to the neighbouring isotopes  $^{52}\text{Ca}$  ( $T_{1/2}=4.6\pm 0.3\text{s}$ ) [1] is due to strong Gamow-Teller transition in the  $\beta$ -decay of  $^{53}\text{Ca}_{33}$ . This effect suggests a rather strong subshell gap at a neutron number  $N=32$  which is confirmed by the large energy of the first  $2^+$ -state in  $^{52}\text{Ca}_{32}$  ( $E=2.563\text{ MeV}$ ) [2]. It is therefore of interest to investigate the decay of the neighbouring  $N=33$  isotones  $^{54}\text{Sc}$ ,  $^{55}\text{Ti}$  and  $^{56}\text{V}$  in order to check whether this spherical gap subsists when adding protons to the calcium nucleus. The isotopes  $^{53-55}\text{Sc}$ ,  $^{54-57}\text{Ti}$  and  $^{56-59}\text{V}$  were produced by fragmentation of a  $64.5\text{ MeV/u}$   $^{65}\text{Cu}$  beam impinging onto a  $90\text{ mg/cm}^2$  Be target. An aluminum wedge-degrader of  $221.5\text{ }\mu\text{m}$ -thickness was placed in the intermediate focal plane of the LISE3 spectrometer in order to reduce the rate of contaminant nuclei. The WIEN-type velocity filter of LISE3 was used in addition to eliminate long-lived nuclei, which would have enhanced the  $\beta$ -background. Nuclei selected were identified by means of two consecutive  $300\text{-}\mu\text{m}$  and  $500\text{-}\mu\text{m}$  silicon detectors. The nuclei were implanted in the second Si-detector, consisting of twelve  $2\text{mm}$ -wide strips ( $24\times 2\times 0.5\text{ mm}$ ). The energies and times for the heavy ions and for the  $\beta$ -particles were measured in each strip. A  $\beta$ -event was only recorded as valid if occurring in the same strip as the precursor nucleus or in one of the neighbouring strips. In addition, each time a nucleus was implanted, the primary beam was switched off for about five times its expected  $\beta$ -half-life in order not to implant contaminant nuclei during the  $\beta$ -measurement. The Si telescope was surrounded by a  $4\pi$   $\gamma$ -detection system, composed of a ring of 8 BGO crystals. This system allowed a very high  $\beta$ - $\gamma$  coincidence efficiency,  $\epsilon_{\beta}\times\epsilon_{\gamma}\approx 0.25\times 0.66$ ,  $\epsilon_{\beta}$  and  $\epsilon_{\gamma}$  being the average total  $\beta$ - and  $\gamma$ -efficiencies respectively. The BGO detectors also allowed to investigate the strongest  $\gamma$ -transitions. Energy levels could be tentatively assigned with a resolution of 18%. Adopted values of the half-lives from ref [3,4] are included in the Table 2. The QRPA model of Möller and Randrup [5] has been used to calculate GT-strength functions and  $\beta$ -decay half-lives. In this approach, Folded Yukawa (FY) wave functions and single-particle energies serve as a starting point to determine

<sup>∇</sup> permanent address : Scientific Computing and Graphics, Inc., P. O. Box 1440, Los Alamos, NM 87544.

<sup>#</sup> present address : Institut für Theoretische Physik, Klingelbergstrasse 82, Universität Basel, CH-4046 Basel, Switzerland.

the deformation-dependent wave functions. Experimental data are compared with QRPA predictions in ref. [4] in order to get the "best possible agreement" and thus learn something about the underlying nuclear structure.

Table 1: Measured half-lives for Sc<sup>[4]</sup>, Ti<sup>[3]</sup> and V<sup>[4]</sup>. The number of nuclei implanted is indicated in the second column

isotope	total	T <sub>1/2</sub> [ms]
<sup>53</sup> Sc	682	> 3000
<sup>54</sup> Sc	363	225(40)
<sup>55</sup> Sc	42	120(40)
<sup>54</sup> Ti	1729	1500 (400)
<sup>55</sup> Ti	3523	620 (60)
<sup>56</sup> Ti	1531	150 (30)
<sup>57</sup> Ti	40	56 (20)
<sup>56</sup> V	1746	230(25)
<sup>57</sup> V	3189	323(30)
<sup>58</sup> V	1347	205(20)
<sup>59</sup> V	55	70(40)

This can be done by varying the deformation parameter  $\epsilon_2$  within and slightly beyond the model predictions in this mass region suggested by FRDM [6] and ETFSI [7] models. The Lipkin-Nogami approximation is applied to calculate pairing correlations. In some cases, the measured probability  $p$  of feeding excited states, or  $p_{g.s.} = 1-p$  to populate the ground state (g.s.), can be used as a constraint on the deformation. For example, in the case of <sup>54</sup>Sc, the experiment has shown that all decay is followed by a gamma emission ( $p \geq 100\%$ ). For a spherical configuration, one would expect a strong  $\nu f_{5/2} \rightarrow \pi f_{7/2}$  GT-transition g.s. to g.s. transition ( $p=0\%$ ) and a short half-life of  $T_{1/2} = 14$  ms. The long measured half-life  $T_{1/2} = 225 \pm 40$ ms, and the high probability of feeding excited states can be obtained for a deformed shape of  $\epsilon_2=0.15$  and a g.s. configuration of  $\pi[330]1/2 \otimes \nu[312]3/2$ . Similar conclusions can be drawn for Ti and V isotopes, pointing towards a region of slightly

prolate shapes. Therefore, one can conclude that this subshell closure is only present for <sup>52</sup>Ca isotope. Indeed for this Z=20 isotope, the configuration mixing is very small, probably due to the magic proton-number that hinders any deformation.

### References:

- [1] M. Langevin et al., Phys. Lett. B **130**, 251 (1983)
- [2] A. Huck et al., Phys. Rev. C **31**, 2226 (1985)
- [3] T. Dörfler et al., Phys. Rev. C **54**, 2894 (1996)
- [4] O. Sorlin et al., Nucl. Phys. A **632**, 205(1998)
- [5] P. Möller and J. Randrup, Nucl. Phys. A **514**, 1 (1990)
- [6] P. Möller et al., At. Data Nucl. Data Tables **59**,185 (1995)
- [7] Y. Aboussir et al., At. Data Nucl. Data tables **61**, 127 (1995)

# A mass measurement experiment to investigate the shell closures far from stability

F.Sarazin<sup>a</sup>, H.Savajols<sup>a</sup>, W.Mittig<sup>a</sup>, P.Roussel-Chomaz<sup>a</sup>, G.Auger<sup>a</sup>, D.Baiborodin<sup>b</sup>,  
A.V.Belozyorov<sup>c</sup>, C.Borcea<sup>d</sup>, Z.Dlouhy<sup>b</sup>, A.Gillibert<sup>e</sup>, A.S.Lalleman<sup>a</sup>, M.Lewitowicz<sup>a</sup>,  
S.M.Lukyanov<sup>c</sup>, F.de Oliveira<sup>a</sup>, N.Orr<sup>f</sup>, Y.E.Penionzhkevich<sup>c</sup>, Z.Ren<sup>a</sup>, D.Ridikas<sup>a</sup>,  
H.Sakurai<sup>g</sup>, A.de Vismes<sup>a</sup>

<sup>a</sup> GANIL, BP 5027, 14076 Caen Cedex 05, France, <sup>b</sup> Nucl.Phys.Inst., 25068 REZ Czech Republic

<sup>c</sup> LNR, JINR, Dubna, P.O. Box 79, 101 000 Moscow, Russia, <sup>d</sup> IAP, Bucharest, Roumania

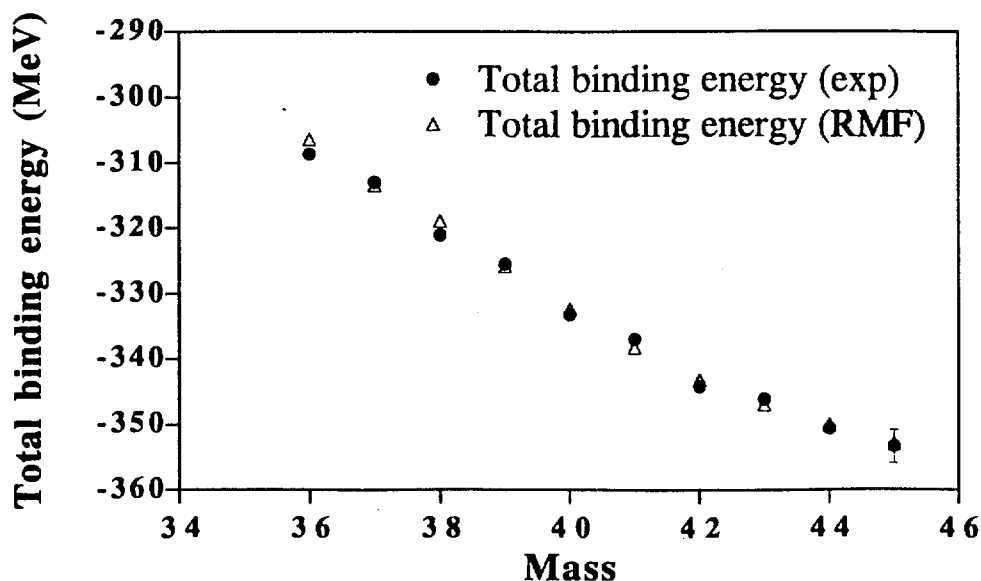
<sup>e</sup> CEA/DSM/DAPNIA/SPhN, CEN Saclay, 91191 Gif-sur-Yvette, France

<sup>f</sup> LPC, Bd Maréchal Juin, 14050 Caen Cedex, France, <sup>g</sup> RIKEN, Wako, Saitama 351-01 Japan

One of the present fundamental question for nuclear structure is whether the magic numbers are universal or whether they change in certain regions far from stability or even disappear altogether. An example of such magicity breaking is given by the N=20 neutron rich nuclei where a collapse of the standard N=20 shell closure has been observed. Recently, there has been an increase of interest in the N=28 isotones far from stability, motivated by the possible existence of anomalies in the shell closures.

An experimental observable that may give a first answer to this question is the binding energy which can be deduced from nuclear masses. We have performed at GANIL a mass measurement experiment with the SPEG spectrometer by using a direct time of flight technique. Our goal was to investigate the N=20 and N=28 neutron shell closures for nuclei from Z=6 to Z=20. The production of these neutron-rich nuclei have been obtained by the fragmentation of a <sup>48</sup>Ca primary beam at 60 A.MeV on a Ta target located in the SISSI device.

Among the N=28 isotones, the <sup>44</sup>S is a nucleus having a mid-shell proton configuration. A previous experiment [1] showed that this nucleus is deformed which can be a signature of a new region of deformation even for the N=28 magic number. The mass of this nucleus have been measured for the first time with an error of less than 500 keV [2]. We performed a Relativistic Mean Field (RMF) calculation for the sulfur isotopes and we found an excellent agreement with the experimental binding energy, as it is shown in the figure, and with the deformation parameter  $\beta_2$ .



## References

- [1] T. Glasmacher et al., Phys.Lett. **B395** (1997) 163-168
- [2] F. Sarazin et al., Proceedings ENAM 98 (in press)

# Observation of the $Z=N+1$ Nuclei $^{77}_{39}\text{Y}$ , $^{79}_{40}\text{Zr}$ and $^{83}_{42}\text{Mo}$

Z. Janas<sup>a,b</sup>, C. Chandler<sup>c</sup>, B. Blank<sup>a</sup>, P.H. Regan<sup>c</sup>, A.M. Bruce<sup>d</sup>, W.N. Catford<sup>c</sup>, N. Curtis<sup>c</sup>, S. Czajkowski<sup>a</sup>, Ph. Dessagne<sup>e</sup>, A. Fleury<sup>a</sup>, W. Gelletly<sup>c</sup>, J. Giovinazzo<sup>e</sup>, R. Grzywacz<sup>b,f</sup>, M. Lewitowicz<sup>f</sup>, C. Longour<sup>e</sup>, C. Marchand<sup>a</sup>, Ch. Miché<sup>e</sup>, N.A. Orr<sup>g</sup>, R.D. Page<sup>h</sup>, C.J. Pearson<sup>c</sup>, M.S. Pravikoff<sup>a</sup>, A.T. Reed<sup>h</sup>, M.G. Saint-Laurent<sup>f</sup>, J.A. Sheikh<sup>c</sup>, S.M. Vincent<sup>c</sup>, R. Wadsworth<sup>i</sup>, D.D. Warner<sup>j</sup>, J.S. Winfield<sup>f</sup>

<sup>a</sup> CEN Bordeaux-Gradignan, Le Haut-Vigneau, F-33175 Gradignan Cedex, France

<sup>b</sup> Institute of Experimental Physics, Warsaw University, PL-00681 Warsaw, Poland

<sup>c</sup> Department of Physics, University of Surrey, Guildford, GU2 5XH, UK

<sup>d</sup> Department of Mechanical Engineering, University of Brighton, Brighton, BN2 4GJ, UK

<sup>e</sup> IReS, BP 28, F-67037 Strasbourg Cedex, France

<sup>f</sup> GANIL, BP 5027, F-14076 Caen Cedex, France

<sup>g</sup> LPC, ISMRA et Université de Caen, Bld. Maréchal Juin, F-14050 Caen Cedex, France

<sup>h</sup> Oliver Lodge Laboratory, Dept. of Physics, University of Liverpool, Liverpool, L69 7ZE, UK

<sup>i</sup> Department of Physics, University of York, Heslington, York, YO1 4DD, UK

<sup>j</sup> CCLRC Daresbury Laboratory, Warrington, WA4 4AD, UK

The very neutron deficient  $Z=N+1$  nuclei  $^{77}_{39}\text{Y}$ ,  $^{79}_{40}\text{Zr}$ , and  $^{83}_{42}\text{Mo}$  have been observed for the first time following the fragmentation of a  $^{92}\text{Mo}$  beam. In contrast, no evidence was found for the existence of  $^{81}_{41}\text{Nb}$  and  $^{85}_{43}\text{Tc}$ . The observation of  $^{77}_{39}\text{Y}$  is of particular interest in light of the instability of the odd-proton,  $Z=N+1$  systems,  $^{69}_{35}\text{Br}$ ,  $^{73}_{37}\text{Rb}$ ,  $^{81}_{41}\text{Nb}$ , and  $^{85}_{43}\text{Tc}$  and may be explained as a consequence of the shape polarising effect of the highly deformed, prolate  $Z=N=38$  core.

Nuclei with nearly equal proton and neutron numbers in the  $A\sim 80$  region are of fundamental interest for two distinct reasons. Firstly, the nuclear structure properties of these nuclei are strongly determined by deformed shell gaps in the nuclear single particle potential [1], which causes dramatic changes of shape with the addition or removal of one or two nucleons [2,3]. In particular, the nucleon numbers 36 and 38 have been identified with highly deformed oblate [4] and prolate [2,5] shell gaps, respectively. Secondly, these systems lie in the vicinity of the proton drip line, the precise position of which is a vital element in determining the path of the postulated astrophysical rapid proton ( $rp$ ) process of nucleosynthesis [6]. The single particle spectrum of orbitals which lie close to the proton and neutron Fermi surfaces varies considerably with deformation, and this nuclear structure aspect can have a subtle, but important effect on the binding energies of odd-proton nuclei and the position of the proton drip line.

Discrepancies in the predictions of mass models [7-9] regarding the proton stability of odd- $Z$ ,  $T_z = -1/2$  nuclei and their bearing on the path or termination of the  $rp$  process have prompted searches for the existence and studies of the decay properties of the  $Z=N+1$  systems  $^{65}_{33}\text{As}$ ,  $^{69}_{35}\text{Br}$ ,  $^{73}_{37}\text{Rb}$  and  $^{77}_{39}\text{Y}$ . Whereas the nucleus  $^{65}_{33}\text{As}$  has been observed and its basic decay properties studied [10,11], the heavier odd- $Z$   $T_z = -1/2$  nuclei were not observed in fragmentation reactions. However, there is evidence that, as the  $T_z = -1/2$ , odd- $Z$  nuclei become more spherical with increasing  $Z$  - due to the increasing influence of the  $N=Z=50$  doubly magic core - the population of higher- $l$  orbitals may increase the binding and the centrifugal barrier for the odd proton. Indeed, Rykaczewski *et al.* [12] have observed  $^{89}_{45}\text{Rh}$ , which constitutes the heaviest odd- $Z$ ,  $T_z = -1/2$  nucleus identified to date.

In the present work, evidence for the particle stability of three isotopes with  $Z=N+1$ , namely  $^{77}_{39}\text{Y}$ ,  $^{79}_{40}\text{Zr}$  and  $^{83}_{42}\text{Mo}$ , together with upper limits for the lifetimes of  $^{81}_{41}\text{Nb}$  and  $^{85}_{43}\text{Tc}$  are presented. The nuclei were produced in the fragmentation of a  $^{92}\text{Mo}^{37+}$  beam of 60 MeV/nucleon provided by the GANIL facility. The primary beam, of typical intensity 100 enA, was incident on a 50 - 100 mg/cm<sup>2</sup> natural nickel targets. The reaction products were collected and separated using the LISE3 spectrometer [13]. At the final focus of the spectrometer, the fragments were stopped in a four-element silicon detector telescope, the first element of which was acted as an energy-loss ( $\Delta E$ ) detector. A time-of-flight (TOF) measurement together with the energy-loss and total-energy measurement was used to obtain an unambiguous identification in  $Z$ ,  $N$  and  $Q$  for each fragment. Figure 1a shows a two-dimensional spectrum of the atomic number  $Z$  determined from the energy loss in the  $\Delta E$  detectors versus the  $A/Z$  ratio determined from the fragment TOF. The projections of the  $T_z = 0$  and  $-1/2$  species onto the  $Z$  axis are presented in figures 1b,c and clearly show the presence of the even- $Z$ ,  $Z=N+1$  nuclei,  $^{75}_{38}\text{Sr}$ ,  $^{79}_{40}\text{Zr}$  and  $^{83}_{42}\text{Mo}$  in our spectra. Evidence for the existence of  $^{75}\text{Sr}$  has been previously reported [10]. Tentative indication for the existence of  $^{79}_{40}\text{Zr}$  has been presented previously by Yennello *et al.* [14]. This isotope is clearly present in the spectrum of figure 1c. Both  $^{79}_{40}\text{Zr}$  and  $^{83}_{42}\text{Mo}$  are predicted by the mass evaluation of Audi and Wapstra [7] to be proton bound, with proton separation energies of approximately 1.9 MeV and 1.2 MeV, respectively.

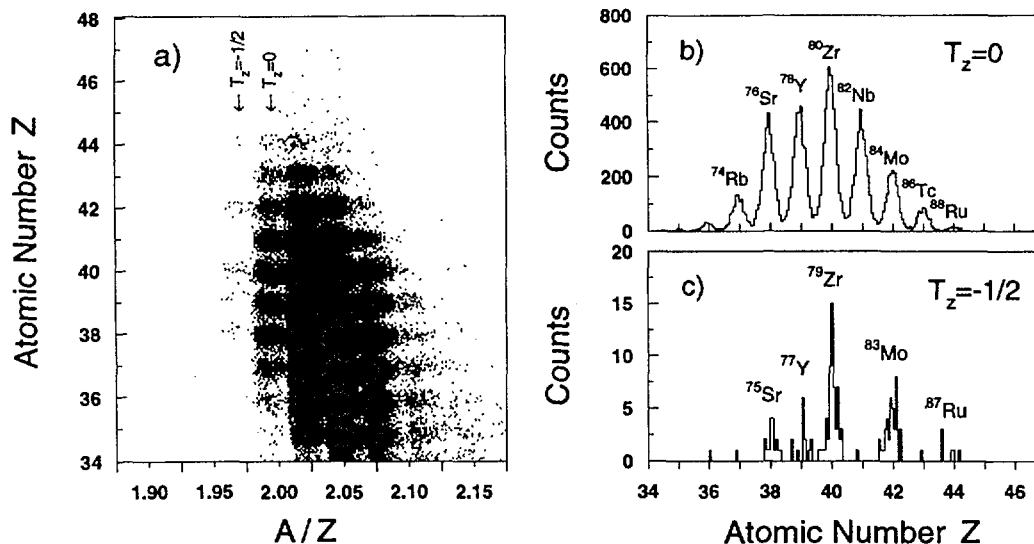


FIG. 1. Two-dimensional atomic number  $Z$  versus  $A/Z$  ratio particle identification plot showing the previously unobserved  $T_z = -1/2$  nuclei  ${}^{77}_{39}\text{Y}$ ,  ${}^{79}_{40}\text{Zr}$  and  ${}^{83}_{42}\text{Mo}$  as well as the absence of  ${}^{81}_{41}\text{Nb}$  and  ${}^{85}_{43}\text{Tc}$  (a). The right-hand side shows projections of the particle identification plot onto the  $Z$  axis for the  $T_z = 0$  (b) and the  $T_z = -1/2$  (c).

For even- $Z$  nuclei, the pairing between the protons provides extra binding and these nuclei are expected to extend further beyond the  $N=Z$  line than odd- $Z$  nuclei. Thus, in common with previous studies [10,15,16], the current data show no evidence for  ${}^{73}_{37}\text{Rb}$ . Moreover, as demonstrated in figure 1c, we found no evidence for the odd-proton nuclei  ${}^{81}_{41}\text{Nb}$  and  ${}^{85}_{43}\text{Tc}$ , indicating that these nuclei are proton unbound and that their lifetimes are short compared to the time of flight through the spectrometer. Assuming the observation limit of one count and considering the yields expected relative to the neighboring isotopes, we derived upper limits of 80 and 100 ns for the half-lives of  ${}^{81}\text{Nb}$  and  ${}^{85}\text{Tc}$ , respectively. In the region expected for  ${}^{77}_{39}\text{Y}$ , figure 1c clearly shows a peak indicating that the half-life of this isotope is longer than  $0.5 \mu\text{s}$ , the flight time through the LISE3 spectrometer. Qualitatively, this observation is consistent with the proton separation energies predicted by Audi and Wapstra [7] which suggest that  ${}^{77}\text{Y}$  is the most bound of the odd- $Z$ ,  $T_z = -1/2$  nuclei in this region. The observation of  ${}^{77}_{39}\text{Y}$  may be interpreted as evidence for the shape polarising effect of the  $N=Z=38$  prolate shell gap, as predicted by the macroscopic-microscopic calculations. Future decay studies of  ${}^{77}\text{Y}$  which would determine spin and parity of the ground state would thus be of interest in either supporting or contradicting this assumption. Such studies should also be able to establish whether or not this isotope is particle bound via observation of the decay mode  $-\beta^+$  (predicted  $\beta$ -decay half-life  $T_{1/2}^\beta = 190 \text{ ms}$  [17]) or direct proton emission, which should be more probable if the proton decay energy is larger than 380 keV.

- 
- [1] W. Nazarewicz *et al.*, Nucl. Phys. **A435**, 397 (1985)
  - [2] C.J. Lister *et al.*, Phys. Rev. **C42**, R1191 (1990)
  - [3] W. Gelletly *et al.*, Phys. Lett. **253B**, 287 (1991)
  - [4] C. Chandler *et al.*, Phys. Rev. **C56**, R2924 (1997)
  - [5] C.J. Lister *et al.*, Phys. Rev. Lett. **49**, 308 (1982)
  - [6] H. Schatz *et al.*, Phys. Rep. **294**, 167 (1998)
  - [7] G. Audi, A.H. Wapstra, Nucl. Phys. **A595**, 409 (1995)
  - [8] P. Möller *et al.*, At. Data Nucl. Data Tables **59**, 185 (1995)
  - [9] Y. Aboussir *et al.*, At. Data Nucl. Data Tables **61**, 127 (1995)
  - [10] M.F. Mohar *et al.*, Phys. Rev. Lett. **66**, 1571 (1991)
  - [11] J.A. Winger *et al.*, Phys. Lett. **299B**, 214 (1993)
  - [12] K. Rykaczewski *et al.*, Phys. Rev. **C52**, R2310 (1995)
  - [13] A.C. Mueller and R. Anne, Nucl. Inst. Meth. Phys. Res. **B56/57**, 559 (1991)
  - [14] S.J. Yennello *et al.*, Phys. Rev. **C46**, 2629 (1992)
  - [15] B. Blank *et al.*, Phys. Rev. Lett. **74**, 4611 (1995)
  - [16] R. Pfaff *et al.*, Phys. Rev. **C53**, 1753 (1996)
  - [17] P. Möller *et al.*, At. Data Nucl. Data Tables **66**, 131 (1997)

# HALF-LIVES OF HEAVY ODD-ODD $N=Z$ NUCLEI SELECTED WITH THE LISE3 SPECTROMETER

C. Longour<sup>a</sup>, J. Garcés Narro<sup>b</sup>, B. Blank<sup>c</sup>, M. Lewitowicz<sup>d</sup>, Ch. Miehé<sup>a</sup>, P.H. Regan<sup>b</sup>, D. Applebe<sup>e</sup>, L. Axelsson<sup>f</sup>, A.M. Bruce<sup>g</sup>, W.N. Catford<sup>b</sup>, C. Chandler<sup>b</sup>, R.M. Clark<sup>h</sup>, D.M. Cullen<sup>e</sup>, S. Czajkowski<sup>c</sup>, J.M. Daugas<sup>d</sup>, Ph. Dessagne<sup>a</sup>, A. Fleury<sup>c</sup>, L. Frankland<sup>g</sup>, W. Gelletly<sup>b</sup>, J. Giovinazzo<sup>c</sup>, B. Greenhalgh<sup>i</sup>, R. Grzywacz<sup>j</sup>, M. Harder<sup>g</sup>, K.L. Jones<sup>b</sup>, N. Kelsall<sup>i</sup>, T. Kszczot<sup>j</sup>, R.D. Page<sup>e</sup>, C.J. Pearson<sup>b</sup>, A.T. Reed<sup>e</sup>, O. Sorlin<sup>k</sup>, R. Wadsworth<sup>i</sup>

<sup>a</sup> *IReS Strasbourg, UMR7500, CNRS-IN2P3 et Université Louis Pasteur, BP28, F-67037 Strasbourg Cedex 2, France*

<sup>b</sup> *Department of Physics, University of Surrey, Guildford, GU2 5XH, UK*

<sup>c</sup> *CEN Bordeaux-Gradignan, Le Haut-Vigneau, F-33175 Gradignan Cedex, France*

<sup>d</sup> *GANIL, BP 5027, F-14021 Caen Cedex, France*

<sup>e</sup> *Department of Physics, Oliver Lodge Laboratory, University of Liverpool, Liverpool, L69 7ZE, UK*

<sup>f</sup> *Department of Physics, Chalmers University of Technology, S-412 96 Göteborg, Sweden*

<sup>g</sup> *Department of Mechanical Engineering, University of Brighton, Brighton, BN2 4GJ, UK*

<sup>h</sup> *Nuclear Science Division, LBNL, Berkeley, CA 94720, USA*

<sup>i</sup> *Department of Physics, University of York, Heslington, York, YO1 4DD*

<sup>j</sup> *Institute of Experimental Physics, Warsaw University, PL-00681 Warsaw, Poland*

<sup>k</sup> *Institut de Physique Nucléaire, 91406 Orsay, France*

(July 20, 1998)

The  $\beta^+$ -decay half-lives of the neutron-deficient, odd-odd,  $N=Z$  nuclei  $^{74}\text{Rb}$ ,  $^{78}\text{Y}$ ,  $^{82}\text{Nb}$  and  $^{86}\text{Tc}$  have been measured following the fragmentation of a primary  $^{92}\text{Mo}$  beam at an energy of 60 MeV per nucleon. The half-lives were measured by correlating  $\beta^+$  decays with the implantation of unambiguously identified fragments. The deduced  $\log ft$  values are consistent with superallowed transitions and the transitions observed may be of Fermi type.

The half-life of a nucleus is a fundamental property of a radioactive species. This value depends on the initial and the final nuclear state wavefunction as well as of the interaction which mediates the decay : Fermi or Gamow-Teller. Fundamental aspects of the weak interaction can be studied with basic ingredients such as half-lives and  $\beta^+$ -decay energies. Specific nuclear structure features can be tested. The technique of projectile fragmentation of medium-mass heavy ions, as used with the LISE/GANIL facility, and the time correlated  $\beta$  decay after implantation has provided an efficient method for the measurement of the fast Fermi-type decays in the heavy odd-odd,  $N=Z$  systems,  $^{74}\text{Rb}$ ,  $^{78}\text{Y}$ ,  $^{82}\text{Nb}$  and  $^{86}\text{Tc}$ .

The nuclei of interest were produced at GANIL by the fragmentation of a  $^{92}\text{Mo}^{37+}$  beam of energy of 60 MeV per nucleon with an average current of 200 enA on a natural nickel target of thickness 120  $\mu\text{m}$ . The fragmentation products were separated using the LISE3 spectrometer [1] with an achromatic beryllium degrader of thickness 50  $\mu\text{m}$ . At the final focus, the fragments were stopped in a three element telescope, the first element of which consisted of a 300  $\mu\text{m}$  thick energy loss ( $\Delta E$ ) silicon detector for element ( $Z$ ) identification. The ions of interest were stopped in a twelve-strip segmented silicon detector of thickness 500  $\mu\text{m}$  situated behind the  $\Delta E$  detector. A third silicon detector, also of thickness 500  $\mu\text{m}$ , was placed behind the strip detector and was used in the off-line analysis to discriminate against any contaminating lighter ions reaching the final focus. A time-of-flight (TOF) of the fragments was measured by taking the time difference between a fast signal extracted from the  $\Delta E$  detector and the cyclotron radiofrequency. This TOF together with the energy loss in the  $\Delta E$  detector and the magnetic rigidity of the dipole magnets in the LISE3 spectrometer was used to obtain an unambiguous identification in  $Z$  and  $N$  for each fragment, using previously described techniques [2]. After implantation of a fragment of interest, the primary beam was immediately shut-off for one second. A millisecond clock was reset each time a detected fragment caused the beam to be cut off so that each radioactivity event was labelled. Subsequent  $\beta^+$ -decays were then correlated with specific implants by looking for signals during this beam-off period in the implanted strip. In the off-line analysis, software cuts were applied to a two-dimensional particle identification matrix  $\Delta E$  versus TOF. This allowed the radioactivity time distributions to be obtained for specific nuclear species.

For the odd-odd,  $N=Z$  systems  $^{74}\text{Rb}$ ,  $^{78}\text{Y}$ ,  $^{82}\text{Nb}$  and  $^{86}\text{Tc}$ , the time distributions are shown in figure 1. The half-lives of the radioactive decays were estimated by applying a least-square fit to the data with a function composed of an exponential decay plus a constant background level.

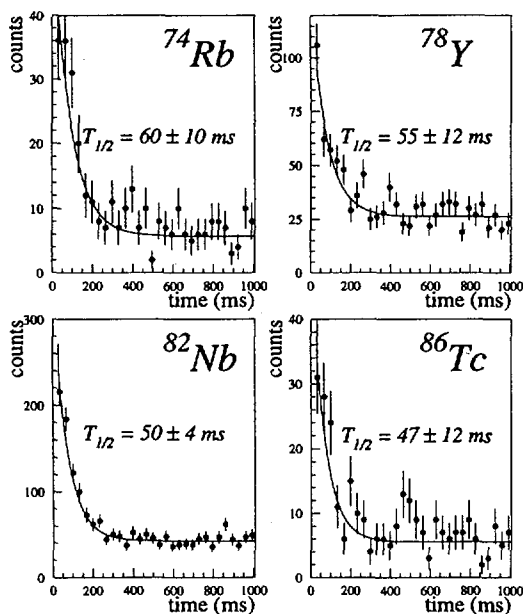


FIG. 1. Time spectra for the odd-odd  $N = Z$  nuclei. The data were recorded for about 90 hours. The fit is shown by the solid line and assumes an exponential decay with a constant level background.

Our analysis yielded half-lives  $T_{1/2}$  of  $(60 \pm 10)$  ms for  $^{74}\text{Rb}$ ,  $(55 \pm 12)$  ms for  $^{78}\text{Y}$ ,  $(50 \pm 4)$  ms for  $^{82}\text{Nb}$ , and  $(47 \pm 12)$  ms for  $^{86}\text{Tc}$ . The half-life of  $^{74}\text{Rb}$  has previously been measured by D'Auria *et al.* [3] to be  $(64.9 \pm 0.5)$  ms which is consistent with our result for this nucleus and provides a cross-check for our method. The time curves gated by the even-even,  $N=Z$  nuclei in this region all showed flat time distributions indicative of decay lifetimes longer than the one second beam-off period. The  $\log ft$  values for these  $\beta^+$ -decays were calculated assuming i) a branching ratio of 100% for the observed transition, ii) a ground-state to ground-state decay and iii) the  $\beta^+$ -decay  $Q$  values from the mass evaluation of Audi *et al.* [4]. The calculated  $\log ft$  values are all compatible within error bars with  $\log ft = 3.5$  which is indicative of a superallowed character for each of these decays. The question now arises what is the ground state of the odd-odd  $N=Z$  nuclei  $^{78}\text{Y}$ ,  $^{82}\text{Nb}$  and  $^{86}\text{Tc}$ . Looking at the systematic, light nuclei, from deuteron to mass 38, have ground state  $T = 0$ ,  $I \neq 0$  and heavier nuclei have  $T = 1$ ,  $I^\pi = 0^+$  ground states. This has been shown for  $^{74}\text{Rb}$  by recent in-beam work [5] and assumed for  $^{78}\text{Y}$  by J. Uusitalo *et al.* [6]. We make the assumption that the ground state is  $T = 1$ ,  $I^\pi = 0^+$  for  $^{78}\text{Y}$ ,  $^{82}\text{Nb}$  and  $^{86}\text{Tc}$ . The daughter nuclei populated following the  $\beta^+$  decay of these odd-odd,  $N=Z$  systems are even-even nuclei ( $T_z = 1$ ), and thus have  $0^+$  ground states. This implies that the decays observed in our studies are all of a  $0^+ \rightarrow 0^+$  Fermi character.

The LISE3 spectrometer, combining electromagnetic dipoles, achromatic degrader and Wien filter, provides a clean selection and identification of nuclei produced by the fragmentation of a  $^{92}\text{Mo}$  beam. Such a facility has allowed the first half-life measurement for the odd-odd,  $N=Z$  nuclei  $^{78}\text{Y}$ ,  $^{82}\text{Nb}$  and  $^{86}\text{Tc}$ .

- 
- [1] A.C. Mueller and R. Anne, Nucl. Inst. Meth. Phys. Res. **B56/57**, 559 (1991)
  - [2] D. Bazin *et al.*, Nucl. Phys. **A515**, 349 (1990)
  - [3] J.M. D'Auria *et al.*, Phys. Lett. **B66**, 233 (1977)
  - [4] G. Audi *et al.*, Nucl. Phys. **A624**, 1 (1997)
  - [5] D. Rudolph *et al.*, Phys. Rev. Lett. **76**, 376 (1996)
  - [6] J. Uusitalo *et al.* Phys. Rev. **C57**, 2259 (1998)



# Mass Measurements near $N=Z$ and $^{100}\text{Sn}$

M. Chartier<sup>1)</sup>, G. Auger<sup>1)</sup>, W. Mittig<sup>1)</sup>, J. C. Angélique<sup>2)</sup>, G. Audi<sup>3)</sup>, J. M. Casandjian<sup>1)</sup>,  
A. Cunsolo<sup>4)</sup>, C. Donzaud<sup>5)</sup>, M. Chabert<sup>1)</sup>, J. Fermé<sup>1)</sup>, L.K. Fifield<sup>10)</sup>,  
A. Foti<sup>4)</sup>, A. Gillibert<sup>11)</sup>, A. Lépine-Szily<sup>1,6)</sup>, M. Lewitowicz<sup>1)</sup>, S. Lukyanov<sup>7)</sup>,  
M. Mac Cormick<sup>1)</sup>, D. J. Morrissey<sup>8)</sup>, M.H. Moscatello<sup>1)</sup>, O.H. Odland<sup>13)</sup>, N. A. Orr<sup>2)</sup>,  
A. Ostrowski<sup>1)</sup>, G. Politi<sup>12)</sup>, C. Spitaels<sup>1)</sup>, B. M. Sherrill<sup>8)</sup>, C. Stephan<sup>5)</sup>,  
T. Suomijärvi<sup>5,8)</sup>, L. Tassan-Got<sup>5)</sup>, D. J. Vieira<sup>9)</sup>, A. C. C. Villari<sup>1)</sup>, J. M. Wouters<sup>9)</sup>

1. GANIL, Bld Henri Becquerel, BP 5027, 14021 Caen Cedex, France
2. LPC-ISMRA, Bld du Maréchal Juin, 14050 Caen, Cedex, France
3. CSNSM, Bâtiment 108, 91406 Orsay Cedex, France
4. INFN, Corso Italia 57, 95129 Catania, Italy
5. IPN Orsay, BP 1, 91406 Orsay Cedex, France
6. IFUSP-Universidade de São Paulo, C.P.20516, 14098 São Paulo, Brasil
7. LNR, JINR, Dubna, P.O. Box 79, 101 000 Moscow, Russia
8. NSCL, MSU, East Lansing MI, 48824-1321, USA
9. LANL, Los Alamos NM, 87545, USA
10. Dep. of Nucl. Phys., RSPHySE, Austr. Nat. Univ., ACT 0200, Australia
11. CEA/DSM/DAPNIA/SPhN, CEN Saclay, 91191 Gif-sur-Yvette, France
12. Università di Catania, Dip. di Fisica, Corso Italia 57, 95125 Catania, Italy
13. Universitetet i Bergen, Fysisk Institutt, Allégaten 55, 5007 Bergen, Norway

Nuclei near  $N=Z$  may be studied in order to determine the shell-closures, the deformations that may particularly strong and symmetries such as mirror symmetries and Wigner terms. An experiment aimed at measuring the masses of proton-rich nuclei in the mass region  $A \approx 60-80$  has been performed, using a direct time-of-flight technique in conjunction with SISSI and the SPEG spectrometer at GANIL. The nuclei were produced via the fragmentation of a  $^{78}\text{Kr}$  beam (73 MeV/nucleon). A novel technique for the purification of the secondary beams, based on the stripping of the ions and using the  $\alpha$  and the SPEG spectrometers, was successfully checked. It allows for good selectivity without altering the beam quality. This work is described in ref. 1.

In the region  $N \approx Z$  of the nuclear chart, fusion evaporation reactions are very competitive with respect to fragmentation reactions. They should be considered, too, for the preparation of Isol beams. Secondary ions of  $^{100}\text{Ag}$ ,  $^{100}\text{Cd}$ ,  $^{100}\text{In}$  and  $^{100}\text{Sn}$  were produced via the fusion-evaporation reaction  $^{50}\text{Cr} + ^{58}\text{Ni}$  at an energy of 5.1 MeV/nucleon, and were accelerated simultaneously in the second cyclotron of GANIL (CSS2). About 10 counts were observed from the production and acceleration of  $^{100}\text{Sn}^{22+}$ . The masses of  $^{100}\text{Cd}$ ,  $^{100}\text{In}$  and  $^{100}\text{Sn}$  were measured with respect to  $^{100}\text{Ag}$  using the CSS2 cyclotron, with precisions of  $2 \times 10^{-6}$ ,  $3 \times 10^{-6}$  and  $10^{-5}$  respectively. More details can be found in ref.2,3.

## References

- [1] M.Chartier et al., Nucl.Phys.**A637**(1998)3.
- [2] G. Auger et al., Nucl.Instr.Meth. **A350**, (1994)235.
- [3] M. Chartier, et al, Phys.Rev.Lett.**77**(1996)2400

**NEXT PAGE(S)  
left BLANK**

## **B - NUCLEAR REACTIONS**

## **B1 - PERIPHERAL COLLISIONS**

## Some regularities in the production of isotopes in $^{32,34,36}\text{S}$ - induced reactions in the energy range 6-75 A MeV

O.B. Tarasov<sup>a</sup>, Yu.E. Penionzhkevich<sup>a</sup>, R. Anne<sup>b</sup>, D.S. Baiborodin<sup>a</sup>, A.V. Belozyorov<sup>a</sup>, C. Borcea<sup>c</sup>, Z. Dlouhy<sup>d</sup>, D. Guillemaud-Mueller<sup>e</sup>, R. Kalpakchieva<sup>a</sup>, M. Lewitowicz<sup>b</sup>, S.M. Lukyanov<sup>a</sup>, V.Z. Maidikov<sup>a</sup>, A.C. Mueller<sup>c</sup>, Yu. Ts. Oganessian<sup>a</sup>, M.G. Saint-Laurent<sup>b</sup>, N.K. Skobelev<sup>a</sup>, O. Sorlin<sup>e</sup>, V.D. Toneev<sup>f</sup>, W. Trinder<sup>b</sup>

<sup>a</sup> *Flerov Laboratory of Nuclear Reactions, Joint Institute for Nuclear Research, 141980 Dubna, Moscow region, Russia*

<sup>b</sup> *Grand Accelérateur National d'Ions Lourds, BP 5027, 14076 Caen Cedex 5, France*

<sup>c</sup> *Institute of Atomic Physics, Bucharest-Magurele, P.O.Box MG6, Rumania*

<sup>d</sup> *Nuclear Physics Institute, 250 68 Rez, Czech Republic*

<sup>e</sup> *Institut de Physique Nucleaire, CNRS-IN2P3, 91406 Orsay Cedex, France*

<sup>f</sup> *Bogoliubov Laboratory of Theoretical physics, Joint Institute for Nuclear Research, 141980 Dubna, Moscow region, Russia*

The investigation of the mechanism of nuclear reactions is closely connected with the projects for radioactive nuclear beam facilities, which will open new possibilities for the study of exotic nuclei and which will generate radioactive secondary beams by using primary beams of very different energies. Questions arise concerning to the extent of coexistence of different reaction mechanisms (e.g. multi-nucleon transfer reactions and fragmentation) at various energies, the dependence of the production rates on the isospins, of the projectile and target etc. Some regularities in the production of the isotopes with  $6 \leq Z \leq 14$  are investigated in the reactions induced by  $^{32,34,36}\text{S}$  beams. The results, discussed in the present work have been obtained in a very broad range of the beam energy ( $6 < E < 75$  A MeV) with various targets:  $^{12}\text{C}$ ,  $^{181}\text{Ta}$  and  $^{197}\text{Au}$ . The isotope yields and the most probable fragment mass are studied in relation to the mass and energy of the target and projectile. The experiments with  $^{32,34}\text{S}$  beam energy were  $E < 20$  A MeV carried out at the U-400 cyclotron of the Flerov Laboratory of Nuclear Reactions (JINR). The yields of the various isotopes were measured using the MSP-144 magnetic spectrometer [1]. The  $^{36}\text{S}$  (75 A MeV) beam was provided by the GANIL accelerator facility (France); the isotope yields were measured by the LISE fragment-separator [2]. The distributions of the carbon, oxygen, neon, magnesium and silicon isotopes produced in  $^{32}\text{S}$  and  $^{34}\text{S}$  (6.3; 9.1 and 16 A MeV) and  $^{36}\text{S}$  (75 A MeV) induced reactions on three targets ( $^{12}\text{C}$ ,  $^{181}\text{Ta}$ ,  $^{197}\text{Au}$ ) were obtained. The experimental data at low energy were compared with the calculation within the framework of the dynamical model of deep inelastic collisions [3]. The yields of the isotopes in the intermediate energy region were calculated with the LISE-code. The isotopic distributions of the final (experimentally observed) nuclei were calculated within the framework of the statistical theory of decay of excited primary fragments. The comparison of the experimental data and the calculations shows (Fig. 1a) that the contribution of deep inelastic reactions to the production cross section of both neutron-rich and neutron-deficient isotopes is dominant at low energies (the dashed lines), while at intermediate energies the main contribution is defined by fragmentation reactions.

On the basis of the data obtained the following conclusions can be drawn:

- In the energy range 7-10 MeV/A quite an abrupt decrease in the cross section is observed in the case of a light target as the number of transferred protons increases. At high energies this difference decreases and is negligible at intermediate energies.

- At high energies the isotopic content of the projectile plays a dominant role in the production of nuclei close to the projectile ( $Z \geq 12$ ), while at energies  $E < 20$  MeV/A the production cross sections for  $^{32}\text{S}$  and  $^{34}\text{S}$  beams are comparable.

A difference in the cross sections is only observed in the region of nuclei heavier than the projectile, where pick-up reactions prevail.

The isotope production cross sections are seen to rise for energies up to about 15-20 MeV/A, after which they either flatten or pass through the maximum and drop in the energy regions where fragmentation is expected to prevail.

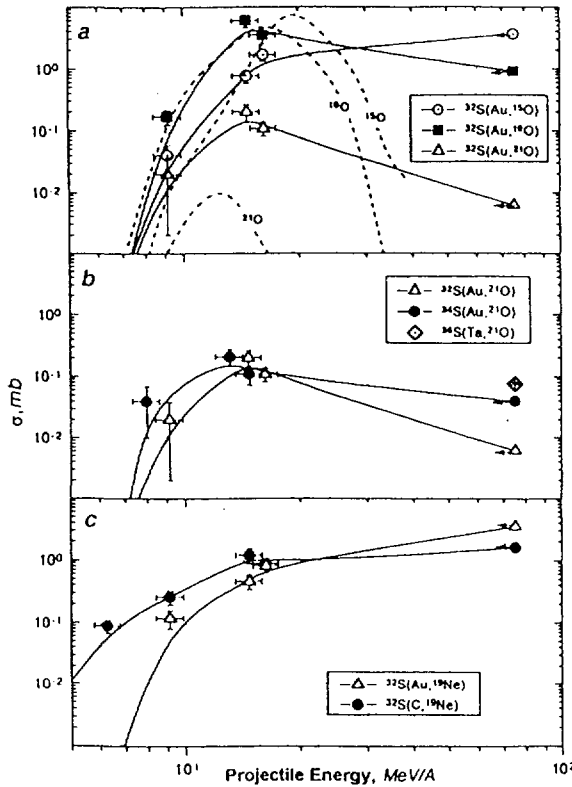


*Fig. 1. Total production cross section for different isotopes as a function of energy. The solid curves are the results of the calculations using a modification of the empirical parametrization. The dashed lines present the calculations of the transfer reaction products.*

### References

1. V.Z.Maidikov et al. Pribori i Tech, Expt. 4 (1979) 68.
2. R.Anne et al. Nucl. Instr. and Meth. A257 (1987) 215.
3. R.Schmidt et al. Nucl. Phys. A311 (1978) 247.

NEXT PAGE(S)  
left BLANK

## **B2 - DISSIPATIVE COLLISIONS**

## Thermal and chemical equilibrium for vaporizing sources

*B. Borderie<sup>1</sup>, F. Gulminelli<sup>2</sup>, M.F. Rivet<sup>1</sup>, L. Tassan-Got<sup>1</sup>  
and the INDRA Collaboration.*

<sup>1</sup> IPN Orsay (IN2P3-CNRS), F-91406 Orsay cedex, France

<sup>2</sup> LPC Caen (IN2P3-CNRS/ISMRA et Université), F-14050 Caen cedex, France

At present there exist many models, describing a simultaneous disassembly of nuclear sources produced in nucleus-nucleus collisions at intermediate energies, which presuppose that before disintegrating these sources achieve partial or complete thermodynamical equilibrium. This hypothesis is essential if one wants to describe the sources by means of macroscopic variables such as pressure and density at finite temperature. We report here on a detailed comparison of the properties of vaporized quasi-projectiles (QP) produced in binary dissipative collisions between  $^{36}\text{Ar}$  and  $^{58}\text{Ni}$  nuclei at 95 A MeV incident energy with a quantum statistical model. Particularly, the completeness of the selected sources made possible the extraction of variances for multiplicities of the different emitted charged particles, thus permitting a more stringent comparison with the model. Apart from the completeness of information, these sources are also interesting because they represent an extreme deexcitation mode for hot pieces of nuclear matter, close to the intuitive expectation of a supercritical nuclear gas. The vaporization events, which correspond to a cross section corrected for efficiency of 1 mb [1], were shown to result mainly (about 90%) from binary dissipative collisions providing us with a well defined set of sources covering a broad range in excitation energy ( $\epsilon^*$ ), from 8 to 28 A MeV for the QP [2].

In the model [4] the emitting source is supposed to undergo a simultaneous disassembly at fixed temperature  $T$ , density  $\rho$  and isospin ( $N/Z$ ) into a gas of fermions and bosons in thermal and also chemical equilibrium [5]. Calculations are performed within the grand canonical ensemble. Corrections to an ideal gas are included in the form of excluded volume effects in the spirit of the Van der Waals gas to deal with collisions and reabsorption at freeze-out [4]. The consequence of the excluded volume is to favour protons, neutrons and alphas over the more loosely bound structures like deuterons and high-lying resonances. Finally the calculated distributions are corrected for the side-feeding of resonance decays. A Metropolis event generator is here introduced to extend

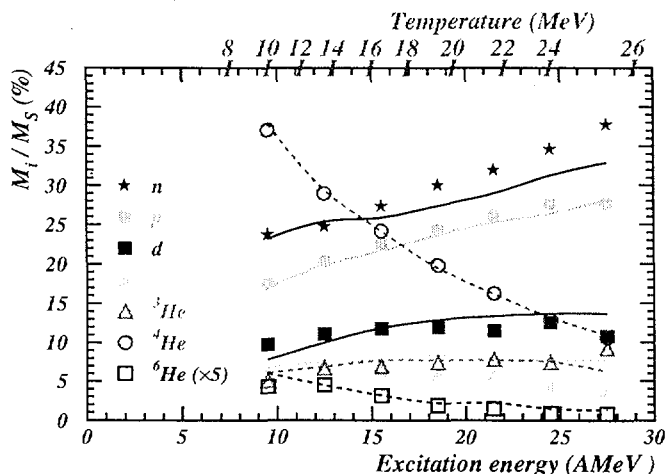


Figure 1: Composition of the QP as a function of its excitation energy. Symbols are for data while the lines are the results of the model. The temperature values used in the model are also given (see text).

the comparison of ref. [3] to the second moment of the multiplicity distributions. To cover

the experimental  $\varepsilon^*$  range the temperature had to be varied from 10 to 25 MeV. Isospin ( $N/Z$ ) was fixed to 1, which is very close to the  $N/Z$  of the system. Finally the freeze-out density has been fixed to  $\rho = \rho_0/3$ , in order to reproduce the experimental ratio between the proton and alpha yields at  $\varepsilon^*=18.5$  MeV calculated from the Metropolis simulation. Fig 1 exhibits the evolution of the relative particle abundance  $M_i/M_s$  where  $M_s$  is the total source multiplicity. The results of the model correspond to lines in Fig 1. Chemical compositions (first moments) as a function of the excitation energy are very well reproduced. Two elements were found essential to get such an agreement. First, the excluded volume correction which was already used in [3]. And second, the extension of the mass table which has been used here (only species up to  ${}^9B$  were included in the partition sum of ref. [3]). As compared to ref. [3], neutron, triton and  ${}^3He$  relative abundances are better reproduced. The comparison data-calculations is displayed in Fig 2 for the variances

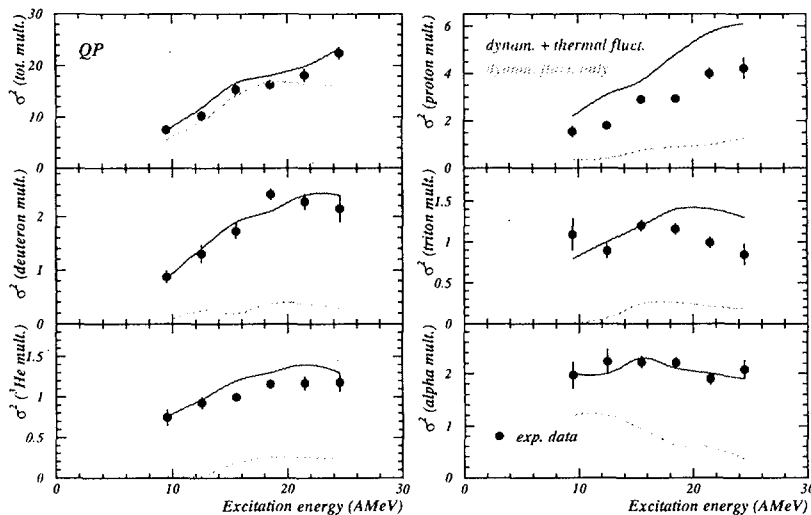


Figure 2: Variances of multiplicity distributions (total, proton, deuteron, triton,  ${}^3He$  and alpha) of the QP as a function of its excitation energy per nucleon. Points refer to the data and the lines are the results of the model (see text). Error bars are statistical errors

associated with the total multiplicity and with the different charged particle multiplicities. The order of magnitude is correctly reproduced by the calculation, as well as the evolution with the excitation energy. The thermal origin of the observed fluctuations is confirmed by a simulation (dashed curves) where only the fluctuations coming from the event selection criteria and/or from the dynamics of the reaction are taken into account and thermal fluctuations are frozen. As expected only variances on the total multiplicity are reproduced in this latter case while the fluctuations observed for the different particles are very small compared to experimental values. The correct prediction of the measured variances validates the value of the freeze-out density fixed in the model and reinforces the idea that thermodynamical equilibrium has been reached.

## References

- [1] C.O. Bacri et al., *Phys. Lett.* **B353** (1995) 27.
- [2] M.F. Rivet et al, *Phys. Lett.* **B388** (1996) 219.
- [3] F. Gulminelli and D. Durand, *Nucl. Phys.* **A615** (1997) 117.
- [4] A. Z. Mekjian, *Phys. Rev.* **C17** (1978) 1051  
S. Das Gupta and A. Z. Mekjian, *Phys. Rep.* **72** (1981) 131.
- [5] B. Borderie et al, *Phys. Lett.* **B388** (1996) 224.



# Energy Sharing in binary collisions

L. Nalpas, Ph. Buchet, J-L. Charvet, R. Dayras, D. Doré  
and the INDRA collaboration

## Abstract

Using the  $4\pi$  multidetector array INDRA at GANIL, we have investigated the reaction  ${}^{36}_{18}\text{Ar} + {}^{58}_{28}\text{Ni}$  for bombarding energies ranging from 52 to 95 MeV/A. Over this energy domain, binary dissipative collisions are the dominant process [1, 2]. The emission sources have been reconstructed from the charged particles emitted in the forward and the backward hemispheres of the center of mass frame. The deposited energy deduced from calorimetry of the decay products is shared equally between the quasi-projectile and the quasi-target suggesting that the thermal equilibrium between the two partners is not achieved.

In order to reconstruct the primary sources from the kinematical properties of the detected charged particles we have developed an event-by-event method based on the “minimum spanning tree” technique [3, 4]. This consists in finding the minimum path linking the particles in the velocity space and break the branch of the tree which maximizes the source separation. The average charge of the reconstructed quasi-projectile ( $Z_{QP} \approx 16$ ) and quasi-target ( $Z_{QT} \approx 24$ ), obtained at 95 MeV/A, are very close to the expected value taking into account the detection efficiency.

Knowing the center-of-mass of the two emitters, the deposited energy ( $\varepsilon_s = E_s^*/A_s$ ) is determined through the calorimetry of the charged particles ( $E_i$ : kinetic energy,  $m_i$  mass):

$$E_s^* = \sum_{i=1}^{M_{tot}} (E_i + m_i) + M_n (\langle E_n \rangle + m_n) - m_s$$

Some assumptions must be done for neutrons which are not detected by the experimental setup. On the one hand, the neutron multiplicity ( $M_n$ ) is deduced from mass and isospin conservation. On the other hand, the neutron energy ( $\langle E_n \rangle$ ) is taken as the mean kinetic energy of protons minus 2 MeV due to the absence of Coulomb barrier.

In order to follow the evolution of the deposited energy into the quasi-projectile ( $\varepsilon_{QP}$ ) and the quasi-target ( $\varepsilon_{QT}$ ) with the violence of the collision, we have considered only well characterized events in momentum (at least 65% of the projectile momentum). This selection allows to explore the lowest dissipative collisions for which the target-like-fragment (TLF) is not detected. Some assumptions about the charge and the momentum of the TLF are needed to complete these events. First of all, we assume that only one fragment is missing, confirmed by the simulations [5] filtered with the INDRA response function. The TLF charge is deduced from charge conservation taking into account the INDRA efficiency (90% of  $4\pi$ ). The TLF velocity is related to the PLF one by the formula:  $V_{TLF} = \frac{M_{proj}}{M_{targ}} (V_{proj} - V_{PLF})$ .

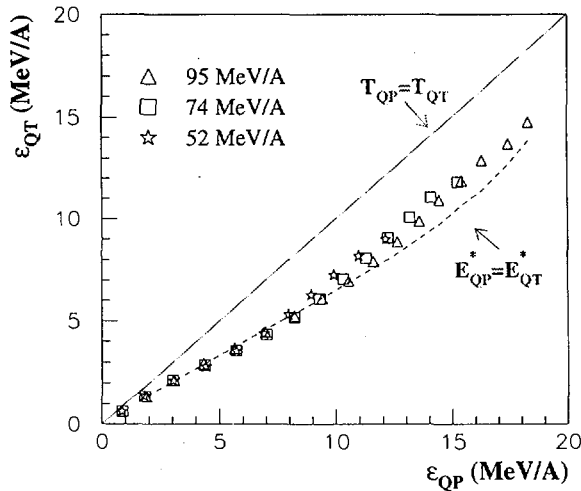


**Figure 1**

Correlation between the energy deposited into the Quasi-Projectile and the Quasi-Target as a function of the degree of dissipation (see text).

The events are sorted according to the energy deposited into the system ( $\frac{E_{QP}^* + E_{QT}^*}{A_{QP} + A_{QT}}$ ). The correlation between the excitation energy imparted to the two interacting partners, plotted in fig. 1, shows that the thermal equilibrium given by the solid line is not reached. The mean QP temperature remains higher than the QT one for the overall dissipation range. The data suggest rather an equal energy sharing given by the dashed line. This trend is compatible with short interaction times as predicted by dynamical calculations ( $\tau_{int} \approx 50 - 80 \text{ fm}/c$ ) [6].

Some deviations occur at high excitation energy ( $\varepsilon > 12 \text{ MeV}/A$ ) which are due to variations in source sizes. In central collisions, the overlap of the two partners is broad. Therefore the decay products at mid-rapidity are distributed in a symmetrical way into the QP and the QT and induce the rise towards the thermal equilibrium which could be meaningless.

The study of the binary collisions observed in the  $^{36}\text{Ar} + ^{58}\text{Ni}$  reactions has shown that beyond 52 MeV/A the deposited energy is equally shared between the quasi-projectile and the quasi-target for the overall dissipation range. This result is inconsistent with a full thermalization of the system even for the central collisions where 80% of the available energy is damped in the exit channel.

## References

- [1] J. Péter et al, Nucl. Phys. A 593 (1995) 95.
- [2] J-L. Charvet et al, Proceeding of the XXXV<sup>th</sup> Int. Winter Meeting on Nucl. Phys., Bormio (1997) 309.
- [3] C.T. Zahn, IEEE Transactions on Computers, vol. 20 (1971) 68.
- [4] L. Nalpas, PhD Thesis, Université Paris XI, 1996.
- [5] D. Durand, Nucl. Phys. A 541 (1992) 266.
- [6] M. Colonna, BNV Calculations (private communication).

## Chemical and kinematical properties of mid-rapidity emissions in Ar+Ni collisions from 52 to 95 A.MeV.

T. Lefort, D. Doré, D. Cussol, J. Péter, for the INDRA collaboration.

The study of particles emitted around mid-rapidity can provide information on the first moments of the collision. At intermediate energies (between 30 and 100 A.MeV), a transition between low energy deep inelastic collision processes to the high energy participant-spectator scenario has been observed. This reflects the increasing role of individual nucleon-nucleon collisions relative to the collective mean-field when the beam energy increases. Dynamical calculations have shown that the particles are emitted at different times. One question is then: is it possible experimentally to have access to the different collision times by looking at the rapidity distributions of light particles ?

The study presented here has been performed on the  $^{36}\text{Ar} + ^{58}\text{Ni}$  system from 52 to 95 A.MeV. This experiment has been done with the  $4\pi$  INDRA detector. Events have been sorted in impact parameter  $b_{exp}$  following their total transverse energy  $E_{trans}$ .

The rapidity distributions of light charged particles and their mean transverse energies are not reproduced by a simulation assuming only a statistical decay from a quasi-target and a quasi-projectile. Additional contributions located around mid-rapidity (labelled MRE) are needed to explain the data [1, 2].

In order to quantify the MRE, three methods have been used: two based on the shapes of the rapidity distributions [1] and one based on the kinetic energy spectra (three source fit analysis labelled TSF) [2]. Figure 1 shows the evolution of the total MRE mass with  $b_{exp}$  for 52 (full circles), 74 (open squares) and 92 (full triangles) A.MeV. The right hand scale of this figure corresponds to the relative amount (in percent) of MRE relative to the projectile mass.

It is clearly seen that MRE mass is weakly dependent on the beam energy, but strongly depends on  $b_{exp}$ . The same observations are made on the particle multiplicities.

One observable to check the energetic properties of MRE is the double ratio parameter  $DRP$  obtained from the isotopic ratios as proposed by S.Albergo. The result of this analysis is shown in figure 2 for four different isotopic ratios. The independence with respect to the violence of the collision and the dependence on the beam energy are observed. The

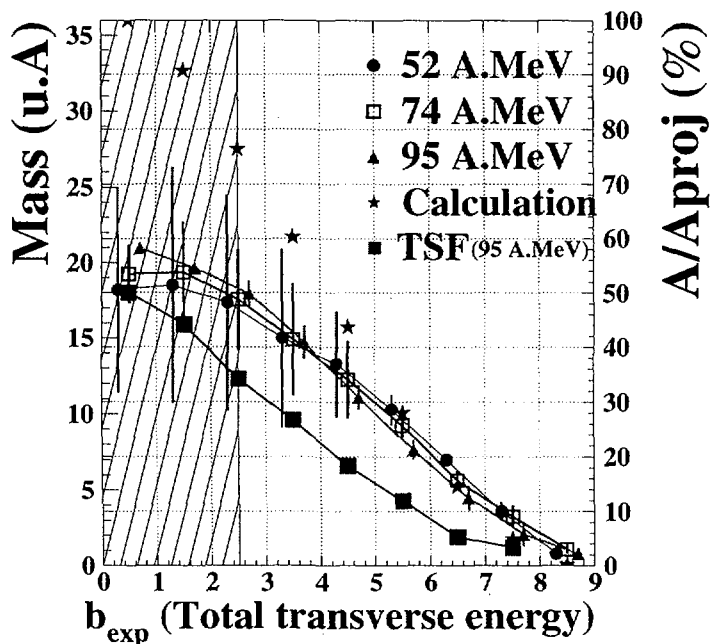


Figure 1

same observations are made on the mean transverse energy and on the slope of the kinetic energy spectra of MRE particles.

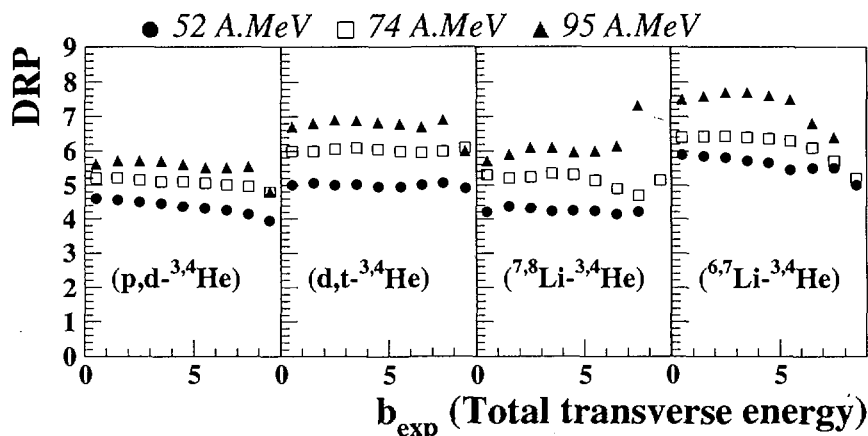


Figure 2

In conclusion, the following trends have been observed in mid-rapidity emissions for Ar+Ni collisions from 52 to 95 A.MeV [3]:

- The amount of particles emitted by MRE is independent of the beam energy, but strongly dependent on the violence (centrality) of the collision. This suggests that this amount is mainly governed by the geometry of the collision.
- The kinematical properties have been found to be strongly dependent on the beam energy but slightly dependent on the violence of the collision. This suggests that the amount of energy exhausted by MRE is only governed by the beam energy.

This strongly suggest a "first-chance collision" process or a "participant-spectator" process. But the rapidity distributions of MRE indicate that several contributions are present, like direct nucleon-nucleon collisions located around  $Y_{nn}=0.5 Y_{proj}$ , fast emission from the deformed quasi-projectile and quasi-target and/or a neck break-up.

## References

- [1] T.Lefort, PhD Thesis (1997), Université de Caen, France.  
T.Lefort *et al.*, Contribution to the XXXVI International Winter Meeting on Nuclear Physics, Bormio (Italy), January 1998.
- [2] D.Doré *et al.*, Contribution to the XXXVI International Winter Meeting on Nuclear Physics, Bormio (Italy), January 1998.
- [3] T.Lefort, D.Doré *et al.*, in preparation.

# Comparison between data measured by INDRA and the prediction of the BNV transport model for $^{36}\text{Ar} + ^{58}\text{Ni}$ reaction at 95 A.MeV

E. Galichet<sup>2</sup>, F. Gulminelli<sup>1</sup>, D.C.R. Guinet<sup>2</sup>,  
the INDRA Collaboration

<sup>1</sup>LPC Caen, IN2P3-CNRS et Université, 14050 Caen Cedex, France.

<sup>2</sup>IPN Lyon, IN2P3-CNRS et Université, 69622 Villeurbanne, Cedex, France.

9th September 1998

The study of reaction mechanisms in heavy ion collisions has much advanced recently with the construction of  $4\pi$  detectors, like INDRA. The formation and the decay of excited nuclei, created in nucleus-nucleus collisions at intermediate bombarding energies ( $10 \text{ MeV/u} < E < 100 \text{ MeV/u}$ ) can be investigated. In this energy regime, it is now well known that the collisions are dominated by binary dissipative processes. In such reactions a quasi-projectile and a quasi-target are formed and their excitation energy increases with decreasing the impact parameter. At variance with the phenomenology of deep inelastic reactions at lower energy ( $\approx 10 \text{ MeV/u}$ ) an intermediate rapidity region between the quasi-projectile and the quasi-target has been observed which is populated by particles and light fragments [1], [2]. The size of this zone increases with energy dissipation, becoming predominant for the most central collisions. Indeed, the nucleons emitted at mid-rapidity should give information about the first steps of the collision. The physical origin of this mid-rapidity emission is most probably a complicated and highly non-equilibrated interplay between one-body and two-body dissipation. If one wants to analyze these events without any a priori hypothesis on the origin of mid-rapidity emission, the reconstruction of sources has to be avoided and all the reaction products have to be studied within a global analysis. The  $4\pi$  detector INDRA was used to study the  $^{36}\text{Ar} + ^{58}\text{Ni}$  reaction at 95 MeV/u. In order to keep a maximum of information, we have chosen to consider only quasi-complete events, in which more than 80% of both total charge ( $Z_{tot} = 46$ ) and total incident momentum of the system have been measured.

The understanding of such reaction mechanisms in which dynamical effects are predominant, demands careful analysis with a choice of adequate variables and a theoretical modelization through a transport model. BNV [3] is a numerical simulation of the nuclear Boltzmann transport equation. In this approach one calculates the space-time evolution of the one-body distribution function under the influence of the the mean

field, the nucleon-nucleon collisions and the Pauli principle. The nucleon-nucleon elastic cross section entering the collision integral was chosen to be the free one  $\sigma_{n-n}(E, \theta, \tau_z)$  where the dependence on energy, scattering angle and isospin is taken from experimental nucleon-nucleon data. With these ingredients, for all impact parameters BNV predicts qualitatively a binary process for the  $^{36}\text{Ar} + ^{58}\text{Ni}$  reaction in the sense that even at  $b=0$  fm, some memory of the entrance channel is kept. But for intermediate impact parameters an important contribution of matter emitted between the projectile and the target is present. And these nucleons are preferentially produced at mid-rapidity. To compare the data with the BNV prediction we have chosen to avoid all definition of sources and construct one-body observables with data. These observables called global variables condensate the experimental information and allow a more simple characterization of the events by a shape description. One of them the charge density  $\rho_z(k)$  [4] is the projection on the main axis of the ellipsoid frame of the charged particles detected in the reaction.

The same technique of analysis can be employed for this model and the data. The results for the charge density  $\rho_z(k)$  are represented in figure 1. The relative position between the quasi-projectile peak and the quasi-target peak is well reproduced as well as the population at mid-rapidity. These results indicate that the dissipation is well described in BNV. We have checked that the quality of the agreement is not due to an autocorrelation between the selection variable  $H(2)$  and the analysis variable  $\rho_z(k)$ . In fact, very similar results are obtained if the charge density is analyzed in bins of other global variables uncorrelated to the parallel velocity axis like transverse energy. From this result we can infer that the only important in medium corrections on the nucleon-nucleon cross section is the Pauli blocking on final states [6].

Finally we have observed that the mid-rapidity zone is neutron rich and it could be related to the density dependence of symmetry energy in the equation of state. For a better understanding of this point we plan to replace the interaction which is presently in BNV with a recently proposed Skyrme interaction involving an isospin dependence optimized to exotic nuclei and neutron matter [5].

## References

- [1] J. Lukasik et al. *Phys. Rev.* C55 (1997) 1906.
- [2] T. Lefort. PhD thesis, Université de Caen, 1997.
- [3] A. Bonasera et al. *Phys. Rep.* 243 (1994) 1.
- [4] J-F. Lecomte et al. submitted for publication.
- [5] E. Chabanat et al. *Nucl. Phys.* A627 (1997) 710.
- [6] E. Galichet. PhD thesis, Université de Lyon, 1998.

### Charge Density (Ar+Ni 95 MeV/u)

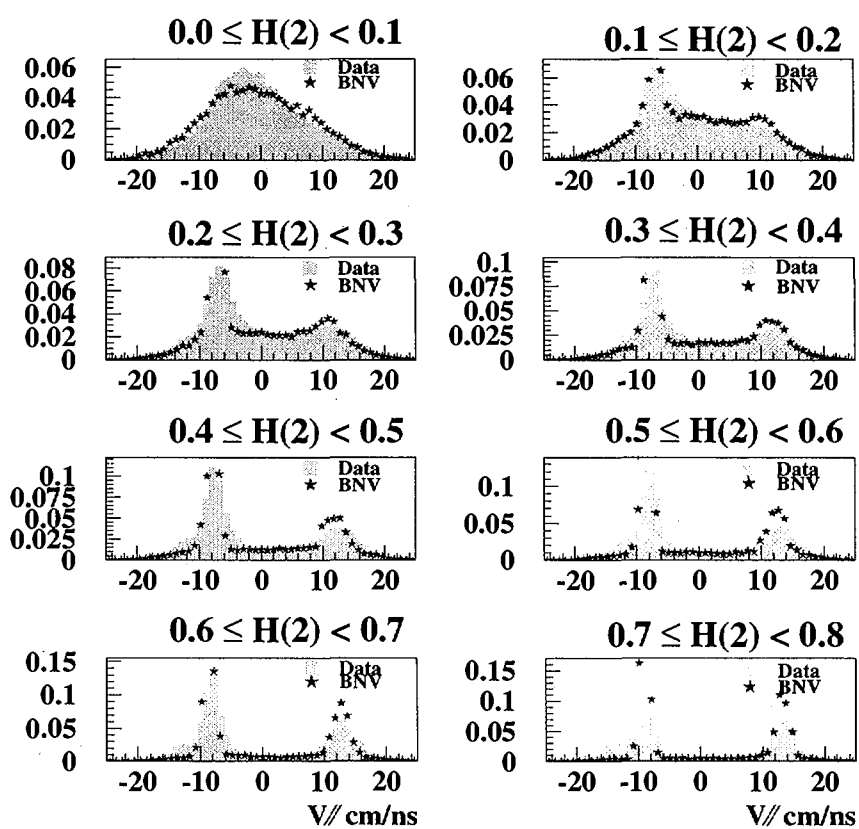


Figure 1: Comparison between data and BNV for charge density and different bins of  $H(2)$ . The parallel velocity is a normalized axis in the ellipsoid frame.

# NON EQUILIBRIUM EMISSION EFFECTS ON QUASI-PROJECTILE PROPERTIES

D. Doré<sup>1</sup>, B. Borderie<sup>2</sup>, Ph. Buchet, J-L. Charvet<sup>1</sup>, R. Dayras<sup>1</sup>, L. Nalpas<sup>1</sup>  
M.F. Rivet<sup>2</sup>  
and the INDRA Collaboration.

(1) DAPNIA/SPhN; CEA/Saclay, F-91191 Gif-sur-Yvette Cedex, France

(2) IPN, IN2P3-CNRS, F-91406 Orsay, France

## INTRODUCTION

It is now well established that binary collisions are the dominant reaction mechanism at intermediate energy. However such collisions are accompanied by non equilibrium emissions observed around mid-rapidity [1]-[2]-[3]-[4].

The quasi-projectile properties of the Ar+Ni reactions at 95A MeV have been studied as a function of the violence of the collision, using a relation between the total transverse energy and the impact parameter. Although the binary character is predominant for all impact parameters [5], an excess of light particles around  $\beta_{nn}$  (nucleon-nucleon velocity) and  $\beta_{cm}$  is observed. It led us to compare a two source analysis, neglecting the mid-rapidity component with a three source analysis which takes into account this emission.

## TWO SOURCE ANALYSIS

The sharing of all particles and fragments is made using a method similar to the thrust. In the centre-of-mass frame of the  $Z \geq 2$  particles, we calculate respectively the QP (QT) source velocity with particles ( $Z \geq 2$ ) having  $v_{//} \geq 1.25v_{CM_{Z \geq 2}}$  ( $v_{//} \leq 0.75v_{CM_{Z \geq 2}}$ ). Next we attribute the other charges according to their velocity relative to the QP and QT source velocities. Neutrons are evaluated and added in order to obtain the total mass of the system. Calorimetry method is then used to calculate the excitation energy per nucleon of each source.

## THREE SOURCE ANALYSIS

To evaluate the mid-rapidity emission, we suppose that this component is equilibrated and we fit the energy distributions of light particles with three maxwellians (transformed in the laboratory frame) :

$$d^2\sigma/dEd\Omega = \sum_{i=1,3} N_i \sqrt{E_l} \exp - ((E_l + Es_i - 2\sqrt{(E_l Es_i)} \cos(\theta_l)) / T_i) \quad (1)$$

$N_i$ ,  $Es_i$  ( $0.5M_{part}V_{source}^2$ ) and  $T_i$  being adjustable parameters and  $E_l$  and  $\theta_l$ , the energy and angle of the particle in the laboratory.

For each light particle and each impact parameter, we fit the sixteen energy distributions (Rings 2 to 17) with the relation (1). The agreement is particularly good at forward angles. For backward angles, over two orders of magnitude, the agreement is still good. We also evaluate the mean multiplicity (above  $\beta_{nn}$ ) of each type of particles. Since the fragments present a negligible intermediate velocity contribution, we will use their mean multiplicities evaluated in a two source



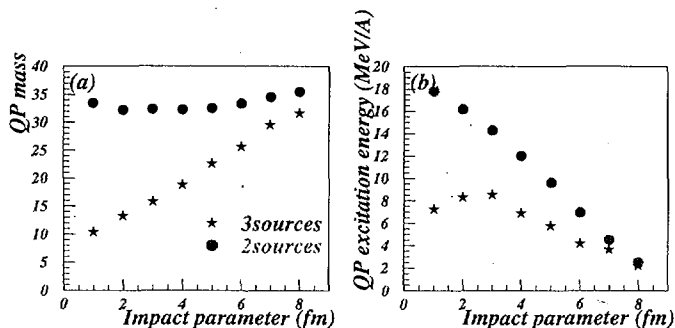


Figure 1: Average QP mass (a) and Excitation energy (b). Two source and three-source analysis lead to quite different results.

analysis in order to calculate the total size of each source.

## RESULTS

The quasi-projectile mass is presented in Fig. 1(a). Results are very different for the two types of analysis. We observe a linear increase with the impact parameter for the three source analysis (stars) while the two source analysis (points) leads to a quasi-constant mass around 33. Qualitatively the three source fit results recall those of geometrical model and fireball [6] but they are quantitatively different. The excitation energy of the quasi-projectile is also different according to the method used. The three source method gives, as expected, smaller excitation energy (9 to 2 MeV/A) than the two source analysis (18 to 2 MeV/A). It is then obvious that, if mid-rapidity particles do not origin from a statistical deexcitation process, the quasi-projectile properties have to be studied after removal of intermediate velocity component. The method proposed here (three source fit) gives a rough estimate but cannot be used for a very detailed analysis.

## References

- [1] J. Péter et al, Nucl. Phys. A593 (1995) 95.
- [2] O. Dorvaux et al, Rapport Interne, CRN Strasbourg 97-04.
- [3] J. Lukasik et al, Phys. Rev. C55 (1997) 1906.
- [4] Ph. Eudes et al, Phys. Rev. C56 (1997) 2003.
- [5] J.L. Charvet et al, XXXVth Bormio Meeting, Italy, 3-8 February 1997.
- [6] G.D. Westfall et al, Phys. Rev. Lett. Vol.37 No 18 (1976) 1202.

# Evidence for dynamical proton emission in Xe+Sn collisions at 50 MeV/u.

M. Germain<sup>1</sup>, D. Gourio<sup>1,a</sup>, Ph. Eudes<sup>1</sup>, J.L. Laville<sup>1</sup>, D. Ardouin<sup>1</sup>, M. Assenard<sup>1</sup>,  
P. Lautridou<sup>1</sup>, C. Lebrun<sup>1</sup>, V. Métivier<sup>1</sup>, A. Rahmani<sup>1</sup>, T. Reposeur<sup>1</sup>,  
and the INDRA collaboration.

<sup>1</sup>SUBATECH, Université, Ecoles des Mines, IN2P3-CNRS, F44072 Nantes, France.

<sup>a</sup>Gesellschaft für Schwerionenforschung, Planckstr. 1, D64291 Darmstadt, Germany.

Experiment : E209/E210.

Particles emitted in intermediate energy (20-200 MeV/u) heavy ion collisions are known to have different origins. In the first stage of the reaction, they are emitted by the interaction zone, during the overlap time of the two colliding nuclei. Then thermal emission by hot nuclei takes place.

In order to get an insight into the presence of non-equilibrium processes in intermediate energy heavy-ion collisions we present in the following a study of proton emission in Xe + Sn data recorded at GANIL by the INDRA multidetector. Selection of the violence of the collision was achieved using the transverse energy  $E_{t12}$  carried out by H and He isotopes [1]. We define two class of events: peripheral ( $E_{t12} < 240$  MeV) and central ( $E_{t12} > 460$  MeV). The mid-rapidity region is then selected between  $60^\circ$  and  $120^\circ$  in the center of mass of the reaction, to avoid thermal emission [1, 2].

We used the relative angle correlation functions between the particles of interest, because they have the property to amplify the effect of low probability processes, and allow to get information on the emission pattern of those particles.

Fig.1 shows the relative angular correlation functions for two protons emitted in the mid-rapidity region as defined above for peripheral (top-left) and central (top-right) collisions. The correlation pattern is rather structureless. To get rid of a possible contamination from both projectile-like and target-like evaporation component at low kinetic energy, we have applied a cut on the proton energy. For  $E_p > 20$  MeV and the peripheral collisions, one observes a clear anisotropy of the relative angle correlation: the two protons are preferentially emitted either closely at  $\alpha \simeq 0$  or back-to-back.

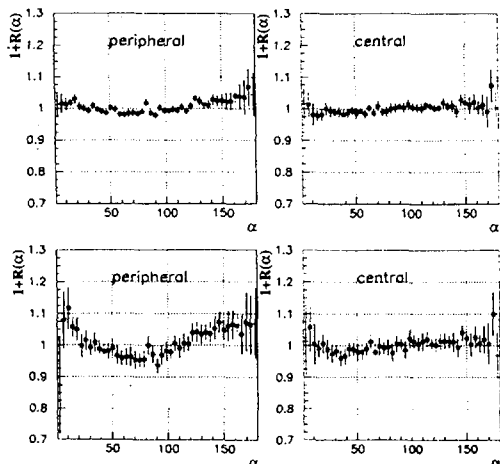


Figure 1: Correlation functions in relative angle between protons emitted in the mid-rapidity region. Top: without any selection of the proton energies, bottom:  $E_p > 20$  MeV in the center of mass of the reaction.

We have ruled out possible detector bias and thermal evaporative scenario [4] by using SIMON [3] whose results were filtered by the INDRA acceptance.

Since one cannot explain the observed correlation by the decay of hot sources, we have to foresee a possible out-of-equilibrium origin with the help of a dynamical computation. Indeed, this observed anisotropy might be explained in the light of recent calculations done in the framework of the Landau-Vlasov model [5]. It has been shown in reference [6, 7] that binary dissipative collisions which dominate the reaction cross-section in this incident energy range are accompanied by an abundant dynamical emission (DE) occurring before the separation time, i.e. the birth of the two exit channel nuclei. We made an analog simulation using the Landau-Vlasov equation solved for the momentum dependent Gogny D1-G1 force [8]. for the Xe+Sn system at 50 MeV/A for rather peripheral collisions ( $b=8\text{fm}$ ). In this case, a separation time of about  $100\text{fm}/c$  is found. To derive the phase space origin of the dynamical emitted particles, their trajectories are followed backward in time, down to  $40\text{fm}/c$  which is the time at which the emission of mid-rapidity particles starts. In fig.2 are displayed equidistant density-profile contours projected on the reaction plane in both the configuration (left) and the momentum space (right). Density profiles are shown for the DE (bottom) and to make the comparison easier, for the whole system (top), i.e. all the particles constituting the two initial nuclei.

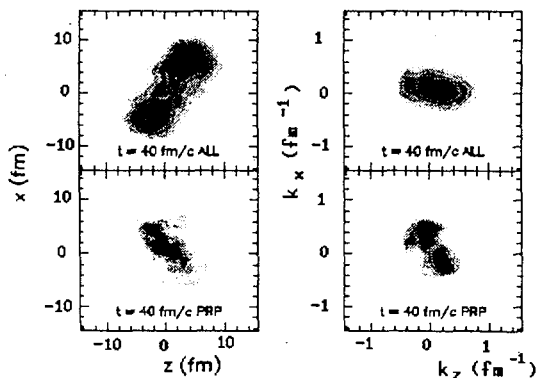


Figure 2: Landau-Vlasov density profiles in space coordinate (left) and momentum coordinate (right) of Xe+Sn at 50 MeV/A and  $b=8\text{fm}$ . For further details, see the text.

The DE contribution comes mainly from the overlapping zone between the two incoming nuclei and is strongly located at mid-rapidity. Moreover, at such a large impact parameter, two components in the momentum space can be observed in DE as previously seen for the Ar + Al system [7]. This effect is a clear signature of a non-global equilibrium in the participant zone which keeps a strong memory of the entrance channel. This is an evidence when only DE is plotted as in figure 2 (bottom) compared to the whole system (top).

These two components could favour correlations at small and large angles. Another strong argument in favour of this interpretation is that such pattern disappears in central collisions, either in experimental data or in the simulation.

In conclusion, we may argue that a clear evidence for a signal of a dynamical process has been found in peripheral Xe+Sn collisions in the mid-rapidity region. This signal appears clearly when an energy cut is imposed eliminating the thermal contributions. The relative angular correlations then appear to be a very suitable

tool to search for dynamical and primordial processes, together with appropriate dynamical simulations as the Landau-Vlasov ones.

## References

- [1] J. Lukasik et al., Phys. Rev. **C55** (1997)1906.
- [2] T. Lefort et al.,  
O. Tirel et al.,  
E. Galichet et al.,  
D. Dore et al.,  
proceedings of the XXXVI Int. Winter Meeting on Nuclear Physics, Bormio (Italy),  
1998, edited by I. Iori.
- [3] D. Durand, Rapport d'habilitation à diriger des recherches, Université de Caen (1995).
- [4] M. Germain, Thèse de l'Université de Nantes (1997) unpublished.
- [5] B. Remaud et al., Nucl. Phys. **A447** (1985)555c.
- [6] P. Eudes et al, Phys. Rev. **C56** (1997)2003.
- [7] P. Eudes et al, proceedings of the XXXVI Int. Winter Meeting on Nuclear Physics,  
Bormio (Italy), 1998, edited by I. Iori.
- [8] F. Sébille et al., Nucl. Phys. **A501** (1989)137.

**NEXT PAGE(S)  
left BLANK**

## **B3 - MULTIFRAGMENT EMISSION**

# Expansion Collective Energies and Freeze-out Volume in the multifragmenting Xe + Sn systems from 32 to 50 AMeV Incident Energies

A. Chbihi, S. Salou and J.P. Wieleczko  
(GANIL)

W.A. Friedman  
(University of Wisconsin)  
For the INDRA Collaboration

The multifragmentation of the nuclear system formed in the central collisions of the Xe + Sn reaction between 32 and 50 AMeV has been studied with the INDRA detector<sup>1)</sup>. We have used the momentum tensor to isolate single sources<sup>2)</sup> for each incident energy.

From these data the extracted single sources are highly fragmented, the fragments are isotropically emitted and their multiplicities increase slowly from 5.9 to 7.2 with the incident energy. The excitation energies of the sources were reconstructed by employing the calorimetric method. They are rather high and evolve from 7 to 12 AMeV when increasing the incident energy from 32 to 50 AMeV.

A comparison between the experimental data and predictions of the statistical multifragmentation model of Compenhaguen<sup>3)</sup> (SMM) shows that in order to reproduce the charge distribution and the other static observables lower excitation energies of the single source than the experimental ones are needed<sup>4)</sup>. Those calculated excitation energies range from 5 to 7 AMeV (compared to the measured ones : 7-12 AMeV) when the incident energies increase. The good agreement between the experimental and calculated charge partitions validate qualitatively the SMM assumption of thermodynamical equilibrium in the freeze-out volume<sup>4)</sup>. However the kinetic observables are more constraining to the model and are difficult to reproduce.

We also used the fragment correlation techniques in order to extract the freeze-out volume and the collective radial energy. With the help of extensive SMM calculations, the freeze-out volume is estimated to be  $2.7 V_0$  ( $V_0$  is the normal volume) at 50 AMeV. It decreases with the incident energy to be nearly  $2 V_0$  at 32 AMeV. For these freeze-out volumes, the collective energy evolves from 0 to 1.3 AMeV with the bombarding energy. However if we perform the SMM calculation with its standard freeze-out value which is  $3 V_0$ , the collective radial energy evolves from 0.5 to 2 AMeV. In both cases the expansion is not thermal and originates probably from a dynamical compression developed in the early stage of the reaction. These results are confirmed by the predictions of the expanding emitting source model<sup>5)</sup> (EES).

## REFERENCES :

- 1) S. Salou, Ph.D. Thesis, Université de Caen, 1997.
- 2) N. Marie et al., Phys. Lett. B391, 15 (1997)
- 3) J.P. Bondorf et al., Phys. Rep. 243 (1995) 1.
- 4) R. Bougault et al., proceedings of the XXXV Intern. (Bormio, February 1997)
- 5) W.A. Friedman, Phys. Rev. C 42, 667 (1990).

# Dynamical effects in peripheral and semi-central collisions at intermediate energy.\*

O.Tirel, INDRA collaboration and J.Aichelin, R.Nebauer

September 11, 1998

The Quantum Molecular Dynamic [1] which describes the time evolution of the nucleon in phase space provides generally a good average description of the dissipative mechanisms occurring all along the interaction between the two colliding nuclei. Some comparisons have been done at different energies for different systems [2]. In our context we will try to get a deeper insight into the reaction mechanisms which could be responsible for the mid-rapidity emission observed in the peripheral and semi-central collision in the reaction Xe+Sn at 50 MeV/nucleon. Simulations have been done for impact parameters between 0 and 12 fm in order to match the total reaction cross section. We have used a soft equation of state ( $K=200$  MeV and  $\sigma_{nn}=55$  mbarn). The calculation has been stopped at 240 fm/c. At this time the fragments are built by a clusterisation method based on a minimum spanning tree [1] and we have checked that their atomic number is stable. A total number of 60 000 events have been calculated on the whole range of impact parameter. All the events have been filtered by the detector efficiency and the same sorting has been applied to define the shape of the events. We observe for all impact parameters (0 to 12 fm) essentially a binary mechanism; two biggest fragments are located in the velocity space close to the beam and the target velocity respectively. They can be associated with the quasi-projectile and the quasi-target residues. Fig 1 visualises this point, and shows that the velocity and the charge distribution of the biggest fragment ( $V_{cm}>0$ ) are very well reproduced for the mid elongated events.

The small deviation, is essentially due to the clusterisation method used here where the binding energy of the alpha particles is not well reproduced so the biggest fragment has a too large atomic number. However production of IMF and LCP appears in the range of velocities between the velocities of QP and QT. For the same set of events, the multiplicity, the charge distribution and the velocity of the IMF, fig. 2, are fairly reproduced. For the other region, corresponding to less violent collisions the different aspects of the IMF production are also well reproduced.

---

\*O.Tirel and al. in preparation

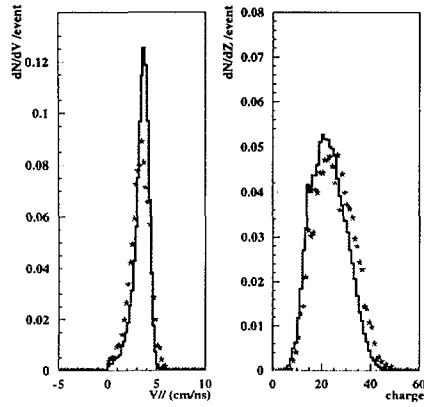


Figure 1: Comparison of velocity and charge distribution of the biggest fragment between experimental data and QMD. The full line and the stars correspond to the data and to QMD calculation, respectively. The comparison has been done for mid-elongated events.

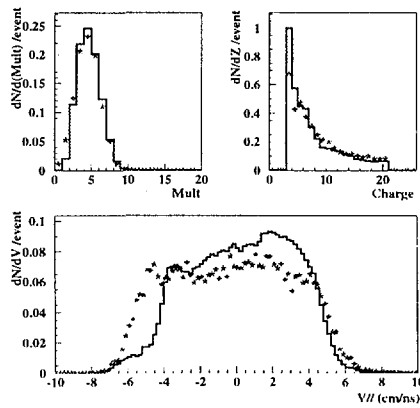


Figure 2: Comparison of the multiplicity, the charge distribution and the velocity of the IMF between experimental data and QMD. The full line and the stars correspond to the data and to the QMD calculation, respectively. The comparison has been done for the mid-elongated events.



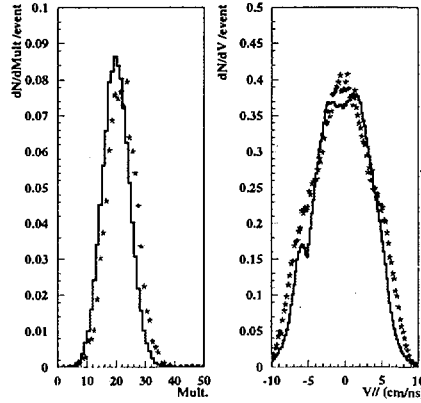


Figure 3: Comparison of the multiplicity and the velocity of the LCP between experimental data and QMD. The full line and the stars correspond to the data and to the QMD calculation, respectively. The comparison has been done for the mid-elongated events.

For LCP, comparison has to be done carefully, essentially for two reasons. QMD model doesn't manage the statistical secondary emission and also the isospin is not well described in this model. In spite of this, the agreement for LCP production (fig 3) is rather good for the two first regions of shape selection. The emission of LCP is preponderant in the mid-rapidity region and can be associated essentially with the first stage of the dynamical process. On the contrary, for the less violent collisions the ratio between dynamical emission and statistical emission is not well reproduced. In these events the proportion of LCP statistically emitted is more important than for the semi-central events. This point reinforces our conclusion concerning the dynamical formation of IMF because although QMD doesn't reproduce well the statistical emission, it reproduces the global characteristics of the fragments. Besides, the fragments in the QMD model are produced in a very fast way, approximately 100-150 fm/c [3] after the contact between the projectile and the target.

## References

- [1] J.Aichelin, Phys. Rep. 202, 233 (1991).
- [2] P.B.Gossiaux and J.Aichelin, Phys. Rev. C56 (1997) 2109
- [3] P. B. Gossiaux, R. Puri, Ch. Hartnack, J. Aichelin, Nuc. Phys. A619 (1997) 379

## Independence of fragment charge distributions of the size of heavy multifragmenting sources

*M.F. Rivet<sup>a</sup>, Ch.O. Bacri<sup>a</sup>, B. Borderie<sup>a</sup>, J.D. Frankland<sup>a</sup>, M. Squalli<sup>a</sup>,  
and the INDRA collaboration  
and A. Guarnera<sup>b,2</sup>, M. Colonna<sup>b,2</sup>, P. Chomaz<sup>b</sup>*

<sup>a</sup> Institut de Physique Nucléaire, IN2P3-CNRS, F-91406 Orsay Cedex, France

<sup>b</sup> GANIL, CEA, IN2P3-CNRS, B.P.5027, F-14021 Caen cedex, France

A comprehensive interpretation of the decay of highly excited nuclear systems through multifragmentation is not yet achieved. Whether this process finds its origin in the dynamics of nuclear collisions, or results from the statistical decay of hot but thermalized nuclear matter is still largely debated. As a contribution to this question, we report on fragment multiplicities and related  $Z$  distributions from single multifragmenting sources with different sizes but with the same available excitation energy per nucleon, resulting from central collisions between heavy nuclei: the 32 MeV/nucleon  $^{129}\text{Xe} + ^{\text{nat}}\text{Sn}$  and 36 MeV/nucleon  $^{155}\text{Gd} + ^{238}\text{U}$  reactions, with total masses evolving from  $\sim 248$  to 393u, can lead to composite systems with an excitation energy around 7 MeV/nucleon. The experiment was performed at GANIL, using the  $4\pi$  multidetector INDRA.<sup>1</sup>

For medium and heavy systems in this energy domain the cross section is dominated by binary dissipative processes, accompanied by dynamical or neck emission. To isolate the events resulting from multifragmentation of a single source, a careful selection is thus needed: i) detection of (80%) of the total charge and of the initial “linear momentum” ( $Z_p V_p$ ); ii) selection of compact shape events from among the most dissipative collisions by means of a shape analysis and of the preferred direction of emission of matter,  $\theta_{cm} \geq 60^\circ$ . Indeed, fragment properties of such events are consistent with the emission from a single source and binary reaction events, if present, are so few as to be negligible.<sup>2</sup> With such a selection the cross section for “fusion” events is about 1% of the reaction cross section.

The fragment multiplicity distributions for the two systems are shown in fig. 1a: the mean fragment number is 1.5 times larger for the heavier system, which corresponds to the ratio of the total charges of the systems. On the other hand the charge distributions are superimposable, over three orders of magnitude (fig. 1b). Thus the experimental observation is that, around 30 MeV/nucleon, the charge distribution for multifragmentation is independent of the system size, and for a given size, of the entrance channel asymmetry.<sup>3</sup> These static properties are also observed for an extended event selection ( $30^\circ \leq \theta_{cm} \leq 60^\circ$ ).<sup>4</sup> The shape and dynamical characteristics of the events in this zone are however different from those of the single source events.

This type of experimental observation is generally taken as a signature of the dominance of phase space, the emission probability of any fragment being, to first order, only dependent on the temperature of the system. Similar charge and multiplicity distributions, however, also come naturally out of a dynamical model in which multifragmentation is related to the development of volume instabilities, and to the spinodal decomposition of finite nuclei<sup>5</sup>, for which it was shown that the partition in primary fragments of typical charge  $Z \sim 10-15$  was favoured. These simulations, in which the evolution of the system is followed during head-on nuclear collisions and up to the cold measurable particles, were performed for each system. The results are shown in fig. 1: a good agreement between

---

<sup>2</sup>present address: Laboratorio Nazionale del Sud, Viale Andrea Doria, I-95129 Catania, Italy

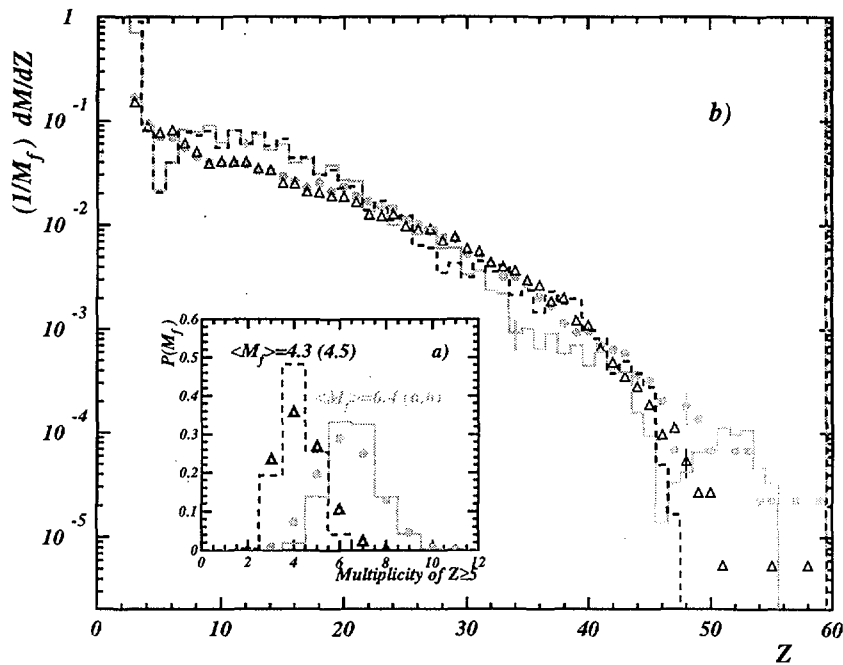


Figure 1: Fragment ( $Z \geq 5$ ) multiplicity ( $M_f$ ) distributions (a) and differential charge multiplicity distributions, normalised to each event's  $M_f$ , (b) for the 32 MeV/nucleon Xe+Sn (triangles; dotted lines) and Gd+U (circles; full lines) systems. Points show the experimental data while the lines are the results of the stochastic mean field simulations. Average experimental (calculated) multiplicity values are given. Some statistical error bars are displayed.

experiment and calculation is observed for the fragment multiplicity and the charge distribution; other variables such as the sizes of the 3 largest fragments are also well reproduced. When decreasing the mass of the system, the experimental conclusions hold for the results of calculations: the charge distribution does not change while the fragment multiplicity decreases. The fragment kinetic energies are however underestimated in the calculation, due to an incomplete account of all possible fluctuations. Works are in progress on this point.

To summarize, we evidenced and characterised the multifragmentation of a single piece of nuclear matter, comprising a large part of two colliding heavy nuclei. When increasing the mass of the system, a scaling law appeared, which consists in increasing the fragment multiplicity proportionally to the charge of the total system while the charge distribution remains unchanged. A possible interpretation is that multifragmentation originates in the spinodal decomposition of nuclei.

## References

- [1] M.F. Rivet et al, Phys. Lett. B (in press)
- [2] J. Frankland et al., Proc. Bormio, (1997), page 323.
- [3] M. D'Agostino et al, Phys. Lett. B371 (1996) 175.
- [4] J.L. Charvet and the INDRA collaboration, this compilation.
- [5] A. Guarnera et al., Phys. Lett. B373 (1996) 267. A. Guarnera, PhD thesis, Caen (1996). B. Jacquot et al, Phys. Rev C 54 (1996) 3025.

## Space Time Characterization of Nuclear Matter in Fragmentation Processes

A.D. Nguyen (LPC Caen) and the INDRA collaboration

Multifragmentation is now a well established process in the Fermi energy range but there is still a large debate concerning the origin of such a phenomenon. A possible way to disentangle among the various processes that have been proposed in the literature is to measure the fragmentation time  $\tau_0$ . The present work gives an estimate of  $\tau_0$  from a detailed analysis of highly fragmented events in central Xe+Sn collisions at 50 MeV/u studied by the INDRA collaboration [1]. In such collisions, matter is almost stopped and is highly excited resulting in the isotropic emission of several fragments with a collective radial motion of about 2 MeV/u representing a sizeable amount of the total available energy. In order to extract the fragmentation time, the process has been simulated with help of the SIMON event generator [2] to extract the velocity and density profiles at freeze-out. To this end, a number of different initial space-time distribution of the matter have been tested and compared with the data until agreement concerning the mean kinetic energies and velocity distributions of the detected fragments was achieved (black points in the figure). Then, these profiles have been compared with the predictions of a microscopic transport model (BNV) [3] at various instants of the collision (lines in the figure). A reasonable agreement between the experimental distributions and those of the model is obtained for a time between 80 and 100 fm/c after contact time. It turns out that this time corresponds almost exactly to the entrance of the system in the so-called spinodal region in which it becomes mechanically unstable. This suggests that fragmentation could be initiated before the system reaches the unstable region and that the nucleons in each fragments should keep memory of their initial space-time correlations as predicted in QMD calculations [4].

However, recent calculations [5] in which genuine quantum effects have been included seem to shorten the fragmentation time scales and favour spinodal decomposition as the mechanism responsible for nuclear disassembly.

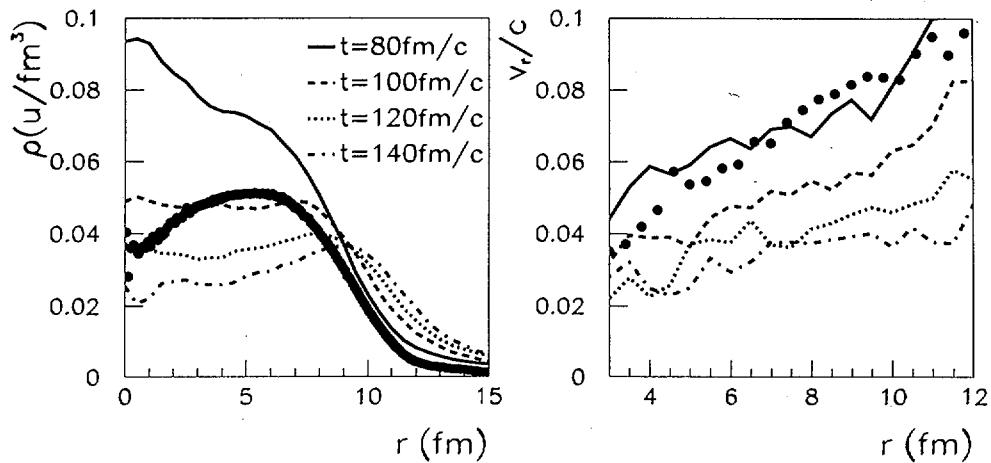


Figure 1: Comparison between the 'experimental' density and velocity profiles (as deduced from the data by comparison with the Simon results) and those obtained in a microscopic transport model with a soft EoS ( $K=200$  MeV).

'La suite au prochain épisode...'

- 1 A.D.Nguyen et al, Proc. of the Winter Meeting, Bormio (1998)  
A.D.Nguyen, Thesis (1998) and to be published
- 2 D.Durand et al, (in preparation)
- 3 A.Bonasera, J. Molitoris, F. Gulminelli, Phys. Rep. 243 (1994) 1
- 4 J. Aichelin, Phys. Rep. 202 (1991) 233
- 5 D. Lacroix, Ph. Chomaz, (in preparation)

# Fragment Excitation Energies in Multifragmentation

A. Chbihi, N. Marie and J.P. Wieleczko  
(GANIL)

J.B. Natowitz  
(Texas A&M)

for the INDRA Collaboration

Central collisions induced by heavy-ion beams at intermediate energies produce highly excited, compressed nuclear matter. After dynamical compression phase, such systems may expand to a low density where the multifragmentation takes place. The produced primary fragments may be excited and in this case, they are expected to decay by statistical processes. An experimental determination of this secondary component and reconstruction of the excitation energies and sizes of the primary fragments can provide a very significant test of the models and of the assumption of thermodynamical equilibrium at the time of disassembly.

An experimental study<sup>1,2,3)</sup> of the central collision of the Xe + Sn at 50 AMeV was made using the IMF-LCP correlation techniques. From the IMF-LCP correlation functions we extracted the average multiplicities and kinetic energies of hydrogen and helium isotopes emitted from the primary fragments. Using this information we reconstructed the sizes (charges and masses) and excitation energies of the primary fragments.

The results of these analysis indicate that the fragments are excited, their mean excitation energies per nucleon are all the same, they are equal to 3 AMeV. In addition, we performed maxwellian fit of the kinetic energy spectra of the LCP emitted from the primary fragments. For each particle type, the apparent temperatures fluctuate about a constant value over the whole range of detected fragments ( $Z = 4$  to  $Z = 20$ ). These two independent pieces of information provide strong evidence that on the average, thermodynamical equilibrium is achieved when the primary fragments are produced.

Another interesting result is that from a comparison between the predictions of the GEMINI model<sup>4)</sup> with the experimentally observed secondary multiplicities of the evaporated light charged particles, we concluded that the primary fragments have the same N/Z ratio as the initial system  $^{129}\text{Xe} + ^{\text{nat}}\text{Sn}$ .

We are performing the same analysis for Xe + Sn system but at other incident energies. Preliminary results indicate that the mean excitation energies of the primary fragments are constant for the whole incident energy range, 32 to 50 AMeV.

Ref.

- 1) N. Marie et al., Phys. Lett. B391, 15 (1997)
- 2) N. Marie et al., Phys. Rev. C (1998) in press.
- 3) N. Marie et al., GANIL P 98 13
- 4) R.J. Charity et al., Nucl. Phys. A483, 371 (1988)

## Collective motion and angular momentum in 50 A.MeV Xe+Sn central collisions.

A. Le Fèvre, O. Schapiro, J.P Wieleczko, A. Chbihi,  
(GANIL)  
For the INDRA Collaboration.

Various features of multifragmentation events for central collisions of Xe+Sn at 50 A.MeV have been recently reported <sup>1)</sup>. Besides a high multiplicity and an isotropical emission of the fragments, it has been observed that mean kinetic energies of the fragments could be understood invoking a collective motion superimposed on Coulomb and thermal motion. However, the origin of such a collective motion remained to be clarified. This collective motion may be associated to the thermal pressure of the hot system, or/and to the expansion flow which follows the initial compression built-up in the first stage of the collision. On the other hand, collective rotation induced by angular momenta stored in the multifragmenting source is another possibility which has to be explored.

Angular momentum has been implemented in a statistical model assuming that multifragmentation is dominated by the equipartition of the many-fragments phase space <sup>2)</sup>. The partitioning is calculated under the constraint of a given size, volume, excitation energy and angular momentum of the source. In the model, it is assumed that the angular momentum is in the orbital motion of the fragments around the center of mass. Respect to a case without angular momentum, the storage of a part of the excitation energy into rotational motion modifies the partition, increasing the yields of the largest fragments and pushing them towards the periphery of the break-up volume.

We have investigated the possible influence of the angular momentum using the Berlin's statistical code of ref. 2 for the multifragmentation events of the central collisions of Xe+Sn at 50 A.MeV. Various calculations have been performed assuming the standard value for the reduced break-up radius (2.2 fm). All the results discussed here have been filtered and selected as the data were. First, we explore the case without angular momentum. For this analysis, the mean size of the biggest fragment together with the total charge bound into fragments have been used to estimate the charge and the excitation energy of the source. Reasonable agreement is observed for the various distributions of the static variables (charge, asymetries of the two or three biggest fragments, fragment multiplicity) with the following parameters respectively for the size, total excitation energy and angular momentum:  $Z_s=79$ ,  $E_s=6$  A.MeV,  $L_s=0$  (see ref. 3). On the other hand, the mean kinetic energies of the fragments are strongly underestimated. For example, the calculated mean kinetic energy of a fragment of charge  $Z=15$  (roughly the charge of the mean biggest fragment) is about twice lower than the experimental value. We have repeated the above procedure for the search of the best parameters, freeing the angular momentum. Static variables are well reproduced with  $Z_s=79$ ,  $E_s=8.5$  A.MeV and  $L_s=640 \hbar$ . A clear improvement is obtained for the kinetic energies of the fragments with charge below 15, but for higher charge, while the experimental values saturate or slightly decrease, the calculated values increase. In the calculation, this behavior is related to the influence of the angular momentum on the location of the biggest fragment which is specific of this kind of modelization but does not seem to be



present in the data. To go further, we have examined the shape of the multifragmentation events in the momentum space. Although variations are seen in the sphericity and coplanarity distributions when one increases angular momentum, the strongest evolution is observed for the aplanarity distribution, since rotational motion tends to induce disk-like shapes. Thus, a high angular momentum, necessary to explain the mean kinetic energy of fragments, fails to reproduce the aplanarity distribution. In fact, as far as the aplanarity distribution is concerned, the agreement with data is better when no rotational motion is assumed. It should be mentioned that this analysis has been performed assuming an unique value for the angular momentum, but it seems difficult to explain simultaneously the aplanarity distribution and mean kinetic energy by imposing a distribution of angular momentum.

To summarize, we have confronted the experimental results of the Xe+Sn central collisions at 50 A.MeV with the predictions of a statistical model which assumes multifragmentation of a rotating hot nuclei. A good agreement is observed for the static variables but the model fails to give a correct picture for the kinematical observables when rotational motion is included. Indeed, the mean kinetic energy of the fragments suggests a high value of angular momentum, and the aplanarity distribution is compatible with no (or a small) angular momentum. Thus, the rotational motion of a thermalized source could not explain the collective motion of the fragments which are produced in the central events of the Xe+Sn reaction at 50 A.MeV.

- 1) N. Marie et al, Phys. Lett. B391 (1997) 15.
- 2) D.H.E Gross, Rep. Progr. Phys. 53 (1990) 605; A.S Botvina and D.H.E Gross, Nucl. Phys. A 592 (1995) 257.
- 3) A. Le Fèvre, PhD Thesis, Université de Paris 7, GANIL T9703.

# MULTIFRAGMENTATION, SCALING LAW AND BINARY DISSIPATIVE COLLISIONS

J-L. Charvet,  
and the INDRA collaboration

## Abstract

A scaling law between the fragment multiplicities and the total charge of the  $^{129}\text{Xe}+^{nat}\text{Sn}$  and  $^{155}\text{Gd}+^{238}\text{U}$  systems has been observed in dissipative binary collisions.

Using the  $4\pi$  multidetector array INDRA at GANIL, we have investigated the reactions  $^{129}\text{Xe}+^{nat}\text{Sn}$  and  $^{155}\text{Gd}+^{238}\text{U}$  at, respectively, 32 and 36 A MeV bombarding energies. In a first analysis, a scaling law between the fragment multiplicity and the total charge of the two systems has been observed in a very peculiar class of events: the multifragmentation of single thermalized sources [1]. This selection required, firstly, the detection of "complete events": at least, 80% of the total charge of the system and 80% of the initial "linear momentum" ( $Z_p V_p$ ). Then, an event shape analysis is performed by calculating the eigenvectors of the 3-dimensional kinetic energy tensor of the fragments ( $Z \geq 3$ ) [2]. This analysis allowed to determine the flow angle ( $\Theta_{flow}$ ), i.e. the angle between the beam axis and the eigenvector associated with the largest eigenvalue. The flow angle distribution is strongly forward peaked indicating that these "complete events" keep a strong memory of the entrance channel, as it is expected in binary dissipative collisions. Nevertheless, events populating  $\Theta_{flow} \geq 60^\circ$  have been interpreted as events coming from the multifragmentation of a unique source formed in "fusion" reactions [3].

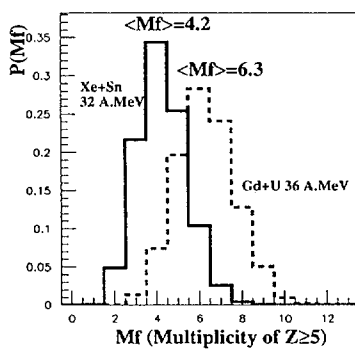


Fig.1:  $Z \geq 5$  multiplicities

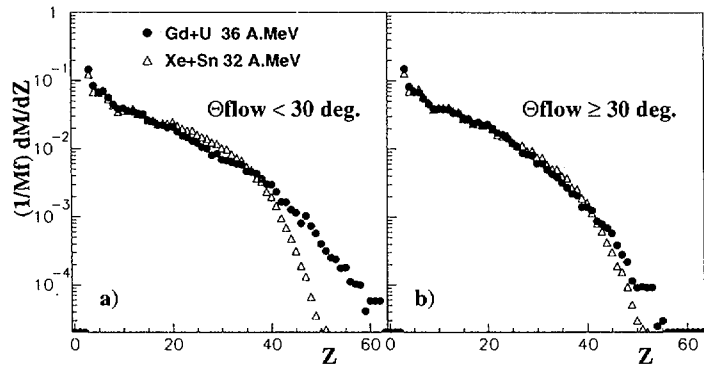


Fig.2: Differential charge multiplicities for  $\Theta_{flow} < 30^\circ$  (a) and  $\Theta_{flow} \ge 30^\circ$  (b)

In the Fig.1 the  $Z \geq 5$  fragment multiplicities are presented for Xe+Sn and Gd+U for the "complete events". We see a perfect scaling law between the

average multiplicities, 4.2 for Xe+Sn and 6.3 for Gd+U, and the total charge of the two systems: 104 and 156, respectively. These values are very close to the ones obtained from the events selected by requiring  $\Theta_{flow} \geq 60^\circ$  which correspond to the multifragmentation of single thermalized sources (4.3 for Xe+Sn and 6.4 for Gd+U) [1]. For the single multifragmentating sources, the cross-sections are around 1% of  $\sigma_R$  (total reaction cross-section) for both systems, whereas the "complete event" selections represent, respectively for Xe+Sn and Gd+U,  $\sim 10\%$  and  $\sim 5\%$  of  $\sigma_R$ .

An interesting point is the comparison of the Z-distribution shapes. In Fig.2, the differential charge multiplicity distributions, normalized to each event's multiplicity ( $M_f$ ) are superimposed, for Xe+Sn and Gd+U, and displayed for two selections: i)  $\Theta_{flow} < 30^\circ$  (Fig.2-a), ii)  $\Theta_{flow} \geq 30^\circ$  (Fig.2-b).

For  $\Theta_{flow} < 30^\circ$  the Z-distributions are not quite independent of the system sizes (Fig.2-a). Fig.2-b ( $\Theta_{flow} \geq 30^\circ$ ) shows a good superposition of the two Z distributions, exactly as it has been observed in the one-source selection ( $\Theta_{flow} \geq 60^\circ$ ) [1]. Moreover, the shape of the Z-distribution of the Xe+Sn system is independent of the flow angle. It is worthwhile to note that the Xe+Sn system is a quasi-symmetrical system and that the maximum detected Z of the fragments, for any  $\Theta_{flow}$ , is around 50. This can imply that the Xe+Sn Z-distributions account for the decays of the quasi-projectile (Xe) and the quasi-target (Sn), both excited after binary dissipative collisions. On the other hand, for the Gd+U system, the maximum detected Z is, for  $\Theta_{flow} < 30^\circ$ , around 60, which is very close to the atomic number of Gd (64). The fission of the uranium target could explain the lack of charge larger than the Gd one.

In conclusion, the scaling law between the IMF multiplicity with the size of the system and the independence of the Z-distributions in  $^{129}\text{Xe}+^{119}\text{Sn}$  and  $^{155}\text{Gd}+^{238}\text{U}$  are two results which are not specific of the multifragmentation of single thermalized sources. They can be found in more standard dissipative binary collisions. These results suggest that the characteristics of the multifragmentation process are determined in an early time before the degrees of freedom of the system, such as relative energy or(and) event shape, reach full relaxation as this occurs in "fusion" reactions.

## References

- [1] M-F. Rivet et al, to be published in Phys. Lett. B, preprint IPNO-DRE-98-08
- [2] J. Cugnon and D. L'Hote, Nucl. Phys. A397(1983)519
- [3] N. Marie et al, Phys. Lett. B391(1997)15

**NEXT PAGE(S)  
left BLANK**

## **B4 - LIFETIMES OF EXCITED NUCLEI**

# A straightforward measurement of fission lifetimes by the crystal blocking technique

M. Chevallier<sup>†</sup>, C. Cohen<sup>†</sup>, D. Dauvergne<sup>†</sup>, J. Dural<sup>§</sup>,  
J. Galin<sup>\*</sup>, F. Goldenbaum<sup>\*</sup>, D. Jacquet<sup>¶</sup>, R. Kirsch<sup>†</sup>,  
E. Lienard<sup>\*</sup>, B. Lott<sup>\*</sup>, M. Morjean<sup>\*</sup>, A. Péghaire<sup>\*</sup>, Y. Périer<sup>\*</sup>,  
J.C. Poizat<sup>†</sup>, G. Prevot<sup>†</sup>, J. Remillieux<sup>†</sup>, D. Schmaus<sup>†</sup>,  
M. Toulemonde<sup>§</sup>

<sup>†</sup>*Institut de Physique Nucléaire de Lyon, IN2P3/CNRS, Univ. Cl. Bernard,  
43 Bd. 11 Novembre 1918, F-69622 Villeurbanne Cedex, France*

<sup>‡</sup>*GPS, 2 place Jussieu, 75251 Paris Cedex 05, France*

<sup>§</sup>*CIRIL, BP 5133, 14040 Caen Cedex, France*

<sup>\*</sup>*GANIL DSM/CEA, IN2P3/CNRS, BP 5027, 14076 Caen Cedex 5, France*

<sup>¶</sup>*Institut de Physique Nucléaire d'Orsay, BP 1, F-91406 Orsay Cedex, France*

The fission lifetime evolution with the initial temperature of an excited nucleus should be a powerful way to get information on the nuclear dissipation processes. Fission lifetimes at high excitation energy have been mainly inferred, up to now, from pre- and post-fission particle multiplicities or GDR- $\gamma$  multiplicities. However, rather large discrepancies can be found between these experiments, due to strong assumptions in the data analyses. The blocking technique used in the present experiment (E257) is certainly the most straightforward way to measure fission lifetimes but, up to now, this technique could be only used to determine rather long lifetimes, associated with fission at low excitation energies. The availability at GANIL of a very high quality beam of  $^{238}\text{U}$  accelerated at 24 MeV per nucleon makes it possible to induce fission events in reverse kinematical reactions, leading to large recoil velocities of the fissioning nuclei. Due to this large velocity, shorter fission times become accessible to the measurement.

The blocking pattern measured for uranium nuclei elastically scattered (figure 1) was used to check during the experiment the crystal properties of the Si target and the quality of the U beam. The fission lifetimes of the uranium-like fragments ( $Z=92\pm 5$ ) (PLFs) produced with temperatures up to about 3

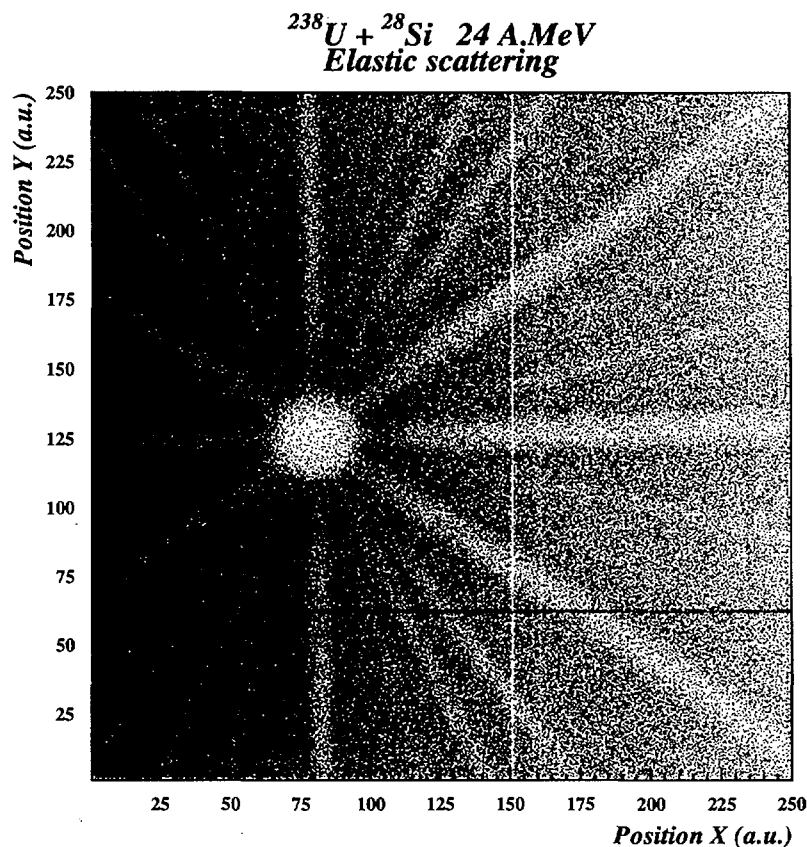


FIGURE 1. Blocking pattern around the  $\langle 110 \rangle$  axis for elastically scattered uranium nuclei.

MeV in the  $^{238}\text{U} + ^{28}\text{Si}$  reactions at 24 A.MeV have been inferred from a single measurement. The PLF excitation energy was calculated event-by-event from the associated neutron multiplicity measured with ORION, a high efficiency  $4\pi$  neutron detector. For uranium-like nuclei with temperatures up to about 3 MeV, the fission lifetimes are found much larger than those obtained previously in more indirect approaches.

**Publications from experiment E257:**

M. Morjean et al., Nucl. Phys. A630 (1998) 200c

M. Morjean et al., Proc. of the Tours Symposium on Nuclear Physics III, ed M. Arnould et al. (AIP Conf. Proc. 425, 1998)

F. Goldenbaum et al., Proc. of the XXXVI Int. Winter Meeting on Nucl. Phys., ed I. Iori (Univ. Milano, 1998)

## Compound Nuclear Lifetimes at High Excitation Energies via a New Statistical Fluctuation Method

J. M. Casandjian<sup>1</sup>, W. Mittig<sup>1</sup>, A. Pakou<sup>2,3</sup>, N. Alamanos<sup>2</sup>, G. Auger<sup>1</sup>, F. Auger<sup>2</sup>,  
M. Chartier<sup>1</sup>, D. Cortina-Gil<sup>1</sup>, V. Fekou-Youmbi<sup>2</sup>, B. Fernandez<sup>2</sup>, A. Gillibert<sup>2</sup>, A.  
Lépine<sup>1,4</sup>, M. MacCormick<sup>1</sup>, A. Ostrowski<sup>1</sup>, P. Roussel-Chomaz<sup>1</sup>, J. L. Sida<sup>2</sup>

1) GANIL (DSM/CEA, IN2P3/CNRS), BP 5027, 14021 Caen Cedex, France

2) CEA/DSM/DAPNIA/SPhN Saclay, 91191 Gif-sur-Yvette Cedex, France

3) Department of Physics, The University of Ioannina, 45110 Ioannina, Greece

4) IFUSP, DFN, C. P. 20516, 01498, Sao Paulo, S. P. Brasil

Compound nuclear lifetimes are connected to statistical properties of nuclei and determine the time scale of statistical de-excitation in heavy ion collisions. Hence, they test the validity of the compound nucleus models at very high excitation energy where it is necessary to compare the various reaction times with the lifetime of a compound nucleus. For example, lifetimes for particle emission at high bombarding energies must be compared to the thermalization process and set the applicability limits for the statistical description of very hot nuclei formed in this type of nuclear reaction. Furthermore, level densities provide a test for nuclear models and their parameters.

A new method to determine compound nuclear lifetimes at high excitation energies was proposed and applied to the system  $^{12}\text{C}(^{28}\text{Si},\alpha)^{36}\text{Ar}$  at two different bombarding energies, 190 and 277 MeV. The first chance alpha particle spectra observed show a structure which directly reflects the fluctuating behavior of the first de-excitation step. Coherence widths and thus lifetimes for the nucleus  $^{36}\text{Ar}$  were obtained via a correlation function analysis. The results at low excitation energies are consistent with standard statistical models while the result at high excitation energy is compatible with a theoretically predicted change of the level density parameter (see fig 1). The new experimental method proposed and used to obtain unambiguously the coherence width of compound nuclei at high excitation energies gives a new insight into the physics of high excitation energy nuclear dynamics. The present work has been published in J.M.Casandjian et al, Phys. Lett. B 430 (1998) 43.

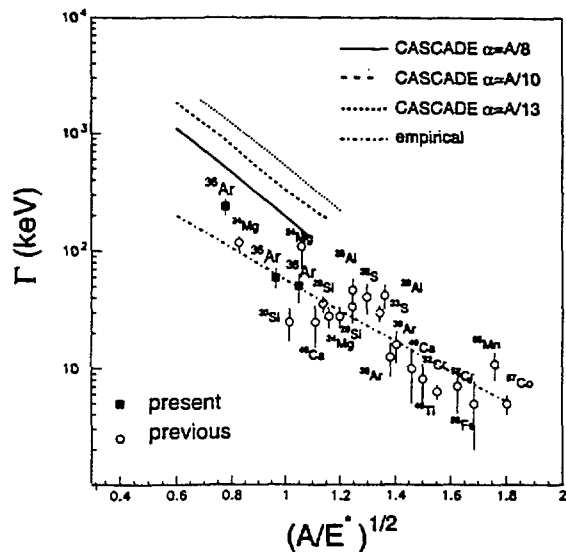


Fig 1: Presently determined widths are compared with the compiled values. The dotted line represents a linear fit to the compiled data. Statistical CASCADE calculations with different density parameters are shown, too.

**NEXT PAGE(S)  
left BLANK**

## **C - MISCELLANEOUS**



TOURNESOL: a new high efficiency, position sensitive, time-of-flight spectrometer for neutrons.

A.Péghaire<sup>1</sup>, J.Galin<sup>1</sup>, E.Liénard<sup>2</sup>, B.Lott<sup>1</sup>, Y.Patois<sup>1</sup>

1 GANIL (IN2P3-CNRS, DSM-CEA), BP 5027, F-14076 Caen Cedex 5, France

2 LPC (IN2P3-CNRS-University of Caen), F-14050 Caen Cedex, France

When studying the interplay between nuclear structure and reaction mechanism in collisions involving neutron halo nuclei it is very rewarding to measure as many correlated observables as possible for any event. This was well illustrated in another contribution of this progress report (ref.1). When dealing with very weak secondary beams a very high efficiency of all detectors working in coincidence is required. These conditions were met in ref.1 when detecting:

1/ The core (or its components) of the <sup>6</sup>He halo nucleus by means of a large area, position sensitive annular telescope.

2/ The thermal energy deposited into the target by means of the high efficiency and 4 $\pi$  neutron multiplicity-meter ORION.

3/ The linear momentum of the halo neutrons as measured with a high efficiency TOF spectrometer.

The latter parameter was then measured with an existing part of the ORION detector, used as a TOF spectrometer. Such a module tested with both mono-energetic neutron beams at Louvain-la-Neuve and later with cosmic rays (ref.2-3) revealed interesting properties of position sensitivity in addition to a very good efficiency. However since this detector had not been designed and thus not optimized for these aims, R&D has been made ending with the design and construction of a new GANIL instrument baptized TOURNESOL.

As explained in ref.3, the position sensitivity of such a detector manifests itself by the differential light yields collected by the phototubes surrounding the detector. Any position of the impact translates into a unique pattern of light yields, thus allowing, after proper calibration and model simulation, the reconstruction of the impact position in both radial distance and azimuthal distance. The position resolution has been observed to depend essentially on the dispersion due to the light distribution during the first collisions when the neutron loses most of its initial energy. Both measured and simulated data lead to a rms of the order of 10 cm indicating that the other sources of dispersion are quite negligible.

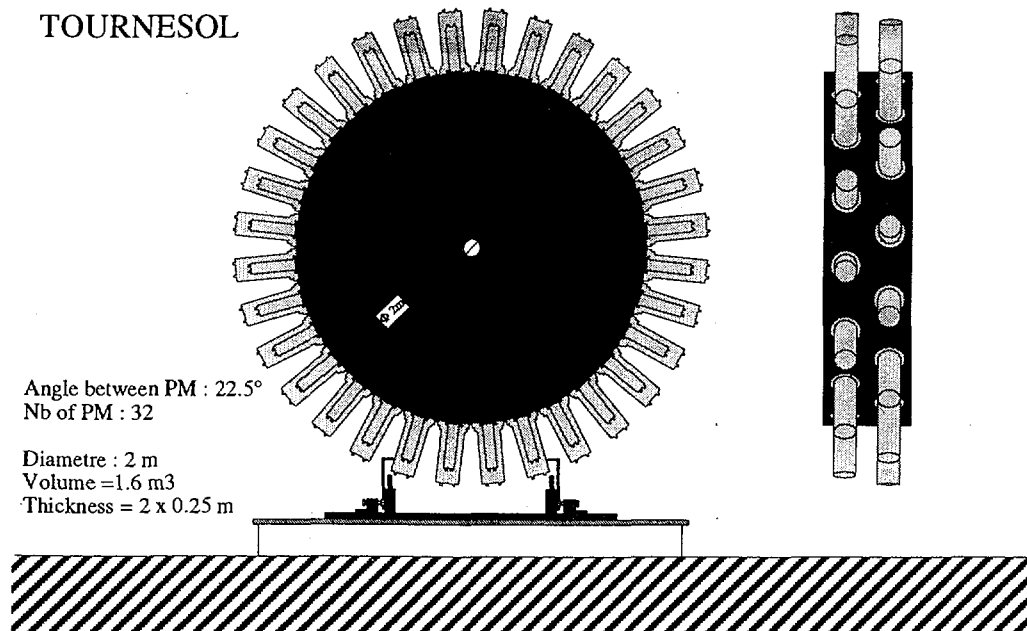


Fig.1 Layout of the TOURNESOL detector

As sketched in Fig.1, the TOURNESOL detector is 2 m in diameter, 50 cm thick, with two optically independent layers 25 cm thick, each. The read out of each cell is made by 16 2" in diameter phototubes, disposed on the detector periphery and viewing the liquid through windows. The scintillator is Gd loaded -as for ORION- enabling the neutron multiplicity measurement as well. TOURNESOL can thus act both as part of the  $4\pi$  multiplicity-meter and as a position sensitive TOF spectrometer. As was shown in a ref.1, and under proper conditions (very high thresholds on both cells), the double cell enables the handling without ambiguity of the two neutrons emitted from the halo. Test work on the proper location of both neutrons has still to be performed.

In summary, a new TOF and large area spectrometer for neutrons, TOURNESOL, has been built at GANIL. Its combined high efficiency, position sensitivity make of this detector an optimized tool for investigating nuclear reactions involving neutron halo projectiles in a novel way.

References:

- 1 Y.Périer, PhD thesis, Caen 1997 and paper in preparation.
- 2 Y.Périer et al. , Nucl. Instr. Meth. A 413 (1998) 312
- 3 E.Liénard et al., Nucl. Instr. Meth. A 413 (1998) 321

## Neutron production in thick Pb targets following spallation reactions

B.Lott, F.Cnigniet, J.Galin, F.Goldenbaum, D.Hilscher\*, A.Liénard, A.Péghaire, Y.Périer, X.Qian

GANIL (IN2P3-CNRS, DSM-CEA), BP 5027, F-14076 Caen cedex05, France

\*Hahn-Meitner-Institut Berlin, Glienicker Strasse 100, D-14109 Berlin, Germany

In the context of several projects (SPIRAL-Phase II, Prospects for a pilot plant for transmutation of nuclear wastes -a so called hybrid reactor coupling a subcritical nuclear reactor with an external neutron spallation source-, ...) it is highly desirable to determine the neutron production following the interaction of light projectiles in thick targets of heavy materials. For this purpose the  $4\pi$  neutron detector ORION at GANIL is particularly well suited with its high efficiency ( $>80\%$ ) for the few-MeV-neutrons of interest. In contrast with all other techniques used so far in order to measure the average neutron production, this instrument allows for an event by event determination of the production and thus leads to the full neutron multiplicity distribution. This information is of particular value when comparing the measured data with those of model calculations: the shape of the distribution brings strong additional constraints.

With a few thousands incident particles per second only needed for such measurements, of energy up to 200 MeV, the proton secondary beams of GANIL were well suited. They were generated from a primary  $^{13}\text{C}$  beam hitting a thick C target and their energies were defined by tuning the magnetic field of the fragment separator. The reaction products were then tagged by means of a thin plastic scintillator located inside the ORION scattering chamber (Fig.1 and ref.1).

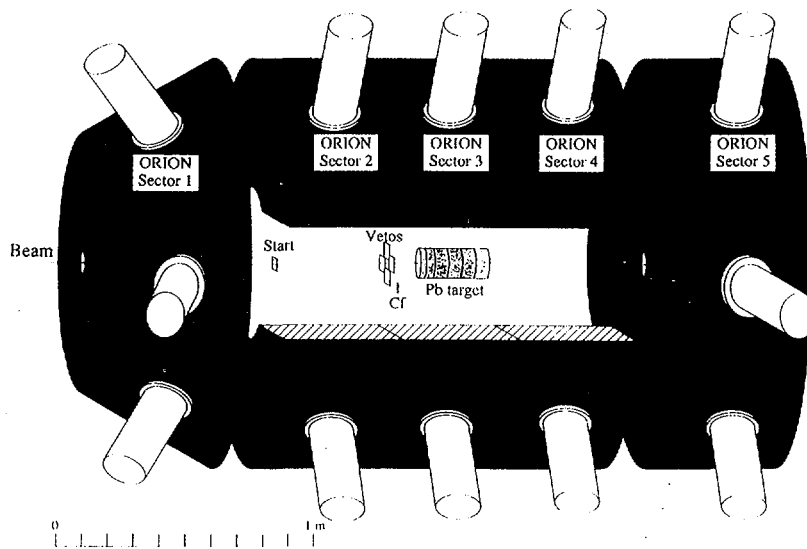


Fig.1 Layout of the experimental setup.

Fig.2 exemplifies the type of multiplicity distributions which were measured for the three scanned projectiles (p, d,  $\alpha$ ) of similar energy in massive targets. The histograms represent the actual neutron distributions as triggered by the detection of the incident particle whereas the symbols represent the distributions requiring in addition a prompt signal from the neutron detector (for more detail see ref.2). If the two hydrogen isotopes lead to similar neutron distributions, it is shown that  $\alpha$ -particles suffer much more the electromagnetic interaction into the target and are thus much less efficient as neutron generators than hydrogen projectiles.

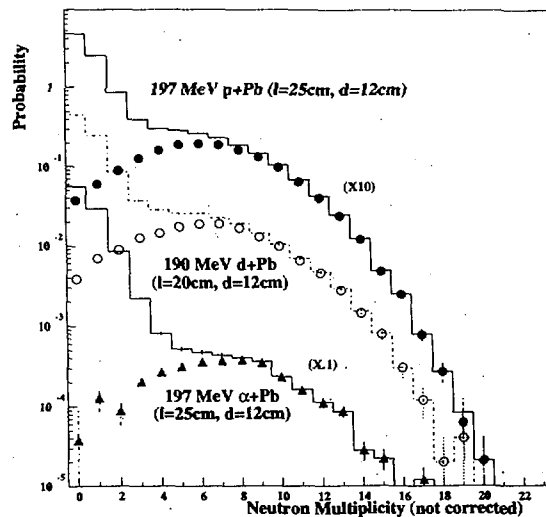


Fig.2 Neutron multiplicity distributions as measured inclusively (histograms) and in coincidence with a prompt signal generated by ORION (symbols) for the p,d and  $\alpha$ -particle projectiles.

The influence of the target geometry has been investigated as shown in Fig.3. The difference in neutron production is quite sensitive to the target thickness as long as the latter is less than about twice the considered particle range -sketched by arrows in the figure- and then remains independent of the thickness. It is quite accidental that the neutron production is found to be the same for both isotope projectiles on thick targets at this bombarding energy.

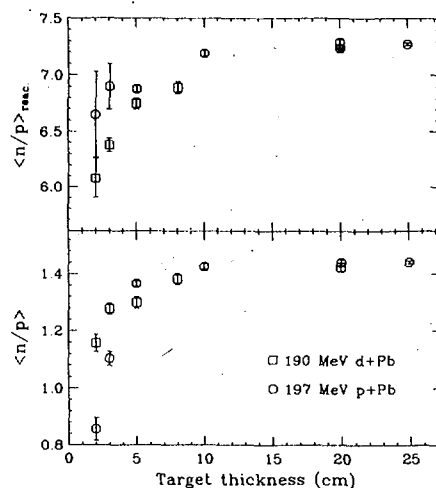


Fig.3. Mean neutron multiplicities (corrected for background and detector efficiency) of the inclusive distributions (lower panel) and those associated with reaction events as defined in the text (upper panel)

Similar measurements have been conducted in a more extensive way at higher energies (Ref.3) at CERN and recently at COSY-Jülich (Ref.4) in order to get an overview of spallation neutron production in a very broad energy range on various materials with varying geometries. It is the first set of data ever recorded, using all the same and very powerful  $4\pi$  measurement approach.

#### References:

- 1 Y.Périer et al. Nucl. Instr. and Meth. A (in press)
- 2 B.Lott et al. GANIL Preprint 97-37 and Nucl. Instr. and Meth. A (in press)
- 3 L.Pjenkowski et al. Phys. Rev. C56 (1997) 1909 and D.Hilscher et al., NIM A (in press)
- 4 NESSI Collaboration (in progress)

# COSMIC RAY INSTRUMENT CALIBRATION (E-285)

L. del Peral<sup>1</sup>, S. Sánchez<sup>2</sup>, E. Bronchalo<sup>1</sup>, M. Carbajo<sup>2</sup>, J. Medina<sup>1</sup> and D. Meziat<sup>2</sup>

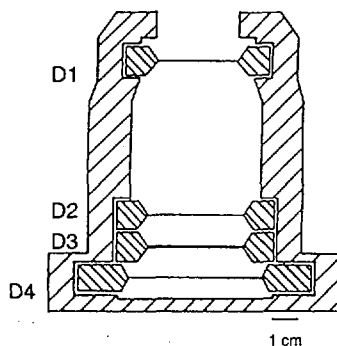
<sup>1</sup>Departamento de Física. <sup>2</sup>Departamento de Automática.  
Universidad de Alcalá. 28871 Alcalá de Henares (Madrid). Spain.

This work has been supported by CICYT (Grant. ESP95-0615) and DGICYT (Grant. UR1995-0168-01).

**Abstract.**— A low-energy cosmic ion detector instrument (called PESCA, Solar Energetic Particles and Anomalous galactic cosmic rays Component) composed of a telescope, its amplification electronic and data processing unit has been designed and will be constructed. The instrument is able to detect ions from hydrogen to iron at energy range of 1– 50 MeV/ nucleon. The electronics have been designed using space components, so its weight, dimensions and power consumption would be small enough to allow the system to be used for cosmic ion detection in space onboard Russian PHOTON satellite. In order to study its actual performances, the instrument need to be calibrated at an heavy ion accelerator.

**1. Instrument description.**— The instrument consists of three main parts: telescope, analog electronics (AE) and digital electronics (DE).

**1.1. Telescope.**— The telescope is made up of four silicon ion implanted detectors placed in a cylindrical aluminum frame (Fig. 1). Table 1 gives the characteristics of these cylindrical detectors. Detector thickness were selected by calculating how far the ions to be detected could penetrate silicon. The first two detectors, D<sub>1</sub> and D<sub>2</sub>, are basically tracking detectors, but D<sub>2</sub> also stops very low energy particles. D<sub>3</sub> is a stopping detector and D<sub>4</sub> is a veto detector for particles which are not stopped at the third detector. The D<sub>1</sub> detector should be thin enough to register the minimum detectable energy range with a cut off at about 2 MeV/nucleon for He and 4 MeV/nucleon for Fe. The D<sub>3</sub> detector must be able to stop the 50 MeV/nucleon Fe ions that hit it after crossing the D<sub>1</sub> and D<sub>2</sub> detectors. Last, the D<sub>4</sub> detector has the most active area, so that it will more efficiently detect ions escaping D<sub>3</sub>, for similar reason the D<sub>3</sub> detector has a less active area. Detectors positions were calculated (Fig. 1) in order to have an acceptance angle of approximately 50° which is wide enough for particles escaping D<sub>3</sub> detector to be caught by D<sub>4</sub> detector and not to escape through the aluminum structure. Additionally, at this acceptance angle, the incident particles should not have a range greater than 15% that of the vertical ones.



	D1	D2	D3	D4
Area (cm <sup>2</sup> )	3	4,5	4,5	9
Thickness (μm)	31	150	1014	100
Resistivity (kΩ cm)	0,408	1,8	12,5	1,9
Dead layer (μg/cm <sup>2</sup> )	40,0 Au 40,1 Al	40,0 Au 40,0 Al	40,1 Au 40,0 Al	40,0 Au 40,0 Al

Fig. 1: Schematic representation of detector telescope.

**1.2. Analog electronics (AE).**— AE consists of five stages. The first stage (Amplification) amplifies the detector pulses. It is composed by four preamplifiers (Amptek A250) and four amplifiers (Amptek A275) with negative feedback to avoid instabilities caused by

active component non-linearities and temperature effects. Detector instabilities in the baseline make the use of a baseline restorer necessary; an Amptek BLR1 integrated circuit was used for this purpose. The peak detector is composed by a PD 06 of WMT-Electronic. The coincidence/anti-coincidence stage is adjusted so that the output signal is only emitted if the  $D_1$  and  $D_2$  coincide while  $D_4$  is in anti-coincidence; therefore the discrimination logic used is  $D_1 D_2 \bar{D}_4$ . Amptek A150 pulse amplitude discriminators with two output gates have been used. This circuit triggers the conversion stage. The control circuit coordinates the conversion of analogue pulse to digital value. Three electronic chains, each composed of a Harris sample and hold HA5330 model and a Maxim analog-to-digital converter (ADC) MAX162 model make up the conversion stage.

1.3. *Digital electronics (DE).*— DE consists of two interfaces one with satellite another with AE and one data processing unit using one MAS281 micro-processor.

2. **Calibration.**— In the calibration we intent to obtain the instrument performance in charge and mass discriminations for ions of energies below 50 MeV/uma. In April 1997 the calibration was performed under the following characteristics:

Beam:  $^{58}\text{Ni}$ , 52 MeV/uma

Targets:  $^{12}\text{C}$  of 18,5 mg/cm<sup>2</sup> and  $^{197}\text{Au}$  of 57,9 mg/cm<sup>2</sup>

Telescope position: 45 cm from target at angles from 2° to 90° with respect to incident beam.

Experimental room: Nautilus.

The Fig. 2 shows two of results obtained.

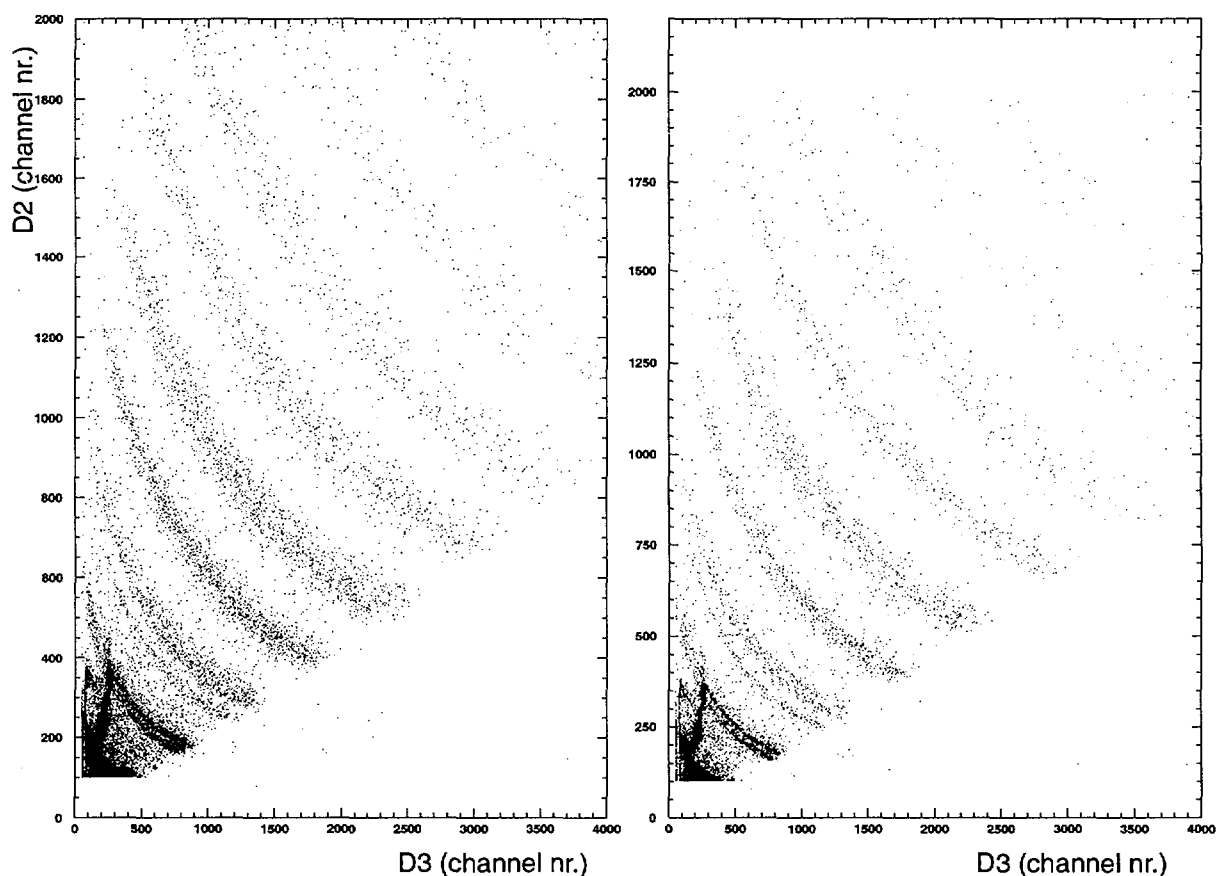


Fig. 2.— Calibration results obtained with  $^{197}\text{Au}$  target at 5° and 7° respectively.

#### References.

Nuclear Instrument and Method in Physics Research. A354 (1994) 539–546.  
IEEE Transaction on Nuclear Science. 44 (1997) 1442–1447.

# ANGULAR DISTRIBUTION OF PROTONS EMITTED FROM ORIENTED NUCLEI: TOWARDS IMAGING SINGLE-PARTICLE WAVE FUNCTIONS

N. Carjan<sup>1,3</sup>, P. Talou<sup>1,3</sup>, and D. Strottman<sup>2,3</sup>

<sup>1</sup>*CEN Bordeaux-Gradignan, 33175 Gradignan Cedex, France*

<sup>2</sup>*LANSCE and* <sup>3</sup>*Theoretical Division, Los Alamos National Laboratory, Los Alamos, NM 87545, USA*

A major drawback of most quantum mechanical measurements is that they produce only quantities averaged over coordinates or time; nuclear physics is no exception. There is, however, an observable (the angular distribution with respect to the deformation axis of single nucleons emitted from metastable states in oriented nuclei) that is directly related to the spatial distribution of the single-particle wave function, as will be shown in this report. It will also be argued that measuring the probability densities of nucleons in nuclei (not only matrix elements) is more promising and that it should become a new trend in evaluating our understanding of nuclear structure in the future.

## Density maps from angular distributions

To calculate the angular distribution with respect to the nuclear symmetry axis of a proton emitted from a metastable state in a deformed nucleus, we have solved numerically the time-dependent Schrödinger equation in two dimensions [1, 2]

$$i\hbar \frac{\partial}{\partial t} \psi(z, \rho, t) = \mathcal{H}(z, \rho) \psi(z, \rho, t) \quad (1)$$

where the hamiltonian  $\mathcal{H}$  is

$$\mathcal{H}(z, \rho) = -\frac{\hbar^2}{2\mu} \left[ \frac{1}{\rho} \frac{\partial}{\partial \rho} + \frac{\partial^2}{\partial \rho^2} + \frac{\partial^2}{\partial z^2} - \frac{\Lambda^2}{\rho^2} \right] + V(z, \rho) \quad (2)$$

Initial single-proton excited states in  $^{208}\text{Pb}$ , as those represented in Fig. 1, were chosen in the frame of a deformed Woods-Saxon potential, characterized by the deformation parameter  $\epsilon$  ( $\simeq \beta_2$  for small  $\epsilon$ ).

Knowing  $\psi(z, \rho, t)$ , one can estimate the tunneling probability as a function of azimuthal angle  $\theta$ :

$$P_{tun}(t, \theta) = \int_{r_B(\theta)}^{\infty} |\psi(r, \theta, t)|^2 r^2 dr \quad (3)$$

where  $r_B(\theta)$  is the radial position of the potential ridge in the direction  $\theta$ . The results are shown in Fig. 2 for the  $'2\hbar'$  quasi-stationary states at  $\epsilon = 0.1$  from Fig. 1.

Except for  $\Lambda = 0$ , none of these wave functions escapes along the path of minimum barrier ( $\theta = 0^\circ$ ). The main directions of emission are determined by the angles between the branches of the initial wave function and the  $z$  axis. The anisotropic barrier acts like a filter modifying the relative intensities of different branches but does not change their directions. Consequently, the emission does not always occur along the nuclear symmetry axis as was intuitively predicted in

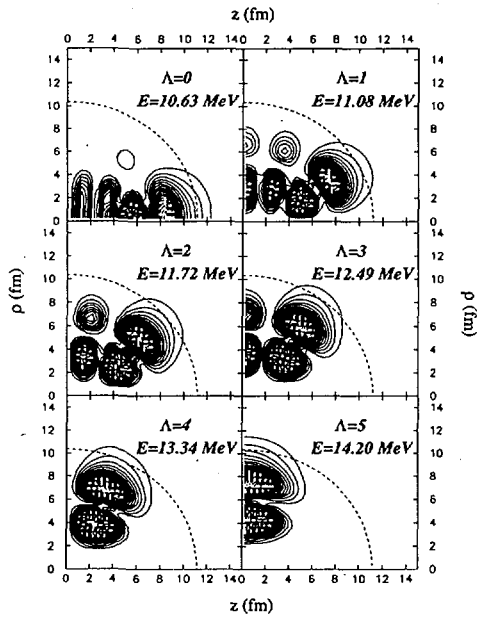


Figure 1:  $|\psi_{2h}(z, \rho)|^2$  at  $\epsilon = 0.1$ .

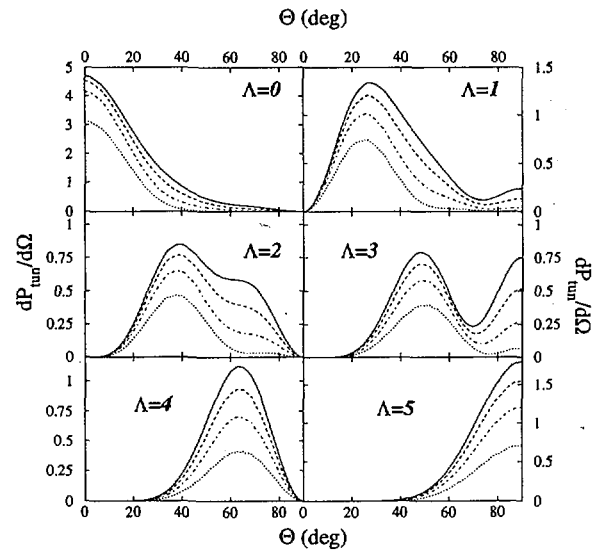


Figure 2: Angular distributions of the '2h' states at  $\epsilon = 0.1$ .

Ref. [3]. It is therefore possible in most cases to deduce the number of branches in the proton density and their orientations just by inspecting the angular distribution. For more complete information it is, however, necessary to simulate the filter, *i.e.*, to calculate the tunneling through a bidimensional barrier. A detailed study of the connection between angular distributions and density maps is in progress.

In conclusion, quite accurate maps of single-particle density distributions in deformed nuclei can be obtained by combining a) angular distribution measurements of single nucleons emitted from metastable states in oriented nuclei, and b) numerical simulations of quantum tunneling through an anisotropic coulomb + centrifugal barrier. This would represent the first direct measurement of probability densities of nucleons in nuclei and would allow one to test nuclear models on a deeper and more detailed level.

After this work was completed we found that pronounced anisotropies – such as those calculated above – have been recently observed during a similar process involving  $\alpha$  emission from oriented nuclei [4]. Although  $\alpha$  decay is easier to measure, proton or neutron decay represents a better tool for exploring in detail the wave functions involved since: a) the modification of the initial wave anisotropy by the tunneling filter is less important, and b) one samples a single particle wave function at a time and not an overlap of the four nucleons entering into the formation amplitude of an  $\alpha$  particle, and c) it carries higher angular momenta.

## References

- [1] P. Talou, N. Carjan and D. Strottman, submitted to Nucl. Phys. A.
- [2] P. Talou, N. Carjan and D. Strottman, submitted to Phys. Rev. C.
- [3] D.L. Hill and J.A. Wheeler, Phys. Rev. **89** (1953) 1102.
- [4] P. Schuurmans *et al.*, Phys. Rev. Lett. **77** (1996) 4720.



## **II. PUBLICATION LIST**

**1996**

**MODEL-UNRESTRICTED NUCLEUS-NUCLEUS SCATTERING POTENTIALS FROM MEASUREMENT AND ANALYSIS OF  $^{16}\text{O} + ^{16}\text{O}$  SCATTERING**

BARTNITZKY G. ET AL.

PHYSIKALISCHES INST. UNIV. TÜBINGEN - TÜBINGEN, HMI - BERLIN, GANIL - CAEN, CE SACLAY - GIF-SUR-YVETTE

**NIM B365 (1996) 23.**

96 01 A1

**SEARCH FOR THE SIGNATURE OF A HALO STRUCTURE IN THE  $p(^6\text{He}, ^6\text{Li})n$  REACTION**

CORTINA-GIL M.D. ET AL.

GANIL - CAEN, CEA SACLAY - GIF-SUR-YVETTE, MCGILL UNIV. - MONTREAL, IPN - ORSAY, IFUSP DFN - SAO PAULO, LPC ISMRA - CAEN

**PHYSICS LETTERS B371 (1996) 14.**

96 09 A

**GIANT DIPOLE RESONANCE IN VERY HOT NUCLEI OF MASS  $A = 115$**

SUOMIJARVI T. ET AL.

IPN - ORSAY, INFN LNS - CATANIA, DAPNIA CEN SACLAY - GIF SUR YVETTE, GANIL - CAEN, NBI - COPENHAGEN

**PHYSICAL REVIEW C53 (1996) 2258.**

96 40 A

**GIANT DIPOLE EMISSION AS A PROBE OF THE ENTRANCE CHANNEL DYNAMICS**

BARAN V. ET AL.

LNS INFN - CATANIA, IFA - BUCAREST, GANIL - CAEN, UNIV. OF ILLINOIS - URBANA

**NUCLEAR PHYSICS A600 (1996) 111.**

96 42 A

**LIMITING TEMPERATURES FOR COLLECTIVE MOTION : THE GIANT DIPOLE RESONANCE IN VERY HOT NUCLEI**

PIATTELLI P. ET AL.

INFN LNS - CATANIA, IPN - ORSAY, DAPNIA CEA SACLAY - GIF SUR YVETTE, GANIL - CAEN, NBI - COPENHAGEN

PROCEEDINGS OF THE GRONINGEN CONFERENCE ON GIANT RESONANCES

GRONINGEN (NL) 1995

**NUCLEAR PHYSICS A599, 1,2 (1996) 63c.**

96 43 A

**ARE GIANT RESONANCES HARMONIC VIBRATIONS?**

VOLPE C. ET AL.

GANIL - CAEN, DEP. FIS.ATOM.MOLEC.NUCL. - SEVILLA, DIP. FIS. AND INFN - CATANIA

PROCEEDINGS OF THE GRONINGEN CONFERENCE ON GIANT RESONANCES

GRONINGEN (NL) 1995

**NUCLEAR PHYSICS A599, 1,2 (1996) 347c.**

96 44 A

**REGULARITY AND CHAOS IN VLASOV EVOLUTION OF NUCLEAR MATTER**

JACQUOT B. ET AL.

GANIL - CAEN, LNS - CATANIA

**PHYSICAL REVIEW C54, 6 (1996) 3025.**

96 48 A

**ELASTIC SCATTERING OF  $^6\text{He}$  AND ITS ANALYSIS WITHIN A FOUR-BODY EIKONAL MODEL**

AL-KHALILI J.S. ET AL.

SOUTHERN CENTRE FOR NUCL. PHYS. - GUILDFORD, GANIL - CAEN, DAPNIA CEA SACLAY - GIF SUR YVETTE, MCGILL UNIV. - MONTREAL, IPN - ORSAY, IFUSP DFN - SAO PAULO, LPC ISMRA - CAEN

**PHYSICS LETTERS B378 (1996) 45.**

96 49 A

**IDENTIFICATION OF HYDROGEN ISOTOPES WITH THE BaF<sub>2</sub> ELECTROMAGNETIC CALORIMETER TAPS**

MATULEWICZ T. ET AL.

GANIL - CAEN, LPC - CAEN

**NIM A378 (1996) 179.**

96 58 A

**FLUID DYNAMICAL APPROACH TO SPINODAL INSTABILITIES IN FINITE NUCLEAR SYSTEMS**

JACQUOT B. ET AL.

GANIL - CAEN, TTU - COOKEVILLE, LNS - CATANIA

**PHYSICS LETTERS B383 (1996) 247.**

96 63 A

**PRE-EQUILIBRIUM EFFECTS IN THE POPULATION OF GIANT DIPOLE RESONANCES**

FLIBOTTE S. ET AL.

DPA McMASTER UNIV. - HAMILTON, AECL - CHALK RIVER, GANIL - CAEN, DP UNIV. OF TORONTO - TORONTO

**PHYSICAL REVIEW LETTERS 77, 8 (1996) 1448.**

96 64 A

**FIRST SPECTROSCOPIC STUDY OF <sup>22</sup>Si**

BLANK B ET AL.

CENBG - GRADIGNAN, GSI - DARMSTADT, INST. FUR KERNPHYSIK TH DARMSTADT, LPC ISMRA - CAEN

**PHYSICAL REVIEW C54, 2 (1996) 572.**

96 65 A

**SPECTROSCOPY OF LIGHT- AND MEDIUM-MASS PROTON-RICH NUCLEI**

BLANK B.

CENBG - GRADIGNAN

EXTREMES OF NUCLEAR STRUCTURE

PROCEEDINGS OF THE INTERNATIONAL WORKSHOP XXIV ON GROSS PROPERTIES OF NUCLEI AND NUCLEAR EXCITATIONS

HIRSCHEGG (AT) 1996

96 72 A

**ELASTIC SCATTERING AND CHARGE EXCHANGE REACTIONS WITH EXOTIC BEAMS**

CORTINA-GIL M.D.

GANIL - CAEN, DAPNIA CE SACLAY - GIF SUR YVETTE, FRL Mc GILL UNIV. - MONTREAL, IPN - ORDAY,

SCNP UNIV. OF SURREY - GUILDFORD, IFUSP DFN - SAO PAULO, LPC ISMRA - CAEN

EXTREMES OF NUCLEAR STRUCTURE

PROCEEDINGS OF THE INTERNATIONAL WORKSHOP XXIV ON GROSS PROPERTIES OF NUCLEI AND NUCLEAR EXCITATIONS

HIRSCHEGG (AT) 1996

96 77 A

**THE MANY FACETS OF GIANT RESONANCES AT HIGH EXCITATION ENERGIES**

BARAN V. ET AL.

IFA - BUCAREST, GANIL - CAEN, LNS INFN - CATANIA, INR - KIEV, ILLINOIS UNIV. - URBANA

PROCEEDINGS OF THE GRONINGEN CONFERENCE ON GIANT RESONANCES

GRONINGEN (NL) 1995

**NUCLEAR PHYSICS A599, 1,2 (1996) 29c.**

96 79 A

**EFFECTIVE GAMMA DEFORMATION NEAR  $A = 130$  IN THE INTERACTING BOSON MODEL**

VOGEL O. ET AL.

INST. FUR KERNPHYSIK - KOLN, GANIL - CAEN

PHYSICAL REVIEW C53, 4 (1996) 1660.

96 89 A

**SUPERSYMMETRIC MULTIPHONON STRUCTURE**

KIM K.H. ET AL.

TOKYO UNIV. - TOKYO, INST. FUR KERNPHYSIK - KOLN, GANIL - CAEN

PHYSICAL REVIEW LETTERS 76, 19 (1996) 3514.

96 90 A

**UNEXPECTED PROPERTIES OF THE SCISSORS MODE IN THE ODD-MASS NUCLEUS  $^{167}\text{Er}$**

SCHLEGEL C. ET AL.

INST. FUR KERNPHYSIK - DARMSTADT, GANIL - CAEN

PHYSICS LETTERS B375 (1996) 21.

96 91 A

**PARTICLE-HOLE EXCITATIONS IN THE INTERACTING BOSON MODEL (I) GENERAL STRUCTURE AND SYMMETRIES**

DE COSTER C. ET AL.

ITP VAKGROEP SUBAT.STRALINGSFYSICA - GENT, GANIL - CAEN, IP FRIBOURG UNIV. - FRIBOURG,

SCHOOL OF PHYSICS - ATLANTA

NUCLEAR PHYSICS A600 (1996) 251.

96 92 A

**SELECTED ASPECTS OF COLLECTIVE MOTIONS IN NUCLEI : ORDER AND DISORDER**

CHOMAZ PH.

GANIL - CAEN

ANNALES DE PHYSIQUE 21 (1996) 669.

96 93 A

**RECENT RESULTS ON ELASTIC AND INELASTIC SCATTERING**

ALAMANOS N. ET AL.

CE SACLAY - GIF-SUR-YVETTE, GANIL - CAEN

ANNALES DE PHYSIQUE 21 (1996) 601.

96 94 A

**STUDY OF THE UNBOUND NUCLEUS  $^{11}\text{N}$  BY ELASTIC RESONANCE SCATTERING**

AXELSSON L. ET AL.

CHALMERS TEKNISKA HOGSKOLA - GOTEBOURG, INST.DE ESTRUCTURA DE LA MATERIA - MADRID,

KURCHATOV INST. - MOSCOW, IPN - ORSAY, ABO ACADEMI - TURKU, GANIL - CAEN, AARHUS UNIV. -

AARHUS, LPC - CLERMONT FERRAND, JINR - DUBNA

PHYSICAL REVIEW C54, 4 (1996) R1511.

96 95 A

**NEW ISOMER  $^{32}\text{Al}^m$**

ROBINSON M. ET AL.

GANIL - CAEN, IAP - BUCHAREST, JINR - DUBNA, LPC ISMRA - CAEN

PHYSICAL REVIEW C53 (1996) 1465.

96 37 C

**MASS MEASUREMENT OF  $^{100}\text{Sn}$**

CHARTIER M. ET AL.

GANIL - CAEN, IFUSP - SAO PAULO, DNP AUSTRALIAN NAT.UNIV., CEN SACLAY - GIF SUR YVETTE,

BERGEN UNIV. FYSIK INST. - BERGEN, LPC ISMRA - CAEN, DIP. DI FIS. CATANIA UNIV. - CATANIA

**PHYSICAL REVIEW LETTERS 77, 12 (1996) 2400.**  
96 67 C

**FIRST OBSERVATION OF THE  $T_z = -7/2$  NUCLEI  $^{45}\text{Fe}$  AND  $^{49}\text{Ni}$**

BLANK B. ET AL.

CENBG - GRADIGNAN, GSI - DARMSTADT, IEP WARSAW UNIV. - WARSAW, GANIL - CAEN

**PHYSICAL REVIEW LETTERS 77, 14 (1996) 2893.**

96 70 C

**MASS MEASUREMENT OF  $^{100}\text{Sn}$  AND  $^{100}\text{In}$  USING THE SECOND CYCLOTRON OF GANIL AS A HIGH RESOLUTION MASS SPECTROMETER**

MITTIG W. ET AL.

GANIL - CAEN, IFUSP - SAO PAULO, DNP AUSTRALIAN NAT. UNIV., CEN SACLAY - GIF SUR YVETTE,

UNIV. BERGEN - BERGEN, LPC ISMRA - CAEN, IPN - ORSAY, UNIV. CATANIA - CATANIA

EXTREMES OF NUCLEAR STRUCTURE

PROCEEDINGS OF THE INTERNATIONAL WORKSHOP XXIV ON GROSS PROPERTIES OF NUCLEI AND

NUCLEAR EXCITATIONS

HIRSCHEGG (AT) 1996

96 73 C

**ASTROPHYSICS WITH NEUTRON-RICH NUCLEI**

SORLIN O.

IPN - ORSAY

EXTREMES OF NUCLEAR STRUCTURE

PROCEEDINGS OF THE INTERNATIONAL WORKSHOP XXIV ON GROSS PROPERTIES OF NUCLEI AND

NUCLEAR EXCITATIONS

HIRSCHEGG (AT) 1996

96 74 C

**SPECTROSCOPY OF LIGHT EXOTIC NUCLEI**

OSTROWSKI A.N. ET AL.

GANIL - CAEN, HMI - BERLIN, OHIO UNIV. - ATHENS, JINR - DUBNA, RRCKI - MOSCOW

EXTREMES OF NUCLEAR STRUCTURE

PROCEEDINGS OF THE INTERNATIONAL WORKSHOP XXIV ON GROSS PROPERTIES OF NUCLEI AND

NUCLEAR EXCITATIONS

HIRSCHEGG (AT) 1996

96 78 C

**NEUTRON-RICH ISOTOPES  $^{54-57}\text{Ti}$**

DORFLER T. ET AL.

GOTTINGEN UNIV. - GOTTINGEN, MAINZ UNIV. - MAINZ, IPN - ORSAY, GANIL - CAEN

**PHYSICAL REVIEW C54, 6 (1996) 2894.**

96 86 C

**RELATIVISTIC MEAN-FIELD STUDY OF LIGHT PROTON-RICH NUCLEI  $^{18}\text{Ne}$ ,  $^{20}\text{Mg}$  AND  $^{22}\text{Si}$**

REN Z. ET AL.,

GANIL - CAEN, NANJING UNIVERSITY - NANJING, FJG INSTITUT FÜR KERNPHYSIK - JÜLICH

**ZEITSCHRIFT FÜR PHYSIKS A353 (1996) 363-365**

96 96 C

**LIGHT PARTICLE-EVAPORATION RESIDUE COINCIDENCES FOR THE  $^{79}\text{Br} + ^{27}\text{Al}$  SYSTEM AT 11.8 MeV/NUCLEON**

GOMEZ DEL CAMPO J. ET AL.

ORNL - OAK RIDGE, GANIL - CAEN, UNIV. NACIONAL AUTONOMA DE MEXICO - MEXICO, DAPNIA CE

SACLAY - GIF-SUR-YVETTE

**PHYSICAL REVIEW C53, 1 (1996) 222.**

96 04 D4

**DISAPPEARANCE OF FLOW AND THE IN-MEDIUM NUCLEON-NUCLEON CROSS SECTION FOR  $^{64}\text{Zn} + ^{27}\text{Al}$  COLLISIONS AT INTERMEDIATE ENERGIES**

ZHI YONG HE ET AL.

LPC ISMRA - CAEN, IMP - LANZHOU, GANIL - CAEN, IPN - LOUVAIN-LA-NEUVE, SUBATECH - NANTES, TEXAS A&M UNIV. - COLLEGE STATION, INST.NUCL.RES. - SHANGHAI, VAPOLI UNIV. - NAPLES

**NUCLEAR PHYSICS A598 (1996) 248.**

96 05 D

**DYNAMICAL ANALYSIS OF DISSIPATIVE COLLISIONS BETWEEN Ar AND Ag NUCLEI IN THE FERMI ENERGY DOMAIN**

HADDAD F. ET AL.

SUBATECH - NANTES, TEXAS A&M UNIV. - COLLEGE STATION, IPN - ORSAY

**ZEITSCHRIFT FÜR PHYSIKS A354 (1996) 321.**

96 10 D

**ORBITING FEATURES IN THE STRONGLY DAMPED BINARY DECAY OF THE  $^{28}\text{Si} + ^{16}\text{O}$  SYSTEM**

OLIVEIRA J.M. ET AL.

IFUSP DFN - SAO PAULO, DCM UNIV. DE SOROCABA, GANIL - CAEN, LABOR. TANDAR - BUENOS AIRES

**PHYSICAL REVIEW C53, 6 (1996) 2926.**

96 38 D

**EVIDENCE FOR COULOMB FISSION OF  $^{238}\text{U}$  IN THE INTERACTION OF 24.3 MeV/NUCLEON  $^{23}\text{U}$  WITH  $^{197}\text{Au}$  : A NEW EXPERIMENTAL APPROACH**

PIASECKI E. ET AL.

IEP WARSAW UNIV. - WARSAW, HEAVY ION LAB. WARSAW UNIV. - WARSAW, WARSAW UNIV. OF AGRICULTURE - WARSAW, SINS - SWIERK, GANIL - CAEN, IF UNIV. SAO PAULO - SAO PAULO, IPN - ORSAY, HMI - BERLIN

**PHYSICS LETTERS B377 (1996) 235.**

96 39 D

**PRODUCTION OF RADIONUCLIDES BY 1.7 GeV PROTON-INDUCED REACTIONS ON CdTe CRYSTALS**

PORRAS E. ET AL.

DEPT. MAT. APLICADA Y ASTRONOMIA - BURJASSOT, PHYS. DEPT. UNIV. OF SOUTHAMPTON, CIEMAT - MADRID, IFC - BURJASSOT, DEPT. DE FIS. UPN - PAMPLONA, GANIL - CAEN

**NIM B111 (1996) 315.**

96 46 D

**ONSET OF COLLECTIVE EXPANSION IN NUCLEUS-NUCLEUS COLLISIONS BELOW 100 MeV/u**

JEONG S.C. ET AL.

LPC ISMRA - CAEN, DP SOONGSIL UNIV. - SEOUL, GANIL - CAEN, DAPNIA CE SACLAY - GIF SUR YVETTE, IPN UCL - LOUVAIN-LA-NEUVE, LPN - NANTES, IMP - LANZHOU, DSF INFN - NAPOLI

**NUCLEAR PHYSICS A604 (1996) 218.**

96 50 D

**HEATING OF NUCLEI WITH ENERGETIC ANTIPROTONS**

GOLDENBAUM F. ET AL.

HMI - BERLIN, CERN - GENEVE, TU-MUNCHEN - GARCHING, GANIL - CAEN, INR RUSSIAN ACAD.SCI. - MOSCOW, WARSAW UNIV. - WARSZAWA, FZ-ROSSENDORF - DRESDEN, IPN - ORSAY

**PHYSICAL REVIEW LETTERS 77, 7 (1996) 1230.**

96 56 D

**NEUTRON FROM THE BREAKUP OF  $^{19}\text{C}$**

MARQUES F.M. ET AL.

LPC ISMRA - CAEN, FI CTH - GÖTEBORG, DP SURREY UNIV. - GUILDFORD, SPSR BIRMINGHAM UNIV.,  
CRN - STRASBOURG, IPN - ORSAY, ULB - BRUXELLES, NSCL MSU-EAST LANSING, GANIL-CAEN, IP  
UCL-LOUVAIN LA NEUVE, IFA AARHUS UNIV.-AARHUS, DL - WARRINGTON

**PHYSICS LETTERS B381 (1996) 407.**

96 61 D

**ONE-NUCLEON TRANSFER REACTIONS TO CONTINUUM STATES INDUCED BY HEAVY  
ION PROJECTILES**

LHENRY I. ET AL.

IPN - ORSAY, GANIL - CAEN, DAPNIA CE SACLAY - GIF SUR YVETTE, NSCL MSU - EAST LANSING, DP  
CENTRAL MICHIGAN UNIV. - Mt. PLEASANT, UNIV. FEDERAL - RIO DE JANEIRO

**PHYSICAL REVIEW C54, 2 (1996) 593.**

96 66 D

**DECAY PATTERNS OF TARGET-LIKE AND PROJECTILE-LIKE NUCLEI PRODUCED IN  $^{84}\text{Kr} + ^{197}\text{Au}$ ,  
 $^{nat}\text{U}$  REACTIONS AT  $E/A = 150$  MeV**

QUEDNAU B.M. ET AL.

GANIL - CAEN, HMI - BERLIN, IFUSP DFN - SAO PAULO, IPN - ORSAY, KVI - GRONINGEN, LN SATURNE -  
GIF SUR YVETTE

**NUCLEAR PHYSICS A606 (1996) 538.**

96 68 D

**STUDY OF SHORT-LIVED ISOMERS PRODUCED IN THE FRAGMENTATION-LIKE  
REACTIONS**

LEWITOWICZ M.

GANIL - CAEN

EXTREMES OF NUCLEAR STRUCTURE

PROCEEDINGS OF THE INTERNATIONAL WORKSHOP XXIV ON GROSS PROPERTIES OF NUCLEI AND  
NUCLEAR EXCITATIONS

HIRSCHEGG (AT) 1996

96 75 D

**REACTION MECHANISM IN HIGHLY FRAGMENTED  $\text{Pb} + \text{Au}$  COLLISIONS AT 29 MeV/u**

LECOLLEY J.F. ET AL.

LPC ISMRA - CAEN, CRN - STRASBOURG

**PHYSICS LETTERS B387 (1996) 460.**

96 80 D

**$^9\text{B}$  PROTON HALO VIA REACTION AND BREAKUP CROSS SECTION MEASUREMENTS**

NEGOITA F. ET AL.

IAP - BUCHAREST-MAGURELE, GANIL - CAEN, IPN - ORSAY, FLNR JINR - DUBNA, NPI - REZ, IEP  
WARSAW UNIV. - WARSAW

**PHYSICAL REVIEW C54, 4 (1996) 1787.**

96 81 D

**KINEMATICAL PROPERTIES AND COMPOSITION OF VAPORIZING SOURCES : IS  
THERMODYNAMICAL EQUILIBRIUM ACHIEVED ?**

BORDERIE B. ET AL.

IPN - ORSAY, LPC ISMRA - CAEN, GANIL - CAEN, IPNL - VILLEURBANNE, DAPNIA CEN SACLAY - GIF  
SUR YVETTE, SUBATECH - NANTES

**PHYSICS LETTERS B388 (1996) 224.**

96 82 D



**VAPORIZATION EVENTS FROM BINARY DISSIPATIVE COLLISIONS**

RIVET M.F. ET AL.

IPN - ORSAY, GANIL - CAEN, SUBATECH - NANTES, IPNL - VILLEURBANNE, LPC ISMRA - CAEN,  
DAPNIA CEN SACLAY - GIF SUR YVETTE

**PHYSICS LETTERS B388 (1996) 219.**

96 83 D

**COMMENT ON "ANALYSIS OF HARD TWO-PHOTON CORRELATIONS MEASURED IN  
HEAVY-ION REACTIONS AT INTERMEDIATE ENERGIES"**

MARQUES F.M. ET AL.

GANIL - CAEN, LPC - CAEN, WARSAW UNIV. - WARSZAWA, KVI - GRONINGEN

**PHYSICAL REVIEW C54, 5 (1996) 2783.**

96 84 D

**PION REABSORPTION IN HEAVY-ION COLLISIONS INTERPRETED IN TERMS OF THE  
DELTA CAPTURE PROCESS**

HOLZMANN R. ET AL.

GANIL - CAEN, GSI - DARMSTADT, KVI - GRONINGEN, IFC - BURJASSOT, GIESSEN UNIV. - GIESSEN, NPI  
- PRAHY, CENBG - GRADIGNAN

**PHYSICS LETTERS B366 (1996) 63.**

96 02 F

**SUBTHRESHOLD PION DYNAMICS AS A SOURCE FOR HARD PHOTONS BEYOND  
PROTON-NEUTRON BREMSSTRAHLUNG IN HEAVY-ION COLLISIONS**

GUDIMA K.K. ET AL.

GANIL - CAEN, GSI - DARMSTADT, KVI - GRONINGEN, IFC - BURJASSOT

**PHYSICAL REVIEW LETTERS 76 (1996) 2412.**

96 06 F

**IMPORTANCE OF ONE- AND TWO-BODY DISSIPATION AT INTERMEDIATE ENERGIES  
STUDIED BY HARD PHOTONS**

VAN POL J.H.G. ET AL.

KVI - GRONINGEN, GANIL - CAEN, GSI - DARMSTADT, GIESSEN UNIV. - GIESSEN, IFC - BURJASSOT,  
SLOVAK ACAD.SCI. - BRATISLAVA, NPI - PRAHY

**PHYSICAL REVIEW LETTERS 76 (1996) 1425.**

96 08 F

**NUCLEAR STOPPING IN HEAVY-ION COLLISIONS AT 100 MeV/NUCLEON FROM  
INCLUSIVE AND EXCLUSIVE NEUTRAL PION MEASUREMENTS**

BADALA A. ET AL.

INFN - CATANIA, CATANIA UNIV. - CATANIA, INFN LNS - CATANIA

**PHYSICAL REVIEW C53 (1996) 1782.**

96 12 F

**THE ROLE OF NUCLEAR INCOMPRESSIBILITY IN THE PRODUCTION OF HARD  
PHOTONS IN HEAVY-ION COLLISIONS**

SCHUTZ Y.,

GANIL - CAEN

PROCEEDINGS OF THE GRONINGEN CONFERENCE ON GIANT RESONANCES

GRONINGEN (NL) 1995

**NUCLEAR PHYSICS A599, 1,2 (1996) 97c.**

96 45 E

**1997**

**STUDY OF MULTIFRAGMENTATION PATTERNS INDUCED BY SPINODAL INSTABILITIES**

COLONNA M. ET AL.

GANIL - CAEN, LNS - CATANIA

**NUCLEAR PHYSICS A613 (1997) 165.**

97 03 A

**THE SCISSORS MODE IN THE PRESENCE OF A NEUTRON SKIN**

WARNER D.D. ET AL.

CCLRC DARESBURY LAB. - DARESBURY, GANIL - CAEN

**PHYSICS LETTERS B395 (1997) 145.**

97 21 A

**THE SPECTROSCOPY OF  $^{22}\text{Al}$ : A  $\beta_p$ ,  $\beta_{2p}$  AND  $\beta_\alpha$  EMITTER**

BLANK B. ET AL.

CENBG - GRADIGNAN, LPC ISMRA - CAEN, GSI - DARMSTADT, INST.FUR KERNPHYSIK - DARMSTADT

**NUCLEAR PHYSICS A615 (1997) 52.**

97 22 A

**SHELL MODEL STUDY OF THE NEUTRON-RICH NUCLEI AROUND  $N = 28$**

RETAMOSA J. ET AL.

CRN - STRASBOURG, GANIL - CAEN, UNIV. AUTONOMA DE MADRID - MADRID

**PHYSICAL REVIEW C55, 3 (1997) 1266.**

97 23 A

**TRANSFER RESULTS FOR ODD-ODD  $^{199}\text{Au}$  AS A TEST OF EXTENDED SUPERSYMMETRY**

BERRIER-RONSIN G. ET AL.

IPN - ORSAY, GANIL - CAEN, IP UNIV. DE FRIBOURG - FRIBOURG

**PHYSICAL REVIEW C55, 3 (1997) 1200.**

97 24 A

**NUCLEAR ASTROPHYSICS WITH RADIOACTIVE BEAMS**

VERVIER J.

IPN - LOUVAIN-LA-NEUVE

**EUROPHYSICS NEWS 28 (1997) 25.**

97 25 A

**FRAGMENT MOMENTUM DISTRIBUTIONS AND THE HALO**

ORR N.A.

LPC ISMRA - CAEN

PROCEEDINGS OF THE FOURTH INTERNATIONAL CONFERENCE ON RADIOACTIVE NUCLEAR BEAMS

OMIYA (JP) 1996

**NUCLEAR PHYSICS A616 (1997) 155c.**

97 28 A

**STUDY OF WEAKLY BOUND AND UNBOUND STATES OF EXOTIC NUCLEI WITH BINARY REACTIONS**

BOHLEN H.G. ET AL.

HMI - BERLIN, FLNR JINR - DUBNA, GANIL - CAEN, DPA OHIO UNIV. - ATHENS

PROCEEDINGS OF THE FOURTH INTERNATIONAL CONFERENCE ON RADIOACTIVE NUCLEAR BEAMS

OMIYA (JP) 1996

**NUCLEAR PHYSICS A616 (1997) 254c.**

97 32 A

**MASS MEASUREMENTS NEAR  $N = Z$**

MITTIG W. ET AL.

GANIL-CAEN, LPC- CAEN, CSNSM-ORSAY, INFN-CATANIA, IPN - ORSAY, IFUSP-SAO PAULO, JINR-DUBNA, NSCL MSU-EAST LANSING, LANL-LOS ALAMOS, RSPHySE-CANBERRA, CE SACLAY-GIF-SUR-YVETTE; UNIV. DI CATANIA- CATANIA, UNIV. I BERGEN - BERGEN

PROCEEDINGS OF THE FOURTH INTERNATIONAL CONFERENCE ON RADIOACTIVE NUCLEAR BEAMS

OMIYA (JP) 1996

**NUCLEAR PHYSICS A616 (1997) 329c.**

97 34 A

**T = 0 VERSUS T = 1 PAIRING IN THE INTERACTING BOSON MODEL**

VAN ISACKER P. ET AL.

GANIL - CAEN, CCLRC DARESBUURY LAB. - DARESBUURY

**PHYSICAL REVIEW LETTERS 78, No.17 (1997) 3266.**

97 35 A

**IONIC CHARGE DEPENDENCE OF THE INTERNAL CONVERSION COEFFICIENT AND NUCLEAR LIFETIME OF THE FIRST EXCITED STATE IN  $^{125}\text{T}_{\text{e}}$**

ATTALLAH F. ET AL.

CENBG - GRADIGNAN, STANFORD UNIV. - STANFORD, CIRIL - CAEN, CSNSM - ORSAY, GANIL - CAEN

**PHYSICAL REVIEW C55, 4 (1997) 1665.**

97 37 A

**BETA-p, 2p,-ALPHA SPECTROSCOPY OF  $^{22,23,24}\text{Si}$  AND  $^{22}\text{Al}$**

CZAJKOWSKI S. ET AL.

CENBG - GRADIGNAN, INST.FUR KERNPHYSIK - DARMSTADT, LPC ISMRA - CAEN, GSI - DARMSTADT

**NUCLEAR PHYSICS A616 (1997) 278c.**

PROCEEDINGS OF THE FOURTH INTERNATIONAL CONFERENCE ON RADIOACTIVE NUCLEAR BEAMS

OMIYA (JP) 1996

97 39 A

**RPA INSTABILITIES IN FINITE NUCLEI AT LOW DENSITY**

JACQUOT B. ET AL.

GANIL - CAEN, CE SACLAY - GIF-SUR-YVETTE, LNS - CATANIA, TENNESSEE TECH.UNIV. -

COOKEVILLE, MIDDLE EAST TECH.UNIV. - ANKARA

**NUCLEAR PHYSICS A617 (1997) 356.**

97 41 A

**PROTON ELASTIC SCATTERING ON LIGHT NEUTRON-RICH NUCLEI**

CORTINA-GIL M.D. ET AL.

GANIL - CAEN, CE SACLAY - GIF-SUR-YVETTE, FOSTER RAD.LAB. MCGILL UNIV. - MONTREAL, LLNL -

LIVERMORE, IPN - ORSAY, IFUSP DFN - SAO PAULO, LPC ISMRA - CAEN

**PHYSICS LETTERS B401 (1997) 9.**

97 42 A

**A CYCLOTRON AS A POWERFUL TOOL FOR MASS MEASUREMENTS OF EXOTIC NUCLEI**

CHARTIER M. ET AL.

GANIL - CAEN, IFUSP - SAO PAULO, AUSTRALIAN NAT. UNIV. - CANBERRA, CEN SACLAY - GIF-SUR-

YVETTE, BERGEN UNIV. - BERGEN, LPC ISMRA - CAEN, CATANIA UNIV. - CATANIA

INTERNATIONAL CONFERENCE ON ELECTROMAGNETIC ISOTOPE SEPARATORS AND TECHNIQUES RELATED TO THEIR APPLICATIONS

PROCEEDINGS OF THE 13th INTERNATIONAL CONFERENCE ON ELECTROMAGNETIC ISOTOPE SEPARATORS AND TECHNIQUES RELATED TO THEIR APPLICATIONS

BAD DURKHEIM (DE) 1996

**NIM B126, 1-4 (1997) 334.**

97 45 A

**PHASE TRANSITION IN NUCLEAR MATTER ?**

AUGER G. ET AL.

GANIL - CAEN, IPN - ORSAY, LPC ISMRA - CAEN, IPN LYON - VILLEURBANNE, CEN SACLAY - GIF-SUR-YVETTE, SUBATECH - NANTES

CRITICAL PHENOMENA AND COLLECTIVE OBSERVABLES

PROCEEDINGS OF CRIS '96 - 1st CATANIA RELATIVISTIC ION STUDIES

ACICASTELLO (IT) 1996

97 50 A

**REACTION MECHANISMS IN MEDIUM ENERGY COLLISIONS : INFLUENCE OF DYNAMICAL FLUCTUATIONS**

COLONNA M. ET AL.

LNS INFN - CATANIA, GANIL - CAEN

CRITICAL PHENOMENA AND COLLECTIVE OBSERVABLES

PROCEEDINGS OF CRIS '96 - 1st CATANIA RELATIVISTIC ION STUDIES

ACICASTELLO (IT) 1996

97 51 A

**INSTABILITIES IN FINITE SYSTEMS**

BELKACEM M. ET AL.

INFN LNS - CATANIA, GANIL - CAEN, INFN SEZIONE DI CATANIA - CATANIA

CRITICAL PHENOMENA AND COLLECTIVE OBSERVABLES

PROCEEDINGS OF CRIS 96 - 1st CATANIA RELATIVISTIC ION STUDIES

ACICASTELLO (IT) 1996

97 52 A

**THE  $^{12}\text{C} + ^{24}\text{Mg}$  ELASTIC SCATTERING : AN EXAMPLE OF ANOMALOUS TRANSPARENCY AT COULOMB BARRIER ENERGIES**

SCIANI W. ET AL.

IFUSP - SAO PAULO, SYNCHROTRON RAD. RES. INST. - HYOGO, DEPT. CIENCIAS EXATAS - SOROCABA, GANIL - CAEN

**NUCLEAR PHYSICS A620 (1007) 91.**

97 56 A

**SPECTROSCOPIC STUDIES OF THE  $\beta_p$  AND  $\beta_{2p}$  DECAY OF  $^{23}\text{Si}$**

BLANK B. ET AL.

CENBG - GRADIGNAN, INST. FUR KERNPHYSIK - DARMSTADT, LPC ISMRA - CAEN, GSI - DARMSTADT

**ZEITSCHRIFT FUR PHYSIK A357 (1997) 247.**

97 69 A

**A NUCLEAR MASS FORMULA BASED ON SU(4) SYMMETRY**

VAN ISACKER P. ET AL.

GANIL - CAEN, FYSISK INST. BERGEN UNIV. - BERGEN

**FOUNDATIONS OF PHYSICS 27, 7 (1997) 1047.**

97 73 A

**HEATING NUCLEI WITH HIGH-ENERGY ANTIPROTONS**

LOTT B. ET AL.

GANIL - CAEN, HMI - BERLIN, CERN - GENEVE, TU MUNCHEN - GARCHING, INR RUSSIAN ACAD. OF SCI. - MOSCOW, WARSAW UNIV. - WARZAWA, FZ ROSSENDORF - DRESDEN, IPN - ORSAY

**NUCLEAR PHYSICS SUPPL. 56A (1997) 114.**

97 83 A

**$^{40}\text{Ti}$  BETA DECAY AND THE NEUTRINO CAPTURE CROSS SECTION OF  $^{40}\text{Ar}$**

TRINDER W. ET AL.

GANIL - CAEN, IPN - ORSAY, NOTRE DAME UNIV. - NOTRE DAME, WASHINGTON UNIV. - SEATTLE  
**PHYSICS LETTERS B415 (1997) 211.**

97 99 A

**ANALYTICALLY SOLVABLE MEAN-FIELD POTENTIAL FOR STABLE AND EXOTIC NUCLEI**

STOITSOV M.V. ET AL.

INST. OF NUCL. RES. & NUCL. ENERGY - SOFIA, BARTOL RES. INST. - NEWARK, GANIL - CAEN, INST.  
DE CIENCIAS NUCLEARES - MEXICO, INST. DE FIS. LAB. DE CUERMACARA - MEXICO

**PHYSICS LETTERS B415 (1997) 1.**

97 100 A

**SPECTROSCOPY OF  $^{11}\text{N}$**

OSTROWSKI A.N. ET AL.

DEPT. PHYS. & ASTR. EDINBURGH UNIV. - EDINBURGH, UNIVERSIDADE DE SAO PAULO - SAO  
PAULO, HMI - BERLIN, INST. ATOMIC PHYS. - BUCAREST, GANIL - CAEN, DSM CE SACLAY - GIF SUR  
YVETTE, LPC - CAEN

INTERNATIONAL WINTER MEETING ON NUCLEAR PHYSICS

PROCEEDINGS OF THE XXXV INTERNATIONAL WINTER MEETING ON NUCLEAR PHYSICS

BORMIO (IT) 1997

**RICERCA SCIENTIFICA ED EDUCAZIONE PERMANENTE SUPPL.110, p.127.**

97 102 A

**COULOMB MULTIPHONON EXCITATION IN HEAVY ION COLLISIONS**

LANZA E.G. ET AL.

CATANIA UNIV. AND INFN - CATANIA, DEPART. DE FIS. ATOM. MOL. NUCL. SEVILLA UNIV. - SEVILLA,  
GANIL - CAEN, IPN - ORSAY

INTERNATIONAL WINTER MEETING ON NUCLEAR PHYSICS

PROCEEDINGS OF THE XXXV INTERNATIONAL WINTER MEETING ON NUCLEAR PHYSICS

BORMIO (IT) 1997

**RICERCA SCIENTIFICA ED EDUCAZIONE PERMANENTE SUPPL.110, p.148.**

97 104 A

**COULOMB EXCITATION EXPERIMENTS AT GANIL**

SORLIN O. ET AL.

IPN - ORSAY, LPC - CAEN, IAP - BUCHAREST, CSNSM - ORSAY, GANIL - CAEN, CE SACLAY - GIF SUR  
YVETTE, FLNR JINR - DUBNA, GSI - DARMSTADT

INTERNATIONAL WINTER MEETING ON NUCLEAR PHYSICS

PROCEEDINGS OF THE XXXV INTERNATIONAL WINTER MEETING ON NUCLEAR PHYSICS

BORMIO (IT) 1997

**RICERCA SCIENTIFICA ED EDUCAZIONE PERMANENTE SUPPL.110, p.566.**

97 108 A

**THERMODYNAMICAL EQUILIBRIUM UP TO THE GAS PHASE ?**

GULMINELLI F. ET AL.

IPN - ORSAY, LPC - CAEN, GANIL - CAEN, IPNL - VILLEURBANNE, CEN SACLAY - GIF SUR YVETTE,  
SUBATECH - NANTES

INTERNATIONAL WINTER MEETING ON NUCLEAR PHYSICS

PROCEEDINGS OF THE XXXV INTERNATIONAL WINTER MEETING ON NUCLEAR PHYSICS

BORMIO (IT) 1997

**RICERCA SCIENTIFICA ED EDUCAZIONE PERMANENTE SUPPL.110, p.396.**

97 111 A

**PROTON EMISSION IN INELASTIC SCATTERING OF  $^{40}\text{Ca}$  ON  $^{40}\text{Ca}$  AT 50 MeV/NUCLEON**

SCARPACI J.A. ET AL.

IPN - ORSAY, GANIL - CAEN, DSM CE SACLAY - GIF SUR YVETTE, KVI - GRONINGEN

**PHYSICAL REVIEW C56 (1997) 3187.**

97 113 A

**ELASTIC AND QUASIELASTIC SCATTERING OF  $^3\text{He}$  FROM  $^{12}\text{C}$**

TOSTEVIN J.A. ET AL.

SURREY UNIV. - GUILDFORD, NOTRE DAME UNIV. - NOTRE DAME, NSCL MSU - EAST LANSING, GANIL - CAEN, ANL - ARGONNE

**PHYSICAL REVIEW C56 (1997) R2929.**

97 114 A

**EVIDENCE FOR A HIGHLY DEFORMED OBLATE  $0^+$  STATE IN  $^{74}\text{Kr}$**

CHANDLER C. ET AL.

SURREY UNIV. - GUILDFORD, CENBG - GRADIGNAN, BRIGHTON UNIV. - BRIGHTON, WARSAW UNIV. - WARSAW, GANIL - CAEN, LPC ISMRA - CAEN, OLIVER LODGE LAB. - LIVERPOOL, IP & NE - BUCAREST, YORK UNIV. - YORK, DARESBUY LAB. - WARRINGTON

**PHYSICAL REVIEW C56 (1997) R2924.**

97 115 A

**NUCLEAR SPIN ALIGNMENT AND STATIC MOMENTS OF LIGHT PROJECTILE FRAGMENTS MEASURED WITH THE LEVEL MIXING RESONANCE (LMR) METHOD**

NEYENS G. ET AL.

INST. VOOR KERN- EN STRALINGSFYSICA - LEUVEN, GANIL - CAEN, CE SACLAY - GIF SUR YVETTE, INST. PHYS. UNIV. SAO PAULO - SAO PAULO

**PHYSICS LETTERS B393 (1997) 36.**

97 07 B

**DYNAMICAL EFFECTS AND INTERMEDIATE MASS FRAGMENT PRODUCTION IN PERIPHERAL AND SEMICENTRAL COLLISIONS OF  $\text{Xe}+\text{Sn}$  AT 50 MeV/NUCLEON**

LUKASIK J. ET AL.,

IPN - ORSAY, GANIL - CAEN, LPC ISMRA - CAEN, IPNL - VILLEURBANNE, CE SACLAY - GIF-SUR-YVETTE, SUBATECH - NANTES

**PHYSICAL REVIEW C55, 4 (1997) 1906.**

97 36 B

**MULTIFRAGMENTATION WITH BROWNIAN ONE-BODY DYNAMICS**

GUARNERA A. ET AL.

GANIL - CAEN, LNS - CATANIA, CE SACLAY - GIF-SUR-YVETTE, NSD LBNL - BERKELEY

**PHYSICS LETTERS B403 (1997) 191.**

97 54 B

**EXPERIMENTS WITH ISOMERIC BEAMS**

PFUTZNER M. ET AL.

INST. EXP. PHYS. WARSAW UNIV. - WARSAW, GSI - DARMSTADT, GANIL - CAEN, CERN - GENEVA  
INTERNATIONAL CONFERENCE ON NUCLEAR PHYSICS AT STORAGE RINGS

PROCEEDINGS OF THE THIRD INTERNATIONAL CONFERENCE ON NUCLEAR PHYSICS AT STORAGE RINGS

BERNKASTEL-KUES (DE) 1996

**NUCLEAR PHYSICS A626 (1997) 259c.**

97 101 B

**A POSSIBLE SCENARIO FOR THE TIME DEPENDENCE OF THE MULTIFRAGMENTATION PROCESS IN  $\text{Xe} + \text{Sn}$  COLLISIONS (AN EXPLANATION OF THE  $3\text{He}$  PUZZLE)**

BOUGAULT R. ET AL.

LPC - CAEN, GANIL - CAEN, IPN - ORSAY, CEN SACLAY - GIF SUR YVETTE, SUBATECH - NANTES, IPNL - VILLEURBANNE

INTERNATIONAL WINTER MEETING ON NUCLEAR PHYSICS

PROCEEDINGS OF THE XXXV INTERNATIONAL WINTER MEETING ON NUCLEAR PHYSICS  
BORMIO (IT) 1997  
RICERCA SCIENTIFICA ED EDUCAZIONE PERMANENTE SUPPL.110, p.251.  
97 103 B

**MULTIFRAGMENTATION OF HEAVY SYSTEMS : CHARACTERISTICS AND SCALING LAWS**

RIVET M.F. ET AL.  
IPN - ORSAY, GANIL - CAEN, LPC - CAEN, IPNL - VILLEURBANNE, CEN SACLAY - GIF SUR YVETTE,  
SUBATECH - NANTES, IPNE IFA - BUCHAREST, LPN - QUEBEC  
INTERNATIONAL WINTER MEETING ON NUCLEAR PHYSICS  
PROCEEDINGS OF THE XXXV INTERNATIONAL WINTER MEETING ON NUCLEAR PHYSICS  
BORMIO (IT) 1997  
RICERCA SCIENTIFICA ED EDUCAZIONE PERMANENTE SUPPL.110, p.225.  
97 105 B

**SEARCH FOR DYNAMICAL EFFECTS IN THE MULTIFRAGMENTATION PROCESS AT INTERMEDIATE ENERGY**

GERMAIN M. ET AL.  
SUBATECH - NANTES, LPC - CAEN, GANIL - CAEN  
INTERNATIONAL WINTER MEETING ON NUCLEAR PHYSICS  
PROCEEDINGS OF THE XXXV INTERNATIONAL WINTER MEETING ON NUCLEAR PHYSICS  
BORMIO (IT) 1997  
RICERCA SCIENTIFICA ED EDUCAZIONE PERMANENTE SUPPL.110, p.343.  
97 107 B

**A COMPREHENSIVE STUDY OF MECHANISMS IN REACTIONS INDUCED BY  $^6\text{He}$  ON Au AND U**

LIENARD E. ET AL.  
GANIL - CAEN, LPC - CAEN  
INTERNATIONAL WINTER MEETING ON NUCLEAR PHYSICS  
PROCEEDINGS OF THE XXXV INTERNATIONAL WINTER MEETING ON NUCLEAR PHYSICS  
BORMIO (IT) 1997  
RICERCA SCIENTIFICA ED EDUCAZIONE PERMANENTE SUPPL.110, p.507.  
97 109 B

**SELECTION OF SINGLE-SOURCE MULTIFRAGMENTATION EVENTS FOR COLLISIONS OF  $^{155}\text{Gd} + ^{238}\text{U}$  AT 36 MeV/u STUDIED WITH INDRA**

FRANKLAND J.D. ET AL.  
IPN - ORSAY, GANIL - CAEN, LPC - CAEN, IPNL - VILLEURBANNE, CEN SACLAY - GIF SUR YVETTE,  
SUBATECH - NANTES, IPNE IFA - BUCHAREST, NAPOLI UNIV. - NAPOLI, LPN LAVAL UNIV. - QUEBEC  
INTERNATIONAL WINTER MEETING ON NUCLEAR PHYSICS  
PROCEEDINGS OF THE XXXV INTERNATIONAL WINTER MEETING ON NUCLEAR PHYSICS  
BORMIO (IT) 1997  
RICERCA SCIENTIFICA ED EDUCAZIONE PERMANENTE SUPPL.110, p.323.  
97 110 B

**TEMPERATURE MEASUREMENTS FROM RELATIVE POPULATIONS OF EXCITED STATES WITH INDRA**

ASSENARD M. ET AL.  
SUBATECH - NANTES, CEN SACLAY - GIF SUR YVETTE, IPN - ORSAY, GANIL - CAEN, LPC - CAEN, IPNL - VILLEURBANNE, IPNE IFA - BUCHAREST, NAPOLI UNIV. - NAPOLI, LPN LAVAL UNIV. - QUEBEC  
INTERNATIONAL WINTER MEETING ON NUCLEAR PHYSICS  
PROCEEDINGS OF THE XXXV INTERNATIONAL WINTER MEETING ON NUCLEAR PHYSICS  
BORMIO (IT) 1997  
RICERCA SCIENTIFICA ED EDUCAZIONE PERMANENTE SUPPL.110, p.465.  
97 112 B



**PRESENT AND FUTURE OF RADIOACTIVE BEAMS AT GANIL : NEW TRENDS IN PHYSICS WITH THE FORTHCOMING SPIRAL FACILITY**

LEWITOWICZ M.,

GANIL - CAEN

PROCEEDINGS OF 1996 KONAN WORKSHOP ON NUCLEAR PHYSICS

KONAN (JP) 1996

97 61 C

**PRESENT AND FUTURE EXPERIMENTS WITH EXOTIC BEAMS AT GANIL/SPIRAL**

MUELLER A.C.

IPN - ORSAY

ZEITSCHRIFT FÜR PHYSIKS A358 (1997) 153.

97 64 C

**NEUTRON TRANSFER REACTIONS WITH RADIOACTIVE BEAMS**

WINFIELD J.S. ET AL.

LPC ISMRA - CAEN, GANIL - CAEN, SURREY UNIV. - GUILDFORD

NIM A396 (1997) 147.

97 67 C

**STUDY OF NEUTRON-RICH NUCLEI NEAR THE N = 20 NEUTRON SHELL CLOSURE USING THE <sup>36</sup>S BEAM**

TARASOV O. ET AL.

FLNR JINR - DUBNA, NPI - REZ, LIVERPOOL UNIV. - LIVERPOOL, LPC - CAEN, GANIL - CAEN, IAP -

BUCHAREST-MAGURELE, IPN - ORSAY

PROCEEDINGS OF THE 8th INTERNATIONAL CONFERENCE ON NUCLEAR REACTION MECHANISMS

CONFERENCE ON NUCLEAR REACTION MECHANISMS

9 Juin 1997

RICERCA SCIENTIFICA ED EDUCAZIONE PERMANENTE SUPPL.111, p.416.

97 91 C

**SEARCH FOR <sup>28</sup>O AND STUDY OF NEUTRON-RICH NUCLEI NEAR THE N = 20 SHELL CLOSURE**

TARASOV O. ET AL.

FLNR JINR - DUBNA, LIVERPOOL UNIV. - LIVERPOOL, LPC ISMRA - CAEN, GANIL - CAEN, IAP -

BUCHAREST MAGURELE, NPI - REZ, IPN - ORSAY

PHYSICS LETTERS B409 (1997) 64.

97 95 C

**SHADOWING EFFECTS AND TRANSVERSE MOMENTUM DEPENDENCE OF PARTICLE EMISSION IN INTERMEDIATE ENERGY HEAVY ION COLLISIONS**

BUTA A. ET AL.

LPC ISMRA - CAEN, IPNE - BUCHAREST, GANIL - CAEN, NSCL MSU - EAST LANSING

ZEITSCHRIFT FÜR PHYSIKS A357 (1997) 9.

97 02 D

**A HOT EXPANDING SOURCE IN 50 A MeV Xe + Sn CENTRAL REACTIONS**

MARIE N. ET AL.

GANIL - CAEN, LPC ISMRA - CAEN, IPN - ORSAY, CE SACLAY - GIF SUR YVETTE, IPNL -

VILLEURBANNE, SUBATECH - NANTES

PHYSICS LETTERS B391 (1997) 15.

97 04 D

**SURVEYING THE NUCLEAR CALORIC CURVE**

MA Y.G. ET AL.

LPC ISMRA - CAEN, CE SACLAY - GIF SUR YVETTE, GANIL - CAEN, IPN - ORSAY, IPNL -

VILLEURBANNE, SUBATECH - NANTES

**PHYSICS LETTERS B390 (1997) 41.**  
97 05 D

**ROLE OF ANHARMONICITIES AND NONLINEARITIES IN HEAVY ION COLLISIONS. A MICROSCOPIC APPROACH**

LANZA E.G. ET AL.

DIPARTI.DI FIS. AND INFN - CATANIA, DEPARTA.DE FIS.MOL.NUCL. - SEVILLA, GANIL - CAEN  
**NUCLEAR PHYSICS A613 (1997) 445.**

97 06 D

**DIRECTED COLLECTIVE FLOW AND AZIMUTHAL DISTRIBUTIONS IN  $^{36}\text{Ar} + ^{27}\text{Al}$  COLLISIONS FROM 55 TO 95 MeV/u**

ANGELIQUE J.C. ET AL.

LPC ISMRA - CAEN, GANIL - CAEN, IPN UCL - LOUVAIN-LA-NEUVE, LPN - NANTES, DSF AND INFN - NAPOLI, IMP - LANZHOU

**NUCLEAR PHYSICS A614 (1997) 261.**

97 09 D

**ELASTIC SCATTERING AND CHARGE EXCHANGE REACTION WITH LIGHT NEUTRON RICH EXOTIC BEAMS**

CORTINA-GIL M.D. ET AL.

GANIL - CAEN, CE SACLAY - GIF-SUR-YVETTE, FOSTER RAD.LAB. Mc GILL UNIV. - MONTREAL, IPN - ORSAY, IFUSP DFN - SAO PAULO, LPC ISMRA - CAEN

PROCEEDINGS OF THE FOURTH INTERNATIONAL CONFERENCE ON RADIOACTIVE NUCLEAR BEAMS

OMIYA (JP) 1996

**NUCLEAR PHYSICS A616 (1997) 215c.**

97 29 D

**$^8\text{B}$  STUDIED AS A SECONDARY BEAM AT GANIL**

BORCEA C. ET AL.

GANIL - CAEN, IAP - BUCHAREST- MAGURELE, IPN - ORSAY, NPI - REZ, FLNR JINR - DUBNA, IEP WARSAW UNIV. - WARSAW

**NUCLEAR PHYSICS A616 (1997) 231c.**

PROCEEDINGS OF THE FOURTH INTERNATIONAL CONFERENCE ON RADIOACTIVE NUCLEAR BEAMS

OMIYA (JP) 1996

97 30 D

**REACTIONS INDUCED BY BEAMS OF NEUTRON AND PROTON HALO NUCLEI**

PENIONZHKEVICH Yu.E.

JINR - DUBNA

**NUCLEAR PHYSICS A616 (1997) 247c.**

PROCEEDINGS OF THE FOURTH INTERNATIONAL CONFERENCE ON RADIOACTIVE NUCLEAR BEAMS

OMIYA (JP) 1996

97 31 D

**FUSION AND BREAKUP AT THE BARRIER WITH UNSTABLE NUCLEI**

SIGNORINI C.

DIPART.DI FIS. AND INFN - PADOVA

**NUCLEAR PHYSICS A616 (1997) 262c.**

PROCEEDINGS OF THE FOURTH INTERNATIONAL CONFERENCE ON RADIOACTIVE NUCLEAR BEAMS

OMIYA (JP) 1996

97 33 D

**NEW  $\mu$  s ISOMERS IN  $T_z = 1$  NUCLEI PRODUCED IN THE  $^{112}\text{Sn}(63\text{A MeV}) + {}^{nat}\text{Ni}$  REACTION**

GRZYWACZ R. ET AL.

IFD WARSAW UNIV. - WARSAW, GANIL - CAEN, IAP - BUCHAREST-MAGURELE, GOTTINGEN UNIV. - GOTTINGEN, FLNR JINR - DUBNA, IPN - ORSAY, GSI - DARMSTADT, LEUVEN UNIV. - LEUVEN, LPC - CAEN, CERN - GENEVE

**PHYSICAL REVIEW C55, 3 (1997) 1126.**

97 40 D

**TWO-PHOTON CORRELATIONS : FROM YOUNG EXPERIMENTS TO HEAVY-ION COLLISION DYNAMICS**

MARQUES F.M. ET AL.

GANIL - CAEN, LPC - CAEN, WARSAW UNIV. - WARSAW, KVI - GRONINGEN

**PHYSICS REPORTS 284, No.3 (1997) 91.**

97 43 D

**HIGHEST TEMPERATURES SUSTAINABLE IN HEAVY NUCLEI PRODUCED IN Ar + Au COLLISIONS AT 60 A MeV**

LECOLLEY F.R. ET AL.

LPC ISMRA - CAEN, UNIV. LIBRE DE BRUXELLES - BRUXELLES, CRN - STRASBOURG, IPN FNRS - LOUVAIN LA NEUVE

**NUCLEAR PHYSICS A620 (1997) 327.**

97 58 D

**THE  $^{12}\text{C} + \alpha$  REACTION RATE FROM THE ELASTIC  $^{16}\text{O}$  BREAKUP**

KIENER J. ET AL.

CSNSM - ORSAY, CRN - STRASBOURG, GANIL - CAEN, RIKKYO UNIV. - TOKYO, IPN - ORSAY  
PROCEEDINGS OF THE FOURTH INTERNATIONAL SYMPOSIUM ON NUCLEI IN THE COSMOS  
NOTRE DAME (USA) 1996

**NUCLEAR PHYSICS A621, 1-2 (1997) 173c.**

97 65 D

**HARD PHOTONS AND NEUTRAL PIONS AS PROBES OF HOT AND DENSE NUCLEAR MATTER**

SCHUTZ Y. ET AL.

GANIL - CAEN, IFC VALENCIA UNIV. - BURJASSOT, KVI - GRONINGEN, GIessen UNIV. - GIessen, GSI - DARMSTADT, CENBG - GRADIGNAN, SOLTAN INST. NUCL. STUDIES - SWIERK, NPI - REZ

**NUCLEAR PHYSICS A622 (1997) 404.**

97 68 D

**PROBABILITY OF FISSION INDUCED BY 1.2 GeV ANTIPROTONS**

SCHMID S. ET AL.

TECHNISCHE UNIV. MUNCHEN - MUNCHEN, HMI - BERLIN, GANIL - CAEN, WARSAW UNIV. - WARSZAWA, FORSCHUNGSZENTRUM ROSSENDORF - DRESDEN, CERN - GENEVE, INR RUSSIAN ACAD. OF SCI. - MOSCOW

**ZEITSCHRIFT FÜR PHYSIKS A359 (1997) 27.**

97 71 D

**NEUTRON MULTIPLICITY DISTRIBUTIONS FOR 1.94 TO 5 GeV/c PROTON-, ANTIPROTON-, PION-, KAON-, AND DEUTERON-INDUCED SPALLATION REACTIONS ON THIN AND THICK TARGETS**

PIENKOWSKI L. ET AL.

HMI - BERLIN, GANIL - CAEN

**PHYSICAL REVIEW C56 (1997) 1909.**

97 80 D

**UNUSUAL BEHAVIOUR OF FUSION-FISSION AT BARRIER ENERGIES FOR A NEUTRON-RICH HALO NUCLEUS**

FEKOU-YOUMBI V. ET AL.

DSM CEA SACLAY - GIF SUR YVETTE, GANIL - CAEN, IPNE - BUCHAREST MAGURELE, IPN - ORSAY,  
DIPAR.DI FISICA & INFN - CATANIA, IFU - SAO PAULO, IMP - LANZHOU  
**JOURNAL OF PHYSICS G23 (1997) 1259.**  
97 81 D

**NEAR- AND SUB-BARRIER FISSION-FUSION STUDIES FOR  $^9,^{11}\text{Be} + ^{238}\text{U}$**

FEKOU-YOUMBI V. ET AL.

DSM CEA SACLAY - GIF SUR YVETTE, GANIL - CAEN, IPNE - BUCHAREST, IPN - ORSAY, DIPART.DI FIS.  
& INFN - CATANIA, IFUSP - SAO PAULO, IMP - LANZHOU  
FRONTIER AND PERSPECTIVE OF NUCLEAR SCIENCE  
PROCEEDINGS 7TH FRANCO-JAPANESE COLLOQUIUM  
DOGASHIMA (JP) 1996  
97 86 D

**MULTIFRAGMENT PRODUCTION IN HEAVY ION INDUCED REACTIONS AT INTERMEDIATE ENERGY**

DAYRAS R. ET AL.

CE SACLAY - GIF SUR YVETTE, GANIL - CAEN, IPN - ORSAY, LPC - CAEN, SUBATECH - NANTES, IPNL -  
VILLEURBANNE  
FRONTIER AND PERSPECTIVE OF NUCLEAR SCIENCE  
PROCEEDINGS 7TH FRANCO-JAPANESE COLLOQUIUM  
DOGASHIMA (JP) 1996  
97 87 D

**THERMODYNAMICAL EQUILIBRIUM FOR NUCLEAR MATTER PRODUCED IN HEAVY ION COLLISIONS AROUND 100 AMeV ?**

BORDERIE B. ET AL.

IPN - ORSAY, LPC ISMRA - CAEN, GANIL - CAEN, IPN LYON - VILLEURBANNE, DAPNIA CEN SACLAY -  
GIF SUR YVETTE, SUBATECH - NANTES, INST. OF PHYSICS & NUCLEAR ENG. - BUCHAREST  
8th INTERNATIONAL CONFERENCE ON NUCLEAR REACTION MECHANISMS  
PROCEEDINGS OF THE 8th INTERNATIONAL CONFERENCE ON NUCLEAR REACTION MECHANISMS  
VARENNA (IT) 1997  
**RICERCA SCIENTIFICA ED EDUCAZIONE PERMANENTE SUPPL.111, p.239.**  
97 89 D

**STUDY OF BINARY COLLISIONS DYNAMICS IN  $^{86}\text{Kr} + ^{165}\text{Ho}$  COLLISIONS AT 60 MeV/u WITH THE NEUTRON DETECTOR Démon**

DORVAUX O. ET AL.

INST. DE RECHERCHES SUBATOMIQUES UNIV. LOUIS PASTEUR - STRASBOURG, UNIV. LIBRE DE  
BRUXELLES - BRUXELLES, LPC ISMRA - CAEN  
8th INTERNATIONAL CONFERENCE ON NUCLEAR REACTION MECHANISMS  
PROCEEDINGS OF THE 8th INTERNATIONAL CONFERENCE ON NUCLEAR REACTION MECHANISMS  
VARENNA (IT) 1997  
**RICERCA SCIENTIFICA ED EDUCAZIONE PERMANENTE SUPPL.111, p.336.**  
97 92 D

**ATOMIC EFFECTS IN HEAVY-ION ELASTIC SCATTERING**

CASANDJIAN J.M. ET AL.

GANIL - CAEN, INST. DE FIS. DA UNIVERSIDADE DE SAO PAULO - SAO PAULO, INST. DE FISICA UNAM -  
MEXICO, DIPART. DI FISICA & INFN - CATANIA, LPC ISMRA - CAEN, IPN - ORSAY, KVI - GRONINGEN  
**PHYSICAL REVIEW C56 (1997) 2700.**  
97 96 D

**MULTI-FRAGMENT PARTITIONS IN THE 32 TO 95 AMeV  $^{36}\text{Ar} + ^{58}\text{Ni}$  REACTIONS**

CHARVET J.L. ET AL.

CE SACLAY - GIF SUR YVETTE, IPN - ORSAY, GANIL - CAEN, LPC - CAEN UOBK - VILLEURBANNE,  
SUBATECH - NANTES, IPNE IFA - BUCHAREST, NAPOLI UNIV. - NAPOLI  
INTERNATIONAL WINTER MEETING ON NUCLEAR PHYSICS

PROCEEDINGS OF THE XXXV INTERNATIONAL WINTER MEETING ON NUCLEAR PHYSICS  
BORMIO (IT) 1997  
RICERCA SCIENTIFICA ED EDUCAZIONE PERMANENTE SUPPL.110, p.309.  
97 106 D

**DEMON AS A NEUTRON PROBE ION HEAVY ION COLLISIONS**

DORVAUX O. ET AL.  
CRN - STRASBOURG, LPC ISMRA - CAEN, UNIVERSITE LIBRE DE BRUXELLES - BRUXELLES  
LARGE-SCALE COLLECTIVE MOTION OF ATOMIC NUCLEI PROCEEDINGS OF THE INTERNATIONAL  
CONFERENCE ON LARGE-SCALE COLLECTIVE MOTION OF ATOMIC NUCLEI  
MESSINA (IT) 1996  
97 120 D

**HARD PHOTON INTENSITY INTERFEROMETRY IN HEAVY ION COLLISIONS AT  
INTERMEDIATE ENERGIES**

BADALA A. ET AL.  
INFN - CATANIA, DIPART. DI FISICA DELL UNIV. DI CATANIA - CATANIA, INFN LNS - CATANIA  
LARGE-SCALE COLLECTIVE MOTION OF ATOMIC NUCLEI  
PROCEEDINGS OF THE INTERNATIONAL CONFERENCE ON LARGE-SCALE COLLECTIVE MOTION OF  
ATOMIC NUCLEI  
MESSINA (IT) 1996  
97 122 D

**TWO-SLIT INTERFERENCE OF BREMSSTRAHLUNG PHOTONS FROM HEAVY-ION  
REACTIONS**

MARQUES F.M. ET AL.  
MARTINEZ G., MATULEWICZ T., OSTENDORF R.W., SCHUTZ Y.  
LPC ISMRA - CAEN, GANIL - CAEN  
PHYSICS LETTERS B394 (1997) 37.  
97 08 E

**HIGH TRANSVERSE MOMENTUM PROTON EMISSION IN Ar + Ta COLLISIONS AT 94  
MeV/u**

GERMAIN M. ET AL.  
SUBATECH - NANTES, LPC ISMRA - CAEN, GANIL - CAEN  
NUCLEAR PHYSICS A620 (1997) 81.  
97 55 E

**TOPOLOGY ANALYSIS FOR THE IDENTIFICATION OF ENERGETIC PHOTONS IN A  
SEGMENTED ELECTROMAGNETIC CALORIMETER**

MARTINEZ G. ET AL.  
GANIL - CAEN  
NIM A391 (1997) 435.  
97 66 E

**PRODUCTION OF  $\pi^0$  AND  $\eta$  MESONS IN CARBON-INDUCED RELATIVISTIC HEAVY-ION  
COLLISIONS**

AVERBECK R. ET AL.  
GSI - DARMSTADT, FRANKFURT UNIV. - FRANKFURT AM MAIN, GIESSEN UNIV. - GIESSEN, KVI -  
GRONINGEN, GANIL - CAEN, NPI - PRAHY, IFC - BURJASSOT  
Z. PHYS. A359 (1997) 65.  
97 70 E

**FAST PARTICLE EMISSION IN INELASTIC CHANNELS OF HEAVY-ION COLLISIONS**

SCARPACI J.A. ET AL.  
IPN - ORSAY, GANIL - CAEN, KVI - GRONINGEN  
8th INTERNATIONAL CONFERENCE ON NUCLEAR REACTION MECHANISMS  
PROCEEDINGS OF THE 8th INTERNATIONAL CONFERENCE ON NUCLEAR REACTION MECHANISMS

VARENNA (IT) 1997

RICERCA SCIENTIFICA ED EDUCAZIONE PERMANENTE SUPPL.111, p.351.

97 90 E

**EXCLUSIVE  $\pi^0$  - AND  $\eta$ -MESON PRODUCTION IN  $^{40}\text{Ar} + ^{40}\text{Ca}$  AT 800 A MeV**

MARIN A. ET AL.

IFIC UNIV. DE VALENCIA - BURJASSOT, GSI - DARMSTADT, GANIL - CAEN, LPC - CAEN, GIESSEN UNIV.

- GIESSEN, KVI - GRONINGEN, NPI - REZ, RES.INST. FOR PART. & NUCL. PHYS. - BUDAPEST

PHYSICS LETTERS B409 (1997) 77.

97 94 E

**CONTRIBUTION OF  $\pi^0$  AND  $\eta$  DALITZ DECAYS TO THE DILEPTON INVARIANT-MASS SPECTRUM IN 1A GeV HEAVY-ION COLLISIONS**

HOLZMANN R. ET AL.

GSI - DARMSTADT, GIESSEN UNIV. - GIESSEN, GANIL - CAEN, IFC - BURJASSOT, FRANKFURT UNIV. -

FRANKFURT, NPI - REZ, KVI - GRONINGEN

PHYSICAL REVIEW C56 (1997) R2920.

97 116 E

**PROBING THE PRE-EQUILIBRIUM STAGE IN HEAVY ION COLLISIONS WITH HARD PHOTONS AND ENERGETIC PROTONS**

SAPIENZA P. ET AL.

INFN LNS - CATANIA, IPN - ORSAY, DAPNIA CE SACLAY - GIF SUR YVETTE, GANIL - CAEN

LARGE-SCALE COLLECTIVE MOTION OF ATOMIC NUCLEI

PROCEEDINGS OF THE INTERNATIONAL CONFERENCE ON LARGE-SCALE COLLECTIVE MOTION OF ATOMIC NUCLEI

MESSINA (IT) 1996

97 124 E

**D) - INTERDISCIPLINARY  
RESEARCH**

# **1 - BASIC COLLISION PROCESSES**



## Search for Resonant Trialectronic Recombination in Channeling Conditions

M. Chevallier<sup>(1)</sup>, P. Chomaz<sup>(2)</sup>, C. Cohen<sup>(3)</sup>, N. Cue<sup>(4)</sup>, D. Dauvergne<sup>(1)</sup>, J. Dural<sup>(5)</sup>, P. Gangnan<sup>(2)</sup>, A. L'Hoir<sup>(3)</sup>, R. Kirsch<sup>(1)</sup>, D. Lelièvre<sup>(5)</sup>, J.-F. Libin<sup>(2)</sup>, P. Mokler<sup>(6)</sup>, J.-C. Poizat<sup>(1)</sup>, H.-T. Prinz<sup>(6)</sup>, J.-M. Ramillon<sup>(5)</sup>, J. Remillieux<sup>(1)</sup>, J.-P. Rozet<sup>(3)</sup>, F. Sanuy<sup>(1)</sup>, C. Stephan<sup>(7)</sup>, D. Schmaus<sup>(3)</sup>, M. Toulemonde<sup>(5)</sup>, D. Vernhet<sup>(3)</sup> and A. Warczak<sup>(6)</sup>

(1) IPN Lyon, IN2P3 and Université Lyon-I, 43 Bd du 11 novembre 1918, 69622 Villeurbanne Cedex, France

(2) GANIL, CEA/IN2P3, BP 5027, 14076 Caen Cedex 5, France

(3) Groupe de Physique des Solides, CNRS URA 017, Universités Paris VI et Paris VII, 75251 Paris Cedex 05, France

(4) Department of Physics, The Hong Kong University of Science and Technology, Kowloon, Hong Kong

(5) CIRIL, UMR 11 CNRS-CEA, rue Claude Bloch, 14040 Caen Cedex, France

(6) Gesellschaft für Schwerionenforschung (GSI), D-64291 Darmstadt, Germany

(7) IPN Orsay and IN2P3, BP 1, 91406 Orsay Cedex, France

During the experiment P372 we have tried to observe the resonant trielectronic recombination by heavy ions. This process, occurring during the collision of the ion with electrons, is the equivalent of the Resonant Transfer and Double Excitation (RT2E) for ion-atom collisions: the capture of a target electron by a projectile having at least two initial electrons is accompanied by the simultaneous excitation of these two electrons. For instance, capture into the L-shell of a He-like incoming projectile would lead to the formation of a Li-like ion with a double K-hole and all electrons in the L-shell. For sufficiently high Z ions, like  $Kr^{34+}$  in our experiment, this triply excited state is expected to decay radiatively.

Theoretical estimates give the probability of the time-reverse process (KK-LLL "double" Auger) to be less than  $10^{-6}$  times that for the single KLL Auger process. Then we expect a similar ratio between probabilities for trielectronic recombination and the well-known dielectronic recombination, already studied at GANIL by our collaboration.

Ion channeling in a crystal has two main advantages for observing such a low cross section capture process: first, channeled ions experience a dense quasi-free electron gas, and, second, close collisions with target atomic cores are strongly attenuated, which lowers the experimental background. The expected signature of the trielectronic recombination was the observation of two  $K\alpha$  photons resulting from the decay of the triply excited state, in coincidence with the detection of a channeled  $Kr^{33+}$  ion, as a function of the incident beam energy around the resonance (37.4, 40.6 and 42.3 AMeV). The experiment was performed in the SPEG beam line, allowing a very high energy resolution of transmitted ions through a thin crystal. In order to optimize the sensitivity and minimize the background, an ion per ion detection was performed at  $3 \cdot 10^6$  incoming projectiles per second. We obtain an upper limit of the cross section in the millibarn range, which represents an improvement of nearly two orders of magnitude over the result of a previous ion-gas experiment. The first results are presented at the HCI-98 conference (Bensheim, sept.98)

# Single and Multiple Excitation Processes in Heavy Ion-Atom Collisions at Intermediate Velocity

L Adoui<sup>∇</sup>, D Vernhet<sup>◊</sup>, J-P Rozet<sup>◊</sup>, J-M Ramillon<sup>∇</sup>, C Fourment<sup>◊</sup>, A Cassimi<sup>∇</sup>, J-P Grandin<sup>∇</sup>,  
C Stephan<sup>†</sup>, L Tassan-Gôt<sup>†</sup>

∇ CIRIL (UMR N° 11 CEA/CNRS), Caen; ◊ GPS (CNRS UMR 75-88), Universités Paris 7 et 6, Paris;  
† IPN, NIM, Université Paris 11, Orsay

The knowledge of the processes involved in swift heavy ion-atom collisions can be considered as the first step in the understanding of ion-matter interactions. This picture corresponds to a given description of the projectile stopping power. In this respect, the intermediate velocity regime ( $v_p \approx v_e$ , where  $v_p$  is the projectile velocity and  $v_e$  the mean orbital velocity of the active electron) is of particular interest: the ion stopping power is nearly maximum and for applied purposes, the understanding of mechanisms accounting for radiation damage in materials is important. However, in this velocity range, experimental determination of mono-electronic process cross sections is not so simple since the excitation, ionization and capture channels are of the same order of magnitude and may influence each other strongly. On the other hand, the role of target electrons as active partners, via *capture channel coupling* and *direct target electron-projectile electron interaction*, is not well known. So far, these effects are not taken into account even by the most sophisticated theories. Furthermore, multiple processes, involving more than one electron of the projectile and of the target as well, are actually under study and ask for much debated questions.

Using high resolution x-ray spectroscopy, we have measured cross sections of single as well as of multiple projectile electron excitations when a two-electron  $\text{Ar}^{16+}$  ion collides with neutral target atoms. For a fixed impact velocity ( $v_p = 23$  a.u.), but using various targets (He,  $\text{N}_2$ , Ne, Ar, Kr and Xe), we have investigated a range of interactions spanning from *the perturbative regime to the strong interaction regime*. More precisely, we have determined cross sections of capture-ionization (CI), capture excitation (CE), capture-excitation-ionization (CEI), double excitation (DE), excitation-ionization (EI) and single excitation (SE) (see table 1).

Initial state	Processes involving only projectile electrons		Processes involving also target electrons	
	Processes	Final states	Processes	Final states
$\text{Ar}^{16+}(1s^2\ ^1S_0) + X$	SE	$\text{Ar}^{16+}(1snp\ ^1P) + X$	CI	$\text{Ar}^{16+}(1s2p\ ^1P\ \text{and}\ ^3P) + X^+$
	DE	$\text{Ar}^{16+}(2l2l'\ ^1L) + X$	CEI	$\text{Ar}^{16+}(2l2l'\ ^1L\ \text{and}\ ^3L) + X^+$
	EI	$\text{Ar}^{17+}(2p,3p) + X$	CE	$\text{Ar}^{15+}(1s2l2l'\ ^2L\ \text{and}\ ^4L) + X^+$

**Table 1 :** Review of all the processes studied (see text) ; the quoted final states are those observed experimentally

The experiment has been performed on the SME facility. A high intensity beam ( $1\ \mu\text{A}_e$ ) of  $\text{Ar}^{16+}$  at 13.6 MeV/u was directed at various atomic targets in an open gaseous cell. The specially designed spectrometer used was composed of a flat mosaic graphite crystal and a localization chamber. Its global efficiency amounted to  $1.3 \times 10^{-7}$  ( $\pm 15\%$ ) and the resolving power reached was  $1.4 \times 10^{-3}$  around 3.7 keV. Spectra we have obtained, presented in Fig.1 in the case of  $\text{N}_2$  and Xe targets, allow to distinguish all the processes involved: in particular, we achieve "spin-selectivity" (i.e. triplet and singlet components are well separated).

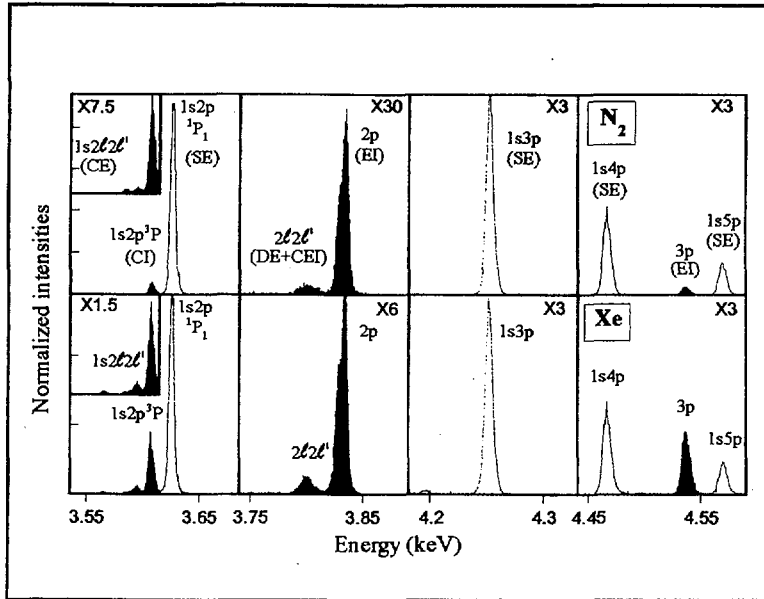


**Figure 1 :** X-ray spectra recorded with the crystal spectrometer in the case of  $Ar^{16+}$  colliding with  $N_2$  and Xe neutral targets. For each target, intensity of the transitions have been normalized to  $1s2p \ ^1P_1 \rightarrow 1s^2 \ ^1S_0$  –the spectra recorded for the  $N_2$  and Xe targets have independent normalization. The transitions filled in black are the lines due mainly to multiple processes.

We have extracted cross sections for each of these processes and the main results may be summarized as follow:

- The evolution of single excitation cross sections,  $\sigma_{SE}^{np}$  (up to  $n=5$ ), for a given projectile, fulfills a scaling law:  $\sigma_{SE}^{np} \approx C_{SE}(Z_t) \times Z_t^2$  (see Fig.2), where  $C_{SE}(Z_t)$  is a  $n$ –independent coefficient (clearly less than 1). Most recent theoretical predictions are in agreement with this evolution. Nevertheless the quantitative values still off by almost a factor of 2 compared to experiment. This disagreement may be assigned to target electron role which is not well taken into account.
- The cross sections of multiple processes involving both target electrons –via capture channels- and projectiles ones, increase more rapidly with  $Z_t$  than those involving only projectile electrons (see Fig.3). In particular, the capture+ionization process cross section, negligible for He target, reaches 54% of the single excitation one for Xe. Those very first measurements performed for a heavy ion bring into light the importance, in the intermediate regime, of these often neglected processes.
- As electron correlations in the initial state can be neglected, a simple independent electron model appears to be successful for predicting the evolution of multiple processes involving only projectile electrons (namely DE and EI cross sections).

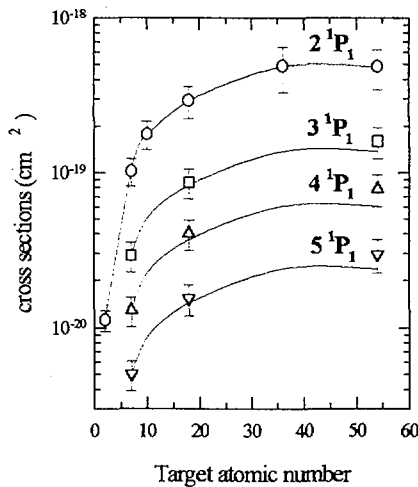


**Figure 2:** single excitation cross sections  $1s^2 \rightarrow 1snp$  up to  $n=5$ , for  $Ar^{16+} \rightarrow Z_t$  collisions (full lines correspond to the scaling law (see text)).

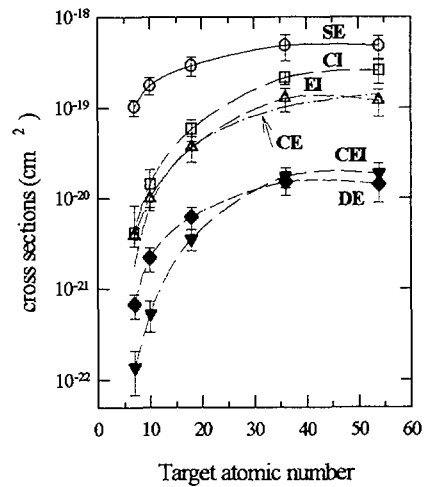


**Figure 3:** single and multiple processes cross sections in  $n=2$  for  $Ar^{16+} \rightarrow Z_t$  collision.

#### References for published works:

- Adoui L 1995 *Thèse de doctorat* Université Pierre et Marie Curie, Paris  
 Adoui L et al. 1995 *Nucl. Instr. and Meth. in Physics Research B* 98 312  
 Vernhet D et al 1996 *Nucl. Instr. and Meth. in Physics Research B* 107 71  
 Vernhet D 1997 *Nouvelles du GANIL* 60 9  
 Vernhet D et al 1997 *Phys. Rev. Lett.* 79 3625

## Production and Transport of Projectile Excited States in Solids

D Vernhet<sup>◇</sup>, J-P Rozet<sup>◇</sup>, C Fourment<sup>◇</sup>  
E Lamour<sup>◇▽</sup>, B Gervais<sup>▽</sup>, A Cassimi<sup>▽</sup>, J-M Ramillon<sup>▽</sup>, D Lelievre<sup>▽</sup>, H Rothard<sup>▽</sup>, L Adoui<sup>▽</sup>,  
J-P Grandin<sup>▽</sup>, C Stephan<sup>†</sup>, L Tassan-Gôt<sup>†</sup>

◇ GPS (CNRS UMR 75-88), Universités Paris 7 et Paris 6, Paris; ▽ CIRIL (UMR N° 11 CEA/ CNRS), Caen; † IPN, NIM, Université Paris 11, Orsay

Two different types of descriptions can be used to calculate the slowing down of a projectile through materials. For both approaches, improvements towards fully *ab initio* calculations are attempted by several groups while, in the past, the prediction of stopping power of heavy ions had to rely on the use of "free parameters" like the effective nuclear charge of the projectile. The first description assumes that ion-solid interaction is the result of a series of binary collisions with the target electrons. In this collisional picture, the evolution of charge state distributions of the projectile at the exit of solid targets, involving core state populations, can be successfully predicted in many cases (like for the ETACHA code). In the other one (the dielectric theory), the target electrons are considered to respond collectively to the passage of the projectile. The polarization of the medium can be described as a wake of electronic density fluctuation trailing the ion. The gradient of the wake potential defines an electric field responsible for the stopping power. This electric field also acts directly on the excited levels of the projectile and will induce, among other effects, binding energy shifts as well as Stark mixing of substates. Until recently, only "quasi-free" target electrons were considered in this approach. Up to now, it exists in fact very few experimental results that can be used to decide which of these pictures is the most appropriate and to define eventually their validity limits. In particular, tests on the predictions of the wake model concerning the spatial extension of the electronic density fluctuations are needed. Atomic physics experiments can be used to shed some light on ion-matter interaction. Looking at one partner of the collision, namely the excited state populations of the projectile, the response of the material may be probed.

Experimental studies on the production and transport of core and Rydberg states have been done for Ar<sup>18+</sup> ( $v=23$  a.u.) on C and Kr<sup>36+</sup> ( $v=36$  a.u.) on C and Cu with target thicknesses ranging from 3.5 to 200  $\mu\text{g}/\text{cm}^2$ . The determination of Ar<sup>17+</sup> and Kr<sup>35+</sup>  $n\ell$  excited states populations has been performed using x-ray spectroscopy techniques on SME and LISE facilities. The Rydberg state populations are measured through long life time deexcitation of Lyman line transitions ( $np \rightarrow 1s$ ), while core state populations are determined looking at prompt emission lines of the projectile.

Two models, relevant to a collisional approach, have been simultaneously developed to describe the transport of projectile excited states in solid targets. Both use the Continuum Distorted Wave cross sections to calculate the production of « initial »  $n\ell$  states populated by the primary capture process. The transport of these states is then described either by a rate equations model (using Plane Wave Born Approximation calculations for excitation and ionization cross sections) or a Monte Carlo simulation of classical dynamics.

A comparison with experiments shows that:

- both collisional approaches allow to interpret the Rydberg  $\ell$  state populations (see Fig. 1). Long life time population measurements for the thinnest as well as for the thickest target are well reproduced by the classical transport model. The discrepancy with the rate equations model, in the case of the 201  $\mu\text{g}/\text{cm}^2$  carbon target, may be assigned to the number of  $n$ -states included so far (indeed, the main limitation of this model is the number of cross sections we are able to calculate).

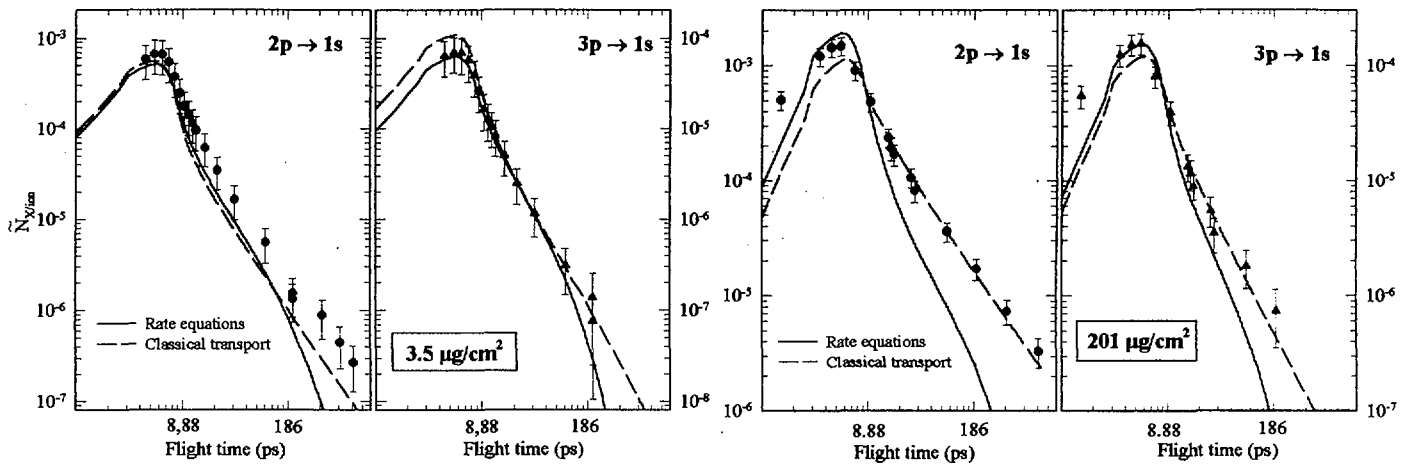


**Figure 1:** Comparison between collisional models and experiment for Rydberg state populations (namely large flight time of  $2p \rightarrow 1s$  and  $3p \rightarrow 1s$  transitions) in the case of  $Ar^{16+} \rightarrow C$  at  $v = 23$  a.u.

- “pure” collisional picture fails to describe the populations of core states ( $n=2,3,4$ ). An illustration of this result (Fig.2) is given by the evolution of the relative populations in  $3\ell j$  excited substates of  $Kr^{35+}$  ion with carbon target thickness. The Stark beats, experimentally observed, with the ion transit time (i.e. target thickness) is a direct signature of the collective response of the medium: the model, which takes into account the wake-field induced by the  $Kr^{36+}$  ion going through the material, gives much better agreement with experiment.

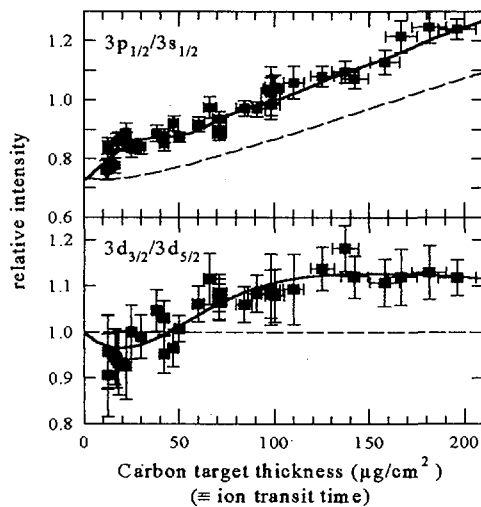


**Figure 2:** Evolution of relative populations in  $3\ell j$  substates of  $Kr^{35+}$  ion with carbon target thickness (dashed line: collisional model; full line Stark model).

and generally used in the dielectric theory ii) the wake field value corresponding to the total stopping power,  $F_{st}$ . Measurements in the case of copper are in agreement with an electric field 5 times larger than  $F_v$  but correspond to the total stopping power  $F_{st}$ . These experimental evidences have already triggered theoretical investigations. Recent calculations go beyond the uniform electron gas model and show that the effect of deeply bound target electrons should be taken into account as non-homogeneities in the jellium.

#### References for published works:

- Lamour E 1997 Thèse de doctorat Université de Caen  
 Rozet J-P et al 1996 Nucl. Instr. And Meth. In Physics Research B 107 67  
 Vernhet D et al 1998 J. Phys. B. 31 117  
 Lamour E et al 1998 J. Phys. B. (to be published)

Target	$F_{exp}$	$F_v$	$F_{st}$
Carbon	$0.9 \pm 0.1$	1	1
Copper	$3.3 \pm 0.3$	0.65	3

**Table 1:** Comparison between experimental electric field values  $F_{exp}$  and theoretical ones :  $F_v$  corresponds only to the contribution of valence electron of the target,  $F_{st}$  corresponds to the total stopping power of the projectile  $Kr^{36+}$  ion. Values are given in  $10^9$  V/cm.

The values of the electric field are directly related to the Stark beat frequency and to the asymptotic value reached for the largest ion transit time. Extracted values from our experimental data are reported in Table 1 and compared to : i) the wake field value  $F_v$ , corresponding to valence electrons only,

**Two- and three-body effects in single ionization of Li by 95 MeV/u Ar<sup>18+</sup> projectiles:  
Analogies with Photoionization**

N. Stolterfoht<sup>1</sup>, J.-Y. Chesnel<sup>1</sup>, M. Grether<sup>1</sup>, B. Skogvall<sup>2</sup>, F. Frémont<sup>3</sup>, D. Lecler<sup>3</sup>,  
D. Hennecart<sup>3</sup>, X. Husson<sup>3</sup>, P. Grandin<sup>4</sup>, B. Sulik<sup>5</sup>, L. Gulyàs<sup>5</sup>, and J.A. Tanis<sup>6</sup>

<sup>1</sup>Hahn-Meitner-Institut Berlin GmbH, Glienickerstr. 100, D-14109 Berlin, Germany

<sup>2</sup>Technische Universität Berlin, Hardenbergstr. 36, D-10623 Berlin, Germany

<sup>3</sup>Laboratoire de Spectroscopie Atomique, ISMRA F-14050 Caen, France

<sup>4</sup>Centre Interdisciplinaire de Recherche avec les Ions Lourds, CEA-CNRS

<sup>5</sup>Institute of Nuclear Research (ATOMKI), H-4001 Debrecen, Hungary

<sup>6</sup>Western Michigan University Kalamazoo, Michigan 49008, USA

Cross sections for single electron emission have been measured in collisions of 95 MeV/u Ar<sup>18+</sup> projectiles with atomic Li for electron energies ranging from 5 –1000 eV and angles ranging from 25° –155° [1]. Because of the high projectile velocity it was possible to separate two- and three-body processes in the angular distributions of the ejected electrons. A comparison the experimental results with theoretical data are shown in Fig. 1.

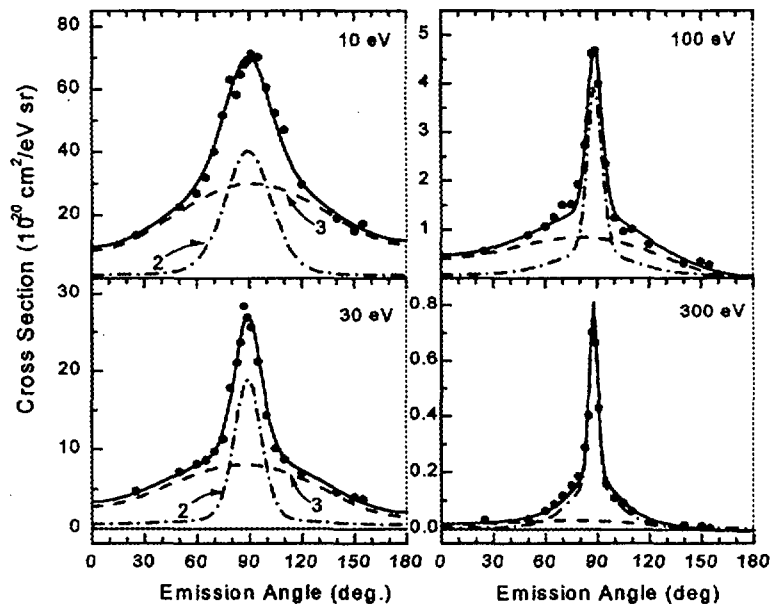


Fig. 1. Angular distributions of electrons emitted at energies of 10, 30, 100, and 300 eV. The dot-dashed curve labeled 2 refers to calculations using the two-body theory [1]. The dashed curve labeled 3 is a fit to the underlying three-body part represented by the function  $A + B \sin^2 \theta + C \cos \theta$

A detailed analysis by means of theoretical results shows that the low-energy emission of the 2s electrons is significantly affected by two-body interactions and, furthermore, the node in the Li 2s wave function is seen to manifest itself in the emitted electron spectrum. The emission of the 1s electron is attributed mainly to three-body effects. The two- and three-body processes are associated with Compton scattering and photoabsorption, respectively.

[1] N. Stolterfoht et al., Phys. Rev. Lett. **80**, 4649 (1998)

## Electron angular distributions as a function of momentum transfer in double ionization of helium by 100 MeV/u $C^{6+}$ impact

B. Bapat<sup>1</sup>, R. Moshhammer<sup>1</sup>, W. Schmitt<sup>2</sup>, A. Cassimi<sup>4</sup>, L. Adoui<sup>4</sup>, R. Dörner<sup>3</sup>,  
H. Kollmus<sup>1</sup>, R. Mann<sup>2</sup>, Th. Weber<sup>3</sup>, K. Khayyat<sup>3</sup>, J.P. Grandin<sup>4</sup>, J. Ullrich<sup>1</sup>

<sup>1</sup>Fakultät für Physik, Universität Freiburg, 79104 Freiburg, Germany

<sup>2</sup>Gesellschaft für Schwerionenforschung, 64291 Darmstadt, Germany

<sup>3</sup>Institut für Kernphysik, Universität Frankfurt, 60486 Frankfurt, Germany

<sup>4</sup>CIRIL, 14040 Caen, France

Double ionization of helium has been a much researched topic because helium is the simplest, but not yet fully understood correlated electron system. Double ionization of this two-electron system is an effective probe of correlation effects. In recent times it has become possible to perform kinematically complete ionization experiments with arbitrary projectiles using the specially developed ion and electron momentum spectrometer, the “reaction microscope” (see [1] and references therein). The momentum components of all ionization products:  $e^-$ ,  $e^-$ ,  $He^{2+}$  can be determined from their position and time of flight spectra, and the precisely known, extremely homogenous electric and magnetic fields in the spectrometer. Thus, every double ionization event is mapped onto a point in the nine-dimensional momentum space. From this map it is possible to determine various differential cross-sections.

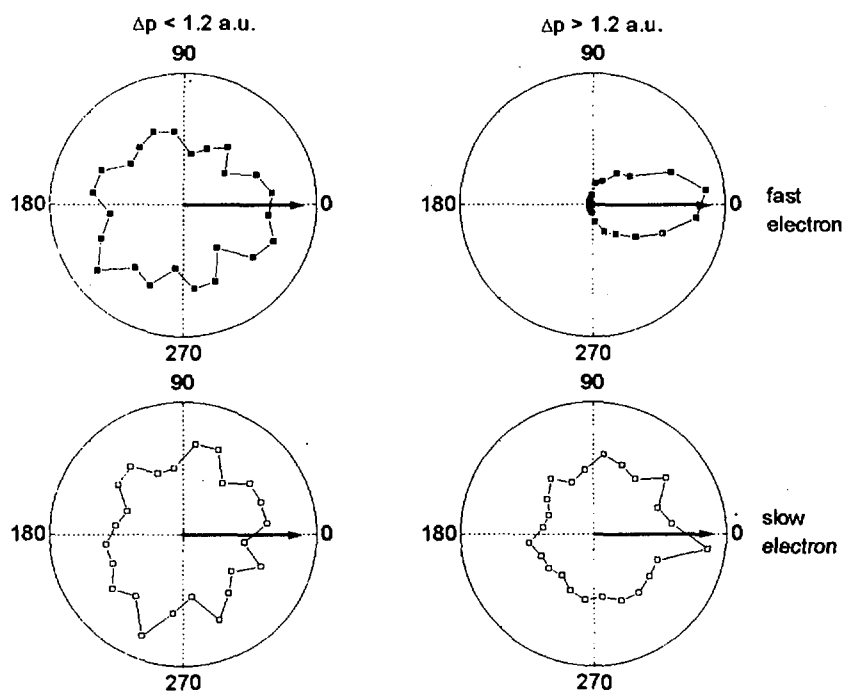


Figure 1: The azimuthal angular distributions of the fast and the slow electrons ejected in the collision  $C^{6+} + He \rightarrow He^{2+} + 2e^-$  for different momentum transfers  $\Delta p$ , as indicated. The arrow represents the direction of momentum transfer to the target in the azimuthal plane. The projectile beam axis is perpendicular to this plane.

The experiments at GANIL were done with 100 MeV/u  $C^{6+}$  ions. The projectile-target interaction strength  $Z_p/v_p$ , in atomic units, is approximately 0.1. For this interaction strength, one expects similarities between photoionization and ion-impact ionization [2,3]. However, there is one important difference between the two processes, which is that momentum transfer in the former is negligible, whereas in the latter any finite momentum transfer is possible. With this point in mind, angular distributions of ejected electrons in double ionization were studied as a function of the momentum transferred by the projectile to the atom.

Preliminary analysis suggests that the events may be separated into two domains, depending on whether the momentum transfer from the projectile to the target atom is less than or greater than 1.2 a.u. This is clearly seen in the azimuthal angular distributions of the electrons shown in the figure. This critical value is close to the mean momentum of the electron in the ground state of the helium atom, and demarcates soft, indirect ionization and hard, direct ionization. Attempts are also on to identify signatures of two-step and shake-off mechanisms of double ionization.

- 
- [1] J. Ullrich, R. Moshhammer, R. Dörner, O. Jagutzki, V. Mergel, H. Schmidt-Böcking and L. Spielberger, *J. Phys. B* **30** 2917 (1997)
  - [2] M. Inokuti, *Rev. Mod. Phys.* **43** 297 (1971)
  - [3] R. Moshhammer *et. al.*, *Phys. Rev. Lett.* **79** 3621 (1997)



# FAST ELECTRON SPECTRA FROM SWIFT HEAVY ION IMPACT ON SOLIDS

G.Lanzanò<sup>1</sup>, E. De Filippo<sup>1</sup>, S. Aiello<sup>1</sup>, M.Geraci<sup>1</sup>, A. Pagano<sup>1</sup>, G. Politi<sup>1</sup>,  
S. Cavallaro<sup>2</sup>, F. LoPiano<sup>2</sup>, E.C. Pollacco<sup>3</sup>, C. Volant<sup>3</sup>, S. Vuillier<sup>3</sup>, C. Beck<sup>4</sup>,  
D. Mahboub<sup>2</sup>, R. Nouicer<sup>4</sup>, D.H. Jakubassa-Amundsen<sup>5</sup>, H. Rothard<sup>6</sup>

<sup>1</sup>Istituto Nazionale di Fisica Nucleare, Sezione di Catania and Dipartimento di Fisica,  
Corso Italia 57, 95129 Catania, Italy

<sup>2</sup>Istituto Nazionale di Fisica Nucleare, Laboratorio Nazionale del Sud, Catania, Italy

<sup>3</sup>CEA, DAPNIA/SPHn, CE Saclay, F-91191 Gif-Yvette-Cedex, France

<sup>4</sup>IReS and Université L. Pasteur, F-67037 Strasbourg, France

<sup>5</sup>Physics Section, University of Munich, Am Coulombwall 1, 85748 Garching, Germany

<sup>6</sup>CIRIL (CEA/CNRS), BP 5133, 14070 Caen Cedex 05, France

Fast electron velocity spectra have been measured with the multidetector ARGOS (mounted in the NAUTILUS scattering chamber at GANIL) in a large angular range for atomic collisions induced by 77 MeV/n Ar<sup>18+</sup> beam on Al target (Experiment E230a, Nov. 1996) [1]. The velocity of electrons can be determined by the time-of-flight method. An example is shown in fig.1, where the measured intensity of emitted electrons is plotted as a function of the electron velocity taken at two different emission angles. One observes a broad peak from a binary collision between the projectile and a target electron (Binary Encounter Electrons, BEE). In beam direction (0 deg.), this peak should be observed at nearly twice the projectile velocity. As can be seen from fig.1, at small emission angles in forward direction, the shape of the BEE peak is well described by a recent relativistic theory [2] (the calculation is shown as full circles in fig. 1). The broadening of the peak at large emission angle is due to the transport of electrons through the solid foil (energy loss and angular scattering). Also, the angular dependence of the emission cross section is in good agreement with this theory and is close to what one would expect from a simple two body Rutherford ("Billiard Ball") scattering if relativistic kinematics are taken into account. Nevertheless, an important shift of the measured peak towards lower velocities is observed. This can be seen from fig. 2, which shows the position of the maximum of the BEE peak as a function of the emission angle in comparison to the theory. This result is not yet understood. Another interesting result concerns backward emission, where evidence for an excess of fast electrons is found. This can also be seen in fig. 2 which shows the "center of mass" of the fast electron distribution in backward direction.

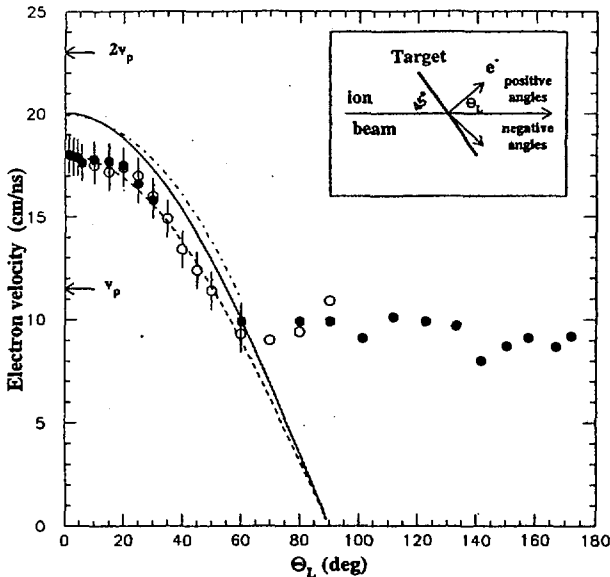


Fig. 2

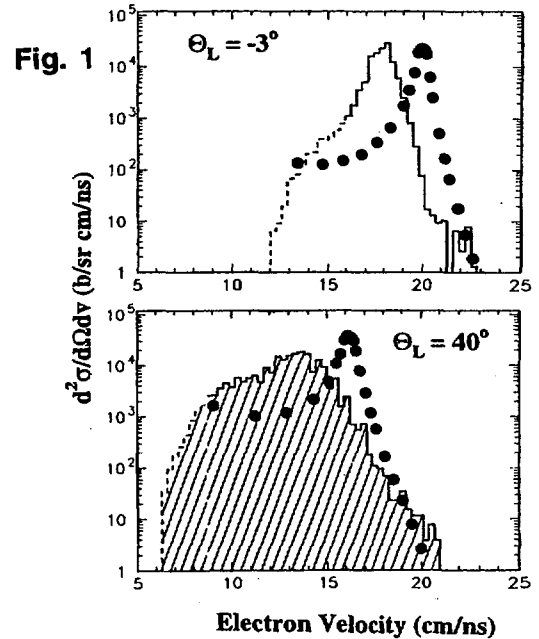


Fig. 1

- [1] G. Lanzanò, E. DeFilippo, S. Aiello, M. Geraci, A. Pagano, G. Politi, S. Cavallaro, F. LoPiano, E.C. Pollacco, C. Volant, S. Vuillier, C. Beck, D. Mahboub, R. Nouicer, H. Rothard, D.H. Jakubassa-Amundsen, submitted to Phys. Rev. A (1998)  
[2] D.H. Jakubassa-Amundsen, J. Phys. B.: At. Mol. Opt. Phys. 30 (1997) 365

## SOLID STATE EFFECTS IN BINARY ENCOUNTER ELECTRON EMISSION

Hermann Rothard<sup>1</sup>, Doris H. Jakubassa-Amundsen<sup>2</sup>, Annick Billebaud<sup>3</sup>

<sup>1</sup>Centre Interdisciplinaire de Recherches avec les Ions Lourds CIRIL, Laboratoire Mixte CEA-CNRS UMR 11, BP 5133, Rue Claude Bloch, F-14070 Caen Cedex 05, France

<sup>2</sup>Physics Section, University of Munich, Am Coulombwall 1, D-85748 Garching, Germany

<sup>3</sup>ISN, IN2P3-CNRS/Univ. J. Fourier, 53 Av. des Martyrs, F-38026 Grenoble Cedex, France

Binary encounter electrons (BEE) stem from a basic ionisation mechanism: the collision of a swift projectile with target electrons which should be ejected with an emission angle  $\theta$  dependent velocity of  $v_{BE} = 2 v_p \cos(\theta)$  if the interaction with the target nucleus, binding energy and relativistic effects are neglected ( $v_p$ : projectile velocity). The observed BEE peak at fixed angle is a distribution centred near  $v_{BE}$  which reflects the initial momentum distribution of the bound target electrons ("Compton profile"). BEE emission from thin foils was studied experimentally at GANIL/SME with  $Ar^{17+}$  of 13.6 MeV/u by means of a magnetic spectrometer [1,2,4] (P299). The results were compared to a theory based on the electron impact approximation (EIA) [3,4], where ionisation takes place via electron transfer to the projectile continuum. The active electron scatters elastically from the projectile field. The corresponding cross section is then folded with the Compton profile. A comparison of experiment and theory (solid line) is shown in figs.1,2 for Carbon foils. The BEE peak shape is well described by theory at small emission angles up to  $20^\circ$ . With increasing emission angle, for the thinnest C foils ( $d = 4.4 \mu\text{g}/\text{cm}^2$ , less than  $260 \text{ \AA}$ ), a shift of the maximum of the BEE peak to lower energies a peak broadening are observed (fig.2). This is due to transport effects (energy loss and angular scattering of electrons in the solid). The importance of such effects can be investigated by increasing the target thickness (fig.1). The overall intensity increases, the maximum shifts to lower energies and the BEE peak finally evolves into a broad distribution without pronounced maximum. The target dependence of BEE emission is discussed in detail in ref. [4].

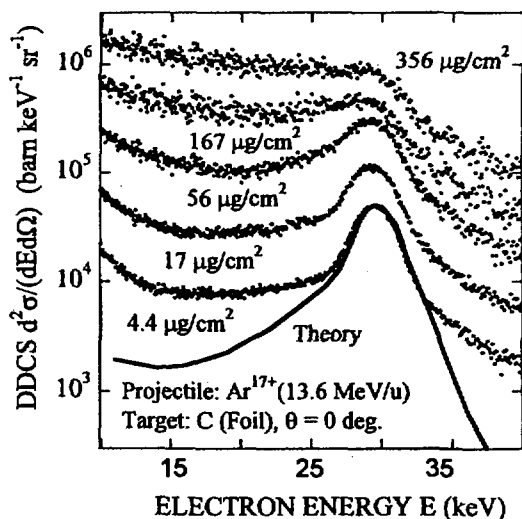


Fig. 1

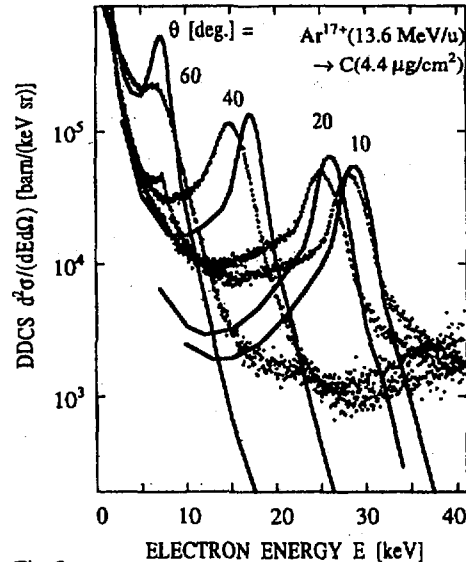


Fig.2

- [1] H. Rothard et al., *Target Thickness Dependent Electron Emission from Carbon Foils Bombarded with Swift Highly Charged Heavy Ions*, Physical Review **A51** (1995) 3066-3078
- [2] H. Rothard, A. Billebaud, M. Chevallier, A. Clouvas, B. Gervais, J.P. Grandin, M. Jung, R. Wunsch, *Transport of Swift Heavy Ion Induced Electrons in Solids*, Nucl. Instrum. Meth. **B115** (1996) 284-287
- [3] D.H. Jakubassa-Amundsen, *Relativistic Theory for Binary Encounter Electron Emission*, J. Phys. B: At. Mol. Opt. Phys. **30** (1997) 365-385
- [4] Hermann Rothard, Doris H. Jakubassa-Amundsen, Annick Billebaud, *Solid State Effects in Binary Encounter Electron Emission from 13.6 MeV/u  $Ar^{17+}$  Collisions with C, Al, Cu and Au Foils*, J. Phys. B: At. Mol. Opt. Phys. **31** (1998) 1563-1578

# ELECTRON YIELDS AS PROBE OF SWIFT HEAVY ION-SOLID INTERACTION

H. Rothard, M. Jung<sup>1</sup>, M. Caron, J.P. Grandin, B. Gervais,

A. Billebaud<sup>2</sup>, A. Clouvas<sup>3</sup>, R. Wünsch<sup>4</sup>

Centre Interdisciplinaire de Recherches avec les Ions Lourds CIRIL  
(CEA-CNRS UMR 11) BP 5133, Rue Claude Bloch, F-14070 CAEN Cedex 05

<sup>1</sup>Now at: ATOMIKA Instruments GmbH, Bruckmannring 40, D-85764 Oberschleissheim

<sup>2</sup>ISN, IN2P3-CNRS/Université J. Fourier, 53 Av. des Martyrs, F-38026 Grenoble Cedex

<sup>3</sup>Dept. of Electrical and Computer Engineering, Aristotelian Univ., GR-54006 Thessaloniki

<sup>4</sup>Inst. für Kernphysik, J.W. Goethe Univ., August-Euler-Str. 6, D-60486 Frankfurt/ Main

A major part of the energy loss of swift heavy ions in matter leads to excitation and ionisation. From an atomic physics point of view, excitation and ionisation are among the most fundamental consequences of energetic atomic collisions. On the other hand, radiation effects due to electronic energy deposition in condensed matter are closely related to the subsequent electron transport (and secondary electron cascade multiplication) where the deposited energy is distributed along and around the ion track. Finally, after relaxation and thermalisation, the energy initially deposited in electronic excitation may result in creation of defects, nuclear tracks, damage and modification of material properties. A fraction of the electrons is ejected from the solid surface and kinetic electron emission is thus an important probe for the interaction of swift heavy ions with solids. Within the proposals P299, P340 and P395, electron yields (the mean number of electrons  $\gamma$  emitted per ion) were studied as a function of the projectile velocity  $E_p$ , the ion charge  $q$  and atomic number  $Z_p$  at GANIL-LISE and GANIL-SME [1-4]. These experiments are based on current measurements as described in detail in [2]. Varying the target thickness (thin foils) allows in particular to study the evolution of electron emission from single collisions (as in atomic collisions with low density gas targets) up to multiple collisions (as in the bulk of solids, where electron transport phenomena become important) [2]. Specific effects can be observed with heavy ions due to the high charge states inside solids involved, resulting high ionisation cross sections, strong induced perturbation and large electronic energy loss [3,4].

The dependence of electron yields on foil thickness is shown in fig.1 for Cu ions of 9.6 MeV/u, and for Ni ions of 74 MeV/u ( $q = 28$  in both cases). Forward yields  $\gamma_f$  evolve over a large thickness range (up to 0.5 mg/cm<sup>2</sup> at 9.6 MeV/u and 3 mg/cm<sup>2</sup> at 74 MeV/u). This is caused by secondary electron production (cascade multiplication) by fast primary electrons. Most of these high energy electrons are emitted in forward direction. Electron transport can be studied quantitatively by an analysis of measured electron yields as a function of foil thickness within the framework of an empirical theory described in detail in [2]. It is found that the diffusion length of low energy electrons ( $E < 100$  eV) does not depend on the ion species or projectile energy and is of the order of 30 Å. In contrast, the attenuation length of fast electrons ( $E \gg 100$  eV) increases strongly with increasing projectile velocity and can be described by a power law  $\lambda[\text{Å}] = 390 (E_p/M_p[\text{MeV/u}])^{1.22}$ . This explains the "velocity effect": damage in solids is different for fixed electronic energy loss  $dE/dx$ , but different ion velocity. Energy is taken away from the track core by fast electrons for faster ions and the density of energy deposition close to the ion track is different. The mean energy  $\langle E \rangle$  of ejected electrons increases with  $E_p/M_p$  as  $\langle E \rangle[\text{eV}] = 92.5 (E_p/M_p[\text{MeV/u}])^{1.08}$ .

It is often assumed that electron yields are proportional to the electronic energy loss per unit path length  $dE/dx$  and thus it is common practice to compare electron yields to  $dE/dx$  by defining a ratio  $\Lambda_T = \gamma_T/(dE/dx)$  if total yields ( $\gamma_T = \gamma_f + \gamma_b$ ) are concerned. The energy dependence of  $\Lambda_T$  for H, C, Ni (Cu) and U ions (as shown in fig.2) can be described by a power law:  $\Lambda_T = C (E_p/M_p)^n$  as indicated by the solid lines in fig.2. The inset shows the projectile dependence of the exponent  $n$ . From fig. 2, one can easily estimate electron yields for all ions in a wide energy range above the maximum of the stopping power curve. This may be useful for the design of ion beam detectors based on secondary electron emission. For proton

**Fig. 1:** Forward (squares) and backward (circles) electron yields ( $\gamma_F, \gamma_B$ ) obtained with  $\text{Cu}^{28+}$  (9.6 MeV/u, full symbols) and  $\text{Ni}^{28+}$  (74 MeV/u, open symbols) as a function of carbon target thickness  $d$ . ( $1 \mu\text{g}/\text{cm}^2$  corresponds to about  $61 \text{ \AA}$  for a carbon foil density of  $\rho = 1.65 \text{ g}/\text{cm}^3$ ).

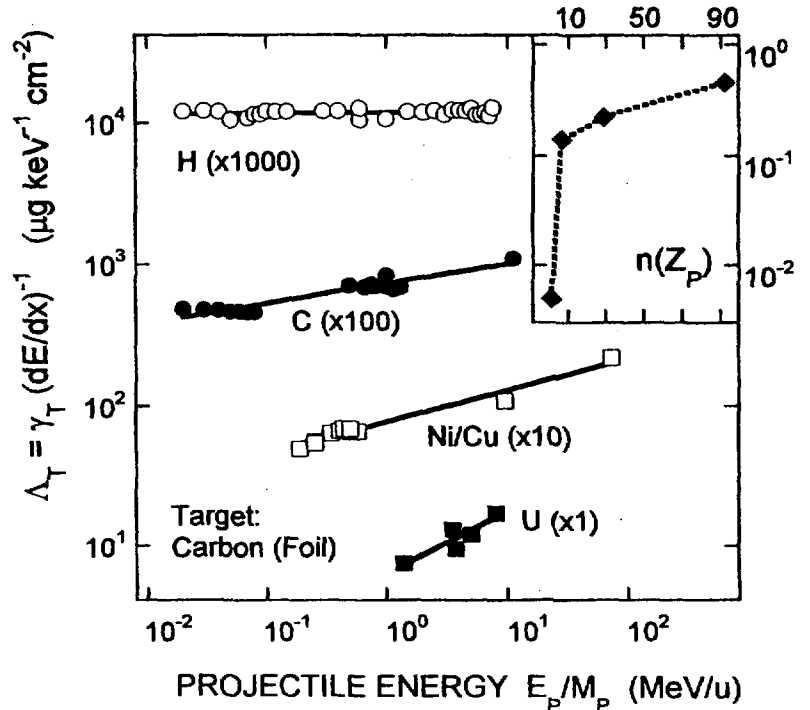
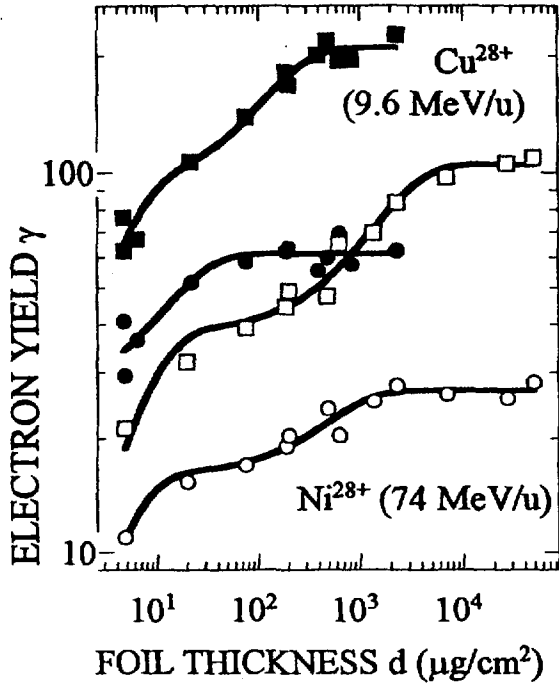


**Fig. 2:** The ratios of total electron yields and electronic energy loss per unit path length  $\Lambda_T = \gamma_T / (dE/dx)^{-1}$  as a function of the projectile energy  $E_p/M_p$  for different ions (the data were multiplied by the indicated factors). The target thickness was chosen so that electron yields have reached the (velocity dependent) asymptotic equilibrium value (see fig. 1, typically  $400 \mu\text{g}/\text{cm}^2$  at  $10 \text{ MeV}/u$ ) and the charge state of the incoming ions was chosen close to the mean final charge.

impact,  $\Lambda_T$  is constant over the whole investigated energy range. In contrast, for C ions, a slight increase is observed. For the heavy Cu and Ni ions, the increase of  $\Lambda_T$  with energy is more pronounced and even slightly stronger for U ions. We note that a strong/forward backward asymmetry with increasing  $Z_p$  of electron yields was observed and refer the reader to ref. [4] for a detailed discussion.

- [1] H. Rothard, M. Jung, B. Gervais, J.P. Grandin, A. Billebaud, R. Wünsch, **Fluence Dependent Electron Emission as a Measure of Surface Modification by Swift Heavy Ions**, Nucl. Instr. Meth. **B107** (1996)108
- [2] M. Jung, H. Rothard, B. Gervais, J.P. Grandin, A. Clouvas, R. Wünsch **Transport of Electrons induced by Highly Charged Ni (74 MeV/u) and Cu (9.6 MeV/u) Ions in Carbon: A Study of Target Thickness dependent Electron Yields**, Phys. Rev. **A54** (1996) 4153
- [3] H. Rothard, M. Jung, J.P. Grandin, B. Gervais, M. Caron, A. Billebaud, A. Clouvas, R. Wünsch, C. Thierfelder, K.O. Groeneveld, **Heavy Ion Track Potentials in solids probed by electron yield measurements**, Nucl. Instrum. Meth. **B125** (1997) 35
- [4] H. Rothard, M. Jung, M. Caron, J.P. Grandin, B. Gervais, A. Billebaud, A. Clouvas, R. Wünsch, **Strong Projectile Dependent Forward/Backward Asymmetry of Electron Ejection by Swift Heavy Ions in Solids**, Phys. Rev. **A57** (1998) 3660

## Enhancement of dielectronic processes in $\text{Ne}^{10+} + \text{He}$ collisions at energies as low as 1 keV

J.-Y. Chesnel<sup>a</sup>, H. Merabet<sup>b</sup>, B. Sulik<sup>c</sup>, C. Bedouet<sup>a</sup>, F. Frémont<sup>a</sup>, X. Husson<sup>a</sup>, M. Grether<sup>d</sup>, A. Spieler<sup>d</sup> and N. Stolterfoht<sup>d</sup>

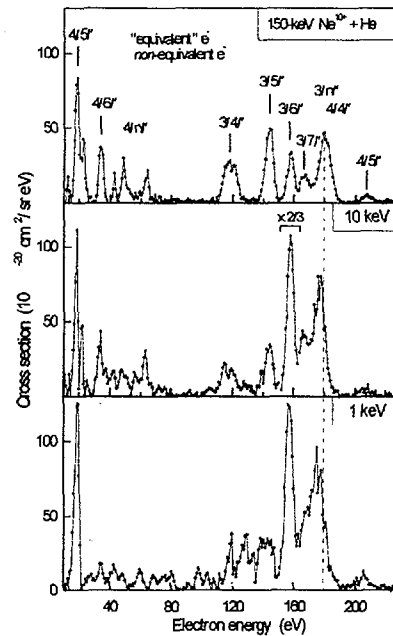
<sup>a</sup>L. S. A., I. S. M. R. A, 6 Boulevard Maréchal Juin, F-14050 Caen Cedex, France

<sup>b</sup>Department of Physics/220, University of Nevada, Reno

<sup>c</sup>I. N. R. of the Hungarian Academy of Sciences, P. O. Box 51, H-4001 Debrecen, Hungary

<sup>d</sup>Hahn-Meitner Institut, Bereich Festkörperphysik, Glienicker Strasse 100, D-14109 Berlin

The method of high-resolution Auger spectroscopy was used to study mechanisms for double-electron capture producing the projectile configurations  $3lnl'$  and  $4lnl'$  ( $n \geq 4$ ) in  $\text{Ne}^{10+} + \text{He}$  collisions. Emphasis was given to slow collisions with projectile energies near 1 keV. At low collision energies the production of the configurations  $3lnl'$  ( $n \geq 6$ ) is found to be dominant. It is shown that dielectronic process produced by electron-electron interaction play a major role in the creation of the  $\text{Ne}^{8+}$  ( $3lnl'$ ) states.



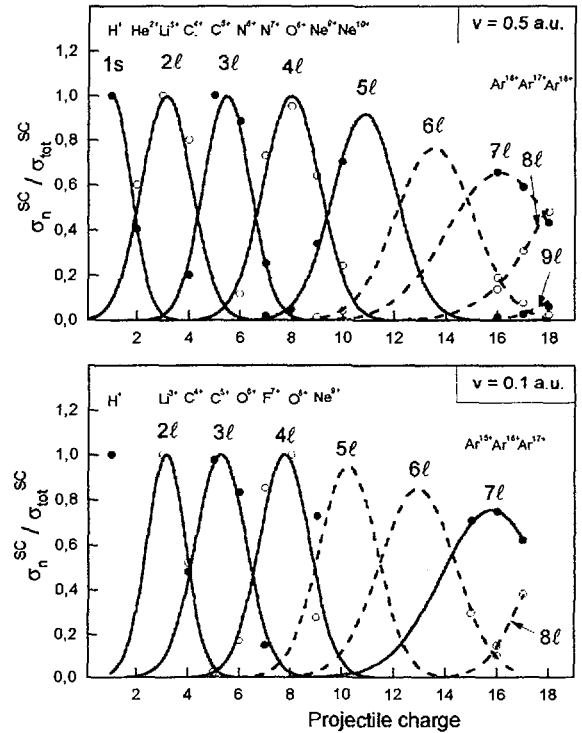
J.-Y. Chesnel, H. Merabet, B. Sulik, C. Bedouet, F. Frémont, X. Husson, M. Grether, A. Spieler and N. Stolterfoht, *Phys. Rev. A* **57**, 3546 (1998)

**Scaling laws for single and double electron capture in  $A^{q+} + \text{He}$  collisions ( $q \geq Z_A - 2$ )  
at low impact velocities.**

F. Frémont<sup>a</sup>, C. Bedouet<sup>a</sup>, J.-Y. Chesnel<sup>a</sup>, X. Husson<sup>a</sup>,

<sup>a</sup>L. S. A., I. S. M. R. A, 6 Boulevard Maréchal Juin, F-14050 Caen Cedex, France

We present empirical scaling laws, as a function of projectile charge state, for single and double electron capture in slow collisions between highly charged ions and He atoms at impact velocities of 0.1 and 0.5 a.u. The fitting parameters are shown to be suitable for predicting the populated states in single and double electron capture. The scaling law for single capture is found to be nearly independent of the projectile velocity in the range from 0.1 to 0.5 a.u. The same fitting procedure is followed for double electron capture at the velocity of 0.5 a.u., since independent mono-electronic transitions, due to electron-nucleus interactions, are dominant. At this velocity, the scaling law for the projectile-charge dependence of double-electron capture cross sections is found to be similar to that for single electron capture. At the lower velocity of 0.1 a.u., where dielectronic processes caused by electron-electron interaction gain importance, the charge dependence of double capture cross sections is strongly modified.



Experimental cross sections for producing a given  $n$ -state as a function of the projectile charge in  $A^{q+} + \text{He}$  collisions. Gaussian curves (solid lines) are used to fit the experimental data. Dashed Gaussian lines extrapolate experiment for  $n$  values larger than 5. Experiments using  $\text{C}^{6+}$ ,  $\text{N}^{7+}$ ,  $\text{O}^{8+}$ ,  $\text{Ne}^{10+}$  and Ar were performed at GANIL.

F. Frémont, C. Bedouet, J.-Y. Chesnel and X. Husson, Phys. Rev. A **57**, 4379 (1998)

# Investigation of charge exchange reactions at low energy by recoil ion momentum spectroscopy

X. Flécharde†, S. Duponchel‡, L. Adoui‡, A. Cassimi‡, A. Lepoutre‡, P. Roncin§, R.E. Olson¶ and D. Hennecart‡

† LSA (ISMRA-CNRS) Caen Cedex, F-14050

‡ CIRIL (CEA-CNRS) BP 5133, Caen Cedex 5, F-14070

§ LCAM (CNRS) Université Paris Sud, Bâtiment 351, F-91405

¶ Physics Department, University of Missouri-Rolla, Rolla, Missouri 65401

In low energy ion-atom collisions (i.e., projectile speeds smaller than the target electron speed), the dominant target removal process is electron capture. Such collision processes are central to the understanding of fusion plasma or for laser development and for diagnostics of astrophysical photoionized plasmas.

Up to now, such processes were studied through the information carried by the scattered projectile either by energy gain or by photon and electron spectroscopy. Unfortunately, these methods are not direct and are affected by post-collisional effects. It is the reason why we use recoil ion momentum spectroscopy to extract the information carried by the recoiling target. In this way, we perform cinematically complete experiments which give us a picture of the very first moment of the collision without any post collisional perturbation.

Several experiments were carried out with various projectiles delivered by the 14 GHz ECR source at the GANIL's test bench. For the first time in the scientific community we have obtained accurate differential state-selective cross-sections for capture reactions where fully stripped ions such as argon were used as projectiles [1].

The good resolution obtained in scattering angle and in Q-value (the inelasticity of the collision) allows first to give a new insight in the

mechanisms involved in double electron capture reactions [2] and second to test precisely the different theories which are available to day.

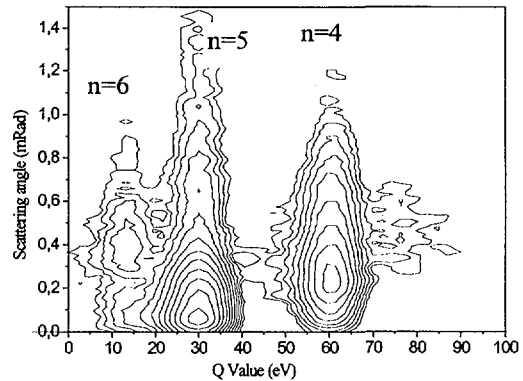


Fig: Example of high resolution doubly differential cross section for the  $Ne^{10+} - He$  at 150 KeV.

Since recoil ions are detected in coincidence with scattered projectiles, we are able to separate the processes leading to stabilized double electron capture from the processes leading to autoionizing double electron capture. This give access to the selective stabilisation ratio and to the Auger yields which are essential in the understanding of post collisional interactions.

1. A. Cassimi, S. Duponchel, X. Flécharde, P. Jardin, P. Sortais, D. Hennecart and R. E. Olson *Phys. Rev.Lett* **76** (1996) 3679.
2. X. Flécharde, S. Duponchel, L. Adoui, A. Cassimi, P. Roncin and D. Hennecart *J. Phys. B: At. Mol. Opt. Phys.* **30** (1997) 3697.

**(n, l, m<sub>l</sub>) selectivity of the single electron capture for low energy X<sup>8+</sup>(X≡Ar,Kr,O)-Li(2s) collisions**

P. Boduch<sup>1</sup>, M. Chantepie<sup>1</sup>, G. Cremer<sup>1</sup>, M. Druetta<sup>3</sup>, E. Jacquet<sup>1</sup>, C. Laulhé<sup>1</sup>, D. Lecler<sup>1</sup>, J. Pascale<sup>2</sup>, M. Wilson<sup>4</sup>.

<sup>1</sup> Laboratoire de Spectroscopie Atomique, 6 Bd Mal Juin F-14050 Caen-cedex, France.

<sup>2</sup> Service des photons, Atomes et Molécules, Centre d'Etudes de Saclay bât 522 F-91191 Gif sur Yvette-cedex, France.

<sup>3</sup> Laboratoire du traitement du signal, CNRS-URA 842, F-42023 Saint-Etienne cedex France.

<sup>4</sup> Royal Holloway University of London, Egham, Surrey TW20 EX, England.

Single electron capture is studied by photon spectroscopy for the X<sup>8+</sup>(Ar, Kr)-Li(2s) collision system between 0.1 and 5 keV/amu in the 200-600 nm wavelength range. From recorded photon spectra, production cross sections  $\sigma(n\ell)$  of each n $\ell$  configuration populated by single electron capture (SEC) process are determined. For both systems, the preferentially populated levels are n=8 and 9. This n distribution is nearly independent of the collision energy between 0.1 and 5 keV/amu.

The  $\ell$  distribution behavior versus the collision energy is completely different. As it is shown in figure 1, at high energy, only high  $\ell$  configurations are mainly populated. For low energy collision, comparison with classical trajectory Monte-Carlo (CTMC) calculations on O<sup>8+</sup>(bare ion)-Li system allows the following conclusion : the effect of the core electron projectile becomes efficient and contributes to the population of the low  $\ell$  configurations<sup>1</sup>.

The polarisation of each observed line due to SEC is measured. Transitions between low configurations are not significantly polarised contrary to transitions between high l configurations. The figure 2 shows the polarisation degree evolution of the 7 $\ell$ -8 $\ell$  Ar<sup>8+</sup>-Li transition. This behavior can be explained in the following way : as the collision energy decreases, the core effect is more efficient and the rotationnal

coupling becomes an intrashell coupling yielding to a m $\ell$  distribution widening and a polarisation degree diminution. At very low energy, the rotationnal coupling efficiency decreases allowing the increase of the polarisation degree<sup>2</sup>.

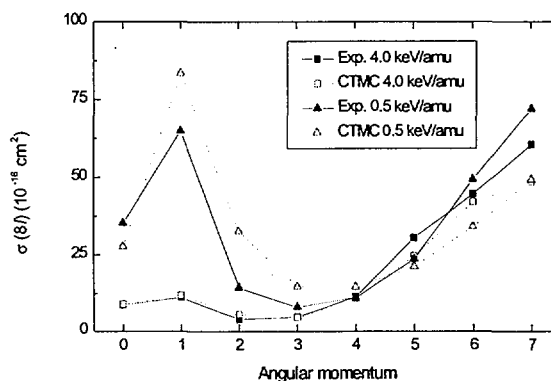


Figure 1

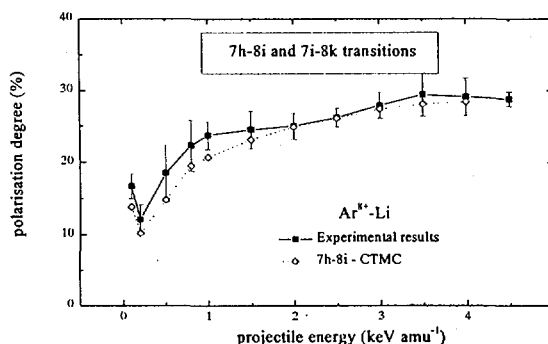


Figure 2

<sup>1</sup> Jacquet E., Pascale J., Boduch P., Chantepie M., Lecler D., J.Phys.B **28** (1995) 2221.

<sup>2</sup> Laulhé C., Jacquet E., Cremer G., Pascale J., Boduch Ph., Rieger G., Chantepie M., Lecler D., Phys.Rev.A **55** (1997) 1088.



## Fast ion-induced molecule fragmentation

C Caraby<sup>1</sup>, A Cassimi<sup>1</sup>, L Adoui<sup>1</sup>, JP Grandin<sup>1</sup>, D.Lelièvre<sup>1</sup> and A Dubois<sup>2</sup>

1 CIRIL (UMR CEA/CNRS N°11) Rue Claude Bloch BP5133 14070 Caen cedex 5 (France)

2 Laboratoire de Chimie Physique-Matière et Rayonnement, Université Pierre et Marie Curie, 11, rue Pierre et Marie Curie, 75231 Paris Cedex 05 (France)

The relaxation of multi-ionized molecules has been a subject of extensive studies during last decade. The ejection of several electrons through core excitation or direct outer-shell ionization leads to fragmentation of the molecule, as soon as the electrons participating to the chemical bond are removed. The use of swift heavy ions provides a powerful tool to remove many electrons in one collision. Thus, it gives access to the study of highly charged transient molecular ions. Moreover, the characteristic time scale for the multi-electron removal by swift ions is of the order of  $10^{-17}$  s, i.e. about  $10^3$  times shorter than the multiphoton ionization produced by up-to-date intense femtosecond lasers.

In this work, we have studied the fragmentation of the carbon monoxide (CO) molecule induced by a 6.7 MeV/A  $Xe^{4+}$  projectile (about 16 a.u. for the projectile velocity). We extend the previous CO fragmentation results in the strong interaction regime ( $q/v_p \gg 1$ , where  $q$  is the projectile charge state and  $v_p$  the projectile velocity), for which no experimental data have been yet reported. The experiment was performed on the LISE (Ligne d'Ions Super Epluchés) line at the GANIL facility. A 1/100 repetition rate has been used for the 10 MHz pulsed projectile beam. The CO target is provided by a supersonic gas jet to avoid the thermal energy spread which limits the momentum resolution. The two fragments are extracted from the collision region, perpendicularly to the ion beam, by a uniform electric field (from 130 to 410 V/cm) and detected on a micro-channel plate detector. The experimental technique is based upon a coincident time of flight measurement of the two fragments, similar to the PIPICO (Photo-Ion Photo-Ion COincidence) method usually performed in photoionization works. We measure the TOF of the first fragment and the time difference between the two ions coming from the molecular fragmentation on the same detector. Then, we use a trajectory simulation in the spectrometer to convert the time difference into total KER distributions.

We have studied the dissociation pathways of the highly charged ions up to  $CO^{9+}$  as well as branching ratios and multi-electron removal cross sections. In the case of such large impact parameter multi-ionizing collisions, the energy transferred to the nuclei of the molecule is small. In a previous ion-atom experiment performed at GANIL with He and Ar gaseous targets, we have measured, for the same projectile, that the most probable value of the recoil ion kinetic energy ranges between 1.17 meV and 9 meV for  $He^{1+}$  and  $He^{2+}$  and between 0.32 meV and 38.5 meV from  $Ar^{1+}$  up to  $Ar^{7+}$  [Jardin *et al.* 1996]. Then, the energy liberated in the dissociation process is directly reflected in the final velocities of the fragments. It is possible to determine the Kinetic Energy Release (KER) distributions from the time of flight (TOF) difference spectra. The main results can be summarized as follow :

- we have determined the KER distributions for 18 dissociation pathways from transient  $CO^{2+}$  to  $CO^{9+}$ . Note that one can deduce from these KER the  $CO^{9+}$  transient molecular excited states. The potential energy curves are well-known only for the very low charge states of the molecular ions ( $Q \leq 2$ ) at least in the Franck-Condon zone and for the lowest excited states. A comparison of these KER is possible as a function of the interaction strength of the perturbation experienced by the target during the collision by using projectiles of various charges and velocities ( $0.1 < k = q/v_p < 2.7$ ). The conclusion is that, if the increase of the interaction strength seems to favour high-lying components in these KER distributions, from the perturbative regime ( $k < 1$ ) to the intermediate one ( $k \approx 1$ ), this extension to the higher energies « saturate » in the strong interaction regime ( $k > 1$ ). Similar behavior has been recently observed in ion-atom collision experiment, made on the GANIL SME (Sortie Moyenne Energie) line, devoted to the *projectile* excitation. The competition between the shift of the impact parameter-dependent ionization probability  $P(b)$  to higher  $b$  values and the increase of the ionizing power results in a nearly constant interaction between the

projectile and the target. The results of the present work strengthen this qualitative interpretation, near from the ion-atom behavior.

- Multi-electron removal is found to represent about 40% of the ionizing events. It exhibits the high ionizing power of such heavy ion in the strong interaction regime, already pointed out in the atom ionization case. In the low molecular ion charge state cases, electron removal is highly dominated by valence electron ionization. However, for high charge states, inner-shell electron capture is estimated to be competitive compared to multiple ionization. Then, this electron capture greatly favours the multi-electron removal events and enhances the corresponding cross sections compared to the single ionization ones.

- In the excitation-ionization channel ( $Xe^{4+} + CO \rightarrow CO^{3+}$ ), only  $(26.8 \pm 0.2)\%$  of the  $CO^{3+}$  ion dissociates. The main fragmentation pathway is the C/O channel. For this one, we have directly measured the KER distribution through the determination of the full momentum vector of the C<sup>+</sup> fragment by Recoil Ion Momentum Spectroscopy (RIMS). This has been achieved by TOF measurement and ion impact position determination, giving access to the angular and KER distributions in coincidence. For a 410 V/cm extraction field, the momentum resolution is around 8 a.u. for the C<sup>+</sup> fragment. It improves the KER distribution resolution and evidences high-lying excited components produced by the excitation-ionization process (figure 1). The higher states ( $\gamma$  and  $\delta$  on figure 1) correspond to a total energy deposited by the projectile of 42.3 eV and 51.2 eV respectively, above the double ionization threshold.

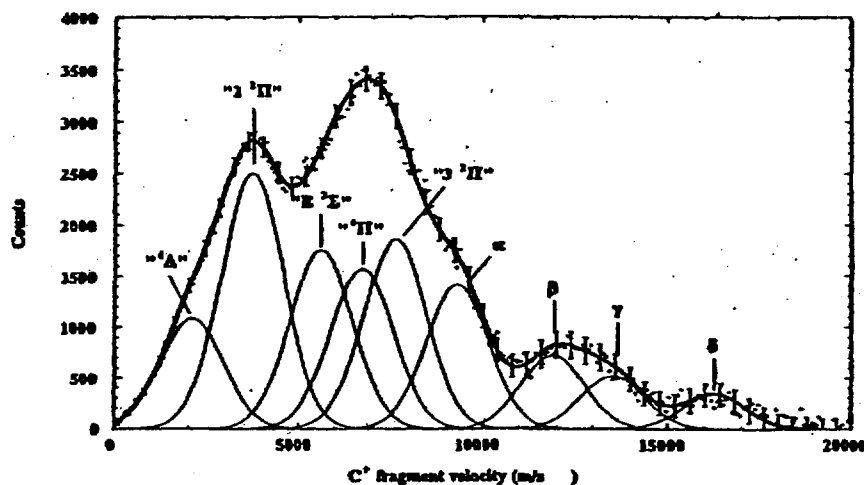


Figure 1 : C<sup>+</sup> momentum distribution for the  $CO^{3+} \rightarrow C^+ + O$  fragmentation channel.

Recently, we have implemented a multi-hit position sensitive detector which allow the full momentum vector determination of all the fragments in coincidence. Thus, in the near future, the attention will be turned to the study of the evolution of the (multi-)ionization cross section versus the angle between the internuclear axis of the diatomic molecule and the ion beam direction. Further experiments on the dissociation of the water molecule are also scheduled. The study of the radiolysis of water becomes a subject of growing interest since, from a radiobiological point of view, most of the energy deposited by ionizing radiations is absorbed by this molecule. The results are still scarce in the case of high Linear Energy Transfer radiations.

**References for published works :**

- Caraby C 1997 Thèse de l'université de Caen (unpublished)
- Caraby et al 1997 Phys Rev A 55 2450
- Caraby et al. 1998 European Physics Journal D 1998 2 53
- Jardin P 1995 Thèse de l'université de Caen (unpublished)
- Jardin P et al 1996 Nucl.Instr.and Meth. B98 363
- Olivera G.H. et al 1998 to appear in Phys.Med.Biol.(accepted)
- Vernhet D et al 1997 Phys.Rev.Lett.79 3625
- Vernhet D 1997 Nouvelles du GANIL60 9

**NEXT PAGE(S)  
left BLANK**

## **2 - SWIFT HEAVY ION INDUCED MODIFICATION IN MATERIALS**

## TEMPERATURE DEPENDANCE OF DAMAGE CREATION IN BISMUTH BY SWIFT HEAVY IONS

Ch. Dufour<sup>\*</sup>, E. Paumier<sup>\*,+</sup>, F. Benu<sup>°</sup> and M. Toulemonde<sup>+</sup>

<sup>\*</sup>LERMAT-ISMRA B<sup>d</sup>du Marechal juin 14050 Caen cédex (F)

<sup>+</sup>CIRIL, CEA-CNRS, BP 5133, 14070 Caen cédex 05 (F)

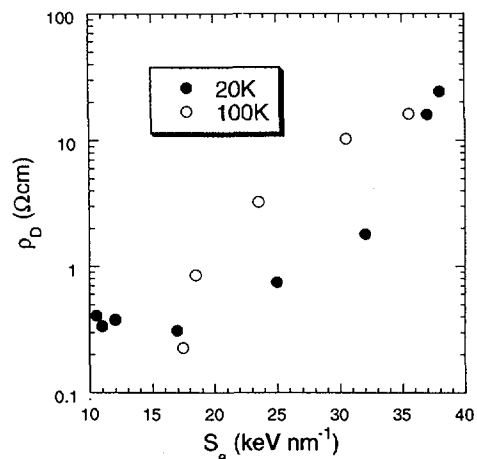
<sup>°</sup>LSI Ecole Polytechnique 91128 Palaiseau cédex (F)

The behavior of metallic materials [1] as well as insulators [2] under swift heavy ion irradiations has been extensively studied and correlated to the thermal spike model [3,4]. In the framework of the thermal spike model the energy deposited on the target electrons is transferred to the lattice causing a local temperature increase. A molten phase could then appear around the ion path and give place to the so-called latent track after ultrafast quenching. A first evidence of an effect of the temperature increase along the ion path is the annealing of the defects created by nuclear collisions [5] below the electronic stopping power threshold of damage creation. This annealing can be quantified by the thermal spike model [6].

In this work we add a new element in favor of the thermal spike model: the effect of the temperature of irradiation. The energy necessary to melt a material is all the lower as the initial temperature of irradiation is high. Bismuth is a good material to test this fact because of its low melting point and its sensitivity to the electronic stopping power  $S_e$  of swift heavy ions [7]. This sensitivity has been experimentally evidenced by measuring the sample resistivity  $\rho$  as a function of the ion fluence  $\Phi t$  ( $\Phi$  is the flux and  $t$  the irradiation time) for

different ions and consequently for different values of stopping power.

In order to quantify the effect of the temperature of irradiation on the damage creation in bismuth, this material has been irradiated with 5.8 GeV of xenon and 6.5 GeV tantalum ions at 20K and 100K. 100K was chosen because at this temperature there is no annealing of defects created by the ion irradiations in the electronic stopping power regime [7]. Aluminum degraders were used to decrease the beam energy and to select several values of  $S_e$  between 17 and 40 keV nm<sup>-1</sup>. In order to characterize the  $S_e$  effect we analyze the evolution of the resistivity increase versus the fluence  $\Phi t$ .



Then we define the following parameter  $\rho_D = (1/\sigma_t)(d\rho/d\Phi t)_{\Phi t=0}$  [7] where  $\sigma_t$  is the damage cross section of elastic collisions. The figure shows the  $\rho_D$  values versus the electronic stopping power for the two temperatures of irradiation. The values of  $\rho_D$  are higher in the case of the irradiations performed at 100K than at 20K. The damage efficiency is therefore higher at 100K than at 20K as expected by the thermal spike model. For values less than 18 keV nm<sup>-1</sup> when only nuclear collisions are responsible of the defect creation,  $\rho_D$  is lower at 100K than at 20K due to the annealing of the Frenkel pairs at 45K [7].

#### References :

- [1] A. Dunlop and D. Lesueur Rad. Eff. Def. Sol. 126(1995)
- [2] M. Toulemonde, S. Bouffard and F. Studer, Nucl. Instr. Meth. B91(1994)108
- [3] Ch. Dufour, E. Paumier and M. Toulemonde, Nucl. Instr. Meth B122 (1997) 445
- [4] M. Toulemonde, J.M. Costantini, Ch. Dufour, A. Meftah, E. Paumier, F. Studer, Nucl. Instr. Meth B116 (1996) 37
- [5] A. Dunlop, D. Lesueur, P. Legrand, H. Dammak and J. Dural, Nucl. Instr. Meth. B90(1994)33
- [6] Z. G. Wang, Ch. Dufour, E. Paumier and M. Toulemonde Nucl. Instr. Meth. B115(1996)577
- [7] Ch. Dufour, A. Audourd, F. Beuneu, J. Dural, J.P. Girard, A. Hairie, M. Levalois, E. Paumier, and M. Toulemonde, J. Phys : Condens. Matter 5(1993)4573

Electronic stopping power threshold of sputtering in yttrium iron garnet: comparison to the latent track appearance.

A. Mefath<sup>§,°</sup>, M. Djebara<sup>+</sup>, J. P. Stoquert<sup>\*</sup>, F. Studer<sup>#</sup> and M. Toulemonde<sup>°</sup>

<sup>§</sup>ENSET, BP26, Merj-eddib, 21000 Skikda (Algérie)

<sup>+</sup>USTHB, Institut de physique, BP32, El-Alia, Bab Ezzouar, 16111 Alger (Algérie)

<sup>\*</sup>Laboratoire PHASE, 23 rue du Loess, 67037 Strasbourg cédex (France)

<sup>#</sup>CRISMAT, ISMRa, Université de Caen, 14032 Caen-cédex (France)

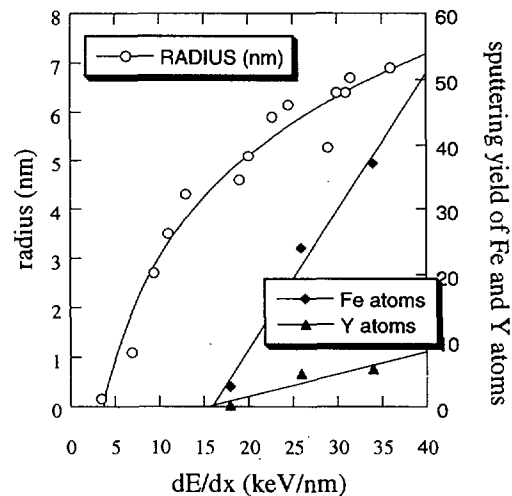
<sup>°</sup>CIRIL, CEA-CNRS, BP5133, 14070 Caen-cédex (France)

The sputtering of yttrium garnet ( $Y_3Fe_5O_{12}$ ) have been studied in the electronic stopping power ( $dE/dx$ ) regime in order to compare the sputtering efficiency to the latent track creation [1].

Single crystal of  $Y_3Fe_5O_{12}$  have been irradiated at room temperature with  $^{86}Kr$  (energy 195 MeV,  $dE/dx=18$  keV/nm),  $^{181}Ta$  (400MeV, 34 keV/nm) and  $^{235}U$  ions (150 MeV, 26 keV/nm) through an aluminum degrader placed 1mm in front of the sample. The sputter atoms are collected on this aluminum foil called the catcher.

The catcher was analyzed using Rutherford backscattering spectrometry using 1MeV of alpha or  $^{12}C$  beam. Using Carbon beam the sensitivity is as low as  $2 \cdot 10^{12}$  Fe per  $cm^2$  allowing low fluence of irradiation to avoid the damage recovery linked to the track creation. Moreover with such fluences the sputtering of the deposited atoms on the catcher is negligible.

The results of the sputtered Fe and Y atoms are presented on the figure and compare to the evolution of the latent track radii versus the electronic stopping power. It should be mention that this electronic sputtering does not follow the stoichiometry of the garnet. By a linear extrapolation of the Fe and Y atom sputtering yield, the electronic stopping power threshold of electronic sputtering is the same for the two species and is equal to  $16 \pm 3$  keV/nm [2].



This threshold is four times higher than the one determined for the damage creation which is  $4 \pm 1.5$  keV/nm [3] in the same energy range of the sputtering experiments.

References:

- [1] A. Meftah, F. Brisard, J.M. Costantini, M. Hage-Ali, J.P. Stoquert, F. Studer and M. Toulemonde Phys. Rev. B48(1993)920
- [2] A.Meftah, M. Djebara, J.P. Stoquert, F. Studer and M. Toulemonde Nucl. Instr. Meth. B107(1996)242
- [3] A. Meftah, M. Hage-Ali, J. P. Stoquert, F. Studer and M. Toulemonde, Rad. Eff. Def. Sol. 126(1993)251

## Angular distribution of neutral atoms sputtered by heavy ion bombardment.

S. Schlutig<sup>\*</sup>, S. Bouffard<sup>\*</sup>, J.P. Duraud<sup>\*</sup> and M. Mosbah<sup>\*</sup>

- <sup>\*</sup> CIRIL (CEA-CNRS), BP 5133, 14070 Caen cedex 5, France
- <sup>\*</sup> LPS (CEA-CNRS), CEA/Saclay, 91191 Gif sur Yvette, France

The experiments done at the surface of the materials can improve our knowledge of the damage mechanism under high electronic excitation. Information about how the atoms are moved off in the track can be obtained from the energy and the angular distribution of the atoms ejected by the ion impact. Since most of the atoms ejected are not ionised, the most used and the simplest technique is to catch the sputtered atoms on a clean surface. In this study, we have chosen a material in which latent tracks have been measured [1] and which presents a high detection efficiency : the Uranium dioxide. The sputtered Uranium atoms are collected on a mica foil which is subsequently irradiated with thermal neutrons to fission the <sup>235</sup>U. The fission fragments create latent tracks in the mica which are revealed by chemical etching. The angular distribution of sputtered Uranium is determined from the spatial distribution of the tracks on the mica detector [2].

The angular distribution can be fitted with a  $\cos^n$  law with  $n \sim 3$  which indicates a preferential emission perpendicular to the surface. The total yield is obtained by integrating over the solid angle. For <sup>116</sup>Sn<sup>36+</sup> (4.6 MeV/A) ions,  $54.4 \pm 9.3$  Uranium atoms are ejected per incident ion, while for <sup>238</sup>U<sup>55+</sup> (3.5 MeV/A), this number increases up to  $4800 \pm 450$ . This huge variation is still debated but could reflect the evolution of the track morphology (from discontinuous to continuous track). The direct observation of the surface of damaged UO<sub>2</sub> by near-field microscopy gives information about the origin of the atoms ejected by the ion impact.

### References :

1. T. Wiss, H.J. Matzke, C. Trautmann, M. Toulemonde and S. Klaumünzer, Nucl.Instr.and Meth. B 122 (1997) 583.
2. S. Bouffard, J.P. Duraud, M. Mosbah and S. Schlutig, accepted in Nucl.Instr.and Meth. B.

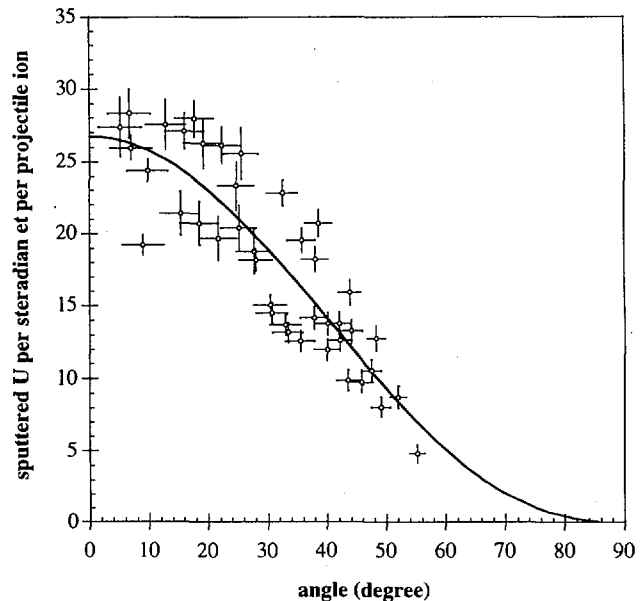


Figure : Angular distribution of Uranium atoms sputtered by the interaction of <sup>116</sup>Sn<sup>36+</sup> (4.6 MeV/A) with an UO<sub>2</sub> target. The line indicates the best fit with a  $\cos^n \theta$  law.

## Effect of the energy density near the ion path on the track formation in mica.

S. Bouffard\*, C. Leroy\* and J.M. Costantini\*

\* CIRIL (CEA-CNRS), BP 5133, 14070 Caen cedex 5, France

\* CEA/Bruyères le Chatel, BP 12, 91680 Bruyères le Chatel cedex, France

Since the first experiment done by near field microscopy [1], the efficiency of this method for the visualisation of the surface modifications induced by the swift heavy ions has been demonstrated. In mica, the evolution of the track diameter has been measured as a function of the electronic stopping power (LET) [2]. For the high-velocity ions ( $E > 1$  MeV/A), above a LET threshold of about 5 keV/nm, the track diameter increases linearly with the LET (figure 1). However this curve is no longer valid for low-velocity ions ( $E < 1$  MeV/A). In this case, the tracks are detectable below this threshold and, for a given LET, a low-velocity ion produces a larger track than a high velocity ion.

Thus the LET of the ions is not a sufficient parameter to characterise the induced modification. A better parameter should be the density of energy deposited near the ion path. This density of energy can be obtained from a simulation of the energy transfer to the solid [3]. Since the energy deposited near the ion path comes essentially from the low energy electrons, we have evaluated the part of the LET which corresponds to the production of these low-energy electrons : the reduced LET. The figure 2 shows that there is no more difference between high- and low-velocity ions if the track diameter is plotted as a function of this reduced LET [4].

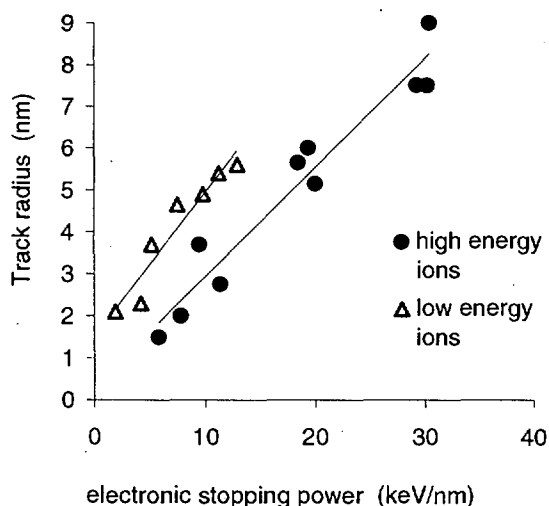


Figure 1 : Track radius measured in mica for high-energy ions (GANIL experiments) and low-energy ions (irradiations done at Bruyères le Chatel).

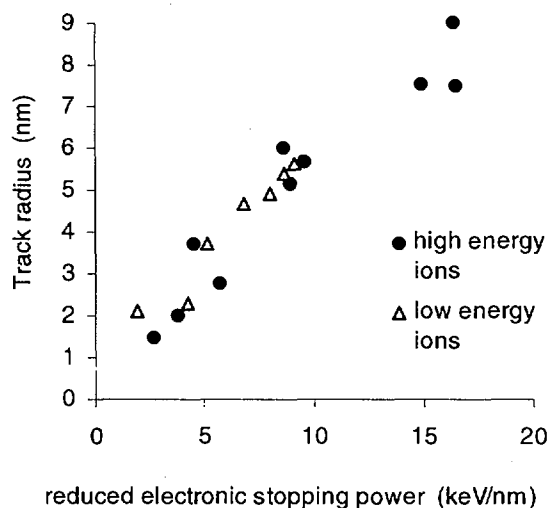


Figure 2 : Track radius plotted as a function of the electronic stopping power corresponding to the production of low-energy electrons (<200eV).

### References :

1. F. Thibaudau, J. Cousty, E. Balanzat and S. Bouffard, Phys.Rev.Lett. 67 (1991) 1582.
2. S. Bouffard, J. Cousty, Y. Pennec and F. Thibaudau, Radiat. Eff. and Def. in Solids 126 (1993) 225.
3. B. Gervais and S. Bouffard, Nucl. Instr. and Meth. B 88 (1994) 355.
4. C. Leroy, Thesis Université de Caen (1996).



## MODIFICATIONS INDUCED BY SWIFT HEAVY ION IRRADIATIONS IN METALLIC OXIDE POWDERS (Y<sub>2</sub>O<sub>3</sub> AND SnO<sub>2</sub>)

Exp P. 373 (E. Dooryhée)

S. Hémon, F. Levesque, CIRIL, CEA-CNRS, rue Claude Bloch, BP 5133, 14040 Caen Cedex

A. Berthelot, C. Dufour, F. Gourbilleau, E. Paumier, LERMAT, UPRESA CNRS 6004, ISMRa, 6 Bd du Maréchal Juin, 14050 CAEN Cedex

E. Dooryhée, avenue des Martyrs, BP 220, 38043 Grenoble Cedex.

The study of the interaction between swift heavy ions and bulk materials shows that the effects depend on the electronic stopping power  $S_e$ , resulting in track creation in  $S_e$  sensitive materials.

In the present study, we are interested in knowing whether the swift ion irradiation effects are influenced by the finite size of the sample. We choose to irradiate powders of materials which are insensitive to  $S_e$  in their bulk form.

In this content, two metallic oxide samples (powders, sintered sample or single crystal in some cases) were used : yttrium oxide (Y<sub>2</sub>O<sub>3</sub>) for which preliminary results were obtained by V. Chailley and tin oxide SnO<sub>2</sub>.

Yttrium oxide was irradiated with several ions in a large range of  $S_e$  value. The different samples exhibit different behaviors under irradiation. In some of them, the structure changes from cubic (stable in normal conditions) to monoclinic (stable under high pressure and high temperature). This transition is studied by X-ray diffraction using the CHEXPIR facility in-situ. The single crystal seems insensitive, while the sintered sample is sensitive only at high  $S_e$  value. The powder remains cubic at low  $S_e$  value, but is more and more sensitive when  $S_e$  increases. The efficiency of the transformation measured by the volumic proportion of cubic phase in the sample, is determined by Rietveld analysis which also gives the evolution of the grain size and of the stresses into the grains during irradiation.

Concerning the tin oxide, the effects of swift heavy ion are studied by transmission and high resolution electron microscopies, before and after irradiation. Thus, with increasing Pb fluences, modifications of grains which occur above a critical fluence of  $2 \cdot 10^{12}$  Pb cm<sup>-2</sup> have been observed. The grains lose their initial shape and some nanodomains are formed presumably due to grain bursting followed by sputtering and redeposition. The smallest grain disappear after irradiation.

The results obtained on each oxide may be interpreted with the aid of the thermal spike model, if modifications are introduced to take into account the increase of pressure due to temperature.

### Publication

- TEM study of irradiation effects on tin oxide nanopowder  
S. Hémon, F. Gourbilleau, C. Dufour, E. Dooryhee, E. Paumier  
Nucl. Inst. Meth. B, 1997, **122**, 526-529
- Phase transformation of polycrystalline Y<sub>2</sub>O<sub>3</sub> under irradiation with swift heavy ions  
S. Hémon, V. Chailley, E. Dooryhee, C. Dufour, F. Gourbilleau, F. Levesque, E. Paumier  
Nucl. Inst. Meth. B, 1997, **122**, 563-565
- The thermal spike model : a possible way to describe the effects induced in matter by swift heavy ion irradiation  
C. Dufour, S. Hémon, F. Gourbilleau, E. Paumier, M. Toulemonde, E. Dooryhee  
Mater. Sci. Forum, 1997, **248-249**, 21-31
- Nanometric size effects on irradiation of tin oxide powder  
A. Berthelot, S. Hémon, F. Gourbilleau, C. Dufour, E. Dooryhee, E. Paumier  
Accepté pour publication dans Nucl. Inst. Meth. B
- Influence of the grain size : yttrium oxide irradiated with swift heavy ions  
S. Hémon, C. Dufour, F. Gourbilleau E. Paumier, E. Dooryhee, S. Begin-Collin  
Accepté pour publication dans Nucl. Inst. Meth. B

## Swelling of insulators under ion irradiation

M. Toulemonde<sup>1</sup>, J.M. Costantini<sup>2</sup>, A. Meftah<sup>3</sup>, K. Schwartz<sup>5</sup>, J.P. Stoquet<sup>4</sup>, C. Trautmann<sup>5</sup>

<sup>1</sup> Ciril, CEA/CNRS, BP 5133, 14070 Caen cedex 5, France, <sup>2</sup> CEA/DPTA/SPMC, BP 12, 91680 Bruyères-Le-Châtel, France, <sup>3</sup> ENSET, BP 26 Merj-eddib, 21000 Skikda, Algeria, <sup>4</sup> Laboratoire PHASE, 67037 Strasbourg cedex 2, France, <sup>5</sup> GSI, Planckstr. 1, 64291 Darmstadt, Germany

Many solids exhibit volume expansion under various types of radiation such as photons, electrons, or neutrons. Recently, swelling effects have also been observed when irradiating  $\text{Al}_2\text{O}_3$  [1] and  $\text{LiNbO}_3$  [2] with energetic heavy ions. In order to test if this macroscopic volume increase is a general modification induced by ions in the electronic energy loss regime, we irradiated several insulating crystals ( $\text{LiF}$ ,  $\text{SiO}_2$  quartz, and  $\text{Gd}_3\text{Ga}_5\text{O}_{12}$  garnets) using a wide variety of ion species [3,4]. About 1 mm thick slabs of single-crystals with polished surfaces were irradiated at the 7 MV tandem Van de Graaff in Bruyères-le-Châtel (F, S, and Cu), at the UNILAC of the GSI (Kr, Au, and U), and at the SME beamline of the GANIL (C, Kr, Mo, Xe, Ta, and Pb). The energy varied from 0.8 to 11.4 MeV/u, corresponding to ion range in the crystals between a few and 100 micrometers.

In all crystals, we observed a significant out-of-plane swelling. Due to the fact that the ions were stopped in a thin surface layer, the free expansion of the irradiated volume is partially limited by the constraint of the undamaged substrate. As a consequence, the sample bulges outwards mainly normal to the sample surface. The quantitative analysis of the swelling was performed with a profilometer (Dektak 8000) where a diamond-tipped stylus scans over the border line between an irradiated and a virgin area. Typical scans of  $\text{Gd}_3\text{Ga}_5\text{O}_{12}$  crystals irradiated with Cr ions of various fluences are shown in Fig. 1. Depending on the ion fluence, the electronic energy loss, the total ion range, and the material, the step height varied between 20 and a few hundred nanometers.

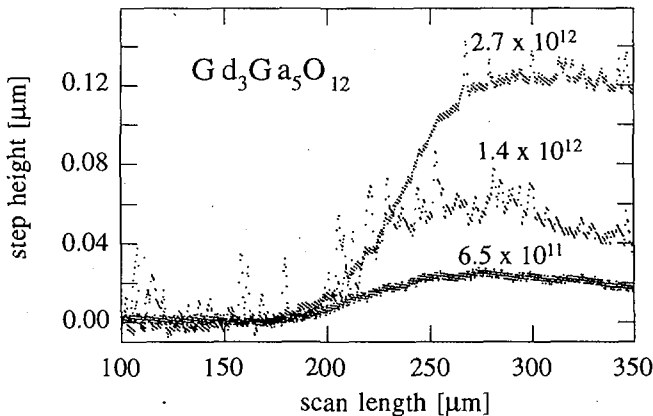


Fig. 1. Profilometer scans from the virgin (left) to the irradiated (right) area of  $\text{Gd}_3\text{Ga}_5\text{O}_{12}$  crystals irradiated with Cr ions (6.2 MeV/u) of various fluences ( $\text{ions}/\text{cm}^2$ ).

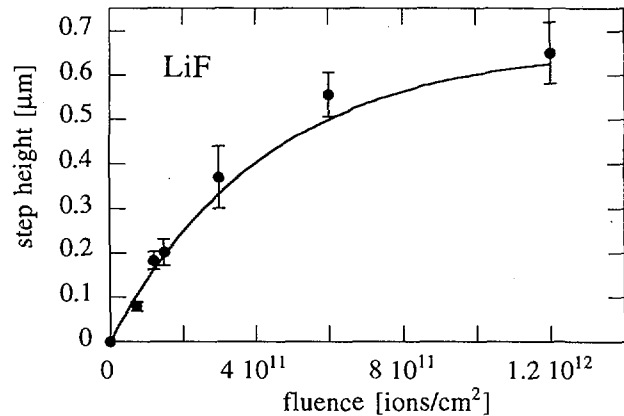


Fig. 2. Step height as a function of the fluence for  $\text{LiF}$  irradiated with Pb ions (4 MeV/u).

The characteristic evolution of the step height as a function of the ion fluence is illustrated for Pb ions in  $\text{LiF}$  in Fig. 2, where an initial linear increase, the curves approached saturation at high fluences.

In order to test the correlation between swelling and energy loss, we determined the relative contribution of each single ion per unit damage length. This was done by plotting the initial rate of swelling ( $\Delta l/\Delta \phi$ ) divided by the projected ion range  $R$  versus the mean energy loss (Fig. 3). Fitting a linear curve to the experimental data, a threshold of  $1.8 \pm 0.5$  and  $7 \pm 2$  keV/nm was deduced for  $\text{SiO}_2$  and  $\text{Gd}_3\text{Ga}_5\text{O}_{12}$ , respectively. Below this critical energy loss, obviously the damage along the ion path does not effect the expansion of the sample

dimension. Both values are in good agreement with the threshold for damage creation as determined from the Rutherford backscattering experiments under channelling condition (C-RBS) [5,6].

Another interesting observation concerns the increase of the swelling effect for larger ion ranges. For a quantitative analysis, the step height was normalised by the damage fraction  $F_d$  as known from C-RBS experiments. Fig. 4 clearly demonstrates that the swelling effect has a linear dependence on the track length. It also shows that the damage induced by the electronic excitation is not efficient along the total range of the incident ion. It is interesting to note that the relative dimensional change of 0.04 is the same for  $Gd_3Ga_5O_{12}$ ,  $SiO_2$ , and  $LiNbO_3$ . In oxides, this observation can be understood based on the finding that tracks consist of amorphised cylindrical zones. As a consequence of the transition from the crystalline to the amorphous phase, each individual track undergoes a volume expansion finally leading to a macroscopic out-of-plane swelling.

For materials such as LiF and other alkali-halides, the situation is different because ionic crystals can not be amorphised. Up to now, the correlation between the type of defects and volume increase is still an open question. In any case, the swelling experiments clearly demonstrated that profilometry can be applied to probe the sensitivity of a wide variety of materials.

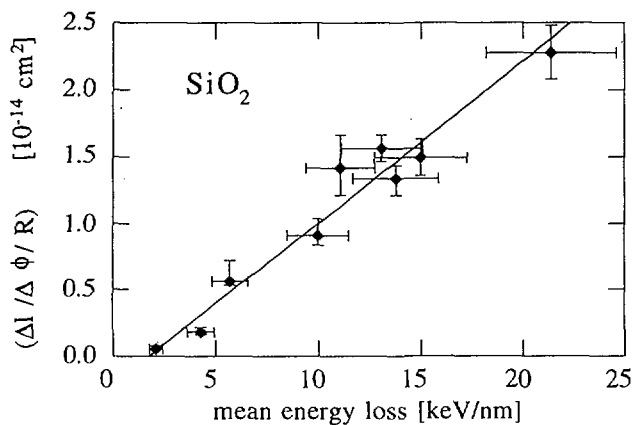


Fig. 3. The initial swelling  $(\Delta I/\Delta\phi)$  per ion normalised by the range  $R$  versus the mean energy loss in  $SiO_2$  quartz.

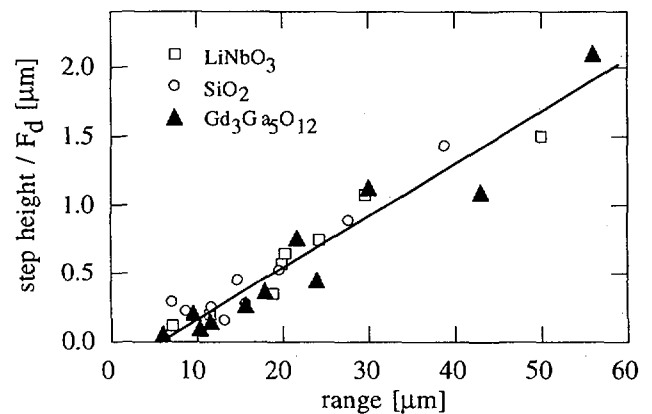


Fig. 4. Step height normalised by the damage fraction  $F_d$  as a function of the ion range for various oxides.

- [1] R. Brenier, B. Canut, S.M.M. Ramos and P. Thévenard, Nucl. Instr. and Meth. B 90 (1994) 339.
- [2] B. Canut, S.M.M. Ramos, R. Brenier, P. Thévenard, J.L. Loubet and M. Toulemonde, Nucl. Instr. and Meth. B 107 (1996) 194.
- [3] C. Trautmann, J.M. Costantini, A. Meftah, K. Schwartz, J.P. Stoquert, M. Toulemonde, to be published in *Atomistic Mechanisms in Beam Synthesis & Irradiation of Materials* (MRS Proceedings, Boston 1997).
- [4] M. Toulemonde, A. Meftah, J. M. Costantini, K. Schwartz, C. Trautmann, to be published in Nucl. Instr. and Meth. Phys. Res. B (1998).
- [5] A. Meftah, F. Brisard, J.M. Costantini, E. Dooryhee, M. Hage-Ali, M. Hervieu, J.P. Stoquert, F. Studer and M. Toulemonde, Phys. Rev. B 49 (1994) 12457.
- [6] A. Meftah et al., unpublished

## Damage morphology of ion irradiated lithium fluoride

C. Trautmann<sup>1</sup>, K. Schwartz<sup>1</sup>, T. Steckenreiter<sup>1</sup>, M. Toulemonde<sup>2</sup>

<sup>1</sup> GSI, Planckstr. 1, 64291 Darmstadt, Germany, <sup>2</sup> Ciril CEA/CNRS, BP 5133, 14070 Caen cedex 5, France

Single-crystals of lithium fluoride were irradiated with various ion species at the GANIL and at the GSI in the energy regime between 1 and 30 MeV/u. The induced radiation damage was studied with techniques such as optical absorption spectroscopy [1], small-angle x-ray scattering (SAXS) [1], chemical etching [2] and profilometry [3], complemented by annealing experiments [3]. Clear evidence is given for a complex track structure and defect morphology.

Fig. 1 shows the number of F- and F<sub>2</sub>-centers as a function of the fluence of Pb ions of 4 MeV/u. From the saturation curve, it can be deduced that such simple defects are produced mainly in a large halo of several tens of nanometers around the ion trajectory. The defect creation in this zone is similar to that under conventional radiation.

New phenomena occur for heavy ions above a critical energy loss of about 10 keV/nm. Within a very small core region of 2-4 nm in diameter, a new type of damage is produced generating a characteristic anisotropic SAXS pattern. Moreover, the tracks can be preferentially attacked by a chemical etchant, resulting in the formation of pyramidal-shaped etch pits (Fig. 2). Due to very similar annealing properties, it is concluded that the etchability and the anisotropic x-ray scattering are both based on the creation of complex defect aggregates possibly small colloids, fluorine clusters and vacancy clusters. Their formation is only slightly influenced by the irradiation temperature and takes place even at 15 K where diffusion processes of primary defects are frozen [4].

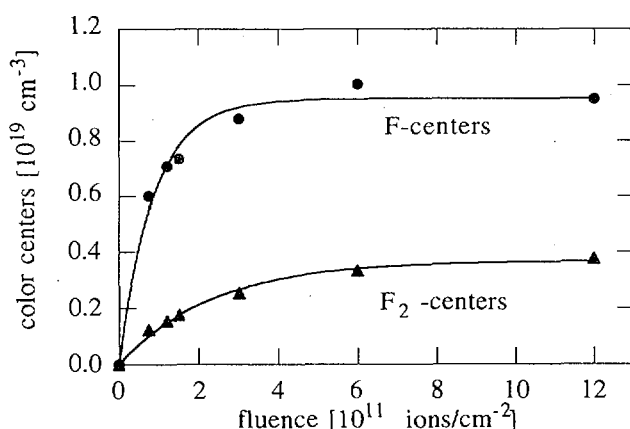


Fig. 1. The concentration of F- and of F<sub>2</sub>-centers as a function of the fluence of Pb ions (4 MeV/u).

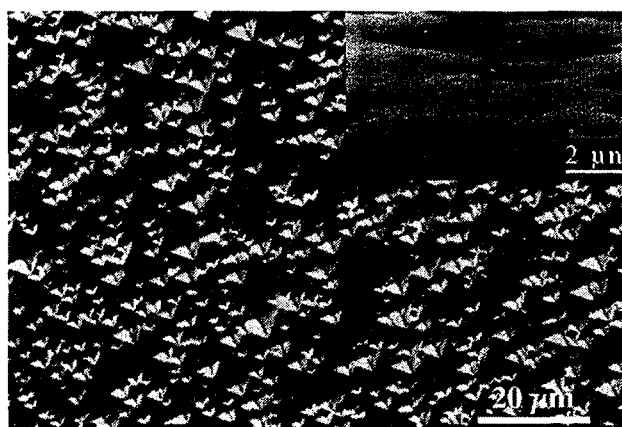


Fig. 2. Surface of an etched LiF crystal irradiated with  $10^7$  U-ions/cm<sup>2</sup> of 11.4 MeV/u. Each track is revealed by a pyramidal-shaped etch pit (inset).

- [1] K. Schwartz, C. Trautmann, T. Steckenreiter, O. Geiß, M. Krämer, accept. for public. in *Phys. Rev. B*.
- [2] C. Trautmann, K. Schwartz, O. Geiß, *J. Appl. Phys.* **83**, 3560 (1998).
- [3] C. Trautmann, K. Schwartz, J.M. Costantini, T. Steckenreiter, M. Toulemonde, to be published in *Nucl. Instr. and Meth. B* (1998).
- [4] K. Schwartz, G. Wirth, C. Trautmann, *Phys. Rev. B* **56** (1997) 10711.

## Structural and magnetic modifications induced by heavy ions irradiation in Fe-R-B amorphous alloys

G. Ravach<sup>a</sup>, A. Fnidiki<sup>a</sup>, J. Teillet<sup>a</sup> and M. Toulemonde<sup>b</sup>

<sup>a</sup> Groupe de Métallurgie Physique, Equipe Magnétisme et Applications, UNR 6634 CNRS  
Université de Rouen, F-76821 Mont Saint-Aignan cédex, France

<sup>b</sup> Laboratoire CIRIL, BP 5133, F-14070 Caen cédex 05, France

Owing to the topological disorder and the spin-orbit coupling, amorphous alloys with Transition Metal and Rare earth (R) elements can exhibit random magnetic anisotropy, which is of fundamental interest accounting for the variety of spin structures that may be reached. A previous Mössbauer study of melt-spun amorphous  $Fe_{80-x}R_xB_{20}$  ribbons ( $R = Ho, Dy, Nd$ ;  $x \leq 16$  at.%) evidenced for a strong modification of the Fe environments in the rare earth concentration range  $x^c \approx 8-9$  at.%, whatever the nature of the rare earth. Above  $x^c$ , the materials display random magnetic anisotropy, while below  $x^c$ , magnetic texture effects depending on the nature and the concentration of R are observed. The present work was undertaken with the aim to study the effect of swift ions irradiation on these properties. The modifications were investigated at room temperature by Mössbauer spectrometry and X-ray diffraction.

Amorphous  $Fe_{80-x}Dy_xB_{20}$  ribbons ( $x = 6, 10, 16$  at.%) were irradiated with Xe and Pb ions at fluences up to  $3 \times 10^{12}$  ions.cm<sup>-2</sup>. For all concentrations, we observe a rotation of the iron hyperfine fields towards the ribbons plane, whatever the initial magnetic texture is. This behaviour is probably related with the positive sign of the magnetostriction constant in the ribbons. In the lower fluences range, the rotation effect is enhanced for the lower rare earth concentrations, in agreement with the higher magnetostriction constant values. From the corresponding variation of the transformed fraction as a function of the fluence, a track radius of the order of 5 nm can be estimated.

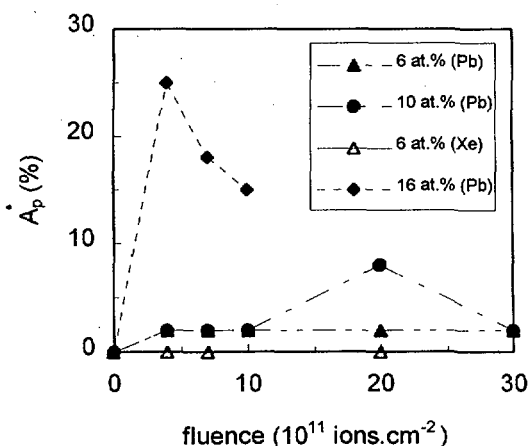


**Fig.1** : Mössbauer abundance of the paramagnetic phase in  $Fe_{80-x}Dy_xB_{20}$  ribbons irradiated with Pb and Xe ions.

We also observe the appearance of a paramagnetic component on irradiation. When the R concentration is increased, its formation occurs at lower fluences, and its fraction is enhanced (Fig.1). Its presence is also favoured in the case of Pb ions. From the Mössbauer and X-ray diffraction measurements, it would be attributed to R-enriched zones. At higher fluences, the paramagnetic phase tends to vanish, as seen for higher R concentrations (Fig.1).

This behaviour suggests a two-step transformation with first, irradiation-induced segregation phenomena in the amorphous state and second, a mixing that reduces the zones previously enriched in rare earth. Further structural investigation of this component is in progress.

# Ion irradiation effects on bcc-Fe/Tb multilayers

J. Juraszek<sup>a</sup>, A. Fnidiki<sup>a</sup>, J. Teillet<sup>a</sup>, F. Richomme<sup>a</sup> and M. Toulemonde<sup>b</sup>

<sup>a</sup>Groupe de Métallurgie Physique, équipe Magnétisme et Application  
UMR 6634 CNRS Université de Rouen,  
F-76821 Mont-Saint-Aignan cedex, France

<sup>b</sup>Laboratoire CIRIL BP5133 F-14070 Caen cedex 05, France

Fe/Tb multilayers are of great interest because of their promising application in magneto-optical recording media. The aim of this work was to study the influence of swift ion irradiation on the structural and magnetic properties of Fe/Tb multilayers in order to improve the perpendicular magnetic anisotropy needed for high-density data storage.

Fe/Tb multilayers with crystallized Fe layers were irradiated with Ar, Kr, Xe, Pb and U ions at various fluences[1]. Damaging processes, investigated by <sup>57</sup>Fe Mössbauer spectrometry at room temperature, give evidence for three thresholds, one for the damage formation ( $5 \text{ keV/nm} < T_0 < 15 \text{ keV/nm}$ ), one for Fe-Tb mixing threshold ( $T_1 \sim 25 \text{ keV/nm}$ ) and one relative to the creation of defects in the bcc-Fe layers ( $T_2 \sim 45 \text{ keV/nm}$ ). If the electronic stopping power  $(dE/dx)_e$  value of the ions is higher than  $T_0$  but less than  $T_1$ , only a demixing of Fe and Tb atoms occurs at the interfaces, producing both a thickening of the pure bcc-Fe layer and a sharpening of the interfaces whatever the ion fluence is. Between  $T_1$  and  $T_2$ , the Fe-Tb demixing is still observed at the lowest fluences, but then the mixing of Fe and Tb layers destroys progressively the layered structure. At high-ion fluences, the samples exhibit the magnetic properties of the corresponding amorphous Fe-Tb alloys. When the energy deposited by the ions exceeds the  $T_2$  value, a third phenomenon appears in addition to the two previous ones: the initial bcc Fe layers are transformed into "pure" disordered Fe layers.

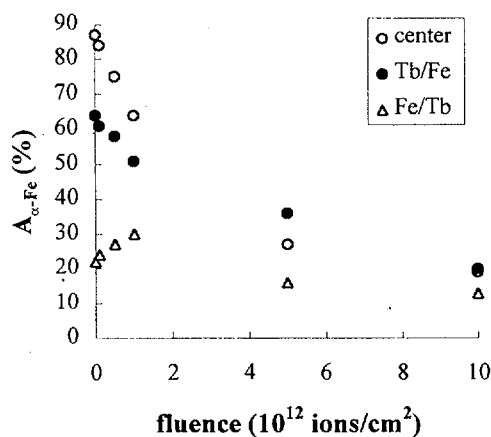


Fig.1: Relative fraction of Fe atoms which are in the  $\alpha$ -phase compared to all Fe atoms for  $(\text{Fe } 3.8\text{nm} / \text{Tb } 1.9\text{nm})_{20}$  multilayer irradiated with 811 MeV U ions.

In order to study more precisely the previous phenomena, probe multilayers have been made by depositing 0.5 nm of pure <sup>57</sup>Fe selectively either at the sharp Tb/Fe interface, or at the diffuse Fe/Tb interface, or in the center of Fe layers [2].

Investigations on Sn and U-ion irradiated probe multilayers by <sup>57</sup>Fe Mössbauer Spectrometry show that the demixing effect is localized exclusively at the diffuse Fe/Tb interface. At the flat Tb/Fe interface, only the mixing is observed (see figure 1).

[1] J. Teillet, F. Richomme, A. Fnidiki and M. Toulemonde, Phys. Rev. B 55 (1997) 11560.

[2] J. Juraszek, A. Fnidiki, J. Teillet, F. Richomme and M. Toulemonde, Solid State Commun. 106 (1998) 83.

## SWIFT HEAVY ION EFFECTS IN POLYMERS

N. BETZ, A. LE BOUEDEC, S. ESNOUF, C. AYMES-CHODUR, S. DAPOZ, E. PETERSOHN, D. SCHLOBER, A. LE MOEL

CEA/Saclay, DSM/DRECAM/SRSIM, 91191 Gif-sur-Yvette Cedex, France

Since 1986, our team in Saclay is interested in radiation effects in polymers. The pioneer work on the swift heavy ion (SHI) effects in polymers was performed in collaboration with the CIRIL, Caen, France. These former studies focused mainly on the polymer surface evolution under ionising radiation. Since then, our interest grew in the field of chemical modifications induced by SHI in the bulk of the polymer. Modification of polymer properties was also investigated<sup>1,2</sup>.

When a polymer is irradiated with ionising radiations such as electrons or  $\gamma$ -rays, modifications occurs which consists in crosslinking, unsaturations (isolated and conjugated), chain scissions, gas evolution, amorphisation and radical formation. These latter can have different life-times. The transient species can be observed at low temperature while the stable ones exist at room temperature and can be detected several days or months later. Among such radicals, those created in poly(vinylidene fluoride) (PVDF) are especially stable and have life-time of several years even if samples are kept at room temperature. Very few publications deal with radicals induced in polymers by SHI, and none of them offers a clear characterisation of the species observed, though these species are necessarily involved in the formation of the other defects. The knowledge of radicals is crucial for the understanding of the formation mechanism of the other defects. In addition, radicals confer to the polymer a chemical reactivity responsible for post-irradiation processes and allowing grafting of monomers.

### 1) The study of radicals by electron spin resonance (ESR)

In earlier studies<sup>3</sup>, it was found that some defects such as alkynes groups are created only when polymers are irradiated with high electronic stopping power  $((dE/dx)_e)$  radiations such as SHI are. Similarly, it was found that in PVDF and in addition to the usual alkyl and peroxy radicals, radicals specific of the SHI/PVDF interaction exist<sup>4</sup>. This latter radical shows an isotropic ESR signal and no hyperfine structure is resolved. The gyromagnetic factor is close to that of the free electron. Its shape is close to a Lorentzian and its line-width is about 0.5 mT. The intensity of the ESR signal which measures the electronic contribution of the magnetic susceptibility follows a Curie law which indicates that these centres are isolated and allows the concentration of the paramagnetic species to be determined. The absence of hyperfine structure indicates that the radical is localised in a highly crosslinked carbon structure. Indeed the radical resembles those formed in pyrolysed polymers. Therefore this radical is attributed to a dangling bond localised in a carbon cluster as observed in amorphous carbon. It can be observed at very low absorbed doses when the polymer is not carbonised. Crosslinking occurs in PVDF. Our solubility results show that the presence of an insoluble fraction correlates with the observation of the dangling bond<sup>5</sup>. Irradiations with various ions ranging from O to Sn from the medium energy line facility in order to study the effect of  $(dE/dx)_e$  on the formation of the dangling bond have been performed. Analysis of the results is in progress. Though the dangling bond is now spectroscopically well characterised, some questions still remain : Could it be formed in other polymers than PVDF ? What is its formation mechanism, direct creation in the track core or is there an effect of the overlapping of tracks ? Is the formation of such centres an indication of pyrolytic effects in the swift heavy ion - polymer interaction ?

## 2) Radiation grafting

Once radicals are generated in the polymer bulk, grafting of monomers able to polymerise is possible. The grafting of polystyrene (PS) occurs in the latent tracks and the anisotropy of the SHI/polymer interaction is maintained<sup>6</sup>. When the grafting yield increases, the surface is progressively covered until a homogeneous layer is obtained. Analysis of the macromolecular weight distribution of the grafted chains was performed<sup>7</sup>. Parameters such as the absorbed dose, the  $(dE/dx)_e$ , the grafting time and the monomer concentration are varied. Very long PS chains (number average molecular weight of 1600000) are formed in the very beginning of grafting (30 min). At very high doses, interpretation of results are complicated by the presence of crosslinking: Only the soluble fraction can be analyzed by steric exclusion chromatography while it is observed that PS is embedded in the insoluble fraction and thus not analysed. The surface structure of the grafted polymer, analysed using X-ray photoelectron spectroscopy, was also studied as a function of  $(dE/dx)_e$ <sup>8</sup>. Several ions were used (O, Ar, Kr, Sn from the medium energy line facility) covering the  $(dE/dx)_e$ -range of 2 to 60 MeV.cm<sup>2</sup>.mg<sup>-1</sup>. Radiation grafting was also performed using 8 MeV electrons in order to compare the different surface structures obtained. The grafting yields used for this study are in all cases small so that the surface is only partially covered. When irradiation conditions are such that a single latent track regime is obtained, the heterogeneity of grafting is large. When overlapping of latent tracks occurs, the homogeneity of the grafted domains becomes comparable to that of the electron grafting. When  $(dE/dx)_e$  increases, the quantity of grafted PS per ion track increases. As the number of radicals per ion track increases when  $(dE/dx)_e$  increases, the length of the grafted chains should become smaller as  $(dE/dx)_e$  grows. This is what was observed in our preliminary experiments<sup>7</sup>.

The structure of SHI PS grafted films is beginning to be well understood. Now, modifying the polymer substrate or changing the PS monomer which terminates by recombination for a monomer terminating by disproportionation can lead to other structures. These studies have been initiated. Another interesting point is to understand the grafting mechanism by identifying the nature of the initiating radicals and the nature of the chemical bond existing between the polymer substrate and the grafted chain. This work is in progress.

---

<sup>1</sup> D. Schoßer, A. Le Moël, "The effect of different energy losses  $(dE/dx)_e$  on the swift heavy ion induced modifications of the Curie transition in fluorinated ferroelectric polymers", *Nuclear Instruments and Methods in Physics Research* **1 0 7** (1996) 313.

<sup>2</sup> E. Petersohn, N. Betz, A. Le Moël, "Modification of dielectric relaxations in ferroelectric polymers induced by swift heavy ion grafting", *Nuclear Instruments and Methods in Physics Research* **1 0 7** (1996) 368.

<sup>3</sup> N. Betz, A. Le Moël, E. Balanzat, J. M. Ramillon, J. Lamotte, J. P. Gallas, J. Jaskierowicz, "A FTIR study of PVDF irradiated by means of swift heavy ions" *J. Polym. Sci.-Polym. Phys.* **B 3 2** (1994) 1493.

<sup>4</sup> N. Betz, E. Petersohn, A. L. Moël, "Free radicals in swift heavy ion irradiated fluoropolymers: an electron spin resonance study", *Radiation Physics and Chemistry* **4 7** (1995) 411.

<sup>5</sup> N. Betz, E. Petersohn, A. L. Moël, "Swift heavy ions effects in fluoropolymers: radicals and crosslinking", *Nuclear Instruments and Methods in Physics Research* **1 1 6** (1996) 207.

<sup>6</sup> G. Gebel, E. Ottomani, J.-J. Allegraud, N. Betz, A. Le Moël, "Structural study of polystyrene grafted in irradiated polyvinylidene fluoride thin films", *Nuclear Instruments and Methods in Physics Research* **1 0 5** (1995) 145.

<sup>7</sup> C. Ducouret, N. Betz, A. Le Moël, "Study of the molecular weight distribution of polystyrene grafted by means of swift heavy ions", *Journal de Chimie Physique* **9 3** (1996) 70.

<sup>8</sup> N. Betz, S. Dapoz, M.-J. Guittet, "Heterogeneity of swift heavy ion grafting: An XPS study", *Nuclear Instruments and Methods in Physics Research* **1 3 1** (1997) 252.



## Cross-linking induced by high density of ionisation in polystyrene.

S. Bouffard\*, C. Leroy\*, E. Balanzat\* and J.P. Busnel\*

\* CIRIL (CEA-CNRS), BP 5133, 14070 Caen cedex 5, France

\* Université du Maine, Laboratoire de Physico-Chimie Macromoléculaire, 72017 Le Mans, France

The high density of ionisation produced in the wake of a high-energy ion is responsible in polymers for a significant increase of the chain scission associated with unsaturated end groups and for the creation of alkyne and allene end groups which are never produced during irradiation with low ionising particles [1,2]. Under these conditions, the creation of new bonds between adjacent chains has been less studied. The difficulty comes from that the cross-links are not induced randomly as under electron or gamma irradiation: the probability to produce several events close to each other is high. Thus under swift heavy ion irradiation, the production of large molecular masses directly in the path of a single ion is favoured [3]. The figure 1 presents the results obtained by steric exclusion chromatography for the cross-linking of polystyrene under Carbon

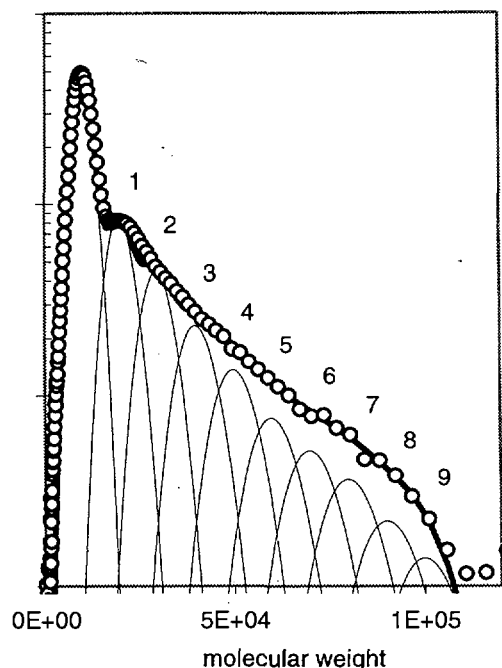


Figure 1: Molecular weight distribution of polystyrene irradiated with  $^{13}\text{C}$  at a dose of 0.5 MGy. The numbers indicate the number of cross-links.

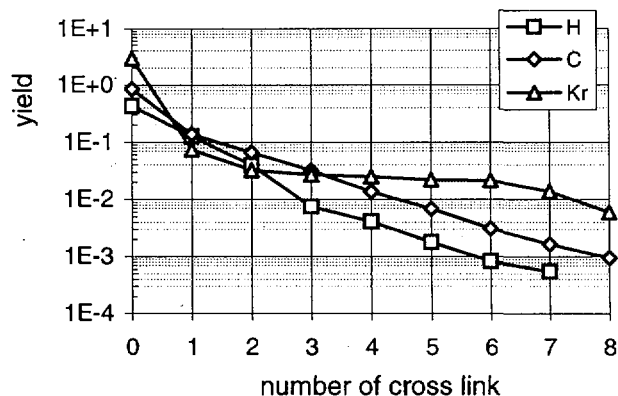


Figure 2: partial yields ( $100 \text{ eV}^{-1}$ ) for cross-link in polystyrene irradiated with 2.5 MeV  $^1\text{H}$ , 118 MeV  $^{13}\text{C}$  and 756 MeV  $^{84}\text{Kr}$  (0 corresponds to the destruction yield).

irradiation. From the evolution of these molecular weight distributions, we can extract the yield to produce  $n$  cross-links per chain (figure 2). The efficiency to the production of large macromolecule increases with the LET. Moreover, the destruction yield of the initial macromolecules increases also with the LET of the ion from 0.4 for Proton to 3 for Krypton.

### References

1. E. Balanzat, N. Betz and S. Bouffard, Nucl.Instr.and Meth. B 105 (1995) 46.
2. N. Betz, A. Le Moel, E. Balanzat, J.M. Ramillon, J. Lamotte, J.P. Gallas and G. Jaskierowicz, J.Polym.Sci., Polym.Phys. B 32 (1994) 1493.
3. S. Bouffard, E. Balanzat, C. Leroy, J.P. Busnel and G. Guevelou, Nucl.Instr.and Meth. B131 (1997) 79.

## Ion induced alkyne formation in polymers

T. Steckenreiter<sup>1</sup>, E. Balanzat<sup>2</sup>, H. Fuess<sup>1</sup>, C. Trautmann<sup>3</sup>

<sup>1</sup> TU-Darmstadt, Petersenstr. 23, 64287 Darmstadt, Germany, <sup>2</sup> Ciril CEA/CNRS, BP 5133, 14070 Caen cedex 5, France, <sup>3</sup> GSI, Planckstr. 1, 64291 Darmstadt, Germany

Although tracks of energetic ions in polymers have been studied for many years, the characterisation of the defects in the ion track is far from being complete. In order to investigate the chemical modifications, a detailed study was performed by Fourier-transform infrared spectroscopy (FTIR). Various commercial polymer films of different aliphatic and aromatic moiety (12  $\mu\text{m}$  polyimide (PI), 16  $\mu\text{m}$  polycarbonate (PC), 12  $\mu\text{m}$  polyethyleneterephthalate (PET), and 24  $\mu\text{m}$  polysulphone (PSU)) were irradiated under vacuum and in oxygen atmosphere with Kr ions (8.6 MeV/u) at the SME beamline of the GANIL. During beam stops, the irradiated samples were transferred from the irradiation chamber to the infrared spectrometer without exposing them to air. The degradation products were found to be very similar to those under classical irradiation, e.g., alkenes, carboxylic acids, alcohols, and  $\text{CO}_2$  [1]. As a unique process induced by the energetic ions, the formation of alkynes was observed. New absorption bands appeared which can be assigned to the characteristic C–H stretching mode of the alkyne end group ( $-\text{C}\equiv\text{C}-\text{H}$ ) at  $3300\text{ cm}^{-1}$  and the  $\text{C}\equiv\text{C}$  stretching vibration at  $2100\text{ cm}^{-1}$ , respectively [2] (Fig. 1). Both peaks increase as a function of the ion fluence. At very high doses, the absorption of these bands saturated due to overlapping of the tracks of single ions (Fig. 2). From this evolution, the track radius at which the created alkyne zones start to overlap was determined to be about 3 nm.

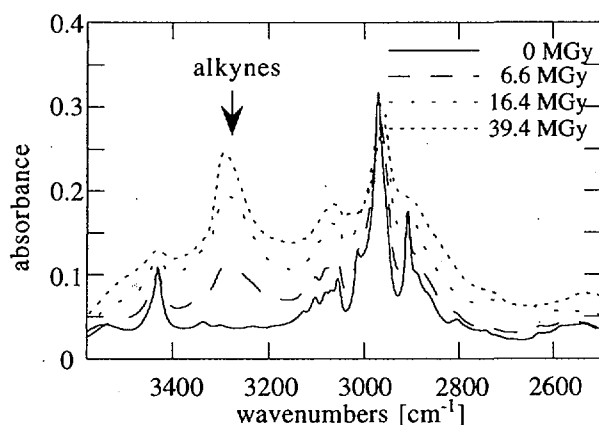


Fig. 1. FTIR spectra of PET irradiated with Kr ions (8.6 MeV/u) at various doses.

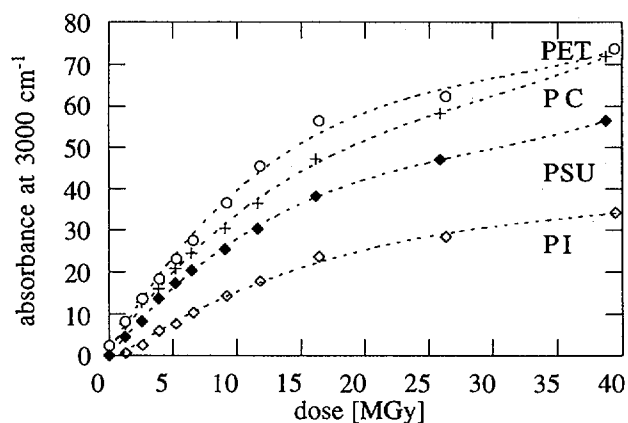


Fig. 2. Absorption of the  $3300\text{ cm}^{-1}$  band typical for alkyne groups as a function of the ion dose for various polymers.

Complementary experiments by mass spectroscopy showed that during irradiation one of the main outgassing product is acetylene. The production of alkynes and acetylene occurs in aromatic as well as in aliphatic [3] polymers and seems to play a crucial role during the track formation. Since the creation of triple bonds requires a remarkable reorganisation of molecular bonds, it is assumed that the process is strongly related to multiple excitation and ionisation events on an extremely short space and time scale. Another interesting aspect is the similarity of the radiation products to those found in pyrolytic processes. Moreover, it is known from the cracking process that above  $1230^\circ\text{C}$  acetylene exhibits the highest stability compared to other hydrocarbons indicating that during track formation possibly high temperatures are involved.

[1] T. Steckenreiter, E. Balanzat, H. Fuess, C. Trautmann, Nucl. Instr. and Meth. B 131 (1997) 159.

[2] N.B. Colthup, L.H. Daly, S.E. Wiberley, in: Infrared & Raman Spectroscopy, (Academic Press 1990) 313.

[3] E. Balanzat, N. Betz and S. Bouffard, Nucl. Instr. and Meth. B 105 (1995) 46.

« Polymer-like » amorphous deuterated carbon films irradiated by swift heavy ions :  
damage and hydrogen pumping.

F. Pawlak<sup>°</sup>, Ch. Dufour<sup>+</sup>, A. Laurent<sup>\*</sup>, E. Paumier<sup>°+</sup>, J. Perrière<sup>\*</sup>, J. P. Stoquet<sup>#</sup> and M. Toulemonde

<sup>°</sup>CIRIL, CEA-CNRS, B.P. 5133, 14070 Caen-cédex 05 (F)

<sup>+</sup>LERMAT, ISMRa, B<sup>d</sup> Maréchal Juin, 14050 Caen-cédex (F)

<sup>\*</sup>GPS Universités Paris VII et VI, Tour 23, 2 Place Jussieu, 75251 Paris-cédex 05 (F)

<sup>#</sup>Laboratoire Phase, CNRS, 23 rue du Loess, 67037 Strasbourg cédex 02 (F)

Mixed hydrogenated and deuterated « polymer-like » amorphous carbon films have been irradiated in the MeV/amu energy range with electronic stopping power varying between  $1 \text{ keV nm}^{-1}$  and  $13 \text{ keV nm}^{-1}$  [1]. These films contains 15% of hydrogen and 50% of deuterium as compared to the number of carbon atoms. Carbon (C), hydrogen (H) and deuterium (D) contents were determined by Rutherford Backscattering spectrometry (RBS) and Elastic Recoil Detection Analysis (ERDA). The figure 1 gives the evolution of the ratio (D/C) and (H/C) versus the fluence.

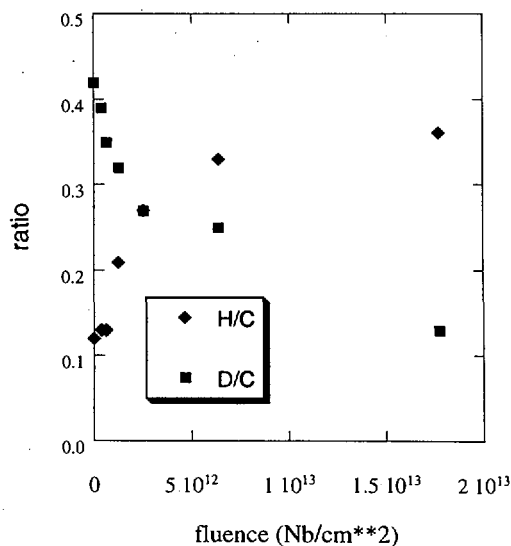
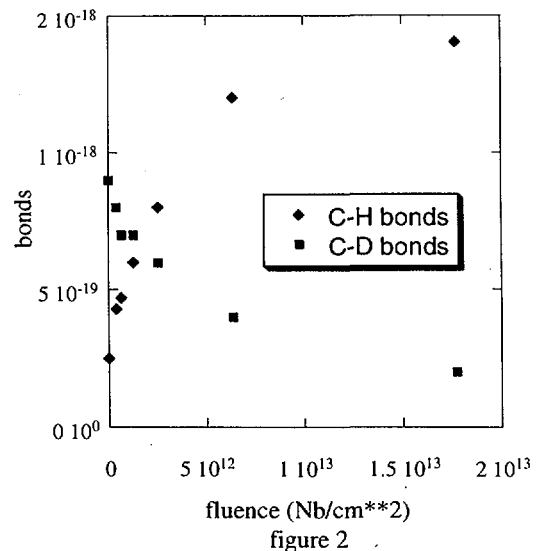


Figure 1

The main effect is the decrease of the deuterium content as compared to the number of carbon atoms versus the fluence. The second observation is the increase of the hydrogen content versus the fluence. Assuming an exponential law to fit the data [1], one can extract a deuterium effusion cross section and an hydrogen absorption cross section which are equal within the experimental errors.



The evolution of C-D and C-H bonds (figure 2) was determined by infrared absorption measurements. As previously observed, the main effect is also the decrease of the C-D bonds and the increase of the C-H bonds. Such an

increase appears only after one month and is stabilised only after five months. Cross sections of C-D bonds breaking and C-H bonds building can be also extracted using an exponential law and they are also equal within the experimental errors.

Moreover the cross sections extracted by the two physical characterisations (ion beam analysis and infra-red absorption) are equal leading to a latent track radius determination which is independent of the physical characterisations. The evolution of the latent tracks radius versus the electronic stopping power is presented in figure 3.

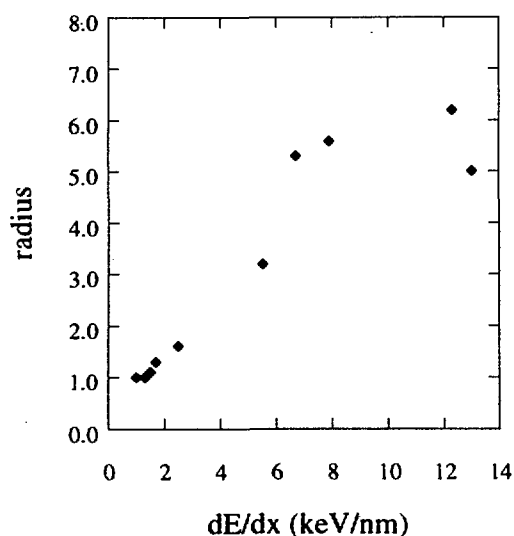


Figure 3

Hence the following interpretation is proposed: during irradiation hydrogen and deuterium atoms are ejected from the latent tracks and afterwards are replaced by hydrogen coming from ambient air and diffuse inside the irradiated material along the latent tracks.

The temperature of bond breaking by irradiation in polymers was determined

by Lewis and Lee [2]. Assuming this temperature for the « polymer-like » amorphous carbon the thermal spike model applied in the electronic stopping power ( $dE/dx$ ) regime is able to predict the evolution of the latent track radii versus  $dE/dx$  [3].

References :

- [1] F. Pawlak , Ch. Dufour, A. Laurent, E. Paumier, J. Perrière, J. P. Stoquert and M. Toulemonde, Nucl. Instr. Meth. B131(1997)135
- [2] M. B. Lewis and E.H. Lee, J. Nucl. Mat. 203(1993)224
- [3] M. Toulemonde, Ch. Dufour, E. Paumier and F. Pawlak to be published in At. Mech. in Beam Synth. and Irrad. Matls MRS proceedings (Boston 1997)

**NEXT PAGE(S)  
left BLANK**

### **3 - RADIATION CHEMISTRY AND RADIOBIOLOGY**

## DIRECT TIME-RESOLVED MEASUREMENT OF RADICAL SPECIES FORMED IN WATER BY HEAVY IONS IRRADIATION

G. BALDACCHINO<sup>\*</sup>, S. BOUFFARD<sup>\*\*</sup>, E. BALANZAT<sup>\*\*</sup>, M. GARDES-ALBERT<sup>\*\*\*</sup>, Z. ABEDINZADEH<sup>\*\*\*</sup>,  
D. JORE<sup>\*\*\*</sup>, S. DEYCARD<sup>\*\*\*\*</sup> and B. HICKEL<sup>\*</sup>

<sup>\*</sup> CEA/Saclay DSM/DRECAM/SCM URA 331 CNRS, 91191 Gif/Yvette cedex

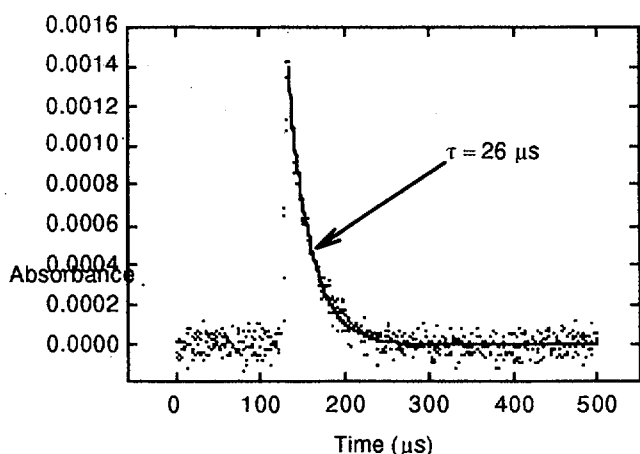
<sup>\*\*</sup> CIRIL (CEA-CNRS) rue Cl. Bloch, BP 5133, 14040 Caen cedex

<sup>\*\*\*</sup> Laboratoire de Chimie-Physique, URA 400, 45, rue des Saints Pères,  
75270 Paris cedex 06

<sup>\*\*\*\*</sup> Faculté de Pharmacie, 1, rue Vaubenard, 14000 Caen, France

Time-resolved absorption spectroscopy has been used to detect radical species in liquid water irradiated by swift heavy ions. These experiments have been performed at the GANIL cyclotron (Caen-France) with  $^{12}\text{C}^{6+}$  (75 MeV/A),  $^{36}\text{S}^{16+}$  (77 MeV/A) and  $^{40}\text{Ar}^{18+}$  (70 MeV/A) particles whose the Linear Energy Transfer ( $\text{LET} = -(dE/dx)_{\text{elec}}$ ) is respectively two and three orders of magnitude greater than electron or gamma rays. The chemistry in water is thus considerably modified at the first moments after the ionisation. In particular the radiolytic yields of the radicals like hydrated electron decrease when the LET is increasing. The temporal structure of the beam is used to perform time-resolved spectroscopy of the transient radicals formed by water radiolysis within the microsecond time scale. It is possible to show the inhomogeneous chemistry around the ion tracks and to compare these results with the Monte Carlo simulations.

**Keywords :** LET, heavy ions, pulse radiolysis, water radiolysis, superoxide anion, hydrated electron



This figure presents the absorbance of hydrated electron generated by 5  $\mu\text{s}$  pulses of  $\text{C}^{6+}$  of 75 MeV/A of energy in pure deaerated liquid water. This curve is obtained by averaging 1000 signals.

### References :

- [1] *J. Chim. Phys.* (1997) **94**, 200-204.
- [2] *Radiat. Res.* (1998) **149**, 128-133.

# RADIATION YIELDS OF THE FREE RADICALS FORMED BY HEAVY IONS WATER RADIOLYSIS

M. Gardès-Albert<sup>1</sup>, D. Jore<sup>1</sup>, Z. Abedinzadeh<sup>1</sup>, A. Rouscilles<sup>1</sup>, S. Deycard<sup>2</sup>,  
S. Bouffard<sup>3</sup>, E. Balanzat<sup>3</sup>

<sup>1</sup>Laboratoire de Chimie-Physique, URA 400 CNRS, Université Paris V,  
45 Rue des Saints-Pères, 75270 Paris cedex 06

<sup>2</sup>Faculté de Pharmacie 14000 Caen

<sup>3</sup>CIRIL 14040 Caen cedex

The radiolysis of liquid water by heavy ions of high LET (Linear Energy Transfer expressed in keV/ $\mu\text{m}$ ) is characterised by the production of  $\text{O}_2^-$  ( $\text{HO}_2$ ) free radicals, even in the absence of dioxygen, whereas in the case of ionising radiations of low LET ( $^{60}\text{Co}$   $\gamma$ -rays), these free radicals are formed in too weak quantities to be measured. Moreover, the production of the other usual free radicals ( $\text{OH}$ ,  $\text{e}^-_{\text{aq}}$ ,  $\text{H}$ ) is considerably decreased, whereas the formation of the molecular products ( $\text{H}_2\text{O}_2$ ,  $\text{H}_2$ ) is enhanced because of the free radicals combination reactions which are favoured in the heavy ions tracks. The G-values (radiation yields expressed in mol. per Joule) of the free radicals depend not only of the LET but also, for a given LET, of the nature and of the rate of the ionising particles. In the literature, the majority of the G-values (see for example [1,2]) have been determined as a function of the *mean* LET (heavy ions being stopped in water). In our case, the experimental conditions of the GANIL allowed to measure the G-values as a function of a *really constant* LET (heavy ions cross the irradiation cell without losing energy).

Experimental data on the radiolytic yields are essential for understanding the mechanisms of formation of the free radical species. For a LET of 250 keV/ $\mu\text{m}$  ( $\text{Ar}^{18+}$ , 95 MeV/A, dose rate 10 Gy/s, doses from 0 to 1000 Gy), we have determined the G-values for  $\text{e}^-_{\text{aq}}$  and  $\text{O}_2^-$  in aqueous solutions containing tetranitromethane,  $\text{C}(\text{NO}_2)_4$ , this compound being known for its scavenging capacity of the reducing species generated by the radiolysis of water [3]. Another LET-value of 127 keV/ $\mu\text{m}$  ( $\text{Ne}^{10+}$ , 60.3 MeV/A) has recently been investigated and this latter experiment has been performed with a new analyzing device, the spectrophotometer being in line (CIRIL, Equipe de Radiolyse du SCM CEA Saclay). The G-values deduced from these experimental data are interpreted according to the usual LET effect and hypothetical mechanisms of formation of superoxide free radicals in heavy ions tracks. The radiobiological consequences of the selective production of  $\text{O}_2^-$  ( $\text{HO}_2$ ) free radicals are discussed.

## REFERENCES

- [1] J.A. Laverne and R. Schuler, J. Phys. Chem., 1987, 91, 6560-6563.
- [2] J.A. Laverne and R. Schuler, J. Phys. Chem., 1992, 96, 7376-7378.
- [3] M. Gardès-Albert, D. Jore, Z. Abedinzadeh, A. Rouscilles, S. Deycard, S. Bouffard, J. Chim. Phys., 1996, 93, 103-110.

## DNA damage induced in plasmid DNA by heavy ions and mutagenic consequences.

*Evelyne SAGE, Céline GIUSTRANTI, Cécile PEREZ, Solange ROUSSET,  
LRC-1 du CEA, CNRS UMR 218, Institut Curie - Section de Recherche  
26 rue d'Ulm, 75248 Paris Cedex 05*

*Emmanuel BALANZAT, CIRIL, CEA/CNRS, BP 5133, 14070 Caen Cedex 05*

Experiments numbers : P374, P397, P464.

The objective of the project is to study the genotoxic effect of high LET radiation in comparison to low LET  $\gamma$  radiation. The first step of the project has consisted in irradiating naked plasmid DNA with heavy ions, in solution or in dry state under vacuum or in the presence of air, exploring various LET. The induction of single and double strand breaks (SSB and DSB), as well as base damage, have been examined. These experiments aim at understanding the interaction of particles with genetic material, and to shed light in the mechanism of formation of DNA damage by ionizing radiation. In living cells, DNA lesions are either removed by various DNA repair pathways, or processed into genetic changes (mutations). The next steps of the project will consist in studying the repair of the irradiated plasmid using cell free extracts, and in monitoring the mutations produced in the irradiated plasmid DNA after introduction into mammalian cells.

pBS plasmid DNA (2961bp) has been irradiated in dry state with  $^{12}\text{C}$  (12.4MeV/a, LET 127 keV/ $\mu\text{m}$ ),  $^{36}\text{S}$  (10.1 & 3.5 MeV/a, LET 1010 & 1650 keV/ $\mu\text{m}$ ) and  $^{125}\text{Te}$  (2.63MeV/a, LET 7830 keV/ $\mu\text{m}$ ), and with  $\gamma$  rays from  $^{137}\text{Cs}$  source. We show that at high LET ( $> 1000$  keV/ $\mu\text{m}$ ), the induction of strand breaks reaches a plateau as detected by electrophoresis, whereas it is higher for irradiation with C ion at low TEL. The ratio of SSB to DSB is 3-4 for irradiation with S or Te, 6 for C. Furthermore, for C irradiation, an increase of strand breaks is observed in the presence of air as compared to irradiation under vacuum, whereas such an oxygen effect is barely detectable with S irradiation. All these observation may be explained by a greater extent of recombination of radicals in the track at high LET. It is also in favor of increasing complexity of damage with increasing LET. Indeed, using electron microscopy, we were able to detect fragments of DNA (a main population centered around 500bp) which could not be revealed by electrophoresis. According to our preliminary data, it seems that the magnitude of fragmentation is enhanced with dose and LET.

pBS plasmid DNA has also been irradiated in solution, at various concentrations, with  $^{36}\text{S}$  (76.2 & 66.6 MeV/a, LET 224 & 429 keV/ $\mu\text{m}$ ) and with  $\gamma$  rays. At similar doses, this last radiation produces more SSB than heavy ions, but the same amount of DSB. The ratio of SSB to DSB is 25 for  $\gamma$  rays and 8 for  $^{36}\text{S}$ . For both types of radiation the induction of SSB decreases with increasing concentration. Both radiations produce base damage (revealed by DNA repair enzymes) to the same extent as SSB. However, when DNA is irradiated in a dry state, base lesions are still present after  $\gamma$  rays, whereas they are not detectable after S irradiation.

All the data are in favor of a complexity of the damage produced by heavy ions.

SAGE E., ROUSSET S., PERDIZ D., MARTIN C. and BALANZAT E. Détection de lésions de l'ADN induites par les radiations ionisantes de faible et fort TEL. *J. Chimie Phys.*, **94**, 331-336 (1997).

**NEXT PAGE(S)  
left BLANK**



## **4 - PHYSICS AND CHEMISTRY WITH TRACKS**

## **SWIFT HEAVY ION RADIATION GRAFTING OF POLYMERS / OBTENTION OF HAEMOCOMPATIBLE SURFACES.**

C. AYMES-CHODUR<sup>1</sup>, S. DAPOZ<sup>1</sup>, N. BETZ<sup>1</sup>, A. Le MOËL<sup>1</sup>, M.-C. PORTE-DURRIEU<sup>1,2</sup>, C. BAQUEY<sup>2</sup>

(1) CEA/Saclay - DSM/DRECAM/SRSIM - 91191 Gif sur Yvette Cedex, FRANCE.

(2) INSERM U.443 - University Victor Segalen-Bordeaux 2, 146 rue Léo Saignat - 33076 Bordeaux Cedex, FRANCE.

Since 1980, numerous studies have been undertaken in the field of vascular prostheses, but no solution has been found to prevent the formation of a blood clot in small diameter ones (internal diameter < 5 mm). Numerous ways of those biomaterials surfaces treatment have been developed, one of which consists in producing « heparin-like » surfaces. This synthesis has been adjusted by Jozefonvicz et al. (1), whose protocol uses polystyrene (PS) chemically modified with the active groups of the heparin, a powerful blood anti-clotting substance. Unfortunately, PS does not exhibit the suitable mechanical properties for vascular implants and its ageing under blood stress is not good enough. This is why our group in Saclay has chosen a different approach based on radiation grafting using swift heavy ions. They are able to induce reactive sites in a polymer at very low doses, without modifying its chemical and mechanical properties. We adapted this synthesis to two fluoropolymer films, poly(vinylidene difluoride) (PVDF) and poly(vinylidene difluoride/hexafluoropropylene) (P(VDF/HFP)), styrene radiografted. P(VDF/HFP) has also been used as tubing (500 µm thick and 4 mm internal diameter) in order to get closer to the vascular prostheses design shape. These fluoropolymers have been chosen for their mechanical and chemical properties as well as for their ionising radiation resistance. The additional HFP group present in the PVDF copolymer, increases its plasticity and confers better mechanical properties on our application.

The synthesis includes three steps: the first step corresponds to the initiating radicals formation, necessary to the polystyrene grafting. In order to irradiate polymers foils, different ions from the Medium Energy Line facility (SME) of GANIL accelerator have been used under an oxygen atmosphere : <sup>50</sup>Sn (2.99 MeV/a), <sup>18</sup>Ar (5.63 MeV/a), <sup>36</sup>Kr (6.82 MeV/a), <sup>8</sup>O (10.05 MeV/a), <sup>36</sup>Ar (10.83 MeV/a) and <sup>18</sup>O (8.26 MeV/a). Stacks of 25 µm thickness foils are taped on an aluminium frame and scanned vertically in front of the beam in order to obtain 4x25 cm<sup>2</sup> irradiated surfaces.

The second step of the biomaterial synthesis corresponds to the styrene monomer grafting by the indirect method (2). The sample is immersed in a styrene filled test tube, which is subsequently desaturated under a nitrogen flow, sealed and then put in a 60°C thermostated bath for a given time in order to study the grafting kinetic. The grafted sample is afterwards extracted with a Soxhlet apparatus to get rid off the homopolymer formed.

The last step consists in three successive reactions that are the chlorosulfonation, the sulfonamidation and the hydrolysis and which allow to add groups as COOH and SO<sub>2</sub>NH to the radiografted styrene, necessary to confer the material « heparin-like » properties (3,4).

The High Energy Line facility is required to irradiate tubing because of their thickness. Irradiations were performed with <sup>36</sup>Ar (84.19 MeV/a) under an oxygen atmosphere. For the swift heavy ion irradiations, two systems have been built, one for a static tubing irradiation and the other, motor equipped, allowing the rotational movement of the tube

on its axis. In the first assembly, 4 tubes, 15 cm length, can be mounted on a frame scanned up and down perpendicularly to the ion beam; this system increases the irradiation capacity as the time necessary to get a dose of 100 kGy is relatively long and as the number of samples needed by the biological tests is very important. The second assembly has been built in order to get a more uniform tubing irradiation. The tubing are mounted on a rotating rod, fixed on the frame which scans vertically in front of the beam. As the irradiation time is much higher in this case than in the former system, only small quantities have been irradiated, the aim being the comparison of grafting yields for both systems. In the first case, the ions go through a thickness varying from 1 mm to 3.1 mm whereas in the second one, the beam is always radial to the tubing and goes through the same 500  $\mu$ m thickness.

The structure of the grafted tubing is presently in study. The functionalisation is feasible.

The biological tests are done in Bordeaux on the different steps of the films synthesis and show that the functionalisation increases the haemocompatibility properties of the material (5).

Testing of the functionalised tubing is a very important step of this research project firstly because the shape of the tubes itself which is closer to the application and secondly because some biological tests can only be done on tubing, such as those made under dynamic blood flow.

Recent tests have shown that such synthesised materials are not cytotoxic. These positive results are encouraging. The next step should be the study of P(VDF/HFP) as waved or knitted tubing.

#### Acknowledgements

The authors thank the regions Basse-Normandie and Aquitaine for supporting 3 grants CTCR « CEA/Région » ; the team from the CIRIL is acknowledged for its precious help during the irradiation at the GANIL.

#### References

- (1) Fougnot C., Jozefonvicz J., Samana M. et Bara L., *Ann. Biomed. Eng.*, 7, 429 (1979).
- (2) Betz N., Le Moël A., Duraud J.P., Balanzat E. et Damez C., *Macromol.* 25, 213 (1992).
- (3) Dapoz S., Betz N., Le Moël A., *J. Chim. Phys.* 93, 58 (1996).
- (4) Dapoz S., Betz N., Guittet M.-J., Le Moël A., *NIM B* 105, 120 (1995).
- (5) Porte-Durrieu M.-C., Aymes-Chodur C., Betz N., Brouillaud B., Rouais F., A. Le Moël et C. Baquey., *NIMB* 131, 364 (1997).

# Simulation des dommages de fission dans les matériaux envisagés pour la transmutation des actinides mineurs

Hj. Matzke<sup>(1)</sup>, M. Beauvy<sup>(2)</sup>, T. Wiss<sup>(1)</sup>

<sup>(1)</sup>European Commission, Joint Research Centre, Institute for Transuranium Elements, P.O. Box 2340, D-76125 Karlsruhe, Germany

<sup>(2)</sup>Commissariat à l'Energie Atomique, Direction des Réacteurs Nucléaires, Centre d'Etudes de Cadarache, F-13115 St Paul-lez-Durance Cedex, France

## 1- Cadre d'étude

Différents matériaux utilisables comme matrice inerte de dilution ont été présélectionnés pour la transmutation des actinides mineurs en réacteur sur la base des propriétés thermophysiques au moins comparables à celles de l'UO<sub>2</sub> (conductivité thermique, point de fusion, et propriétés mécaniques), et sur la base de la compatibilité chimique. Parmi les critères de sélection, l'endommagement sous irradiation constitue un aspect essentiel (modifications structurales et changements des propriétés thermophysiques) mais celui-ci demeure difficile à étudier expérimentalement. Afin de caractériser l'endommagement par les fissions en réacteur, certains de ces matériaux ont été irradiés au GANIL pour simuler les dommages dus aux produits de fission.

## 2- Irradiations

Deux séries de matériaux ont été irradiées aux ions lourds <sup>86</sup>Kr et <sup>106</sup>Cd afin de simuler les effets de l'irradiation des matrices inertes en réacteur. Les deux irradiations dénommées „Matinon“ ont été réalisées sous vide, à température ambiante, sur le banc IRASME de la Sortie Moyenne Energie du GANIL. Elles ont permis d'atteindre des fluences de 4.10<sup>13</sup> ions/cm<sup>2</sup> pour des énergies de projectiles comprises entre 1 et 10 MeV par nucléon.

Les échantillons sous forme de disques de 5 ou 9mm de diamètre et de 100µm à 3mm d'épaisseur ont été fabriqués et caractérisés dans nos laboratoires. Les caractéristiques de quelques échantillons irradiés sont présentées dans le tableau 1.

Tableau 1 - Caractéristiques des échantillons irradiés

Matériau	Fabrication			Epaisseur		Ion		Fluence, ions/cm <sup>2</sup>	
	CEA1	ITU	CEA2	lamé 100µm	>1mm	Kr	Cd	10 <sup>11</sup>	4.10 <sup>13</sup>
MgO	x		x	x	x	x	x	x	x
MgAl <sub>2</sub> O <sub>4</sub>	x	x	x	x	x				x
CePO <sub>4</sub>		x			x	x		x	x
ZrSiO <sub>4</sub>		x			x	x	x	x	x
CeO <sub>2</sub>	x	x	x	x	x	x	x	x	x
Y <sub>2</sub> O <sub>3</sub>	x		x	x	x	x	x	x	x
YAG	x		x	x	x	x	x	x	x

### **3 - Etudes des échantillons irradiés**

Les différents mécanismes produisant les dommages dans les matériaux lors de l'irradiation ionique (ionisation et cascade de déplacements) permettent de simuler tous les effets intervenant lors des irradiations en réacteur mais à différents niveaux : effets des produits de fission et de transmutation, effets des neutrons, et effets des rayonnements. Toutefois deux paramètres doivent être systématiquement quantifiés pour pouvoir exploiter correctement les résultats de la simulation : la fluence de l'irradiation et les dimensions des différentes zones irradiées des échantillons. Les fluences maximales de  $4 \cdot 10^{13}$  ions/cm<sup>2</sup> avec Cd atteignent dans Matinon produisent des effets équivalents à ceux obtenus lors d'une irradiation aux neutrons à environ  $10^{18}$  n/cm<sup>2</sup> lorsque l'on considère uniquement les cascades de déplacements. Comparativement aux conditions réelles envisagées pour la transmutation des actinides, ces fluences restent faibles et ne permettent d'étudier que le début de l'endommagement des cibles en réacteur. De plus les dimensions des zones endommagées par les ions sont très petites par rapport aux volumes atteints par les neutrons (généralement moins de 80µm pour l'ensemble et quelques µm pour la zone des cascades). Il reste que l'irradiation aux ions est une excellente simulation de l'irradiation par les produits de fission qui de loin produit le plus de dommages dans les matériaux.

Les échantillons irradiés ont été étudiés par microscopie optique et MEB. Beaucoup d'échantillons ont perdu leur intégrité après irradiation aux fluences élevées : fissures et clivage. Les plus dégradés sont CePO<sub>4</sub>, ZrSiO<sub>4</sub>, et YAG. Seuls les échantillons de MgO ont tous gardé leur intégrité. Le comportement différent observé pour des échantillons de MgAl<sub>2</sub>O<sub>4</sub> originaires de fabrications différentes montre l'importance de ce dernier paramètre sur les effets d'irradiation.

Les zones irradiées présentent une coloration étudiée par spectrophotométrie sur les lames minces. Toutefois le doute n'est pas encore levé sur l'origine de cette coloration : formation de centres F ou excitation des impuretés ?

Nous n'avons pas mesuré ni observé de gonflement pour les matériaux ayant conservé leur intégrité (profilométrie et MEB). Ces mesures n'ont toutefois pas été possibles pour les matériaux les plus dégradés.

L'étude par diffraction des rayons X a été effectuée parallèlement sur la face irradiée et sur la face non irradiée des disques échantillons. Celle-ci montre en particulier une légère variation du paramètre cristallin pour MgO et MgAl<sub>2</sub>O<sub>4</sub>, et une déformation des pics de diffraction correspondant aux plans riches en Al.

Concernant le phosphate de cérium, des propriétés thermiques médiocres ainsi que le piètre comportement sous irradiation par des ions lourds énergétiques a conduit à éliminer ce matériau des possibles candidats matrices inertes sans toutefois le rejeter en tant que matrice de stockage [1].

### **Perspectives**

Des irradiations à fluences plus élevées sont nécessaires pour analyser l'évolution des mécanismes de création de dommages pendant l'irradiation en réacteur, et valider cette simulation par rapport aux irradiations expérimentales dans le réacteur Phénix. Des irradiations à température élevée seraient également utiles pour évaluer la recombinaison des défauts d'irradiation.

### **Références**

- [1] K. Bakker, H. Hein, R.J.M. Konings, R.R. van der Laan, H.J. Matzke and P. van Vlaanderen, J. Nucl. Mater., 252 (1998) 228.

**A comparative study of the irradiation effects in high resistivity silicon used in the semiconductor detectors manufacturing.**

P. Mangiagalli, M. Levalois and P. Marie.

LERMAT-ISMRA 6, Boulevard Maréchal Juin, 14050 CAEN-cedex, FRANCE.

As part of the collaboration between the LERMAT Laboratory and the ISTITUTO NAZIONALE di FISICA NUCLEARE (sezione di Milano), preliminary studies of high fluences radiation damage in very high resistivity bulk silicon have been carried out with the intention of understanding the defect formation process. This is very useful to explain the behaviour of detectors, manufactured from this material, which will be used in new generation accelerators (LHC,SSC).

Systematic irradiations of high resistivity silicon and detectors, with heavy ions from GANIL, swift neutrons and energetic electrons allow us to point out very important modifications in the material properties after high dose irradiation. Hall effect measurements carried out on irradiated substrate show that, above a critical fluence which depends on the incident particle, silicon stabilizes in a *near intrinsic* state, whose properties are independent on the incident particle. This state is due to the material compensation by high concentration of radiation induced deep centers. These centers have been identified by Deep Level Transient Spectroscopy and Photoluminescence measurements: they are vacancy-related complex defects (vacancy-oxygen, vacancy-phosphorus, divacancy,...). By fitting the experimental Hall measurements, we have estimated the concentrations of the various defects created by the irradiations.

The substrate modifications induce an alteration of the irradiated electronic devices properties. The I(V) and C(V) characteristics show that at low fluences the saturation value of the leak current of the detectors increases linearly with the fluence. On the other hand, above a threshold fluence, the detector characteristics are deeply altered and it is no more possible to consider the device as an abrupt junction.

The comparison of the results obtained with the different types of particles show that the inelastic energy loss cannot explain the observed differences, which cannot either be taken into account with the total elastic displacement cross-section. Indeed, crucial parameters are also the spatial distribution of defects and the mean nuclear energy deposited into the cascades.

P. MANGIAGALLI, Thèse de l'Université de CAEN, Juillet 1997.

P.MANGIAGALLI, M.LEVALOIS, P.MARIE, P.G.RANCOITA and M.RATTAGGI,

Nucl. Phys. B 61 (Proc. Suppl.) (1998) 464.

P.MANGIAGALLI, M. LEVALOIS and P. MARIE,

IV<sup>th</sup> International Symposium on Swift Heavy Ions in Matter (SHIM 98), Berlin, May 1998, to be published in Nucl. Instr. and Meth. B.

## Vortex pinning by columnar defects in high- $T_c$ superconductors

V. Hardy<sup>1</sup>, S. Hébert<sup>1</sup>, F. Warmont<sup>1</sup>, Ch. Simon<sup>1</sup>, J. Provost<sup>1</sup>, M. Hervieu<sup>1</sup>, G. Villard<sup>1</sup>, P. Lejay<sup>2</sup>. (P385, P424)

(1) CRISMAT (UMR 6508), ISMRA, Bd M<sup>st</sup>Juin, 14050 Caen.

(2) CRTBT, 25 Av. des Martyrs, BP 166, 38042 Grenoble.

Irradiation of superconducting cuprates by swift heavy ions, e.g. 6 GeV-Pb ions, can lead to the creation of columnar defects (CDs) consisting of continuous, amorphous latent tracks with a core diameter of order 100 Å. These CDs can act as very efficient pinning centers for the vortices, and yield huge improvements of transport properties.

During the period 1996-1997, we carried on the study of various pinning parameters by magnetic measurements, and we began to perform transport measurements. We essentially used single crystals of two compounds: Bi<sub>2</sub>Sr<sub>2</sub>CaCu<sub>2</sub>O<sub>8</sub> (Bi-2212) which has a very large electronic anisotropy between the c axis and the ab planes, and the much less anisotropic YBa<sub>2</sub>Cu<sub>3</sub>O<sub>7</sub> (YBCO). These crystals have a plate-like shape, with the shortest dimension along the c axis.

The electrical resistance has been studied in a Bi-2212 crystal irradiated at  $\theta_i = +45^\circ$ , as a function of the angle  $\theta$  between the field and c [1]. We observed a pronounced dip in the  $R(\theta)$  curves at  $\theta = +\theta_i$  (and not for  $\theta = -\theta_i$ ), demonstrating that, even for a very anisotropic compound in the reversible regime, the presence of CDs is able to induce a vortex line behavior. The magnetic studies were carried out with  $H//c$ . The persistent current densities  $J$  were derived from hysteresis loops. CDs of different mean radius  $R$  have been introduced along c in Bi-2212 crystals, by using various experimental conditions (e.g.  $R \approx 45$  Å for 6 GeV Pb ions, whereas  $R \approx 65$  Å for 0.9 GeV Pb ions). It was found that the  $J$  values increase with  $R$  in the whole range of field and temperature [2]. This demonstrates that the theoretically expected increase of the pinning energy with  $R$  directly affects a macroscopic quantity like  $J$ . Another way to vary the effective defect size in the ab planes consists in tilting the ion beam with respect to c. Fig. 1 illustrates the occurrence of a regime where the pinning efficiency (still with  $H//c$ ) is larger for highly angled tracks ( $\theta_i = 75^\circ$ ) than for tracks parallel to c [3]. A further pinning improvement related to entanglement effects can be induced by a dispersion in track directions (splay). The occurrence of such a splay effect in very anisotropic is still very controversial. Various configurations of tracks have been compared in Bi-2212 and did not provide any evidence for a splay effect [4]. This could be due to the low vortex cutting barriers associated to high anisotropy. In YBCO, for which the existence of splay effects is well established, we have studied the influence of various parameters: value of  $\theta_i$  in bimodal distribution  $\pm \theta_i$  around c; number of directions at a fixed  $\theta_i$  value; cone-like distributions etc... Several results have been obtained, allowing for a better knowledge of the active processes in a splay. For instance, it was found that the number of track directions (2, 3 or  $\infty$ ) at a fixed  $\theta_i$  value ( $10^\circ$ ) has no effect on the pinning efficiency (Fig. 2).

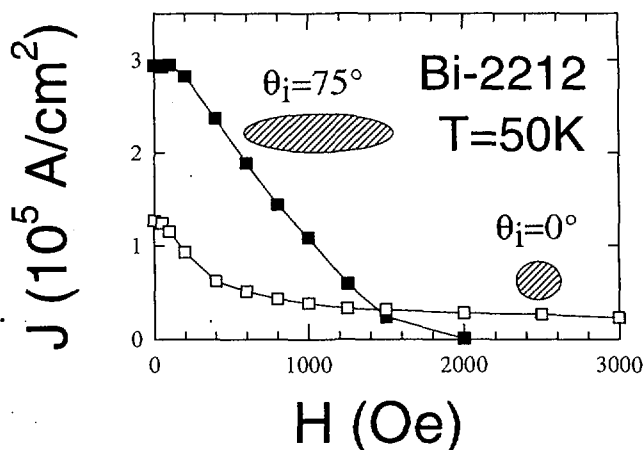


Fig. 1 : Persistent current density vs magnetic field (applied along c), in crystals irradiated by  $5 \cdot 10^{10}$  Pb/cm<sup>2</sup> at an angle  $\theta_i$  from c.

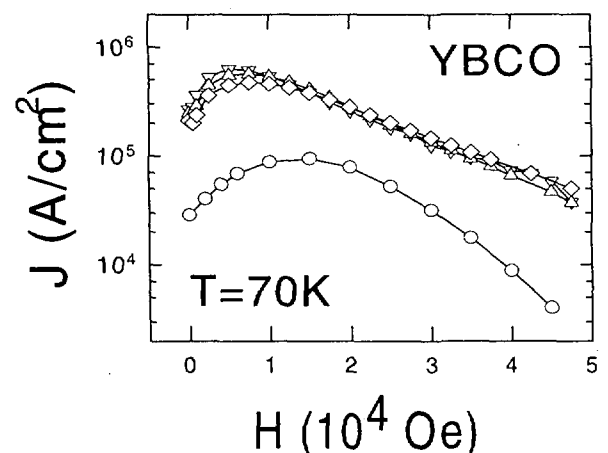


Fig.2 : Persistent current density vs magnetic field (applied along c), in a virgin sample ( $\circ$ ) and samples irradiated by  $10^{11}$  Pb/cm<sup>2</sup> along 2 ( $\Delta$ ), 3 ( $\nabla$ ) or  $\infty$  ( $\diamond$ ) directions inclined of  $10^\circ$  from c.

### References

- [1] F. Warmont et al., Physica C 277, 61 (1997).
- [2] S. Hébert et al., submitted to Nucl. Instr. & Meth. B.
- [3] S. Hébert et al., Physica C 299, 259 (1998).
- [4] S. Hébert et al., Phys. Rev. B 57, 649 (1998).

# **AUTHOR INDEX**



## AUTHOR INDEX

- ABEDINZADEH Z. 151; 152  
ADOUÏ L. 112; 114; 117; 125; 127  
AICHELIN J. 78  
AIELLO S. 119  
ALAMANOS N. 11; 14; 32; 95  
ALLATT R. 39; 40  
ANGELIQUE J.C. 20; 21; 39; 40; 51  
ANNE R. 39; 40; 44; 57  
APPLEBE D. 49  
ARDOUIN D. 72  
ASSENARD M. 72  
AUDI G. 20; 51  
AUGER F. 11; 14; 32; 95  
AUGER G. 46; 51; 95  
AXELSSON L. 25; 42; 49  
AYMES-CHODUR C. 142; 157  
AZAIEZ F. 21  
BACRI Ch.O. 82  
BAIBORODIN D. 46; 57  
BALABANSKI D.L. 30  
BALANZAT E. 144; 145; 151; 152; 153  
BALDACCHINO G. 151  
BAPAT B. 117  
BAQUEY C. 157  
BARRETTE J. 32  
BEAUVY M. 159  
BECK C. 119  
BEDOÛET C. 123; 124  
BELLEGUIC M. 21; 42  
BELOZYOROV A.V. 46; 57  
BENEU F. 131  
BENOIT B. 25  
BERAUD R. 42  
BERGMANN U. 25  
BERTHELOT A. 136  
BETZ N. 142; 157  
BILLEBAUD A. 120; 121  
BIZARD G. 9  
BLANK B. 47; 49  
BLASEVIC A. 19  
BLUMENFELD Y. 11; 14; 32  
BODUCH P. 126  
BOHLEN H.G. 19  
BÖHMER W. 44  
BORCEA C. 19; 21; 39; 40; 42; 46; 57  
BORDERIE B. 61; 70; 82  
BORREL V. 44  
BOUFFARD S. 134; 135; 144; 151; 152  
BOURGEOIS C. 21  
BRONCHALO E. 103  
BRUCE A.M. 47; 49  
BUCHET Ph. 63; 70  
BURJAN V. 39  
BUSNEL J.P. 144  
CANCHEL G. 42  
CARABY C. 127  
CARBAJO M. 103  
CARJAN N. 105  
CARON M. 121  
CASANDJIAN J.M. 20; 32; 51; 95  
CASSIMI A. 112; 114; 117; 125; 127  
CASTEL B. 14  
CATFORD W.N. 25; 39; 47; 49  
CAVALLARO S. 119  
CHABANNAT E. 42  
CHABERT M. 51  
CHANDLER C. 47; 49  
CHANTEPIE M. 126  
CHAPPELL S.P.G. 25  
CHARTIER M. 20; 32; 51; 95  
CHARVET J.L. 63; 70; 89  
CHBIHI A. 77; 86; 87  
CHESNEL J.Y. 116; 123; 124  
CHEVALLIER M. 93; 111  
CHISTE V. 14  
CHOMAZ P. 82; 111  
CLARK R.M. 49  
CLARKE N.M. 25  
CLOUVAS A. 121  
CNIGNIET F. 101  
COHEN C. 93; 111  
COLONNA M. 82  
CORTINA-GIL M.D. 30; 32; 95  
COSTA G. 25  
COSTANTINI J.M. 135; 137  
COULIER N. 30  
COUSSEMENT R. 30  
CREMER G. 126  
CUE N. 111  
CULLEN D.M. 49  
CUNSOLO A. 20; 51  
CURTIS N. 25; 47  
CUSSOL D. 65  
CZAJKOWSKI S. 47; 49  
D'ARRIGO A. 25  
DAPOZ S. 142; 157  
DAUGAS J.M. 21; 42; 49  
DAUVERGNE D. 93; 111  
DAYRAS R. 63; 70  
De FILIPPO E. 119  
de GOES BRENNARD E. 25  
de OLIVEIRA F. 21; 25; 30; 42; 46  
de VISMES A. 46  
DEL PERAL L. 103

DELONCLE I. 21  
DESEQUELLES P. 9  
DESSAGNE Ph. 47; 49  
DEYCARD S. 151; 152  
DJEBARA M. 133  
DLOUHY Z. 39; 40; 46; 57  
DONZAUD C. 21; 39; 40; 42; 51  
DONZEAUD C. 20  
DOORYHEE E. 136  
DORE D. 63; 65; 70  
DÖRFLER T. 44  
DORNER R. 117  
DORVAUX O. 9; 25  
DRUETTA M. 126  
DUBOIS A. 127  
DUFOUR C. 131; 136; 146  
DUPONCHEL S. 125  
DUPRAT J. 21  
DURAL J. 93; 111  
DURAND D. 9  
DURAUD J.P. 134  
EMSALLEM A. 42  
ERAZMUS B. 9  
ESNOUF S. 142  
EUDES Ph. 72  
FEKOU-YOUMBI V. 32; 95  
FERME J. 51  
FERNANDEZ B. 32; 95  
FIFIELD L.K. 51  
FLECHARD X. 125  
FLEURY A. 47; 49  
FNIDIKI A. 140; 141  
FOTI A. 20; 51  
FOURMENT C. 112; 114  
FRANKLAND J.D. 82  
FRANKLAND L. 49  
FRASCARIA N. 11; 14; 32  
FREER M. 25  
FREMONT F. 116; 123; 124  
FRIEDMAN W.A. 77  
FUSS H. 145  
FULTON B.R. 25  
GALICHET E. 67  
GALIN J. 23; 93; 99; 101  
GANGNAN P. 111  
GARCES NARRO J. 49  
GARDES-ALBERT M. 151; 152  
GARDINA G. 25  
GELLETLY W. 47; 49  
GEORGIEV G. 30  
GERACI M. 119  
GERMAIN M. 72  
GERVAIS B. 114; 121  
GILLIBERT A. 11; 14; 20; 21; 32; 46; 51; 95  
GIOVINAZZO J. 47; 49  
GIUSTRANTI C. 153  
GLASCHAMER T. 11  
GODWIN M. 11  
GOLDENBAUM F. 93; 101  
GOURBILLEAU F. 136  
GOURIO D. 72  
GRANDIN J.P. 112; 114; 116; 117; 121; 127  
GREENHALGH B. 49  
GREGORI C. 25  
GREYHER M. 116; 123  
GREVY S. 21; 25; 39; 40; 44  
GRZYWACZ R. 47; 49  
GUARNERA A. 82  
GUILLEMAUD-MUELLER D. 21; 25; 39;  
40; 42; 44; 57  
GUIMARAES V. 19  
GUINET D.C.R. 67  
GULMINELLI F. 61; 67  
GULYAS L. 116  
HANAPPE F. 9; 25  
HARDER M. 49  
HARDY V. 162  
HEBERT S. 162  
HEMON S. 136  
HENNECART D. 116; 125  
HERVIEU M. 162  
HEUSCH B. 25  
HICKEL B. 151  
HILSCHER D. 101  
HIRATA D. 20  
HUSSON X. 116; 123; 124  
JACQUET D. 93  
JACQUET E. 126  
JAKOBSSON B. 9  
JAKUBASSA-AMUNDSEN D.H. 119; 120  
JANAS Z. 47  
JONES K.L. 49  
JONSON B. 25  
JORE D. 151; 152  
JOUANNE C. 14  
JUNG M. 121  
JURASZEK J. 141  
KALPAKCHIEVA R. 19; 57  
KELLY G. 25  
KELSALL N. 49  
KHAN E. 11  
KHAYYAT K. 117  
KIENER J. 21  
KIRSCH R. 93; 111  
KOLLMUS H. 117  
KRATZ K.L. 44  
KSZCZOT T. 49  
L'HOIR A. 111  
LABICHE M. 25  
LALLEMAN A.S. 46  
LAMOUR E. 114  
LANZANO G. 119  
LAPOUX V. 11; 14; 19  
LAULHE C. 126  
LAURENT A. 146  
LAURENT H. 32

LAUTRIDOU P. 72  
LAVILLE J.L. 72  
LE BOUEDEC A. 142  
LE BRUN C. 25  
LE FEVRE A. 87  
LE MOËL A. 142; 157  
LEBRUN C. 9; 72  
LECLER D. 116; 126  
LECOLLEY F.R. 9  
LEDNICKY R. 9  
LEENHARD S. 42  
LEENHARDT S. 21; 25  
LEFORT T. 65  
LEJAY P. 162  
LELIEVRE D. 111; 114; 127  
LEPINE-SZILY A. 19; 20; 30; 32; 51; 95  
LEPOUTRE A. 125  
LEROY C. 135; 144  
LESZCZYNSKI P. 9  
LEVALOIS M. 161  
LEVESQUE F. 136  
LEWITOWICZ M. 20; 21; 25; 30; 39; 40;  
42; 44; 46; 47; 49; 51; 57  
LHENRY I. 11  
LIBIN J.F. 111  
LICHTENTHALER R. 19; 20  
LIENARD A. 101  
LIENARD E. 23; 93; 99  
LIMA G.F. 20  
LONGOUR C. 42; 47; 49  
LOPEZ M.J. 42  
LOPIANO F. 119  
LOTT B. 23; 93; 99; 101  
LUKYANOV S. 20; 39; 40; 46; 51; 57  
MACCORMICK M. 19; 20; 51; 95  
MAHBOUB D. 119  
MAIDIKOV V.Z. 57  
MANGIAGALLI P. 161  
MANN R. 117  
MARCHAND C. 47  
MARECHAL F. 11  
MARIE F. 14; 21  
MARIE N. 86  
MARIE P. 161  
MARKENROTH K. 25  
MARQUES F.M. 25; 39  
MARTINEZ G. 39  
MATZKE H.J. 159  
MEDINA J. 103  
MEFTAH A. 133; 137  
MEHREN T. 44  
MERABET H. 123  
METIVIER V. 72  
MEZIAT D. 103  
MIEHE Ch. 47; 49  
MIKHAILOV K. 9  
MITTIG W. 14; 20; 30; 32; 46; 51; 95  
MOKLER P. 111  
MÖLLER P. 44  
MORISSEY D.J. 11  
MORJEAN M. 23; 93  
MORRISSEY D.J. 20; 51  
MOSBAH M. 134  
MOSCATELLO M.H. 51  
MOSHAMMER R. 117  
MOTTA M. 25  
MUELLER A.C. 21; 25; 39; 40; 44; 57  
MURGATROYD J.T. 25  
MUSUMARA A. 11  
NALPAS L. 63; 70  
NATOWITZ J.B. 86  
NEBAUER R. 78  
NEYENS G. 30  
NGUYEN A.D. 84  
NILSSON T. 25  
NINANE A. 25  
NOLAN P.J. 39  
NOREN B. 9  
NOUICER R. 119  
NOVAK J. 39  
NOWACKI F. 40  
NYMAN G. 25  
ODLAND O.H. 51  
OGANESSIAN Yu.Ts. 57  
OLIVEIRA F. 19  
OLIVEIRA J.M. 19  
OLSON R.E. 125  
ORR N. 11; 19; 20; 21; 23; 25; 32; 39; 40;  
46; 47; 51  
OSTROWSKI A. 19; 20; 44; 51; 95  
OTTINI S. 11  
OTTINI-HUSTACHE S. 14  
PAGANO A. 119  
PAGE R.D. 39; 40; 47; 49  
PAKOU A. 32; 95  
PASCALE J. 126  
PASCALON V. 32  
PATOIS Y. 99  
PAUMIER E. 131; 136; 146  
PAWLAK F. 146  
PEARSON C.J. 47; 49  
PEGHAIRE A. 23; 93; 99; 101  
PENIONZHKEVICH Y.E. 21; 39; 40; 46; 57  
PEREZ C. 153  
PERIER Y. 23; 93; 101  
PERRIERE J. 146  
PETER J. 65  
PETERSOHN E. 142  
PFEIFFER B. 44  
PIATTELLI P. 11  
PIQUERAS I. 25  
PLUTA J. 9  
POIZAT J.C. 93; 111  
POLITI G. 51; 119  
POLLACCO E.C. 11; 119  
PORQUET M.G. 21

PORTE-DURRIEU M.C. 157  
POUGHEON F. 21; 39; 40; 42; 44  
PRAVIKOFF M.S. 47  
PREVOT G. 93  
PRINZ H.T. 111  
PROVOST J. 162  
PRZEWLOCKI M. 9  
QIAN X. 101  
QUEDNAU B.M. 23  
RAHMANI A. 72  
RAMILLON J.M. 111; 112; 114  
RAUSCHER T. 44  
RAVACH G. 140  
REED A. 39; 40; 47; 49  
REGAN P.H. 39; 47; 49  
REMILLIEUX J. 93; 111  
REN Z. 46  
REPOSEUR T. 72  
RICHOMME F. 141  
RIDIKAS D. 46  
RIISAGER K. 25  
RIVET M.F. 61; 70; 82  
ROGERS W.F. 30  
RONCIN P. 125  
ROTHARD H. 114; 119; 120; 121  
ROUSCILLES A. 152  
ROUSSEL-CHOMAZ P. 11; 19; 30; 32;  
46; 95  
ROUSSET S. 153  
ROYNETTE J.C. 11; 14  
ROZET J.P. 111; 112; 114  
SAGE E. 153  
SAINT-LAURENT M.G. 21; 25; 39; 40;  
42; 44; 47; 57  
SAKURAI H. 46  
SALOU S. 77  
SANCHEZ S. 103  
SANTONOCITO D. 11  
SANUY F. 111  
SARAZIN F. 25; 46  
SAUVESTRE J.E. 11; 42  
SAVAJOLS H. 46  
SCARPACI J.A. 11; 14; 32  
SCHAPIRO O. 87  
SCHLOSSER D. 142  
SCHLUTIG S. 134  
SCHMAUS D. 93; 111  
SCHMIDT-OTT W.D. 44  
SCHMITT W. 117  
SCHWAB W. 40  
SCHWARTZ K. 137; 139  
SHEIKH J.A. 47  
SHERRILL B.M. 20; 51  
SIDA J.L. 32; 95  
SIISKONEN T. 39  
SIMON Ch. 162  
SINGER S. 25  
SKEPPSTEDT O. 9  
SKOBELEV N.K. 57  
SKOGVALL B. 116  
SOBOLEV Yu. 21  
SOKOL E. 39; 40  
SORLIN O. 21; 25; 39; 42; 44; 49; 57  
SPIELER A. 123  
SPITAELS C. 51  
SQUALLI M. 82  
STAVINSKY A. 9  
STECKENREITER T. 139; 145  
STEPHAN C. 20; 51; 111; 112; 114  
STOLLA Th. 19  
STOLTERFOHT N. 116; 123  
STOQUERT J.P. 133; 137; 146  
STROTTMAN D. 105  
STUDER F. 133  
STUTTGE L. 9; 25  
SUHONEN J. 39  
SULIK B. 116; 123  
SUOMIJARVI T. 11; 20; 32; 51  
TALOU P. 105  
TAMAIN B. 9  
TANIS J.A. 116  
TARASOV O. 39; 40; 57  
TASSAN-GOT L. 20; 51; 61; 112; 114  
TEILLET J. 140; 141  
TERNIER S. 30  
TEUGHEL S. 30  
TIREL O. 78  
TONEEV V.D. 57  
TOULEMONDE M. 93; 111; 131; 133; 137;  
139; 140; 141; 146  
TRAUTMANN C. 137; 139; 145  
TRINDER W. 39; 40; 57  
ULLRICH J. 117  
VERNHET D. 111; 112; 114  
VIEIRA D.J. 20; 51  
VILLARD G. 162  
VILLARI A.C.C. 20; 23; 51  
VINCENT S. 39; 47  
VOLANT C. 119  
von OERTZEN W. 19  
VUILLIER S. 119  
VYVEY K. 30  
WADSWORTH R. 47; 49  
WARCZAK A. 111  
WARMONT F. 162  
WARNER D.D. 47  
WATSON D.L. 25  
WEBER Th. 117  
WIELECZKO J.P. 77; 86; 87  
WILSON M. 126  
WINFIELD J.S. 19; 21; 40; 47  
WISS T. 159  
WOUTERS J.M. 20; 51  
WÜNSCH R. 121

## INDRA(\*) :

M. Assenard<sup>6</sup>, G. Auger<sup>2</sup>, Ch.O. Bacri<sup>4</sup>, N. Bellaize<sup>5</sup>, J. Benlliure<sup>2</sup>,  
E. Bisquer<sup>3</sup>, F. Bocage<sup>5</sup>, B. Borderie<sup>4</sup>, R. Bougault<sup>5</sup>, R. Brou<sup>5</sup>, Ph. Buchet<sup>1</sup>,  
J.L. Charvet<sup>1</sup>, A. Chbihi<sup>2</sup>, J. Colin<sup>5</sup>, D. Cussol<sup>5</sup>, R. Dayras<sup>1</sup>, A. Demeyer<sup>3</sup>,  
E. De Filippo<sup>1</sup>, P. Désesquelles<sup>2</sup>, D. Doré<sup>1</sup>, D. Durand<sup>5</sup>, P. Ecomard<sup>2</sup>,  
P. Eudes<sup>6</sup>, J.D. Frankland<sup>4</sup>, P. Gagné<sup>2</sup>, E. Galichet<sup>3</sup>, E. Genouin-Duhamel<sup>5</sup>,  
E. Genoux-Lubain<sup>5</sup>, E. Gerlic<sup>3</sup>, M. Germain<sup>6</sup>, L. Gingras<sup>2</sup>, D. Gourio<sup>6</sup>,  
E. Grelet<sup>1</sup>, D. Guinet<sup>3</sup>, F. Gulminelli<sup>5</sup>, B. Hurst<sup>5</sup>, R. Laforest<sup>5</sup>, P. Lautesse<sup>3</sup>,  
J.L. Laville<sup>2</sup>, L. Lebreton<sup>3</sup>, C. Le Brun<sup>5</sup>, J.F. Lecolley<sup>5</sup>, A. Le Fèvre<sup>2</sup>,  
T. Lefort<sup>5</sup>, R. Legrain<sup>1</sup>, N. Leneindre<sup>5</sup>, O. Lopez<sup>5</sup>, M. Louvel<sup>5</sup>, J. Lukasik<sup>4</sup>,  
Y.G. Ma<sup>5</sup>, N. Marie<sup>2</sup>, A.M. Maskay<sup>3</sup>, V. Metivier<sup>5</sup>, L. Nalpas<sup>1</sup>,  
A.D. N'Guyen<sup>5</sup>, A. Ouatzerga<sup>4</sup>, M. Parlog<sup>8</sup>, J. Péter<sup>5</sup>, E. Plagnol<sup>4</sup>,  
E. Pollacco<sup>1</sup>, G. Politi<sup>2</sup>, A. Rahmani<sup>6</sup>, T. Reposeur<sup>6</sup>, M.F. Rivet<sup>4</sup>, E. Rosato<sup>7</sup>,  
F. Saint-Laurent<sup>2</sup>, S. Salou<sup>2</sup>, M. Samri<sup>2</sup>, A. Siwek<sup>5</sup>, M. Squalli<sup>4</sup>,  
J.C. Steckmeyer<sup>5</sup>, M. Stern<sup>3</sup>, G. Tabacaru<sup>8</sup>, B. Tamain<sup>5</sup>, L. Tassan-Got<sup>4</sup>,  
O. Tirel<sup>2</sup>, E. Vient<sup>5</sup>, C. Volant<sup>1</sup>, J.P. Wieleczko<sup>2</sup>, A. Wieloch<sup>5</sup>.

- (1) -DAPNIA/SPhN, CEA/Saclay, 91191 Gif-sur-Yvette Cedex, France.
- (2) -GANIL (DSM-CEA/IN2P3-CNRS), B.P. 5027, 14076 Caen Cedex 5, France.
- (3) -IPN Lyon (IN2P3-CNRS/Université), 69622 Villeurbanne Cedex, France.
- (4) -IPN Orsay (IN2P3-CNRS), 91406 Orsay Cedex, France.
- (5) -LPC Caen (IN2P3-CNRS/ISMRA et Université), 14050 Caen Cedex, France.
- (6) -SUBATECH (IN2P3-CNRS/Université), 44070 Nantes Cedex, France.
- (7) -Dipartimento di Scienze Fisiche, Univ. di Napoli, 180126 Napoli, Italy.
- (8) -Nuclear Institute for Physics and Nuclear Engineering, Bucharest, Romania.

\* The names refer to the INDRA group since its creation up to the analysis presented in this report. Nowadays the number of physicists involved in our experiments represents 54% of this list. The collaboration wants here to thank all the physicists, especially the visitors and the students, for their contribution.

---

# **GANIL**

**GRAND ACCELERATEUR D'IONS LOURDS  
BP 5027 - 14076 CAEN CEDEX 05 FRANCE  
TEL. 02 31 45 46 47 - FAX. 02 31 45 46 45**

---